Expect the Unexpected: An institutional case series of rare mimicking common pathology within the head and neck

1 Expect the Unexpected: An institutional case series of rare mimicking common pathology within the head and neck

CA Tork, BD Martin, AM Betts

Brooke Army Medical Center
United States

Purpose Lesions within the head and neck involve many different anatomical spaces and tissue types. While these lesions can often be readily distinguishable by their imaging characteristics, some require advanced imaging or tissue sampling for a definitive diagnosis. Occasionally, tissue diagnosis demonstrates a rare pathology unexpected based on imaging characteristics. These mimickers share imaging characteristics with common lesions that are indistinguishable via conventional imaging. This exhibit will show an institutional case series of rare pathology mimicking common lesions within the parotid gland, carotid space, cervical spine, nasal cavity, and oral cavity. Description Benign primary parotid neoplasms such as benign mixed tumor/pleomorphic adenoma and Warthin tumor encompass 80% of lesions found within the parotid gland. Additional common lesions are normal intraparotid lymph nodes, primary malignancy such as mucoepidermoid carcinoma and adenoid cystic carcinoma, and metastases. The malignant lesions can often be separated from the benign with the presence of invasive or aggressive imaging features. In a subset of cases we show other rare malignant tumors such as neuroendocrine carcinoma that share imaging features of the more common benign entities, only diagnosed following tissue analysis. The carotid space is home to the classic carotid body tumor/paraganglioma centered at the carotid bifurcation. A case in our institution demonstrated what was originally thought to be an atypical appearance of a carotid body tumor. Instead, the tissue revealed synovial sarcoma, of which only a handful of cases are reported in the literature at the carotid bifurcation. A dumbbell shaped mass expanding the cervical spine neural foramen showed the common imaging characteristics of a nerve sheath tumor, until tissue markers elicited a diagnosis of the more uncommon solitary fibrous tumor. What was believed to be a solitary nasal polyp on imaging resulted with a pathology diagnosis of solitary fibrous tumor. A large cystic mass within the sublingual space was initially suspected as a simple ranula. However, additional imaging features raised suspicion of a dermoid or epidermoid. Aspiration revealed caseous material, and sublingual excision revealed a sublingual dermoid. The imaging findings for the common lesions within each of these spaces will be discussed, followed by the case(s) from our institution of rare pathology that mimics these lesions. In addition, potential differences in the imaging will be discussed to distinguish these lesions or demonstrate the need for tissue diagnosis, as the diagnosis could alter the need for surgery, surgical approach, and additional treatment. Summary Many common lesions within the head and neck have distinguishing imaging characteristics that enable the diagnosis, but as evidenced with these cases, even the slightest variation in imaging can result in the need for tissue sampling to ensure the diagnosis is not a rare pathology that can alter further clinical management.

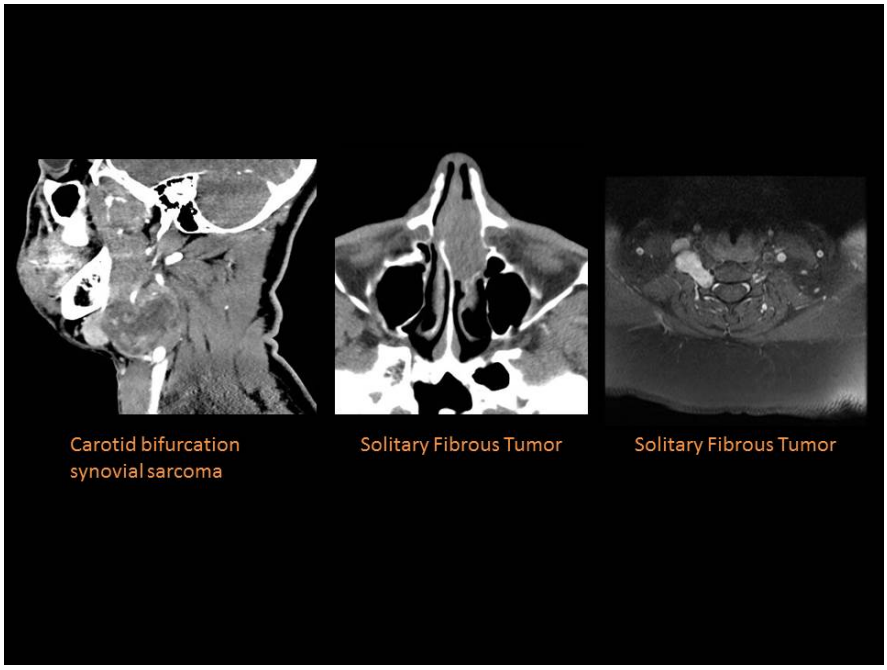

Carotid bifurcation synovial sarcoma

Solitary Fibrous Tumor

Solitary Fibrous Tumor

Carotidynia: Symptom or Disease State?

2 Carotidynia: Symptom or Disease State?

E Rawie, D Roberie, L Mitchell, T Biega

Landstuhl Regional Medical Center, Landstuhl, Germary
United States

1. Purpose In the late 1980s, the International Headache Society (IHS) included carotidynia in its classification system of disorders. Less than twenty years later they removed it. Two cases follow that suggest that carotidynia is, in fact, a valid disorder. 2. Description A. Case Reports The first case concerns a 41 year old male patient who presented to the Emergency Department with a three day history of moderately severe left-sided neck pain and swelling with odynophagia. A contrast enhanced CT (CECT) of the neck demonstrated circumferential soft tissue thickening of the left carotid artery bulb and bifurcation without luminal narrowing (Figures 1, 2, and 3). The second case concerns a 48 year old male who presented to his primary care physician for a routine physical. During the visit the patient reported three weeks' left-sided neck tenderness. The patient underwent a CECT of the neck which demonstrated asymmetric left-sided mural thickening and inflammation of the common carotid artery bifurcation without luminal narrowing and (Figures 3 and 4). B. Discussion Many carotidynia case reports followed in the decades after Temple Fay's first description of carotidynia in 1927 and in 1988 the IHS included carotidynia in The International Classification of Headache Disorders (ICHD). In the years following the appearance of the ICHD several journal articles demonstrated flaws with its criteria. Consequently, in the 2004 second edition of the ICHD (ICHD-II) the IHS moved carotidynia from the classification system to the appendix where it listed entities requiring additional research validation. The disagreement between carotidynia detractors and proponents likely reflects an inconsistent use of the term. On the one hand, carotidynia may refer to the symptom of carotid pain. When defined this way, it is non-specific finding. Other diseases of the carotid, migraine headaches, and infections of the oral cavity, oropharynx, and salivary glands may all present with unilateral carotid or neck pain. On the other hand, carotidynia may refer to an idiopathic diagnosis made after exclusion of the above entities. Idiopathic carotidynia appears to have relatively consistent clinical findings largely reflecting the original ICHD criteria. With imaging, one usually sees soft tissue enhancement and inflammation around the carotid on CT. The two cases presented in this exhibit largely adhere to the carotidynia profile. 3. Summary Initially, some questioned, perhaps rightly, carotidynia's validity as a clinical entity. However, subsequent development of hematologic analysis and imaging better allowed the exclusion of other etiologies. With their exclusion, an uncommon idiopathic syndrome of carotid inflammation characterized by carotid pain and tenderness, mural inflammation on imaging, and a self-limiting course does appear to exist.

Figure 1. Coronal CECT image shows inflammation of the fat around the distal left common carotid artery.

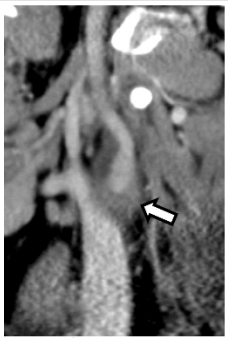

Figure 2. Sagittal CECT image demonstrates inflammation of the fat around the left carotid bulb and proximal internal carotid artery.

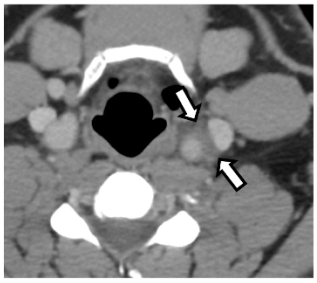

Figure 3. Axial image demonstrates asymmetric inflammation around the left carotid artery.

An Unwanted Union: A Case of TMJ Ankylosis

3 An Unwanted Union: A Case of TMJ Ankylosis

MP Balaccua

Quezon City General Hospital
Philippines

Temporomandibular joint (TMJ) ankylosis is a disorder in which there is fibrous or bony fusion of the components of the temporomandibular joint leading to a limitation of joint movement and arrest of mandibular growth in the affected side. TMJ ankylosis is a rare condition with varying incidence rates in the world, with most recorded cases in India and Egypt. Most of the cases resulted from trauma to the TMJ and, in developing countries, it is mostly due to an adjacent infection. The author presents a case of a five year old male who came in with a chief complaint of limitation of mouth opening associated with deviation of the chin to the right. Facial computed tomography (CT) scan revealed shortening, flattening and irregularity between the right condylar head of the mandible and glenoid fossa, thickening and irregularity of the ipsilateral temporal bone with a fine bony bridge between the right condylar head and the ipsilateral temporal bone. Treatment for TMJ ankylosis involves surgical excision of the pathologic fibrous or osseous tissue and joint reconstruction coupled with aggressive and early post-operative physiotherapy.

Appendix B. Coronal section showing the flattening of the right condylar process (red arrow) with ipsilateral loss of the TMJ joint space, thickening of the temporal bone (green arrow) and shortened mandibular ramus (yellow arrow).

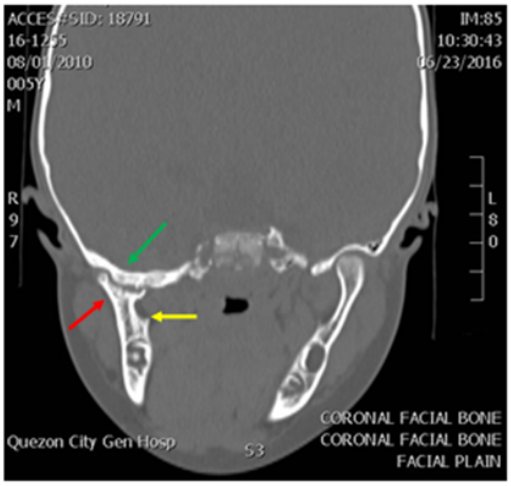

Case series of temporal bone Granulomatosis with Polyangiitis

4 Case series of temporal bone Granulomatosis with Polyangiitis

KD Seifert, A Malhotra, X Wu, L Tu

Yale New Haven Hospital
United States

Purpose: Granulomatosis with polyangiitis classically presents as a triad of pulmonary, upper respiratory, and kidney symptoms. The majority of patients present with otorhinolaryngologic symptoms, with the paranasal sinuses and nasal cavities being the most common sites of involvement. Ear involvement is less common, and temporal bone involvement is rare. Often, patients initially present to their otolaryngologist for complaints of recurrent ear infections and/or hearing loss. These patients frequently undergo some type of imaging study with CT or MRI for further evaluation. Therefore, it is important to have knowledge of the clinical presentation, imaging and pathologic characteristics, and laboratory tests for GPA so the astute radiologist can aid in diagnosis. The purpose of this exhibit is to present a case series of rare temporal bone involvement of GPA, and subsequently review the more common findings of GPA in the head and neck. Description: This education exhibit will present a case series review of 4 patients with temporal bone involvement of GPA, including their clinical presentation, radiologic and pathologic findings, and any pertinent laboratory data. This educational exhibit will also review other more common clinical presentation and imaging findings of GPA involving the head and neck. Summary: With knowledge of rare temporal bone involvement of GPA, an educated radiologist can add in diagnosis of rare presentations of GPA.

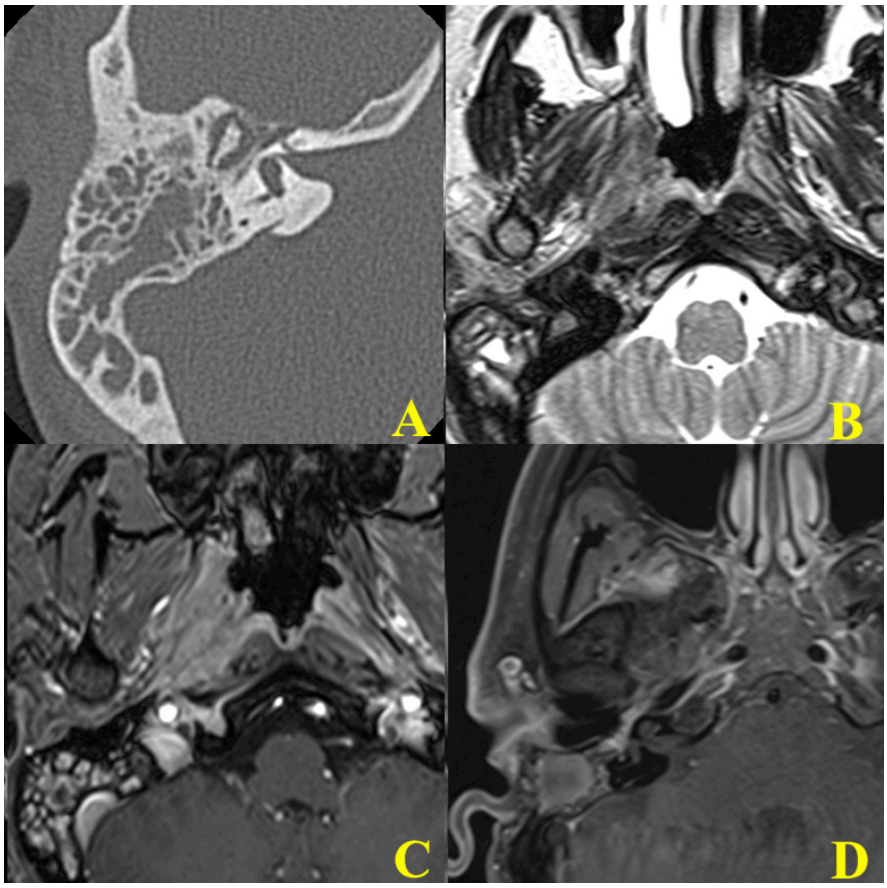
A
B
C
D

Imaging of Early & Delayed Complications in Head and Neck Cancer Treatment

5 Imaging of Early & Delayed Complications in Head and Neck Cancer Treatment

N Harn, J Thompson, M Witek, G Avey, L Ledbetter, T Kennedy

University of Wisconsin, Hospitals and Clinics
United States

Purpose: Summarize imaging findings of early and late complications of head and neck cancer treatment. Description: Knowledge of common early and late complications of head and neck cancer treatment should aid in adding value to post treatment imaging by potentially reducing morbidity associated with early detection. Imaging evaluation should not only include identification of disease response, recurrence of disease, and metastases but should also identify treatment related changes that can produce significant morbidity. Early complications amenable to imaging diagnosis include: mucositis/mucosal edema, sialoadenitis, periodontal disease, flap necrosis, pharyngocutaneous fistula, vocal cord paralysis and other nerve injuries. Late complications amenable to imaging diagnosis include: osteoradionecrosis, lymphedema and fibrosis, flap necrosis, accelerated atherosclerosis, carotid blowout, myelopathy, and secondary malignancy. Imaging findings of these conditions are presented as a pictographic summary with key points. Summary: Post treatment imaging evaluation of head and neck cancer is important to evaluate for early and late complications of treatment in addition to disease recurrence/response and metastasis.

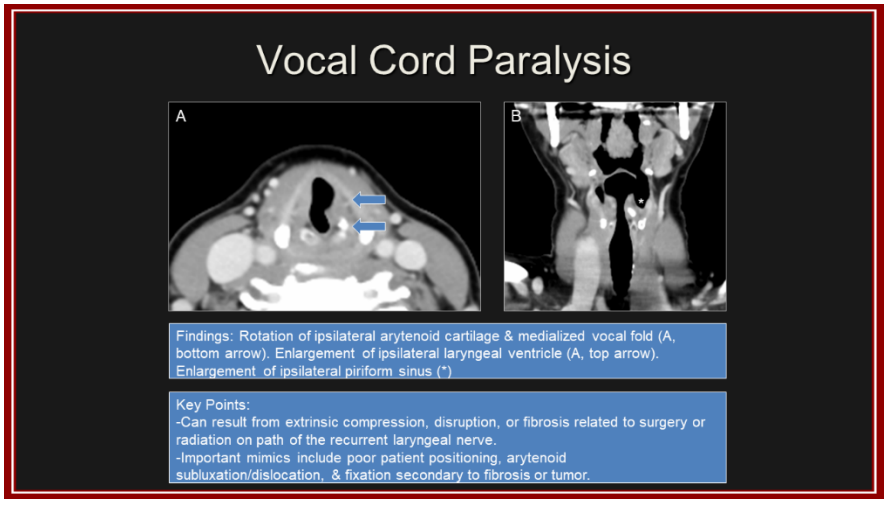

Imaging Findings Related to the Valsalva Maneuver in Head and Neck Radiology

6 Imaging Findings Related to the Valsalva Maneuver in Head and Neck Radiology

AA Madhavan, C Carr, J Lane

Mayo Clinic - Rochester, MN
United States

PURPOSE: Attempted exhalation against a closed glottis, known as the Valsalva maneuver, is an important clinical diagnostic and therapeutic tool due to its physiologic effects. The maneuver rapidly increases intrathoracic pressure, causing a decrease in systemic venous return to the heart with complex downstream effects.1 Several unique conditions can occur with repetitive or acute changes in pressure from Valsalva. We will discuss and review the pertinent imaging features of head and neck entities resulting from induced pressure gradients DESCRIPTION: Several cases from our practice that had significant head or neck imaging findings related to induced pressure gradients were reviewed by two neuroradiologists. Those with especially compelling or educational imaging features and corroborative clinical histories were selected for presentation. Cases selected included laryngocele, hyperpneumatization of the skull base, Valsalva retinopathy, transient global amnesia, spontaneous subcutaneous emphysema, orbital varices and jugular phlebectasia that vary in size with Valsalva, and chronic pneumoparotitis. These cases have characteristic imaging findings related to induced pressure gradients and are accompanied with appropriate clinical history accounting for the radiologic features. SUMMARY: Recognizing imaging findings and knowing the expected clinical histories that are frequently related to induced pressure gradients aids in the diagnosis of these pathologies. Cases from our practice demonstrate the breadth of these findings in head and neck radiology. For reference, an example of one of our cases (jugular phlebectasia) has been provided. Images from all of the cases will be included in the final electronic exhibit.

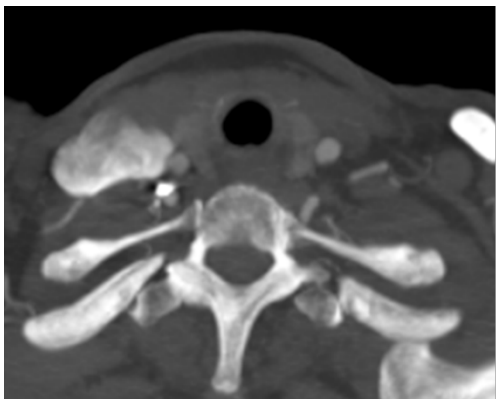

The Secret of the Sniffle: An Orbital PET-CT Correlation for An Orbital Metastasis Mimic

7 The Secret of the Sniffle: An Orbital PET-CT Correlation for An Orbital Metastasis Mimic

V Yedavalli, Z Dymon, M Gabriel

Stanford University
United States

Purpose: Corynebacterium bovis is a subtype of gram-positive family that most often causes pyelonephritis in cattle and dacrocystitis in mice. It is not known as an infectious bacterium in humans. Corynebacterium subforms have been implicated in adult conjunctivitis but bovis specifically has a handful of human conjunctivitis and no known dacrocystitis cases. We present a 69-year-old male with known metastatic rectosigmoid carcinoma with left eye discomfort showing a hypermetabolic left orbital mass on PET/CT thought to be metastasis, but ultimately diagnosed as Bovis dacrocystitis. Description: We present a 69-year-old male with history of colon cancer complaining of left eye discomfort for over four months without resolution after penicillin therapy. A PET study was then performed after the initial diagnosis for restaging of the patient's rectosigmoid carcinoma on which an incidental hypermetabolic left medial orbital mass was found. A postcontrast CT then demonstrated a peripherally enhancing mass in the left orbit. Findings were concerning for metastasis with lymphoma and infection considered less likely. A biopsy was then performed with cultures with pathology demonstrating squamous metaplasia without evidence of malignancy or invasive fungal infection. Cultures showed colonies of penicillin resistant Corynebacterium bovis leading to the diagnosis of infectious dacrocystitis. Symptoms resolved after appropriate antibiotic therapy. Image Findings: A 69-year-old male with history of rectosigmoid colon cancer. A) Axial PET/CT demonstrates an abnormal focally increased uptake within the medial canthus of the left globe with an SUV max of 5.3. B) Corrected PET image corresponds to the area of increased uptake. C-D) Axial and coronal postcontrast CT shows extent of the corresponding peripherally enhancing mass. Summary: We present a rare case of a Corynebacterium bovis dacrocystitis mimicking an orbital metastasis. Although metastasis is the main consideration in the known history of primary neoplasm, rare infections should not be overlooked. Accurate and timely diagnosis can lead to prompt clinical management.

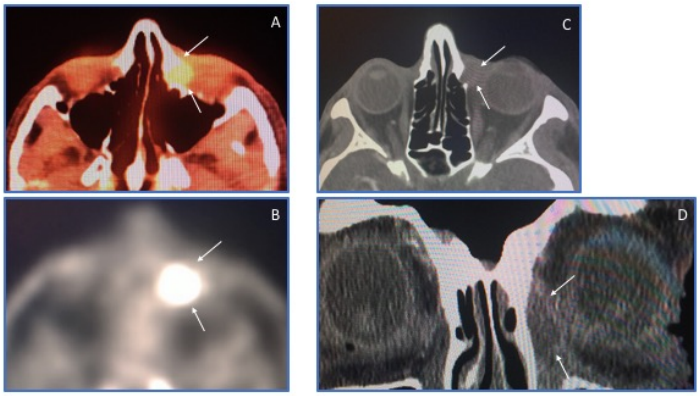

A 69 year old male with history of metastatic rectosigmoid colon cancer. A) Axial PET CT demonstrates an abnormal focal increased FDG uptake within the medial canthus of the left globe with SUX max of 5.3. B) Axial corrected PET image corresponds to the area of increased uptake. C) Axial CT with contrast shows the corresponding mass with faint rim enhancement. D) Coronal CT with contrast also shows the extent of the peripherally enhancing mass.

An Incidentally Found Primary Thyroid Carcinoma on US and Parathyroid Sestamibi Imaging

8 An Incidentally Found Primary Thyroid Carcinoma on US and Parathyroid Sestamibi Imaging

V Yedavalli, Z Dymon, M Gabriel

Stanford University
United States

Purpose: Follicular thyroid carcinoma is the second most common primary thyroid subtype, seen in 10-32% of all thyroid cancers. Although prevalent amongst thyroid cancers, follicular carcinoma is rarely found incidentally on imaging for other pathologies with only a handful of reported cases. Thyroid cancers have relatively increased concentration of mitochondria resulting in increased uptake of sestamibi, leading to diagnostic dilemmas on dedicated parathyroid studies. It is therefore essential not to overlook primary thyroid carcinoma on a sestamibi evaluation. Description: We present a 44-year-old female with known primary hyperparathyroidism. A thyroid ultrasound, performed to assess for thyroid pathology, demonstrated a solitary solid vascular right lobe nodule and a hypoechoic nodule posterior to the inferior left thyroid lobe. A subsequent SPECT/CT sestamibi scan showed intense uptake within the right thyroid lobe with faint uptake posterior to the inferior left thyroid lobe, both correspond to the sonographic findings. Biopsy confirmed a right sided follicular thyroid carcinoma and concomitant left inferior parathyroid adenoma. The patient underwent total thyroidectomy and parathyroid adenoma resection. Image Findings: Figure 1. A) Color sonographic images demonstrating a vascular right thyroid lobe solid hyperechoic nodule. B) Color sonographic image showing a hypoechoic vascular nodule immediately posterior to the inferior left thyroid lobe compatible with a parathyroid adenoma. C) SPECT/CT showing an intense hypermetabolic focus within the right thyroid lobe consistent with thyroid cancer. D) SPECT shows the intense right thyroid lobe focus in addition to the faint focus posterior the left thyroid lobe (red arrow). Summary: Follicular thyroid carcinoma is a common primary thyroid malignancy, yet is rarely seen incidentally on imaging for other entities. We present a case of incidental follicular thyroid carcinoma in a patient with primary hyperparathyroidism. It is therefore essential to consider thyroid masses for uptake on parathyroid imaging as seen in this case.

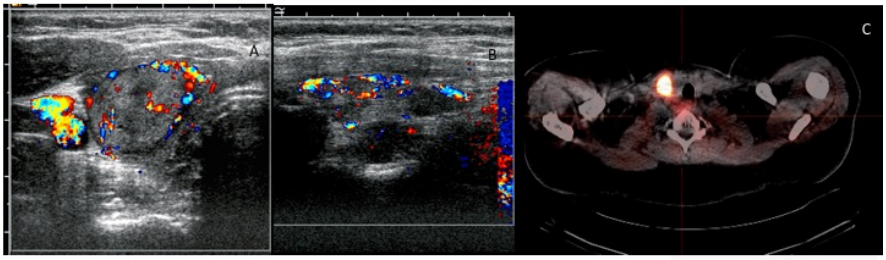

Figure 1. A) Color sonographic images demonstrating a vascular right thyroid lobe solid predominantly hyperechoic nodule. B) Color sonographic image showing a hypoechoic vascular nodule immediately posterior to the inferior left thyroid lobe compatible with a parathyroid adenoma. C) SPECT/CT showing an intense hypermetabolic focus within the right thyroid lobe consistent with thyroid cancer. D) SPECT shows the intense right thyroid lobe focus in addition to the faint focus posterior the left thyroid lobe (red arrow).

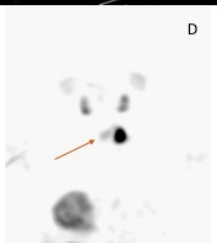

The Masquerading Metastasis: A Multimodality and Pathological Analysis of Renal Cell Carcinoma Metastasis to the Thyroid Gland

9 The Masquerading Metastasis: A Multimodality and Pathological Analysis of Renal Cell Carcinoma Metastasis to the Thyroid Gland

V Yedavalli, Z Dymon, M Gabriel

Stanford University
United States

Purpose: Thyroid lesions have a comprehensive differential diagnosis which include benign and malignant entities such as metastases. Primary renal cell carcinoma (RCC) metastases is extremely rare and seen in only 0.1% of cases. This entity is a diagnostic dilemma as symptoms may not manifest for up to 26 years even after removal of the RCC. Because of the nonspecific appearance on CT and ultrasound, distinguishing such lesions from primary thyroid malignancies is of utmost importance for timely patient management. Description: We present a 66-year-old male with known RCC status post complete left nephrectomy. After presenting with anterior chest pain, the patient underwent a PET/CT demonstrating metastases to the thoracic spine, lungs, and left thyroid lobe. The hypermetabolic thyroid mass was initially thought to be a new primary malignancy. However, PTH, TSH, T3, and T4 were normal. Thyroid ultrasound then demonstrated heterogeneous appearance of the thyroid with a focal hypervascular left lobe mass. Subsequent FNA biopsy confirmed metastatic RCC to the thyroid. Image Findings: Figure 1. A 66-year-old male with resected left RCC presents with chest pain. A) PET/CT demonstrates a focal hypermetabolic mass within the left thyroid lobe (white arrow) compatible with primary RCC thyroid metastasis. Adjacent left posterolateral hypermetabolic focus represents metastatic lymphadenopathy. B) Doppler ultrasonography of the left thyroid lobe shows internal vascularity within the mass. C) Postcontrast CT neck image of the thyroid demonstrates irregular peripherally enhancing thyroid hypodensities (white arrows) consistent with necrotic metastases. D) Microscopic pathology confirms RCC origin with positive CD10 staining. Summary: Thyroid metastases are rare entities with varied appearances. In this case, we present a resected RCC with subsequent thyroid masses initially thought to be a synchronous primary thyroid malignancy, later pathologically proven to be RCC metastases. Although rare, it is essential to include thyroid metastasis in any thyroid mass differential for prompt diagnosis and management.

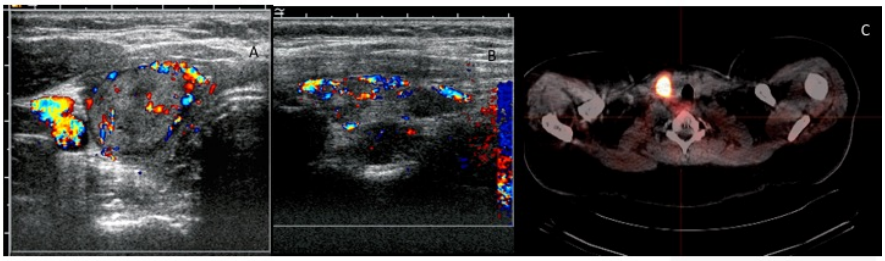

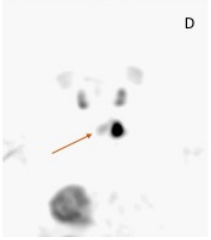

Figure 1. A) Color sonographic images demonstrating a vascular right thyroid lobe solid predominantly hyperechoic nodule. B) Color sonographic image showing a hypoechoic vascular nodule immediately posterior to the inferior left thyroid lobe compatible with a parathyroid adenoma. C) SPECT/CT showing an intense hypermetabolic focus within the right thyroid lobe consistent with thyroid cancer. D) SPECT shows the intense right thyroid lobe focus in addition to the faint focus posterior the left thyroid lobe (red arrow).

The Many Faces of the Carotid Spaces

10 The Many Faces of the Carotid Spaces

CM Tomblinson, JM Aulino

Vanderbilt University
United States

Purpose: 1. Describe the anatomic boundaries of the carotid space (CS) and relationship to surrounding structures 2. Discuss the imaging findings of primary and secondary CS pathologies 3. Develop an algorithm for identifying the structure of origin of a CS mass 4. Demonstrate several mimics of CS pathology Description: The CS is an anatomically complex region extending from the skull base to aortic arch and is invested in all three layers of the deep cervical fascia. The major neurovascular bundle of the head and neck traverses through the CS, including the carotid arteries, internal jugular vein (IJV), cranial nerve X in the infrahyoid neck, and portions of cranial nerves IX, XI, and XII in the suprahyoid neck. CS pathologies include benign and malignant tumors, vascular pathologies, and infectious or inflammatory processes. These diseases can be primary if originating in the carotid space or secondary when spreading from a contiguous space. Each entity possesses imaging features and structural relationships that can aid in distinction from other lesions in the differential diagnosis. The most common benign tumors of the CS are paraganglioma and neurogenic tumors. Subtypes of paraganglioma include carotid body tumors, glomus vagale, and glomus jugulare, which occur at predictable locations, demonstrate avid post-contrast enhancement, and flow voids on T2-weight images indicating intralesional vessels. Because the structures of the CS are anatomically consistent, the direction of vessel displacement can be useful in determining the origin of a CS mass. For example, an avidly enhancing mass with flow voids splaying the internal and external carotid arteries near the carotid bifurcation is a carotid body tumor (Figure A,B), while a more cephalad mass with similar imaging characteristics interposed between the IJV and carotid artery reflects glomus vagale (Figure C,D). Contrast-enhanced MRA may be utilized to further distinguish between paraganglioma and schwannoma, where lack of enhancement on MRA virtually excludes paraganglioma (Figure E,F). Lymph nodes are intimately associated with the carotid sheath. Metastatic nodes with extracapsular spread can invade the carotid sheath and obscure the perivascular fat planes. Squamous cell carcinoma and metastatic papillary or medullary thyroid cancer are common culprits. Primary vascular lesions include carotid dissection, pseudoaneurysm, IJV thrombosis, fibromuscular dysplasia, and carotid rupture. Tortuous carotid arteries and asymmetric IJVs may present as a pseudotumor mimicking pathology. Close approximation to neighboring parapharyngeal and retropharyngeal spaces can permit ingress of infectious or inflammatory processes, leading to cellulitis or abscess. Carotidynia demonstrates circumferential wall thickening and should not be mistaken for arterial dissection, as management is supportive. Given close proximity to adjacent but distinct anatomic spaces, several lesions can present as CS mimics, such as salivary gland neoplasms of the pre-styloid parapharyngeal compartment. Summary: With a thorough understanding of the anatomy of the CS, common pathologies located therein, and an algorithm for assessing nearby displaced structures, one can reasonably narrow the differential or arrive at a diagnosis of diseases of the CS.

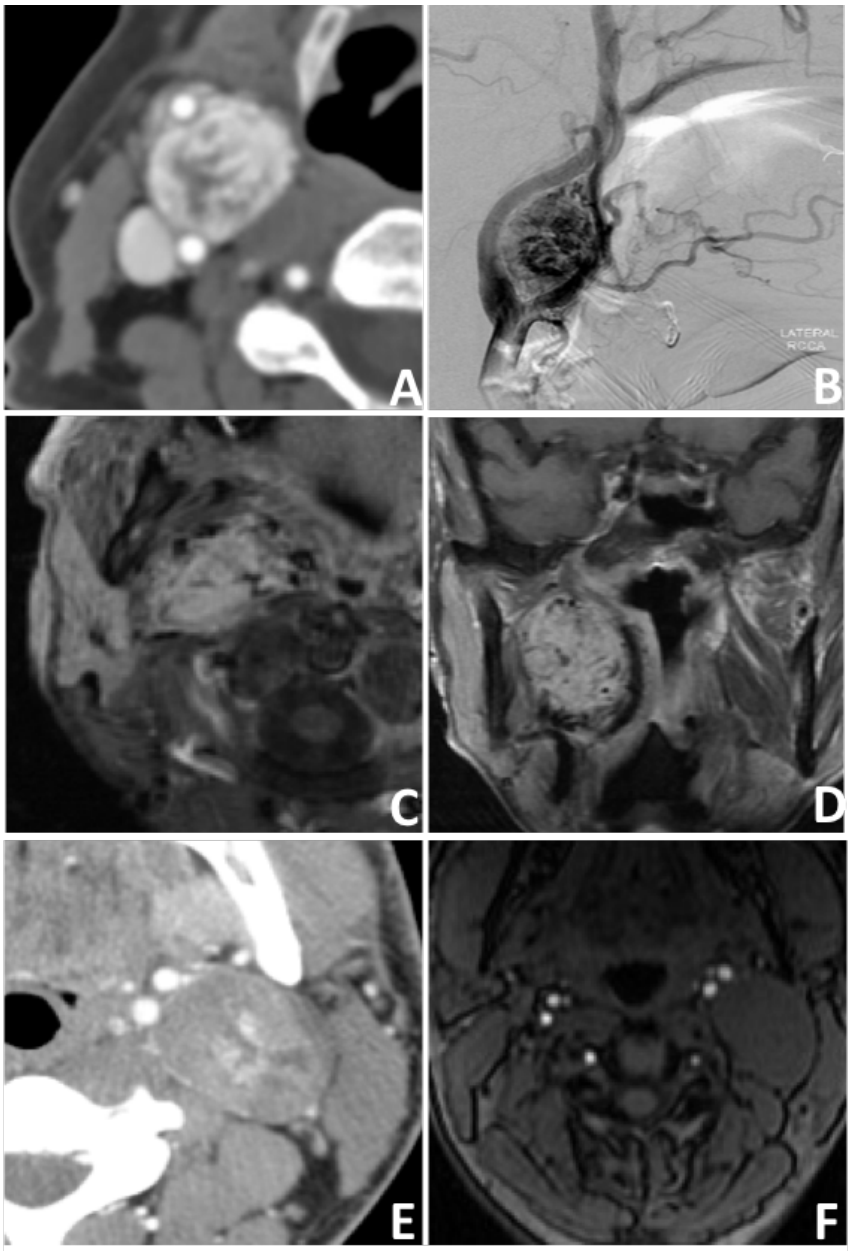

Figure. Three carotid space masses. A-B, Carotid body tumor. C-D, Vagal paraganglioma. E-F, vagal schwannoma.

Cementoblastoma of Mandible

11 Cementoblastoma of Mandible

J Chaudhry, SJ Chaudhry

Mohammed Bin Rashid University of Medicine and Health Sciences
United Arab Emirates

Introduction: Cementoblastoma is an uncommon benign neoplasm of mesenchymal origin. It is characterized by formation of cementum-like tissue that forms round to ovoid mass around the root of a tooth.1 It is more often associated with mandibular premolar and molar teeth although a quarter of the reported lesions were in maxilla. Males are affected more than females with no racial predilection. The reported age range is 12 - 65 years, however, most patients are in their 20's and 30's at the time of detection.2 Description: Our patient is a 27-year-old male who was referred to an oral maxillofacial surgeon for evaluation of asymptomatic bony swelling on lingual surface of right posterior mandible noticed by his general dentist. Mucosa overlying the swelling was intact and of normal color. A maxillofacial cone beam computed tomography (CBCT) exam was acquired and evaluated. An ovoid, well-defined, mixed-density, expansile lesion with low-density margin, 2 x 1.7 x 1.7 cm in greatest dimensions, was attached to the mesial root of tooth #30 with loss of periodontal ligament (PDL) space and lamina dura. The lesion extended anteriorly to involve the periapical area of tooth #29 with effacement of the distal root surface, and posteriorly to the distal root of tooth #30 with loss of PDL space and lamina dura. It resorbed the adjacent buccal and lingual cortical plates and extended 5 mm into the lingual soft tissues resulting in lingual swelling noted clinically. The lesion resorbed the medial wall of adjacent right inferior alveolar canal with extension into canal lumen; there was no displacement of the canal. Diagnosis: Differential diagnosis included periapical osseous dysplasia, however, the resorption & perforation of the cortical plates with extension of the lesion into lingual soft tissues, ovoid shape, and prominent soft tissue capsule manifesting as well-defined, low-attenuation margin favored the diagnosis of Cementoblastoma. 1. Benign Tumors. White, Stuart C., Michael Pharoah. Oral Radiology: Principles and Interpretation, 7th Edition. Mosby. 2. Benign cementoblastoma of the anterior mandible: an unusual case report. J Korean Assoc Oral Maxillofac Surg. 2016 Aug; 42(4): 231-235.

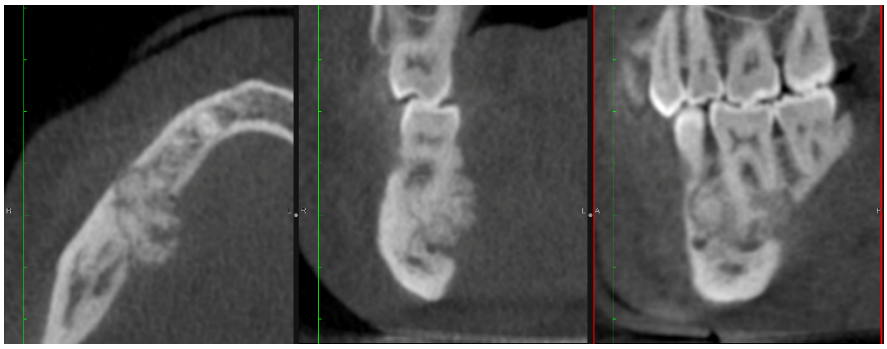

Widely Invasive Follicular Thyroid Carcinoma with Jugular Vein Extension

12 Widely Invasive Follicular Thyroid Carcinoma with Jugular Vein Extension

AR King, D Sylvestre, A Schilling

Memorial Health University Medical Center
United States

A 67-year-old female with history of insulin-dependent diabetes mellitus, hypertension, and hyperlipidemia presents with dizziness and abnormal gate. CT and MRI of the brain demonstrated no evidence of acute ischemia. Carotid ultrasound revealed thrombus with internal Doppler flow within the right jugular vein with demonstrable direct extension from the thyroid gland. CT neck with contrast confirmed the findings of an invasive thyroid based neoplasm with intraluminal jugular vein extension. Ultrasound guided fine needle aspiration of the mass revealed a BSRTC IV invasive follicular-type thyroid cancer. Surgical excision of the mass was subsequently performed, followed by radiation and I-131 treatment. Highlighted are the incidence, presentations, and diagnostic approaches to follicular thyroid carcinoma.

Know Your Boundaries: A Survival Guide to Key Anatomical Landmarks in the Head and Neck

13 Know Your Boundaries: A Survival Guide to Key Anatomical Landmarks in the Head and Neck

MJ Lee, R Lobo, SB Chinn, A Srinivasan

University of Michigan
United States

Purpose: The purpose of this educational exhibit is to discuss important anatomical landmarks in the head and neck that define boundaries for differentiating spaces, serve as pathways for spread of malignancy, and feature in accurate staging of head and neck cancer. Description: Imaging findings in head and neck cancer vary widely, and it is often difficult to accurately assess the extent of disease without knowledge of key anatomical landmarks. These anatomical landmarks with clinical and surgical relevance that will be discussed include but are not limited to: - Buccopharyngeal fascia - Mylohyoid muscle - Lingual artery/Hypoglossal nerve bundle - Extrinsic tongue muscles - Laryngeal ventricle - Thyroid cartilage - Pterygopalatine fossa - Retropharyngeal space For example, mylohyoid muscle is an important anatomical landmark in the floor of the mouth that serves as a boundary separating sublingual from submandibular space. Lesions in the sublingual space require a more limited approach compared to lesions that span both the spaces, making it important to identify this involvement on imaging. In addition, the mylohyoid muscle is often directly involved during spread of submucosal malignancy, with the extent of involvement best seen on the coronal image. Similarly, identifying whether the lingual artery is involved in tongue cancer serves as a key point for deciding limited versus more extensive glossectomy. Summary: After reviewing this exhibit, the reader will gain familiarity with important head and neck landmarks that will aid in defining boundaries for different spaces, assessing pathways for malignancy spread, and determining staging of head and neck cancer.

Eye See It: Reviewing acquired pathologies of the ocular globe in adults.

14 Eye See It: Reviewing acquired pathologies of the ocular globe in adults.

R Jordan, E Supsupin, E Friedman

UT Houston McGovern Medical School
United States

Purpose: Orbital pathology is often overlooked on brain imaging performed for neurological abnormalities or following head trauma. This exhibit will review the anatomy of the ocular globe and demonstrate a spectrum of pathologies and surgical/ treatment changes of the globe. Description: Loss or decreased vision can be detrimental to a patient's quality of life, which is why it is crucial to understand and identify pathology of the orbit. If not included in a radiologist's search pattern, orbital pathology can be easily overlooked, especially when it is not suspected clinically. In this review we will discuss the normal anatomy of the globe as well as demonstrate a wide-range of acquired ocular pathologies in adults, including ocular hemorrhage, endophthalmitis, glaucoma, various calcifications of the globe, retinal and choroidal detachment, and melanoma, among others. We will also review a variety of postsurgical and treatment-related changes. Summary: The globe is a small but important structure that can easily be overlooked on imaging, but should always be assessed on every cranial radiologic examination. By understanding normal anatomy and pathologies associated with the globe, radiologists may make incidental findings or catch early disease which may benefit the patient's quality of life and at times, survival.

Figure 1: Right subchoroidal hemorrhage and lens extrusion in elderly patient who fell.

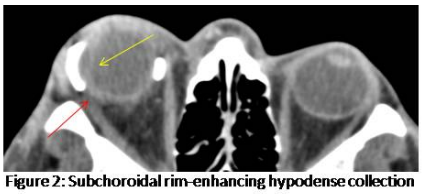

Figure 2: Subchoroidal rim-enhancing hypodense collection (yellow arrow) with thickening and enhancement of the sclera (red arrow), compatible with endophthalmitis.

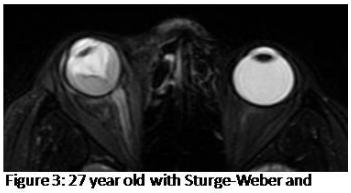

Figure 3: 27 year old with Sturge-Weber and chronic right eye blindness as a result of chronic retinal detachment.

Figure 4: Foreign body in the right anterior chamber with lens extrusion and overlying soft tissue swelling

Pediatric Head and Neck Infections: Spectrum of Radiologic Findings and Complications

15 Pediatric Head and Neck Infections: Spectrum of Radiologic Findings and Complications

KS Traylor, SF Kralik

Indiana University School of Medicine
United States

Purpose: Pediatric head and neck infections involve a number of anatomic locations similar to adults, however, in children there is a greater frequency of spread of infections from these anatomic sites resulting in more complicated disease. The purpose of this educational exhibit is to demonstrate the spectrum of radiologic findings in pediatric neck infections in order to highlight important potential complications that the radiologist must be able to detect. Approach/Methods: A radiology database search will be performed to identify pediatric patients (age < 18) with imaging of infections involving the head and neck. X-rays, CT, MRI, and ultrasound findings will be used to demonstrate the anatomic sites of infection and complications of infection. Findings/Discussion: Radiologic findings of pediatric head and neck infections and spectrum complications of infection will be demonstrated for the following anatomic locations: 1. Paranasal sinuses - acute sinusitis complicated by subgaleal abscess, subperiosteal abscess, and epidural empyema; Invasive fungal sinusitis 2. Orbits - orbital cellulitis complicated by cavernous sinus thrombosis 3. Temporal bones - acute otomastoiditis complicated by sinus thrombosis, epidural abscess and bezold abscess; labyrinthitis secondary to meningitis. 4. Aerodigestive tract - pharyngotonsillitis complicated by tonsillar/peritonsillar abscess; septic thrombophlebitis (Lemierre Syndrome); epiglottis; croup; retropharyngeal abscess 5. Parotid glands - acute parotitis complicated by abscess 6. Lymph nodes - lymphadenitis; suppurative lymph nodes; granulomatous disease 7. Congenital - infected thyroglossal duct cyst; thymic cyst; branchial cleft cyst Summary/Conclusion: It is detrimental for radiologists to have a thorough understanding of the various anatomic sites of head and neck infections and the potential for complications of infection in the pediatric population.

Calvarium and Skull Base Musculoskeletal Findings: What Every Neuroradiologist Should Know

16 Calvarium and Skull Base Musculoskeletal Findings: What Every Neuroradiologist Should Know

JA Rotman, H Baradaran, A Schweitzer

NYP-Weill Cornell medicine
United States

Purpose: The purpose of this exhibit is to educate neuroradiologists about musculoskeletal conditions and tumors that can affect the skull. Description: For educational purposes, computed tomography (CT) and magnetic resonance imaging (MRI) studies acquired at our institution demonstrating musculoskeletal conditions (such as Paget's disease) and/or tumors (such as osteosarcomas) affecting the skull were collected. Certain images were selected to delineate each entity's distinguishing features. Summary: The following entities will be presented: 1. Eosinophilic granuloma: CT shows a characteristic soft tissue mass with osseous destruction and MRI demonstrates a T2 isointense to hyperintense homogeneously enhancing mass (see figure 1 attached). 2. Giant cell tumor: CT shows an expansile lytic lesion with an associated soft tissue mass and MRI demonstrates a fibrous T2 hypointense mass with enhancing solid components, differentiating it from an aneurysmal bone cyst (see figure 2 attached). 3. Chondromyxoid fibroma: CT shows a lobulated calcified mass and MRI demonstrates a T2 hyperintense mass with peripheral nodular enhancement (see figure 3 attached). 4. Osteoma: CT shows a dense bony protuberance and MRI demonstrates a bony lesion similar in intensity to underlying cortex without evidence of invasion into adjacent structures. 5. Fibrous dysplasia: CT shows the diffuse expansile ground-glass appearance of the calvarium and MRI demonstrates the typical patchy enhancement and expanded T1 hypointense appearance of the skull (see figure 4 attached). 6. Chondrosarcoma: CT shows a lytic lesion with ring and arc calcifications characteristic of a cartilaginous lesion and MRI demonstrates curvilinear areas of T1 hypointensity within the enhancing mass suggestive of a chondroid lesion. 7. Chordoma: CT shows a lytic lesion in the clivus with cortical destruction and MRI demonstrates a heterogeneously enhancing mass. 8. Osteosarcoma: CT shows a mass with associated osseous destruction and invasion of adjacent structures and MRI demonstrates high signal in the soft tissue component and low signal in the mineralized components. 9. Hemangioma: CT shows a focal area of lucency in the bone without an associated soft tissue component and MRI demonstrates an enhancing T2 hyperintense lesion, unchanged over multiple years. 10. Ossifying fibroma: CT shows a round ground-glass lesion confined to the bone and MRI demonstrates a heterogeneously enhancing T1 hypointense and T2 isointense lesion. 11. Osteochondroma: CT shows a pedunculated mass with medullary continuity with underlying bone and MRI shows an enhancing cartilage cap overlying the bony stalk. 12. Paget's disease: CT shows the patchy cotton wool appearance of the skull and diploic widening with involvement of both the inner and outer calvarial tables and MRI demonstrates a speckled appearance of the fatty bone marrow. 13. Renal osteodystrophy: CT shows skull thickening with loss of distinction between the inner and outer tables as well as a "salt and pepper" appearance. Conclusion: It is imperative for neuroradiologists to recognize and accurately diagnose musculoskeletal conditions and tumors that can affect the skull. Early and proper recognition of such findings can alter management, whether it is a "do not touch" lesion, a lesion-requiring follow-up, or a lesion necessitating surgical management.

Figure 1

Eosinophilic Granuloma

(a) Axial CT of the brain of a 7-year-old female demonstrates an expansile soft tissue mass centered along the left greater sphenoid wing with associated osseous destruction of the lateral and superior orbital walls and extension into the lateral extraconal space causing proptosis. (b) Axial T2-weighted MRI shows the mass to be T2 isointense to hyperintense. (c) Coronal contrast-enhanced T1-weighted image shows that the mass enhances homogeneously. The medially displaced lateral rectus muscle abuts the left optic nerve. There is involvement of the temporalis muscle.

Figure 2

Giant Cell Tumor

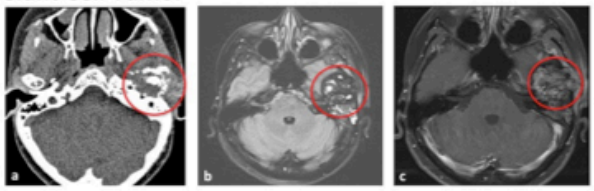

(a) Axial CT of the brain of a 56-year-old female demonstrates a large expansile lytic lesion centered in the left glenoid fossa with involvement of the squamosal portion of the left temporal bone and erosion of the anterior wall of the middle ear cavity. There is an associated soft tissue mass. (b) Axial fat-saturated T2 FLAIR MRI shows areas of low signal intensity, likely reflecting hemosiderin and/or fibrosis. The mass invades the left middle fossa skull base and temporomandibular joint. There is a left mastoid effusion, likely secondary to obstructed secretions. (c) Axial contrast-enhanced fat-saturated T1-weighted MRI demonstrates enhancement of its solid components, helping differentiate it from an aneurysmal bone cyst.

Figure 3

Chondromyxoid Fibroma

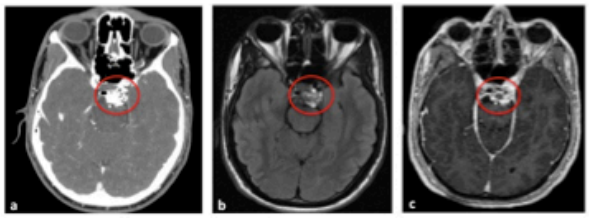

(a) Axial contrast-enhanced CT of the brain of a 26-year-old male demonstrates a lobulated calcified mass involving the left aspect of the clivus invading the left cavernous sinus causing mass effect on the midbrain. (b) Axial T2 FLAIR MRI demonstrates a lobulated T2 hyperintense mass centered in the clivus invading the cavernous sinus causing mass effect on the left internal carotid artery. (c) Contrast-enhanced T1-weighted image shows that the mass demonstrates peripheral nodular enhancement.

Figure 4

Fibrous Dysplasia

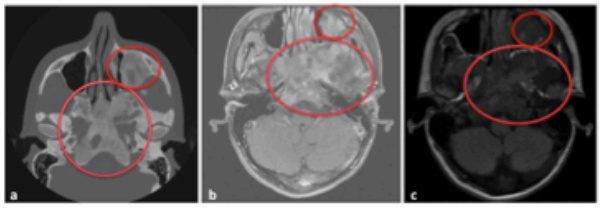

(a) Axial maxillofacial CT of a 24-year-old female demonstrates a diffuse expansile ground-glass appearance of the calvarium with well-defined borders involving the frontal, parietal, temporal, and sphenoid bones as well as the skull base. (b) Axial contrast-enhanced fat-saturated T1- weighted and (c) unenhanced T1-weighted MRI of the brain demonstrates involvement of the clivus, left pterygoid, left sphenoid and left maxilla by fibrous dysplasia. The bone is expanded and T1 hypointense with patchy enhancement.

Non-contiguous Dural-based Esthesioneuroblastoma Recurrence in Absence of Local Recurrence, Mimicking Intracranial Meningioma

17 Non-contiguous Dural-based Esthesioneuroblastoma Recurrence in Absence of Local Recurrence, Mimicking Intracranial Meningioma

J Fujimoto, J Chang, A Ozturk, N Pham, O Raslan

UC Davis Medical Center
United States

Purpose: To describe the different MRI presentations of a rare case of non-contiguous dural-based Esthesioneuroblastoma (ENB) recurrence in absence of local recurrence, highlighting the importance of careful scrutiny of the leptomeninges on the surveillance MRI exams, screening of the spine in positive cases and the prognostic implications of such finding. Description: A 64-year-old male with a history of ENB presented with intermittent epistaxis. Eight years earlier the tumor had been treated with gross total craniofacial resection with negative margins followed by adjuvant radiation therapy. During the initial post-operative period, he was followed with serial MRI but had been lost to follow-up for three years prior to presentation. Upon presentation, MRI showed no local recurrence; however there was multiple enhancing convexity and falcine plaque-like dural thickening, dural nodularity and dural based masses, several of them demonstrating cystic changes. The solid components of the lesions showed increased relative cerebral blood volume (rCBV) on the MR perfusion images. The largest lesion was located in the left parietal convexity and resulted in mass effect on the underlying brain parenchyma and lateral ventricles. Although rare, diffuse dural based recurrent disease was favored as the etiology of the lesions over radiation induced atypical meningiomas, as most of the lesions lie outside of the radiation field. MRI of the spine excluded dropped leptomeningeal metastases. The diagnosis was confirmed pathologically after surgical resection of the largest lesion in the left parietal convexity. Summary: Esthesioneuroblastoma (also known as olfactory neuroblastoma) is a rare locally aggressive neoplasm arising from the olfactory epithelium comprising about 2% of all sinonasal tract tumors. Distant metastasis is rare, and is most commonly limited to regional lymph nodes. Leptomeningeal metastasis is extremely rare, with fewer than 20 reported cases. Risk factors for dural recurrence include patients with preoperative intracranial extension, tumor involving the surgical margins, and subtotal resection. Surgical seeding or hematogenous spread were described as mechanisms of the dural failure. Routine scrutiny of the leptomeninges on surveillance MRI is advised as the leptomeningeal disease usually occurs several years after a disease free interval, and in absence of local recurrence. Our case shows all 3 presentations of the disease including enhancing plaque-like dural thickening, dural nodularity and dural based masses with cystic changes. To our knowledge this is the first study documenting the increased rCBV in such lesions. Imaging of the entire spine must be performed next in order to rule out dropped metastases. Unlike other cancers, leptomeningeal metastasis from ENB indicates an extremely poor prognosis, has fewer treatment options and limits the efficacy of repeated radiotherapy due to prior radiotherapy for primary lesion.

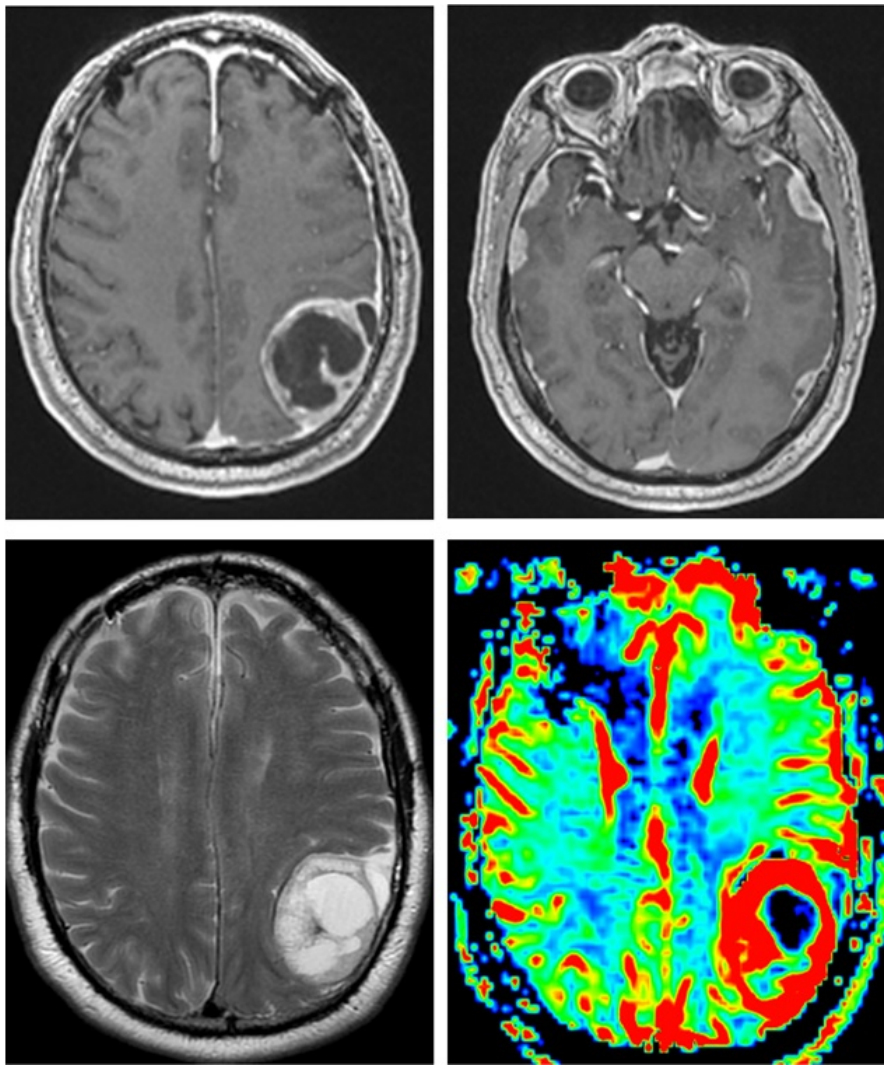

A rare cause of intraorbital masses

18 A rare cause of intraorbital masses

KD Seifert, A Malhotra, X Wu, L Tu

Yale New Haven Hospital
United States

Purpose: The purpose of this exhibit is to review a rare cause of bilateral intraorbital masses. Description: A 60 year old female with history of Lyme's disease and diagnosis of pituitary hypophysitis with resultant diabetes insipidus presented for MRI brain and was found to have bilateral intraorbital masses, which displayed avid enhancement on post contrast imaging. Masses encased the optic nerves with no evidence of infiltration of the nerves, vascular structures, or extraocular muscles. Ultimately, a biopsy was performed and the patient was given a diagnosis of Erdheim-Chester disease. This case will review the full clinical presentation of the patient, review imaging studies, and review laboratory and pathology results that ultimately led to the diagnosis. Subsequently, we will review other manifestations of ECD, as well as current treatment options and prognosis. Summary: This exhibit will review a rare cause to consider when a patient presents with bilateral intraorbital masses.

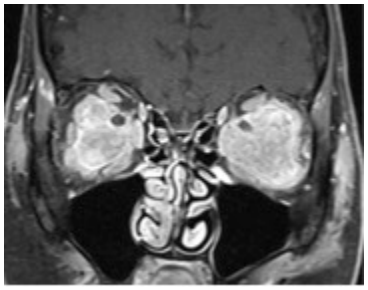

Underlying bone change in patients with oral squamous cell carcinoma

19 Underlying bone change in patients with oral squamous cell carcinoma

K Huh, G Jo, J Kim, M Heo, S Lee, S Choi

Department of Oral and Maxillofacial Radiology, School of Dentistry, Seoul National University Republic of Korea

Purpose When oral squamous cell carcinoma (OSCC) invades the jaw bone, abnormal attenuation on CT or pathologic signal intensity (SI) on MR image is frequently observed in underlying bone marrow, which makes it difficult to determine the extent of tumor invasion. The purposes of this study were to assess the prevalence of underlying bone change on preoperative CT and MR image, and to investigate the relationship between the underlying bone change and tumor aggressiveness. Materials & Methods CT and MR images and electronic medical records of consecutive 213 patients with OSCC in mandibular gingiva, who underwent partial mandibulectomy, were retrospectively reviewed. The presence of bone invasion was histopathologically proven. Patients with recurrent OSCC and those who undertook preoperative radiotherapy or chemotherapy were excluded. Total of 137 subjects were enrolled in the present study. All images were evaluated by consensus of two experienced oral and maxillofacial radiologists using the picture archiving and communication system (Infinitt PACS, Infinitt Healthcare, Seoul, Korea).The presence, degree, and extent of underlying bone change were assessed on preoperative CT and MR images, and correlated with other data including radiographic pattern of bone infiltration margin (erosion limited to cortical bone, marrow invasion with smooth, irregular, or infiltrative margin), degree of differentiation on histopathological examination, TNM staging, and recurrence. The relationships were evaluated using Pearson's Chi-square test. Results The overall prevalence of underlying bone sclerosis was 69.6% on CT images and the prevalence of pathologic SI in underlying bone marrow was 90.9% on MR images. The degree and extent of underlying bone change increased with invasive bone infiltration pattern and depth of invasion. However, no other clinical or histopathological data showed significant relationship with underlying bone change on CT and MR images. Conclusions Underlying bone sclerosis, which was frequently observed in patients with bone invasion by OSCC, may reflect tumor invasiveness or protective reaction of our body.

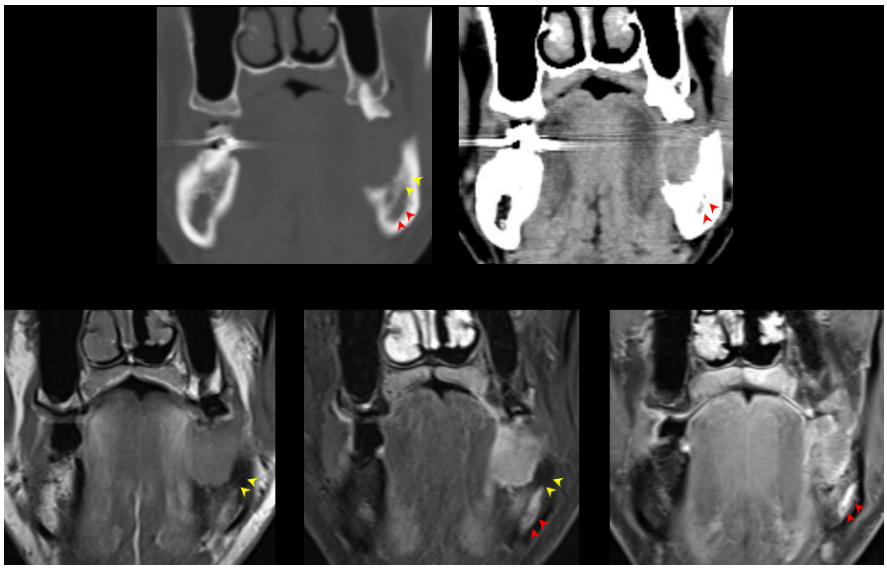

Imaging Pediatric Facial Bone Tumors - Do They All Look Alike?

20 Imaging Pediatric Facial Bone Tumors - Do They All Look Alike?

M Magarik, S Pruthi, U Barad

Vanderbilt University Medical Center
United States

Title: Imaging Pediatric Facial Bone Tumors - Do They All Look Alike? Authors: Meaghan Magarik MD, PHD, Sumit Pruthi MD, Udaykamal Barad, MBBS PURPOSE: 1. Review the appropriate imaging modalities to evaluate suspected facial bone tumors 2. Compare and contrast the key imaging findings and characteristics of selected odontogenic and non-odontogenic tumors 3. Briefly discuss facial bone tumor mimics DESCRIPTION: Facial bone tumors, although rare, can result in significant functional impairment, facial deformation and disfigurement. Most pediatric facial bone tumors are benign and non-odontogenic in origin, with the majority occurring in the mandible. Patients are most often asymptomatic although some may present with facial bone swelling or asymmetry, pain or paresthesias. Appropriate identification and characterization is critical to guide prognosis and further management. OUTLINE: 1. Review the appropriate imaging modalities used in the workup of facial bone tumors. a. Ultrasound b. CT c. MRI d. Nuclear Medicine: PET-CT, MIBG 2. Illustrate the imaging findings of pediatric odontogenic tumors. a. Ameloblastoma b. Odontogenic Keratocyst c. Odontogenic cyst d. Odontoma e. Torus 3. Illustrate the imaging findings of pediatric non-odontogenic facial bone tumors. a. Benign i. Osteoma ii. Langerhans cell histiocytosis iii. Fibrous dysplasia iv. Aneurysmal bone cyst v. Juvenile ossifying fibroma vi. Giant cell reparative granuloma b. Malignant i. Ewing Sarcoma ii. Osteosarcoma iii. Lymphoma/Chloroma c. Metastatic Facial Bone Tumors i. Neuroblastoma 4. Illustrate the imaging findings of facial bone tumor mimics. a. Periapical Abscess b. Osteomyelitis

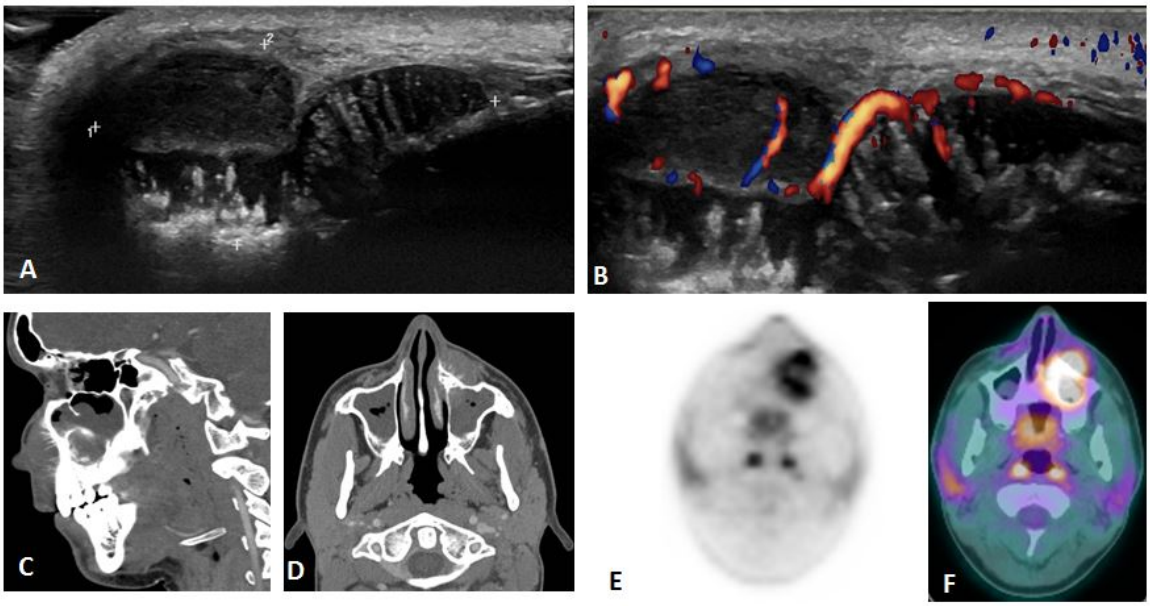

Figure 1. A 15 year old boy presented for imaging having failed outpatient antibiotic treatment of a sinus infection and complaining of a left maxillary mass. Targeted gray-scale and Color Doppler sonogram demonstrates a mixed cystic and solid, heterogenous, hypervascular mass anterior to the left maxilla, concerning for neoplasm (A and B). Further characterization with contrast-enhanced CT of the face demonstrates an enhancing mass centered in the left frontal process of the maxilla and extending into the left maxillary sinus. There is associated permeative bony erosion and "sunburst" periostitis (C, sagittal) and (D, axial). A PET-CT demonstrates intense FDG uptake within the soft tissue mass and left maxilla (E, axial non-attenuation corrected and F, fused axial). Tissue sampling of the soft tissue component of the mass revealed lymphoma.

Implementing Online TI-RADS Calculator

21 Implementing Online TI-RADS Calculator

J Wang, T Ellchuk, R Otani, G Groot, P Babyn

University of Saskatchewan
Canada

Thyroid nodules are common and fine needle aspiration (FNA) or surgery are used to assess for malignancy. Thyroid Imaging, Reporting and Data System (TI-RADS) uses ultrasound for non-invasive risk stratification of thyroid nodules and reduce unnecessary biopsies. The use of TI-RADS has been quite limited despite its value. This project used an online calculator and education to facilitate the application of TI-RADS in clinical practice. Retrospective review defined the baseline reporting of thyroid nodule ultrasound features. Web-based resource and presentation were used to integrate TI-RADS in reporting thyroid ultrasounds and measure the improvements in comprehensive reporting of thyroid nodules and guiding management. The percentage of thyroid ultrasound reporting using TI-RADS within six months increased from 0% to 27% during the project period. Reports with TI-RADS provided twice as many recommendations compared to reports without TI-RADS. The online TI-RADS calculator is utilized internationally with over 2000 visitors per month. Online TI-RADS calculator and education has successfully facilitated the integration of TI-RADS in thyroid ultrasound reporting to provide more accurate and comprehensive reports and guide management.

Stuck in the Middle: Nervus Intermedius Related Neuropathologic Imaging Spectrum

22 Stuck in the Middle: Nervus Intermedius Related Neuropathologic Imaging Spectrum

JM Yetto, S Elakkad, M Landon, A Germana, M Cathey

Naval Medical Center San Diego
United States

Purpose: The nervus intermedius (NI), so-named due to the intermediate course it takes between the facial and vestibular nerves within the cerebellopontine angle (CPA), ultimately gives rise to the greater superficial petrosal nerve, chorda tympani, and the lesser known posterior auricular nerve. Primary pathologies of the NI can present as nervus intermedius neuralgia (NIN). Alternatively, pathology in the distribution of any nerves derived from NI can present with symptoms referred to the NI. Advances in imaging technology have improved our ability to see this nerve and its branches, which may allow for greater diagnostic accuracy when pathology referable to the NI is suspected. The purpose of this exhibit is to review the anatomy and function for the NI using case based approach, highlighting the NI neuro-pathologic spectrum of disease. Approach/Methods: We will illustrate normal anatomy of the NI and its branches, emphasizing the use of high resolution state of the art CT of the temporal bones and 3T MRI. Further, we will show specific imaging examples of a variety of pathologies that involve the NI and its branches. Finally, we will provide an updated review of the literature on this topic. Findings / Discussion: The NI innervates the lacrimal, submandibular, sublingual glands, provides sensory input from portions of the external auditory canal, paranasal sinuses and nasal mucosa as well as conveys taste input from the anterior two-thirds of the tongue, floor of the mouth, and the palate. Pathologies either directly involving NI, such as CPA mass or vascular compression, or its branches, such as sinonasal tumor, perineural tumor spread, contact point headache, may be referable to the NI. Overlapping innervation with branches of the trigeminal, glossopharyngeal and vagus nerves can confound diagnosis and / or lead to mis-localization, resulting in delayed diagnosis or inappropriate therapy. Summary / Conclusion: Understanding the anatomy of the NI, its branches and pathologic spectrum allows radiologists to take a nuanced approach to these complex cases, improving diagnostic accuracy and providing value added to our referring providers and patients.

Chorda Tympani

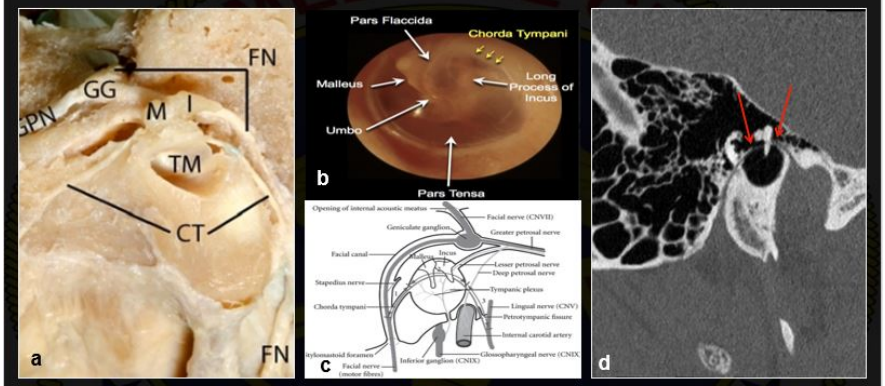

Figure 9. a. Gross specimen shows the chorda tympani (CT) as it courses across the tympanic membrane (TM) between the handle of the malleus (M) and the long process of incus (I). b. Chorda tympani (arrows) can be visualized on otoscopic examination. c. Schematic of the chorda tympani. d. High resolution temporal bone CT curved planar reformat demonstrates the course of the chorda tympani (→) as it arises from the mastoid segment of CN VII and courses between the handle of the malleus and long process of the incus.

Carcinoma of Unknown Primary - Understanding the AJCC8 guidelines and how to identify the primary lesion.

23 Carcinoma of Unknown Primary - Understanding the AJCC8 guidelines and how to identify the primary lesion.

J Junn, C Heaton, C Glastonbury

Emory University Hospital
United States

Objectives: 1. Understand the definition/implication of cancer of unknown primary (CUP) 2. Overview of imaging modalities for evaluating CUP 3. Illustration of lymph node drainage 4. Discussion of the new AJCC 8th edition guideline for CUP staging system Carcinoma of unknown primary (CUP) is defined as carcinoma in cervical lymph node with clinically occult primary site after clinical examination. Approximately 1-3% of head and neck cancer patients presents with CUP with more than 90% eventually being determined to be squamous cell carcinoma (SCC) of oropharyngeal origin1,2 (Keller et. al, Motz et. al). In order to facilitate targeted treatment to reduce morbidity associated with wide-field radiation, identification of the primary tumor site is important. Thus, initial diagnostic imaging plays a key role in the management of CUP. Contrast enhanced CT (CECT), MR, and FDG-PET may each be used, or in combination, to find the primary site or to identify the most likely primary site to help targeted biopsy at endoscopy. Hence, radiologists have an instrumental role in management of CUP patients. AJCC8 presents specific guidelines for clinical work-up of SCC CUP tumors. P16 should be initially performed. If this is positive, then an oropharyngeal SCC (OPSCC) is likely; however, if imaging is not fruitful for a primary OPSCC, then HPV testing should also be performed. Other SCC including skin SCC may also be p16 positive but will be HPV negative. If p16 is negative, then EBV should be performed. If it is EBV positive, it suggests a nasopharyngeal origin of the primary tumor. When p16/HPV and ENV are negative, then a T designation cannot be assigned to the tumor unless a skin primary site is strongly suspected or known. While CUP most frequently present as level II nodes, they may also present as level IV/ supraclavicular nodal masses. This is a common site of thyroid carcinoma and lymphoma; however, if FNA determines the nodal mass to be SCC, the primary site is more likely to be below the clavicle in the chest, abdomen or pelvis. In this situation, FDG-PET is a more useful initial imaging examination. This exhibit will demonstrate the preferred pathway for evaluation of CUP tumors and illustrate the role of different imaging modalities multiple clinical examples. 1. Keller LM, Galloway TJ, Holdbrook T, Ruth K, Yang D, Dubyk C, Flieder D, Lango MN, Mehra R, Burtness B, Ridge JA. p16 status, pathologic and clinical characteristics, biomolecular signature, and long-term outcomes in head and neck squamous cell carcinomas of unknown primary. Head Neck. 2014 Dec;36(12):1677-84. doi: 10.1002/hed.23514. Epub 2014 Jan 13. PubMed PMID: 24115269; PubMed Central PMCID: PMC3972378. 2. Motz K, Qualliotine JR, Rettig E, Richmon JD, Eisele DW, Fakhry C. Changes in Unknown Primary Squamous Cell Carcinoma of the Head and Neck at Initial Presentation in the Era of Human Papillomavirus. JAMA Otolaryngol Head Neck Surg. 2016 Mar;142(3):223-8. doi: 10.1001/jamaoto.2015.3228. PubMed PMID: 26769661.

The Ptotic Tongue - A Segmental Approach to Detecting Common Pathology along the Hypoglossal Nerve

24 The Ptotic Tongue - A Segmental Approach to Detecting Common Pathology along the Hypoglossal Nerve

R Tade, X Wu

Emory University
United States

Purpose: Describe and discuss the CT and MRI findings of tongue ptosis and common pathological causes of hypoglossal nerve dysfunction, outlining a segmental, anatomically based approach to assessing for the cause of tongue ptosis and atrophy. Description: This educational exhibit will begin by briefly reviewing the CT and MRI findings of tongue ptosis and atrophy, which should alert radiologists to potential pathology along the complex anatomic course of the hypoglossal nerve (Cranial nerve XII). While relatively specific for hypoglossal nerve pathology, the findings of unilateral tongue atrophy and ptosis do not accurately localize the site or cause of nerve dysfunction. Therefore, one must understand the anatomic extent of the entirety of the nerve's course in order to identify possible pathology. The exhibit will therefore review hypoglossal nerve anatomy and key surrounding structures in a segmental fashion, starting from the hypoglossal nucleus in the dorsal medulla, to the cisternal segment, skull base segment, extracranial carotid space/anterior segment, and sublingual segment with its terminal motor branches. Knowledge of the common segments and understanding normal anatomical relationships allows for accurate localization of common pathology. The exhibit will then review CT and MRI imaging protocols that adequately evaluate the course of the hypoglossal nerve in its entirety as well as key surrounding structures, providing image-rich examples of diverse pathology which may affect the nerve at each anatomic location. The exhibit will then summarize differential considerations for pathology based on location and specific imaging findings. Summary/Conclusion: When faced with imaging findings of unilateral tongue ptosis, detailed knowledge of hypoglossal nerve anatomy and its surrounding structures is necessary in identifying and diagnosing potential pathology. This exhibit will help radiologists review the complex nerve anatomy in a segmental approach and provide imaging examples of diverse pathology that may contribute to tongue ptosis.

Patient #1 – Glomus Jugulare

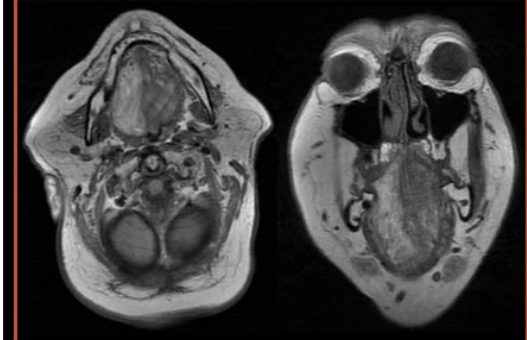

Axial and coronal T1w images through the level of the mandible demonstrating marked fatty atrophy of the intrinsic muscles of the right tongue secondary to denervation related to tumor involvement at the hypoglossal canal.

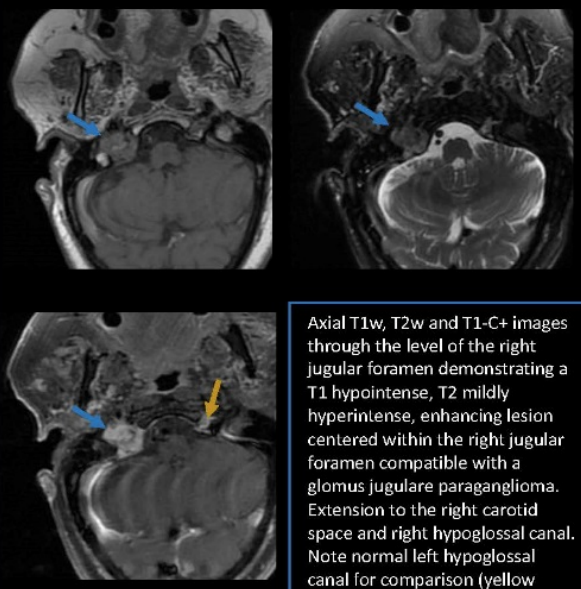

Axial T1w, T2w and T1-C+ images through the level of the right jugular foramen demonstrating a T1 hypointense, T2 mildly hyperintense, enhancing lesion centered within the right jugular foramen compatible with a glomus jugulare paraganglioma. Extension to the right carotid space and right hypoglossal canal. Note normal left hypoglossal canal for comparison (yellow arrow).

A rare pediatric case of mandibular chronic non-bacterial osteomyelitis

25 A rare pediatric case of mandibular chronic non-bacterial osteomyelitis

BD Owen, N Pham, J Chang, O Raslan, M Bobinski, A Ozturk

University of California Davis
United States

Purpose We present a rare pediatric case of mandibular chronic non-bacterial osteomyelitis (CNO) with imaging and clinical findings. Description A 10 year old male with no significant past medical history was referred to infectious disease clinic with a 10 month history of jaw pain and swelling for which he had seen by multiple dentists, had multiple teeth removals, and received multiple different antibiotic treatments. On physical examination, his left mandible was tender to palpation with a firm palpable lesion just anterior to the mandibular angle. There was mild erythema, but no evidence of abscess formation. There were no dental caries or gingival lesion. His blood tests demonstrated a mildly elevated erythrocyte sedimentation rate, a normal white blood cell count, and normal C - reactive protein. Computed Tomography (CT) of the face with contrast demonstrated left mandibular ramus and posterior body expansion with heterogeneous sclerosis and smooth periosteal reaction. There was no associated abscess formation or enhancing soft tissue component. Clinical history of good oral hygiene and waxing and waning clinical symptoms despite proper medical treatment were suspicious for CNO. Full-body Magnetic Resonance Imaging (MRI) with coronal single shot fast spin-echo and inversion recovery was also obtained. There were no other lesions identified on total body MRI. The patient proceeded to biopsy, and the pathology result revealed focal devitalized bone, prominent fibrosis, and scattered neutrophils, consistent with recurrent and partially treated osteomyelitis. Summary CNO is a rare entity affecting children and characterized by waxing and waning periods of non-infectious pain and swelling, which has similar presentation with chronic multifocal noninfectious osteomyelitis (CRMO). CNO and CRMO are rare idiopathic entities which are on a spectrum of severity with a typical radiologic progression from early osteolysis evolving to hyperostosis and sclerosis, and associated with periosteal reaction occurring at any stage of the disease. MRI characteristics include marrow and soft tissue edema as well as fractures and synovitis. Prior studies have demonstrated the mandible to be the most frequently involved structure in the head and neck in patients with CNO, with a frequency of 21%. Clinical presentation plays a key role in the diagnosis of CNO from other etiologies which may have similar imaging findings such as infectious osteomyelitis. As the growing body of literature illustrates CNO as an autoimmune disorder, treatment has progressed from use of non-steroidal anti-inflammatories (NSAIDs) to disease-modifying anti-rheumatic drugs (DMARDs) and TNF-a inhibitors depending on disease severity. As radiologists, we should consider CNO in our differential diagnosis as an idiopathic sterile chronic inflammatory response for the patients with appropriate waxing and waning clinical presentation, and laboratory test results that requires a completely different medical management.

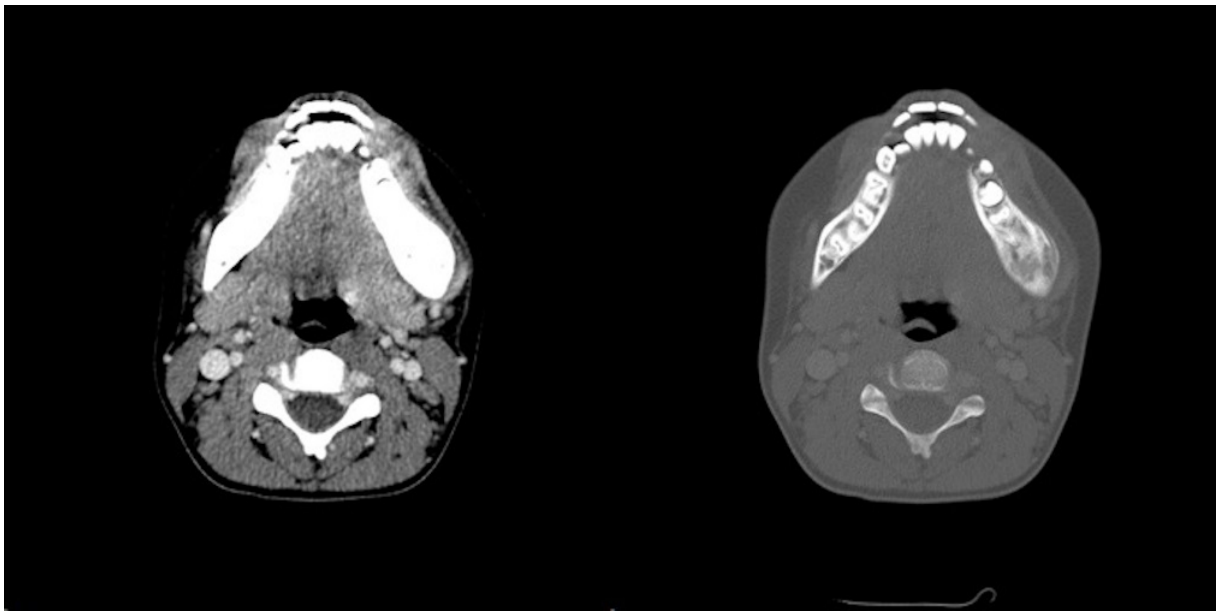

Temporal Bone Metastasis Presenting as “Bell palsy”

26 Temporal Bone Metastasis Presenting as “Bell palsy”

MA Love, A Matthews, N Emerson

Ochsner Medical Center
United States

Purpose: Provide a brief overview of the associated etiology and common clinical presentations of temporal bone metastases, use a case to highlight an uncommon presentation in the form of isolated facial nerve palsy, and ultimately encourage heightened suspicion amongst providers when caring for a patient with a history of malignancy. Description: Neoplastic metastasis to the temporal bone is thought to be uncommon, if not rare. Most lesions are hematogenously spread with breast, lung, renal, and prostate cancers providing the majority of primary cancers. Many patients have no associated symptoms while those that do often present with hearing loss or pain. Less often, patients may present with facial nerve paralysis. We present a case of a 69 y.o. woman with remote history of breast cancer, presumed cured, who’s initial presentation of left-side facial weakness was the first clinical symptom of her wide-spread metastatic breast cancer. Our patient was diagnosed with breast cancer (stage IIB - T2,N1a,M0) at an outside facility in 2005 and underwent modified radical left mastectomy with adjuvant chemotherapy, radiation therapy, and hormone therapy with the last continuing until November of 2011. She routinely underwent mammographic surveillance with her latest mammogram in January, 2017, demonstrating no abnormal findings and with the overall interpretation of Bi-RADS 1. Within this same month, the patient presented to the emergency department with symptoms of facial weakness diagnosed as Bell palsy and was conservatively managed as an outpatient only to seek additional medical care a few weeks later for dyspnea. Chest radiograph was obtained at this time and showed right lower lung consolidation with possible pleural effusion which was treated as a pneumonia, again on an outpatient basis. After a week-long course of antibiotics and no alleviation of symptoms, the patient presented to the emergency department and, via additional imaging, was found to have a large right-sided pleural effusion. The patient was admitted to the hospital and underwent successful thoracentesis with specimen sent to the laboratory for further analysis. She was discharged the next day with pathology from the thoracentesis finalizing multiple days after and resulting positive for malignant cells (metastatic mammary carcinoma). The patient was contacted by her hospitalist who explained her lab results and arranged for a hematology/oncology appointment. As a part of her oncologic workup, PET/CT and MRI of the brain were obtained on 3/14/18 and revealed diffuse metastatic spread including a left temporal bone metastasis involving her facial nerve. After discussions with her multidisciplinary team, she has restarted letrozole, begun taking palbociclib, and undergone whole brain radiation therapy. Summary: Although metastatic spread to the temporal bone is rare, and facial nerve palsy as the sole clinical sign/symptom ever rarer, providers must be aware that facial weakness may be a complication of temporal bone neoplasm and maintain a high level of suspicion in patients with a known history malignancy.

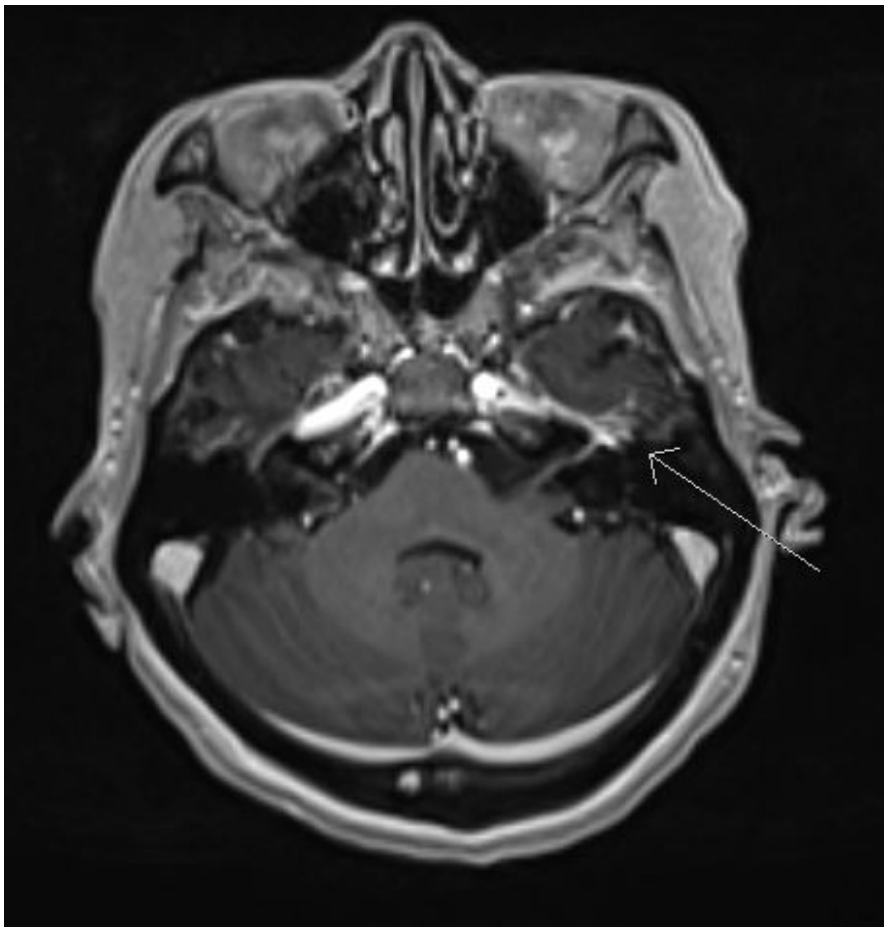

Prolapse of Orbital Fat Through the Inferior Orbital Fissure: Description, Prevalence, and Possible Pathologic Association

27 Prolapse of Orbital Fat Through the Inferior Orbital Fissure: Description, Prevalence, and Possible Pathologic Association

PM Bunch, H Kelly

Massachusetts General Hospital
United States

Background: Several patterns of orbital fat prolapse have been described (1-3). Some prolapse patterns have been associated with pathologic processes such as Graves disease, whereas others are clinically relevant because they may mimic neoplasm. We have observed prolapse of orbital fat into the temporal fossa via the inferior orbital fissure on MR imaging. The clinical relevance of this finding, if any, is unknown. Purpose: The goals of this study are: 1) to describe the MR imaging appearance of orbital fat prolapse through the inferior orbital fissure, 2) to estimate the prevalence of this finding, 3) and to assess for possible pathologic associations. Materials & Methods: In this HIPAA-compliant retrospective study, 150 consecutive orbital MR examinations meeting inclusion criteria performed at a single institution between January 2017 and April 2017 were reviewed. The presence or absence of orbital fat prolapse through the inferior orbital fissure was determined by visual examination of the axial and coronal T1-weighted images (Figure 1). When orbital fat prolapse was observed, the prolapsed fat was measured, and additional sequences were evaluated for the presence or absence of associated septae, increased fluid signal, and enhancement. Clinical data were obtained from the electronic medical record. Statistical analyses were performed using one-way analysis of variance and Fisher's exact test. Results: Prolapse of orbital fat through the inferior orbital fissure was observed in 6 patients (4%) ranging in age from 29 to 70 years. This finding was unilateral in 5 patients (83%) and bilateral in 1 patient (17%). The prolapsed fat ranged in long axis from 5 to 12 mm (mean 9 mm). Associated septae were present in 86%, faintly increased STIR signal was present in 71%, and faint enhancement was seen in 14%. There was a statistically significant association between prolapse of orbital fat through the inferior orbital fissure and Graves disease (p=0.0337). There was no statistically significant association with age (p=0.6706), sex (p=0.4059), body mass index (p=0.3803), or prior orbital surgery (p=1.0000). Conclusions: In this study, prolapse of orbital fat into the temporal fossa via the inferior orbital fissure was observed in 4% of patients and was most commonly unilateral. There was no association between prolapse of orbital fat through the inferior orbital fissure and patient age, sex, body mass index, or prior orbital surgery. The data from this small study suggest a possible association with Graves disease, however, a larger study would be needed for confirmation. References: 1. Birchall D, Goodall KL, Noble JL, et al. Graves ophthalmopathy: intracranial fat prolapse on CT images as an indicator of optic nerve compression. Radiology 1996;200:123-7. 2. Lin CC, Liao SL, Liou SW, et al. Subconjunctival Herniated Orbital Fat Mimicking Adipocytic Neoplasm. Optom Vis Sci 2015;92:1021-6. 3. Cellina M, Floridi C, Panzeri M, et al. The role of computed tomography (CT) in predicting diplopia in orbital blowout fractures (BOFs). Emerg Radiol 2018;25:13-9.

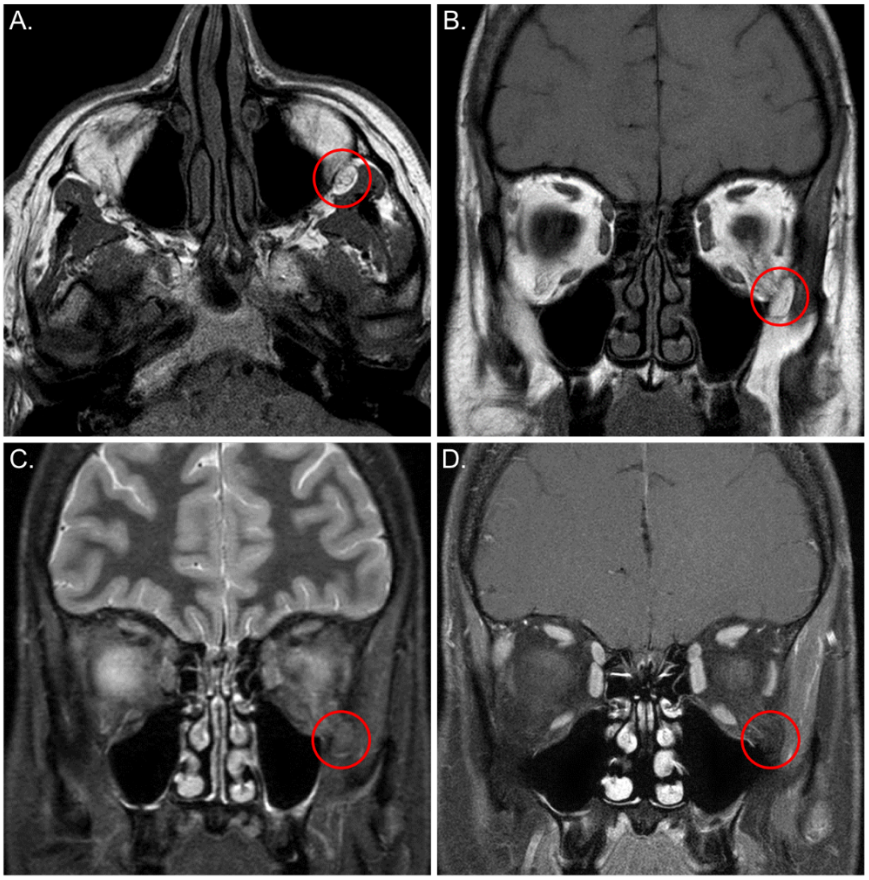

Figure 1. Axial (A) and coronal (B) T1-weighted images through the orbits demonstrate prolapse of left orbital fat (red circles in A, B) through the left inferior orbital fissure into the left temporal fossa along the deep margin of the left temporalis muscle. Associated septae are visible on the axial T1-weighted image (A). The coronal STIR (C) and coronal gadolinium-enhanced, fat-suppressed, T1-weighted image (D) demonstrate no associated increased STIR signal or enhancement within the prolapsed fat (red circles in C, D), respectively.

Assessing junior radiology resident preparedness for on call head and neck emergencies

28 Assessing junior radiology resident preparedness for on call head and neck emergencies

J Choi, E Friedman, M Patino

UT McGovern Medical School University of Texas at Houston
United States

Assessing junior radiology resident preparedness for on call head and neck emergencies Purpose: The training of 1st year radiology residents (PGY 2) at our institution includes a year long Fundamentals course. Each of the subspecialties is given a several week block to instruct the residents once a week in 3 ½ hour lectures on anatomy and imaging diagnoses commonly encountered when on call. At the end of the year long course, residents take a final exam to measure their preparedness for starting overnight call. The past 2 years of the Fundamentals course, we have instituted more subspecialized head and neck (HN) lectures, given the nature of the patient population at the county hospital and need for the residents to be more familiar with HN emergencies as well as HN oncology that may present at a county hospital. This year we began an additional one hour of temporal bone instruction. We intend to include a variety of HN questions on the final exam this year and will measure residents' responses this year as a baseline for longitudinal assessment. Description: A final exam is administered at the end of the Fundamentals course and is used as a measure to test preparedness for taking overnight call. Overnight call for the PGY 3 residents is supervised by an overnight radiology attending, however only one of the rotating overnight attendings has neuroradiology fellowship training. Therefore, many of the neuroradiology cases, including the HN cases, are viewed and preliminarily read overnight by the PGY 3 resident until the morning. At the county hospital, there is a wide spectrum of HN inflammatory, infectious and oncologic pathology. To prepare the newly minted PGY 3 residents to handle these cases, we recently introduced a total of 3 hours of HN didactic and case based lectures to the Fundamentals course. Lecture based introduction to radiology courses during the PGY 1 clinical internship year have shown to improve preparedness for radiology call. (Darras, et al.) Similarly, simulation modules have also shown to be helpful in preparing junior residents for call. (Ganguli, et al.) Summary: With the recent introduction of focused HN lectures into our institution's Fundamentals course, we will assess the residents' performance on the final exam and use this year's exam as a baseline to assess longitudinally the residents' gain in knowledge of HN diagnoses they may encounter on overnight call. We predict that the exposure to HN teaching during the Fundamentals course will facilitate the residents' preparedness for handling a variety of HN pathology when on call. References: 1. Darras KE, Worthington A, Russell D, Hou DJ, Forster BB, Hague CJ, Mar C, Chang SD. Implementation of a longitudinal introduction to radiology course during internship year improves diagnostic radiology residents' academic and clinical skills: a Canadian experience. Acad Radiol 2016; 23: 848-860. 2. Ganguli S, Camacho M, Yam CS, Pedrosa I. Preparing first-year radiology residents and assessing their readiness for on-call responsibilities: results over 5 years. AJR 2009; 192: 539-544.

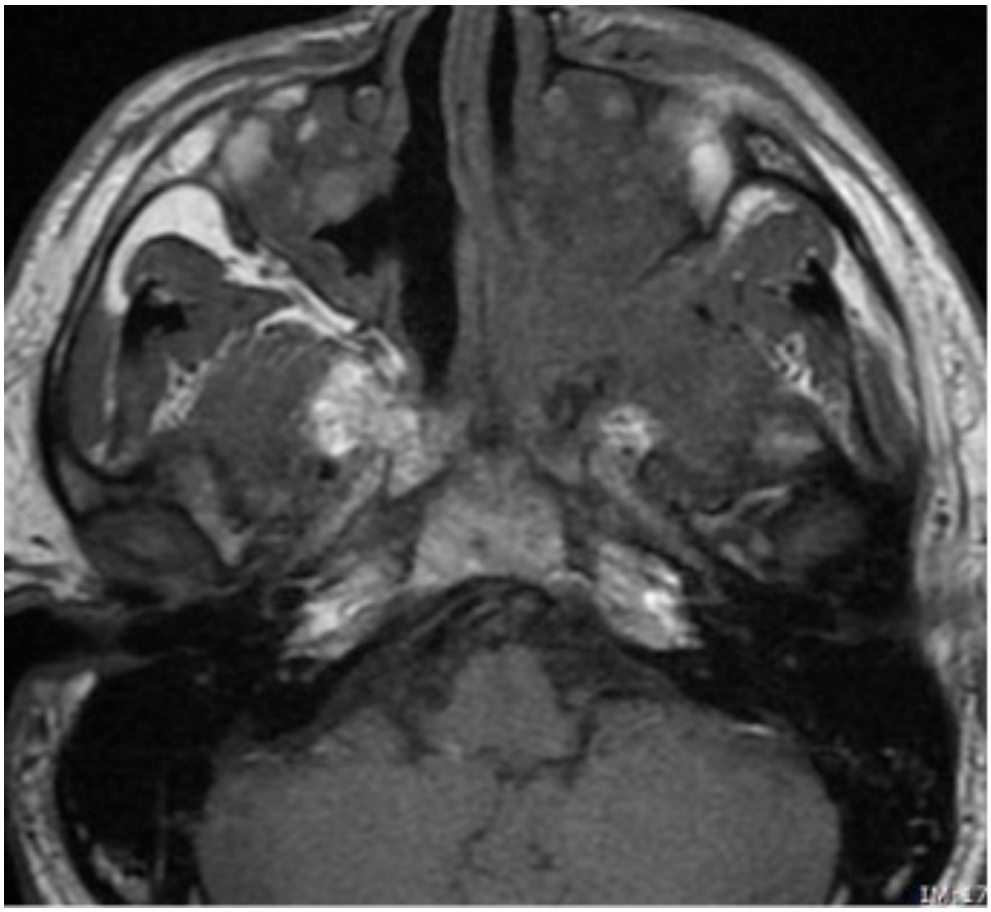

Pigmented villonodular synovitis of the temporomandibular joint: a rare case report

29 Pigmented villonodular synovitis of the temporomandibular joint: a rare case report

A Tesfay, R Bashiti, M Mirza, M Chakko

Michigan State University Southeast Campus, Providence Hospital and Medical Centers
United States

Purpose: Pigmented villonodular synovitis (PVNS) is an idiopathic, benign disorder occurring primarily in young and middle-aged adults. The pathologic process can involve any joint, bursa, or tendon sheath. It is a proliferative disorder of unknown etiology. The disease is characterized by synovial hypertrophy with diffuse hemosiderin deposits within the joint. The knee is the most commonly involved joint in PVNS. Involvement of the temporomandibular joint (TMJ) is very rare. We report a case of PVNS of the temporomandiular joint in a patient that presented with left ear pain and some dizziness. Total surgical excision of the lesion was performed through a preauricular craniotomy approach with temporal extension. Methods: Pigmented villonodular synovitis (PVNS) is an idiopathic, benign disorder occurring primarily in young and middle-aged adults. Knee is the most commonly involved joint, with hips, shoulder, ankle or wrist being involved less frequently 5-6 . Although any joint can be involved, involvement of the temporomandibular joint is reportedly very rare. Lapayowker et al. first described PVNS of the TMJ in 1973. Discussion: 57Yo M patient presented with hearing problems, ear pain and dizziness. CT of the head showed a lesion faintly hyperdense to grey matter in the posterlateral aspect of the middle cranial fossa associated with bone erosion and destruction extending from the anterior margin of the external auditory canal to the posterior margin of the pterygoid plate. MRI of the brain showed destructive process with faintly enhancing tissue centered at the left lateral pterygoid muscle and medial aspect of the temporal mandibular joint, extending into the into anterior epitympanum and middle cranial fossa with mild mass effect on the temporal lobe. Patient was taken to surgery and had left middle fossa craniotomy and extradural skull base approach to left middle cranial fossa, which showed a granular mass eroding the anterior temporal bone and floor of the middle fossa extending laterally and eroding the squamous portion of the temporal bone, and appeared adherent to the carotid artery and the external auditory canal. Patient was discharged in a stable condition and was being followed with MRI of the brain. MRI of the brain 2 years later showed mild increase in size of the residual mass within the infratemporal fossa medial to the left temporal mandibular joint, causing slight increased mass effect upon the inferior left temporal lobe. Patient was taken to surgery and had left preauricular middle cranial fossa approach with cranioplasty, which showed a granular tumor eroding a large portion of the bony middle fossa floor extending up to the dura, inseparable from it, and extending into the infratemporal fossa. A subtotal/near total resection of the tumor obtained. Intraoperative frozen section consistent with pigmented villonodular synovitis. Patient was discharged home in a stable condition after uneventful postoperative course in the hospital. Summary/Conclusion: Pigmented villonodular synovitis (PVS) is a locally aggressive proliferative lesion that mostly affects the joints of long bones. It rarely affects the temporomandibular joint (TMJ), and only 73 cases were reported in the literature up to 2015.

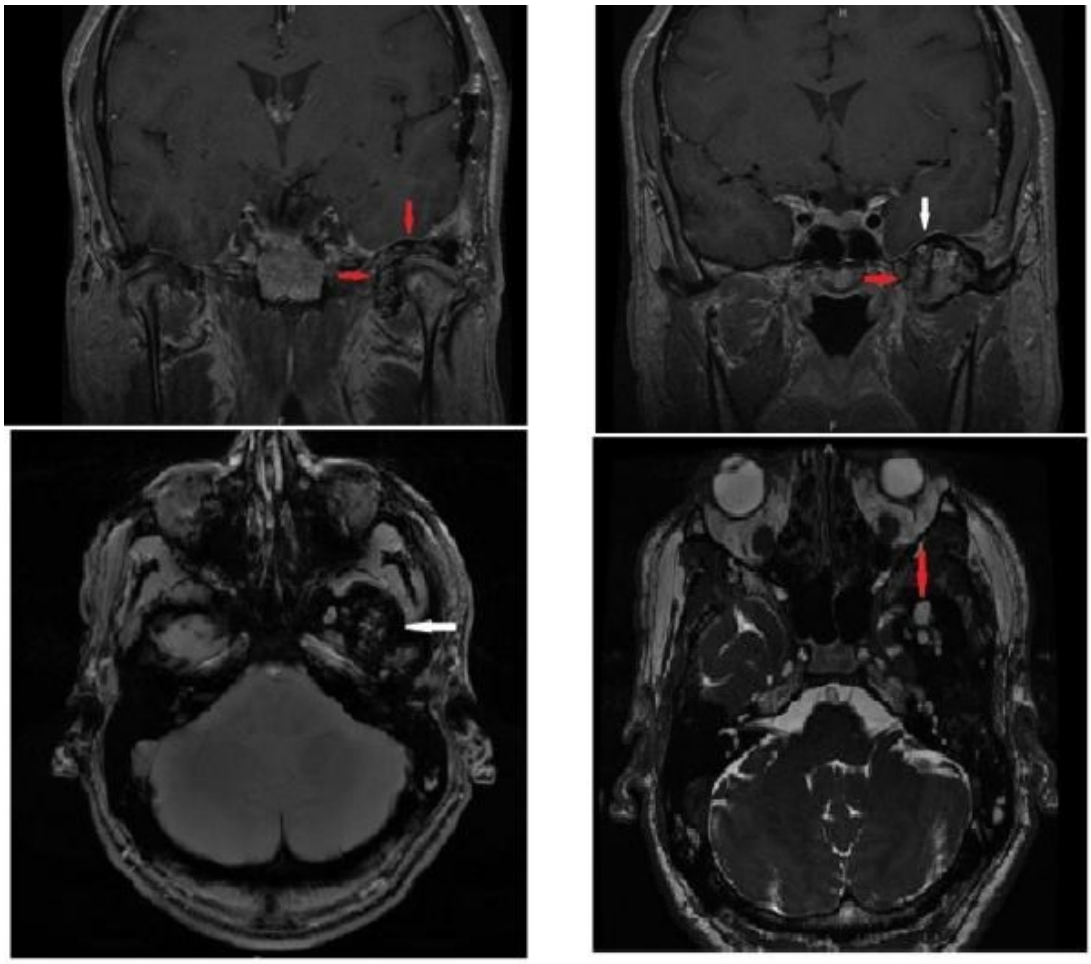

Scratch That - A Radiologic Approach to the Hoarse Voice

30 Scratch That - A Radiologic Approach to the Hoarse Voice

S Montoya, A Portanova, A Kessler, A Bhatt

University of Rochester Medical Center
United States

Purpose: The goal of this presentation is to review many of the different etiologies of dysphonia, with an emphasis on anatomic location. Description: The biomechanics of phonation is a complex process, which can be altered by a wide range of local and systemic processes. Many of these are not readily apparent on laryngoscopy, so the head and neck radiologist must be familiar with the anatomy and pathology of the larynx as well as the complex supporting laryngeal nerve network. First, the normal anatomy of the larynx and pathways of the vagus and recurrent laryngeal nerves will be presented. Next, several of the diverse pathologic entities that can result in dysphonia will be presented in an image-rich format. Summary: Dysphonia is a common symptom which can be due to a wide range of pathologic processes. Familiarity with the relevant anatomy as well as the broad spectrum of disease processes will prove useful for the radiologist presented with this clinical entity.

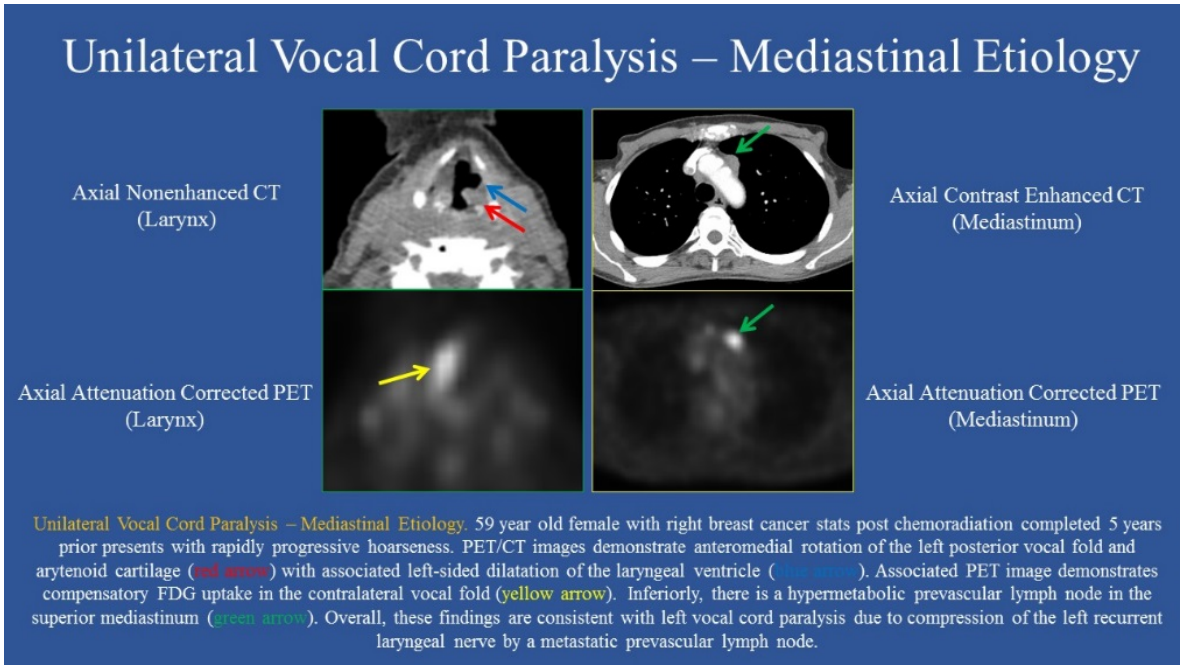

Imaging evaluation of radiation-induced osteonecrosis and chondronecrosis in the head and neck

31 Imaging evaluation of radiation-induced osteonecrosis and chondronecrosis in the head and neck

DJ Oliveira, RC Leao, B Policeni

Hospital do Cancer da Universidade Federal de Uberlandia
Brazil

Imaging evaluation of radiation-induced osteonecrosis and chondronecrosis in the head and neck Purpose: Review the imaging findings associated with radiation-induced osteonecrosis and chondronecrosis in head and neck structures, through different imaging modalities, including computed tomography (CT), magnetic resonance imaging (MRI) and positron emission tomography/computed tomography (PET/CT). We will also discuss the differential diagnosis among such entities and tumor recurrence. Description: Osteoradionecrosis is defined as a bone necrosis in previously irradiated tissues in the absence of residual or recurrent disease. In most of the cases, it occurs 1 to 3 years after radiation therapy. In 90% of the cases, it is induced by secondary trauma or surgery, such as dental extraction. The most vulnerable areas are the buccal cortices of the premolar and retromolar trigone supplied by the inferior alveolar artery. The hyoid bone can also be affected, in post radiation cases where the primary tumor was located close to the hyoid bone. Imaging findings include focal lytic area and associated cortical erosion on CT scan and abnormal signal intensity within the bone marrow on MRI. In both methods, there is a marked enhancement of the surrounding soft tissues, in the absence of focal mass-like tumor. Similarly, chondronecrosis occurs in 1 to 5% of the irradiated laryngeal tumors. Most of the patients develop it within the first 3 months after radiotherapy but it can also take several years to occur. The associated risk factors are alcohol, tobacco, previous tumoral invasion, post-operative infection, trauma, and high radiation dosage. The arytenoid cartilages are the most frequently involved. Imaging findings are also similar to osteonecrosis: both CT scan and MRI will show fragmentation and cortical erosion of the affected cartilage, although MRI is able to rule out tumor recurrence (enhancing space-occupying lesion). Additionally, we will also discuss the role of PET/CT to differentiate tumor recurrence from radiation therapy effects. Summary: Fragmentation and cortical erosion of the bone and cartilage, and associated inflammatory changes of the surrounding tissue are the major imaging findings of radiation-induced osteonecrosis and chondronecrosis in head and neck. Such knowledge can prevent potentially harmful interventions, and permit adequate treatment of patients.

Imaging review of salivary gland oncocytic lesions

32 Imaging review of salivary gland oncocytic lesions

R Rivera-de Choudens, F Syed, E Liao

University of Michigan
United States

In this review, we describe the usual imaging appearance of oncocytic lesions and propose features that may hint at the diagnosis. Oncocytic lesions are rare and comprise approximately 0.4-1% of salivary gland neoplasms. They arise from oncocytes, a type of epithelial cell which on histological analysis demonstrate a characteristic bright eosinophilic granular cytoplasm. These cells are found throughout the head and neck including the salivary, thyroid, parathyroid glands and aerodigestive tract mucosa. Oncocytic lesions are found in conditions ranging from hyperplasia to aggressive malignant lesions. The World Health Organization (WHO) classified them into three distinct types: oncocytosis, oncocytoma, and oncocytic carcinoma. Additionally, oncocytic differentiation is seen within other major salivary gland tumors and has been described synchronous with Warthin's tumor. On imaging, they are generally thought of as having non-specific characteristics. However, upon review of multiple cases, some imaging commonalities have been noted which may help to distinguish them prospectively.

Hyperintensity of the Optic Nerve on 3D FLAIR Imaging is Effective for Identifying Papilledema in Patients with Idiopathic Intracranial Hypertension

33 Hyperintensity of the Optic Nerve on 3D FLAIR Imaging is Effective for Identifying Papilledema in Patients with Idiopathic Intracranial Hypertension

ED Golden, R Krivochenitser, N Mathews, C Longhurst, Y Chen, J Yu, T Kennedy

University of Wisconsin School of Medicine and Public Health
United States

Purpose High-diffusion signal of the optic nerve (ON) and the optic nerve head (ONH) on diffusion-weighted imaging (DWI) is associated with papilledema in patients with idiopathic intracranial hypertension (IIH). However, no studies to date have examined the potential for 3-D Fluid Attenuated Inversion Recovery (FLAIR) sequences to sensitively detect papilledema in IIH patients. The purpose of this study is to evaluate whether hyperintensity of the ON and ONH on 3-D FLAIR imaging is associated with papilledema in patients with IIH. Materials and Methods In this Institutional Review Board approved study, a retrospective chart review from January 2012-December 2015 was performed. Consecutive patients with known IIH, as diagnosed by funduscopic exam by a staff ophthalmologist, with concurrently performed contrast-enhanced (CE) MR imaging with post contrast 3-D FLAIR sequences were included in this single-institution study. Two CAQ-neuroradiologists blinded to clinical data independently reviewed each MRI. Each ON on CE 3-D FLAIR was evaluated and graded independently on a scale of 0-3: 0=normal ON; 1= hyperintensity within the nerve without involvement of the ONH; 2=hyperintensity within the ON with mild inversion of the ONH; and 3=hyperintensity within the ON with significant inversion of the ONH. Descriptive statistics were then calculated. Results 47 patients (3 males, 44 females, mean age 29.53 ±11.04) with known papilledema and 61 age- and sex-matched control patients (5 males, 56 females, mean age 30.89 ±11.74) with normal MRIs were included in this study. For reader one, hyperintensity of at least one ON was 84.38% sensitive (95% CI 75.69, 90.41) and 100% specific (95%CI 96.33,100) for presence of papilledema. For reader two, hyperintensity of at least one ON was 77.08% sensitive (95%CI 67.67, 84.41) and 87.70% specific (95%CI 80.59, 92.51) for the presence of papilledema. Inter-reader reliability was assessed using a weighted kappa score and was 0.8108 (95%CI 0.6938, 0.8846). Conclusions We present the first application of CE 3-D FLAIR imaging towards the detection of papilledema. We demonstrate that hyperintensity of the ON on 3-D FLAIR imaging is sensitive and specific for detection of papilledema in patients with IIH, allows for high inter-reader agreement, and may outperform DWI in the detection of papilledema. CE 3-D FLAIR imaging is a feasible neuroimaging technique for the detection of papilledema that can supplement the funduscopic exam.

Transoral Robotic Surgery - Role of the Head and Neck Radiologist

34 Transoral Robotic Surgery - Role of the Head and Neck Radiologist

BY Kwan, J de Almeida, D Goldstein, V Paleri, R Forghani, E Yu

University of Toronto
Canada

Purpose The objective of this exhibit is to review the indications for transoral robotic surgery (TORS) and its role in treatment de-escalation for oropharyngeal cancer. The role of imaging in patient selection will be specifically reviewed. Description Transoral robotic surgery is a recently developed technique that allows minimally invasive surgeries to be performed in the head and neck. TORS has a role in the de-escalation of oropharyngeal cancers which allows for treatment with surgery with or without neck dissection in place of definitive chemoradiation therapy. Additionally, this technique allows for less invasive surgery and decreases associated complications. The head and neck radiologist has a prominent role to identify suitable candidates for this type of surgery. This exhibit will review important anatomy and staging related to TORS. Additionally, all the key imaging features for patient selection (indications and contraindications) will be presented along with case illustrations. Summary TORS is an emerging technique for de-escalation of oropharyngeal cancer. This exhibit will guide the radiologist for interpretation of pre-operative MRIs for patient selection.

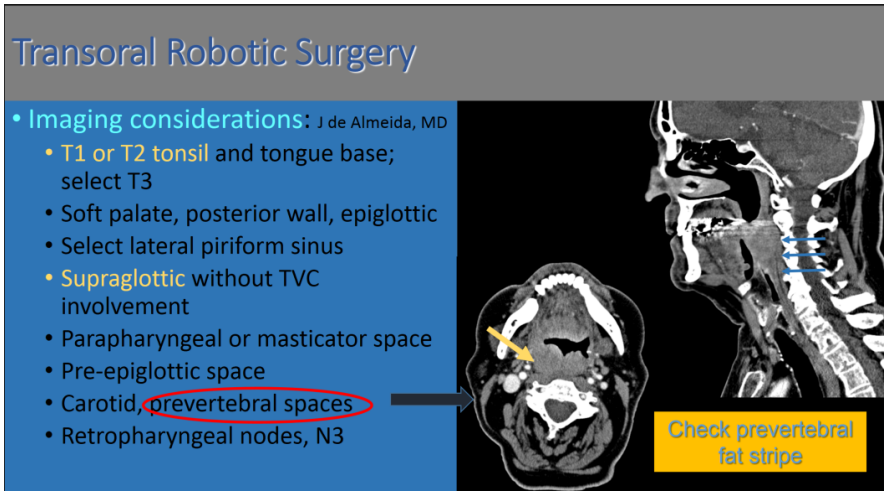

Often Forgotten, But not Lost Art: A Pictorial Review of Dacryocystography and Associated Nasolacrimal Appartus and Lacrimal Pathology

35 Often Forgotten, But not Lost Art: A Pictorial Review of Dacryocystography and Associated Nasolacrimal Appartus and Lacrimal Pathology

A Shah, M Bhatt, S Noujaim

Beaumont Health/Oakland University-William Beaumont School of Medicine
United States

Purpose: Epiphora, or excessive tearing, is a frequently encountered clinical complaint in ophthalmology practices. A variety of etiologies have been described in the literature, prompting the need for further evaluation. A key area for inspection is the lacrimal apparatus, consisting of the lacrimal gland and nasolacrimal drainage pathway. A thorough grasp on the technical aspects of Dacryocystography is essential, as obtaining the appropriate images can be key to making the diagnosis. Additionally knowledge of the normal nasolacrimal apparatus anatomy and review of associated pathologies is important in providing the clinician with an appropriate and accurate interpretation. Description: With the use of fluoroscopic and cross-sectional imaging, in addition to 3-D reconstructions and original illustrations, the anatomy of the lacrimal and nasolacrimal apparatus will first be reviewed. Following, multiple images will be displayed, highlighting the necessary equipment in performing Dacryocystography, including the catheter, topical anesthetic, headset, contrast and fluoroscopic unit. This will be followed by detailed technical review of the steps involved in Dacryocystography, from cannulating the lacrimal puncta, to obtaining the necessary images. We will then show a variety of associated pathologies, that include, but are not limited to Dacryolithiasis, Dacryocystitis, Dacryocystocele, Lacrimal duct stenosis, Trauma, as well as lacrimal gland pathology, including Lymphoma, Carcinoma, Minor salivary gland tumors. Summary: Dacryocystography is often overlooked in terms of radiology education, however remains an important skill for the radiologist. Combination of understanding the detailed anatomy of the nasolacrimal apparatus and grasping the technical aspects of the exam are key to accurate interpretations. Additionally understanding the pathological entities occurring in this an anatomic region is essential to the radiologist.

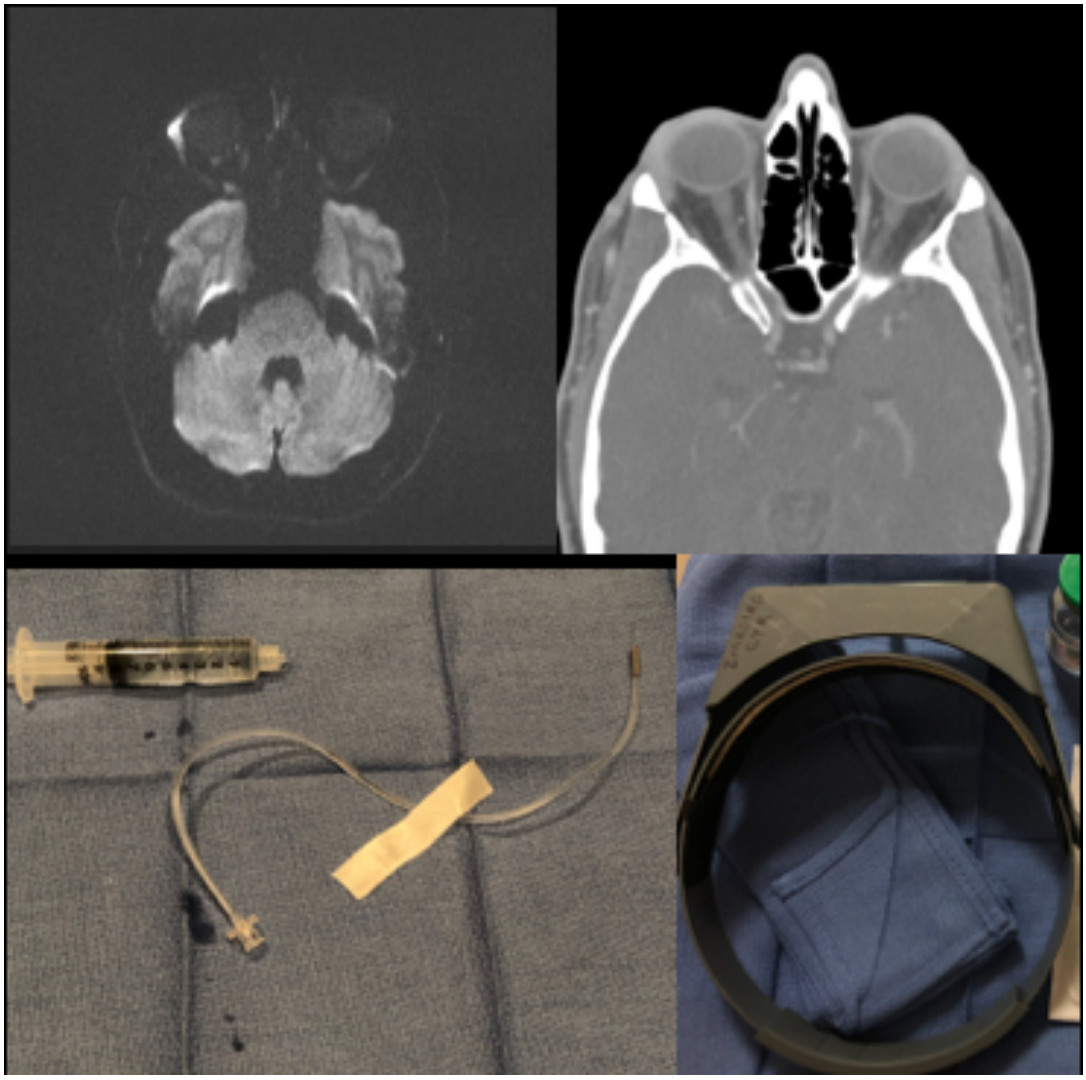

Sudden Onset Deafness in a Pediatric Patient due to Acute Labyrinthitis: An Illustrative Case Report

36 Sudden Onset Deafness in a Pediatric Patient due to Acute Labyrinthitis: An Illustrative Case Report

PK Naidu, WT O'Brien, DI Choo, BL Koch

Cincinnati Children's Hospital
United States

Purpose: We present an unusual case of sudden-onset profound deafness in a 10-year-old that was due to acute labyrinthitis. The case not only highlights the imaging findings of acute labyrinthine inflammation but also emphasizes the need for prompt imaging when this condition is suspected in order to allow for appropriate treatment (cochlear implantation) prior to the third phase of ossific labyrinthine obliteration. Description: A 10-year-old presented to the otolaryngologist after the sudden onset of severe deafness ten days prior. Per her mother, she had been on a trip to Mexico and swam in a "dirty" river. The day after, she became ill and complained of ear pain, hearing loss, dizziness, and vomiting. There was no history of prior meningitis or ear infection. She saw multiple doctors and was ultimately placed on steroids and referred to ENT at our institution. The dizziness and vomiting resolved, but the deafness persisted. Audiometry confirmed bilateral profound sensorineural hearing loss (SNHL). The otolaryngologist continued the patient on steroids and ordered an MRI of the IACs. MRI demonstrated decreased fluid signal within the labyrinthine structures bilaterally on FIESTA sequences and labyrinthine enhancement consistent with the fibrous stage of acute labyrinthitis. Both cochlear nerves were present. A CT of the IACs confirmed patency of the cochlea bilaterally. The patient subsequently underwent successful bilateral cochlear implantation. Summary: While sensorineural hearing loss (SNHL) occurs in 6 of every 1000 children (1), sudden SNHL (SSNHL) is much more rare, occurring in 5-20 of every 100,000 individuals of any age each year (2). SSHNL is an urgent/emergent otologic condition; a delay in treatment can result in permanent hearing loss (3). As such, prompt imaging is imperative to both look for a cause and evaluate integrity of the cochlea and cochlear nerve in preparation for potential cochlear implantation. SSNHL necessitates a rapid clinical and radiological evaluation in order to optimize treatment outcomes, as depicted by the case presented here. References 1. Huang BY, Zdanski C. Pediatric Sensorineural Hearing Loss, Part 2: Syndromic and Acquired Causes. Am J of Neuradiol 2012; 33: 399-406. 2. Inci E, Edizer DT, et al. Prognostic Factors of Sudden Sensorineural Hearing Loss in Children. Int. Adv. Otol. 2011; 7: 62-66. 3. Na SY, Kim SG, et al. Comparison of Sudden Deafness in Adults and Children. Clin Exp Otorhinolayngol. 2014; 7: 165-169.

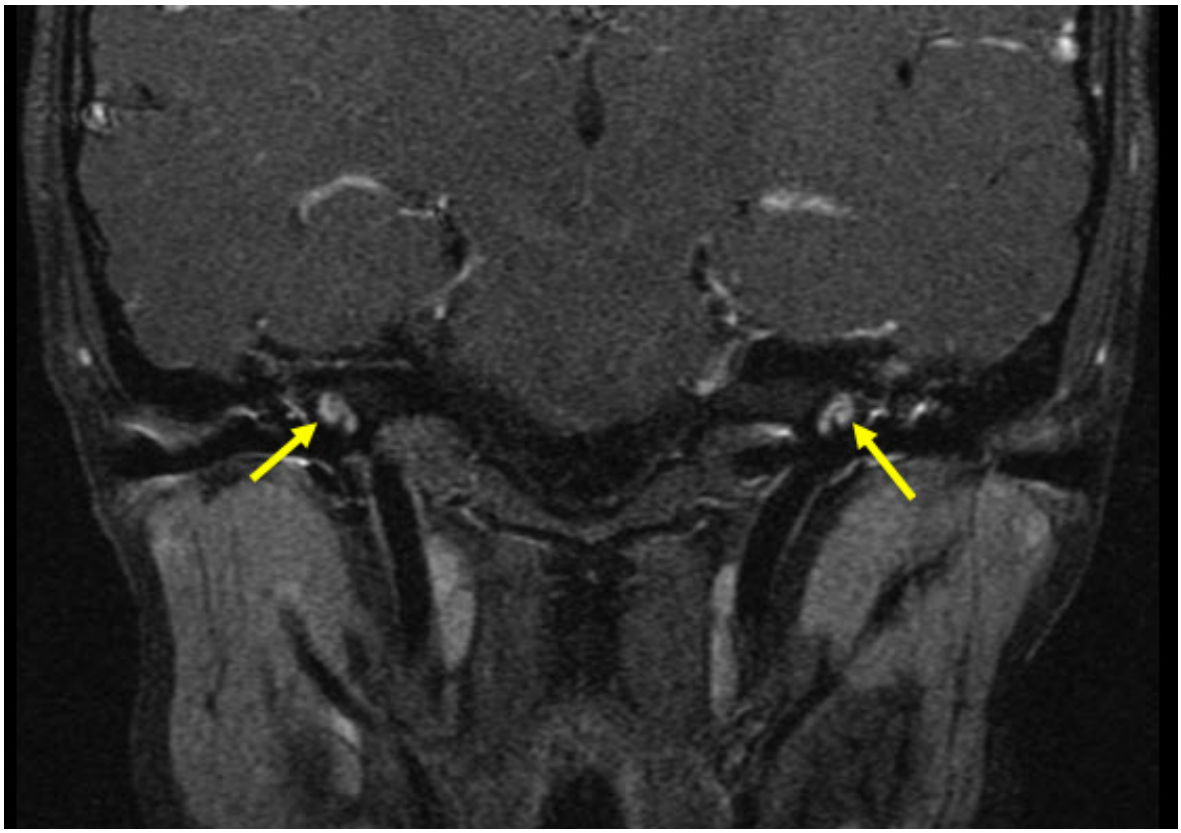

Fibrous Dysplasia: Notorious Mimic of Skull Base Pathology

37 Fibrous Dysplasia: Notorious Mimic of Skull Base Pathology

OL Dayton, I Schmalfuss

University of Florida
United States

Fibrous dysplasia is a disorder of the osseous skeleton, which results in progressive replacement of cancellous bone with a combination of immature woven bone and fibrous tissue. The skull base and craniofacial skeleton are involved in up to 25% of patients with monostotic fibrous dysplasia and up to 50% of patients with polyostotic fibrous dysplasia. The classic CT findings of fibrous dysplasia include a medullary-centered process causing osseous expansion and replacement of the medullary space with ground-glass density related to mineralization of immature osseous matrix. The classic MR findings of fibrous dysplasia include osseous expansion with intrinsic T1 and T2 hypointensity related to mineralization of osteoid matrix with variable contrast enhancement depending on degree of osseous and fibrous tissue. This classic imaging appearance is only observed in 2/3 of patients while marked variability is seen in other patients. This variability is related to the ratio of mineralized osseous matrix to fibrous tissue, presence of cystic changes, and presence or absence of residual fatty marrow in the involved bone. As such, fibrous dysplasia of the skull base is a great mimicker of other disease entities that have a propensity to involve the skull base. In this electronic exhibit we will illustrate a range of CT and MR findings of skull base fibrous dysplasia and discuss differentiating imaging features to other skull base pathologies that may cause diagnostic dilemmas. Examples of fibrous dysplasia mimicking the following disease entities will be presented: Chronic sinusitis, pituitary gland adenoma, intraosseous meningioma, Paget disease, chondrosarcoma, and osseous metastatic lesions. Hints to the correct diagnosis will be discussed. After review of this electronic exhibit the conference-attendee will be able to differentiate fibrous dysplasia from other skull base pathology with higher degree of confidence.

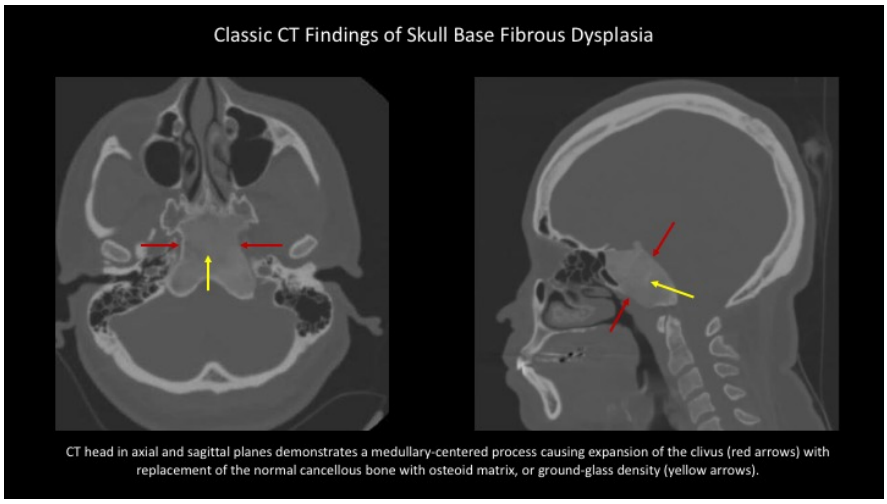
Classic CT Findings of Skull Base Fibrous Dysplasia
CT head in axial and sagittal planes demonstrates a medullary-centered process causing expansion of the clivus (red arrows) with replacement of the normal cancellous bone with osteoid matrix, or ground-glass density (yellow arrows).

Imaging Review of New and Emerging Sinonasal Tumors and Tumor-like Entities from the 4th Edition of the World Health Organization Classification of Head and Neck Tumors

38 Imaging Review of New and Emerging Sinonasal Tumors and Tumor-like Entities from the 4th Edition of the World Health Organization Classification of Head and Neck Tumors

KE Dean, C Phillips, D Shatzkes

NYP-Weill Cornell
United States

The sinonasal tract is histologically and anatomically complex providing for an environment diverse with neoplastic pathologies. Further advancements have resulted in the discovery or redefinition of several new entities and other emerging tumor and tumor-like entities generally specific to the sinonasal tract. The 4th edition of the World Health Organization Classification of Head and Neck Tumors released in 2017 specifically describes three, new, well-defined entities and several, less-defined, emerging entities. The new entities include seromucinous hamartomas, NUT carcinomas, and biphenotypic sinonasal sarcomas. The emerging entities including both provisional diagnoses and those described only in the context of differential diagnoses. These emerging entities include HPV-related sinonasal carcinomas with adenoid cystic-like features, SMARCB1 (INI-1) deficient sinonasal carcinomas, renal cell-like adenocarcinomas, and chondromesenchymal hamartomas. A recent expanded series of HPV-related sinonasal carcinomas with adenoid cystic-like features suggests the tumor may be, in fact, a distinct entity with the proposed name of HPV-related multiphenotypic sinonasal carcinomas. Thus far, literature has largely focused on the pathologic and histologic features of these entities. I plan to discuss the imaging features and patterns of these entities both on CT and MR. Additionally, I will provide brief descriptions of the demographics and natural histories of these diseases and discuss differential considerations. In doing so, I aim to provide an expanded framework for neuroradiologists in their diagnostic approach to sinonasal tumors.

Provided below is an example of one of the emerging entities described in the 4th edition of the World Health Organization Classification of Head and Neck Tumors, the SMARCB1 (INI-1) deficient sinonasal carcinoma.

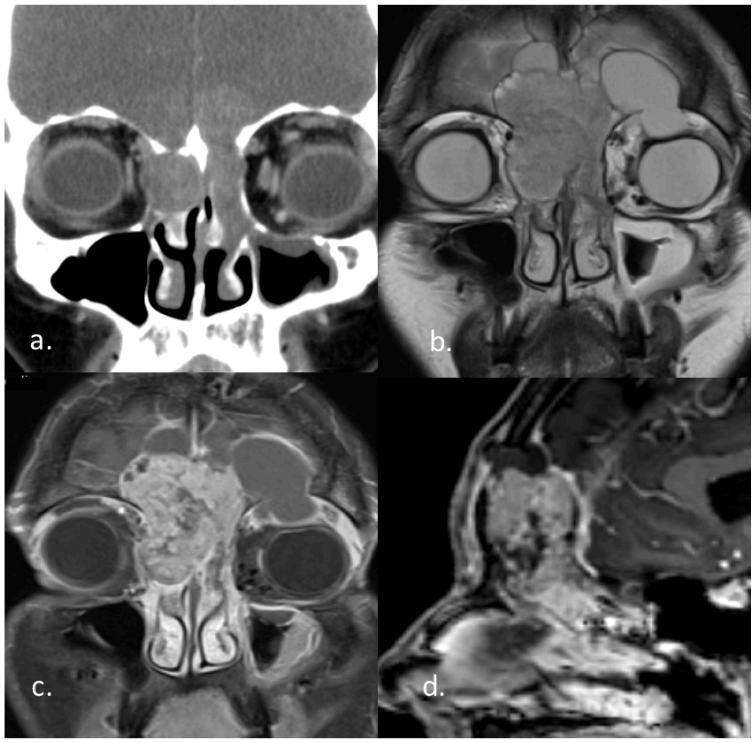

SMARCB1 (INI-1) deficient carcinoma of sinonasal tract is an emerging entity in the latest edition of WHO Classification of Head and Neck Tumors. SMARCB-1 deficient carcinomas have largely been described as centered within the superior nasal vault/ethmoid sinuses and demonstrate highly aggressive imaging findings. The tumors are isointense to and enhance similar to muscles on CT and approximately half of the cases have associated calcifications (a). Frank expansion into or erosion of the skull base is often noted (a-d). Extension into the orbit is seen in approximately half of described cases (a-c). T2 signal is variable, through predominantly isointense to hyperintense, and there is avid associated enhancement on MR imaging (b-d). Tumoral necrosis and peritumoral cysts were noted in this case (b-c).

Multimodal Measures of Perineural Tumor Spread: Does PET FDG correlate with MR Diffusion Anisotropy?

39 Multimodal Measures of Perineural Tumor Spread: Does PET FDG correlate with MR Diffusion Anisotropy?

KS Traylor, NA Koontz, VD Aaron, JB Sims, K Mosier

Indiana University School of Medicine
United States

Introduction: Perineural spread is defined as spread of tumor along named cranial nerves and although estimates vary, is reported to occur in approximately 15-40% of head and neck cancers. Perineural spread is important to identify as the presence of perineural spread significantly decreases overall survival. Previous studies have shown that interactions between glial cell derived neurotrophic factor (GDNF) from nerves and chemokines from adjacent tumor draws the tumor onto the nerve. This process is dependent on glucose utilization. These interactions suggest that a combination of FDG avidity and diffusion imaging measures may improve the sensitivity and specificity of perineural spread. However, the relationship between FDG uptake and diffusion measures including the apparent diffusion coefficient (ADC) and fractional anisotropy (FA) in perineural spread remains unclear. Purpose: To determine the relationship between the apparent diffusion coefficient (ADC), fractional anisotropy (FA), and standardized uptake value in perineural tumor spread Materials/Methods: We conducted a retrospective review of patients in our institutional database from 2010-2018. Inclusion criteria included patients with proven or suspected perineural spread with MRI and PET-MRI or PET-CT exams. A total of 12 patients met inclusion criteria. ROI analysis was performed on the involved nerve as well as the contralateral uninvolved nerve and the brainstem as controls for the ADC and FA measurements. Standard uptake values (SUV) were obtained from the co-registered PET and MR images of the involved nerve. Statistical analysis was performed using ANOVA and non-linear Poisson regression methods accounting for small sample size and ROI volume. Results: Perineural spread was identified primarily along V2 and V3 branches of the trigeminal (n = 11) as well as the V1 branch of CN 5 (n = 1). Pathology included squamous cell carcinoma (n = 6), adenoid cystic carcinoma (n = 1), poorly differentiated salivary carcinoma (n = 1), sinonasal small cell carcinoma (n =1), neuroblastoma (n=1), and rhadomyosarcoma (n = 1). All involved nerves (n=12) demonstrated enlargement and enhancement on post-contrast MRI. There was a statistically significant effect of the SUV on FA, as well as ADC (p=0.01). Further, our preliminary data suggests that as the SUV increases, the FA also increases. These results suggests that a higher metabolic activity may be associated with formation of directional structure. Conclusion: The results of this study show a relationship between the FA and SUV in perineural spread and suggest that increased FDG uptake is associated higher FA values. This may reflect anisotropy secondary to directional vector of tumor spread along the nerve, or alternatively may represent the signature of neural-tumor tracking.

Imaging anatomy of the distal branches of the trigeminal nerve, as demonstrated by perineural tumor spread

40 Imaging anatomy of the distal branches of the trigeminal nerve, as demonstrated by perineural tumor spread

J Sommerville, M Gandhi

Royal Brisbane and Women's Hospital, University of Queensland
Australia

Purpose: To demonstrate radiological anatomy of the distal branches of the trigeminal nerve as depicted in cases of perineural tumour spread. Description: The trigeminal nerve is the largest of the cranial nerves and supplies sensation to the face as well as motor function to the muscles of mastication. It is the nerve most commonly involved in perineural tumour spread. This is a rare manifestation of tumour spread, most commonly seen with cutaneous squamous cell carcinoma, but it's presence has a significant impact on the patient's prognosis and treatment. If the disease is picked up early, while in the distal branches of the trigeminal nerve and prior to involvement of the Gasserian ganglion, patients have improved survival and reduced morbidity from treatment. As such, it is important to have an understanding of the anatomy of the nerve as seen on MRI, so that it can be diagnosed early. This exhibit will demonstrate cases of perineural tumour spread involving the main branches of the trigeminal nerve including branches of V1 (frontal, lacrimal and nasociliary nerves), V2 (greater and lesser palatine and infraorbital nerves) and V3 (auriculotemporal, inferior alveolar, lingual nerve).

Multi-modality approach to Congenital Cystic Abnormalities of the Neck

41 Multi-modality approach to Congenital Cystic Abnormalities of the Neck

M Cedillo, M Cai, N Voutsinas, J Song, P Belani

Mount Sinai Hospital
United States

Purpose: To provide a multi modality review on approaching congenital cystic masses of the neck and their complications. Description: Powerpoint presentation reviewing a multimodality approach to diagnosis of congenital cystic masses of the neck with a particular emphasis on the following cystic disease: brachial cleft cysts, cystic metastatic disease, cystic hygroma and thyroglossal duct cysts. Each pathology will be reviewed in depth to include embryogenesis, epidemiological data on incidence, imaging appearances via ultrasound/CT/MRI, complications, and treatment options. Imaging characteristics of common complications such as infection will also be reviewed. Summary: Concise and informative powerpoint presentation reviewing a multimodality approach to congenital cystic masses of the neck and their complications.

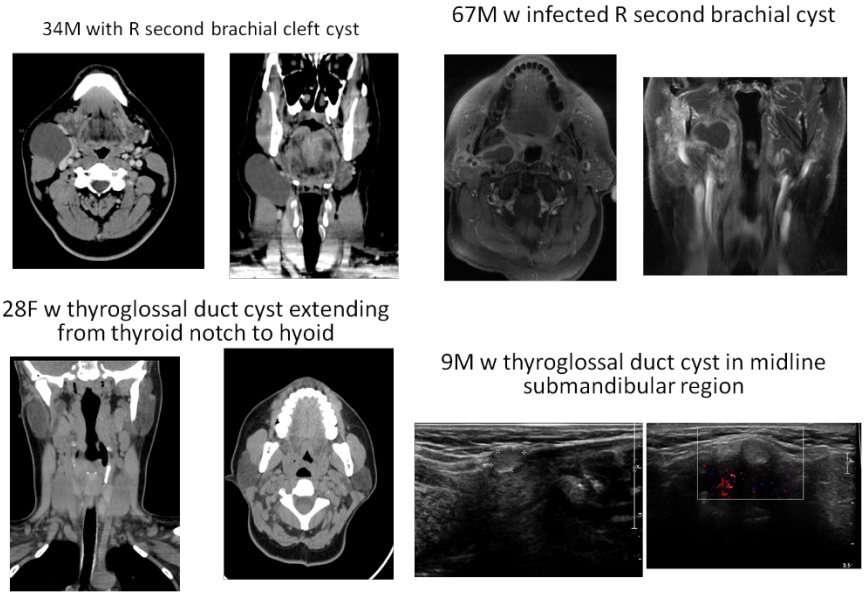

Vallecular presentation of extruded fragments of hyoid osteoradionecrosis: clinical, videostroboscopic and radiologic findings in two cases

42 Vallecular presentation of extruded fragments of hyoid osteoradionecrosis: clinical, videostroboscopic and radiologic findings in two cases

MM Chen, A Gillenwater, J Lewin, LE Ginsberg

MD Anderson Cancer Center
United States

Purpose: To present clinical, videostroboscopic and imaging features of hyoid osteoradionecrosis presenting as extruded bone fragments in the vallecula Description: Osteoradionecrosis of the hyoid is a complication of radiation therapy in the treatment of head and neck malignancies. We present 2 cases of hyoid osteoradionecrosis in patients with low base of tongue squamous cell carcinomas that progressed to extruded hyoid bone into the vallecula. In one patient, the fragmentation of hyoid bone extruding into the vallecula is correlated with videostroboscopy. In another case, the hyoid auto-amputated, and the patient expelled the hyoid fragment. Gross pictures of the fragment (given by the patient to the senior author for teaching purposes) will be correlated to imaging findings. FDG avid activity in the left base of tongue was initially misdiagnosed as recurrent tumor at an outside institution. After biopsy, the patient developed hyoid osteoradionecrosis. Summary: Radiation of mucosal cancer in proximity to the hyoid (vallecula, inferior tongue base), and particularly re-irradiation, are known predictors of hyoid osteoradionecrosis.

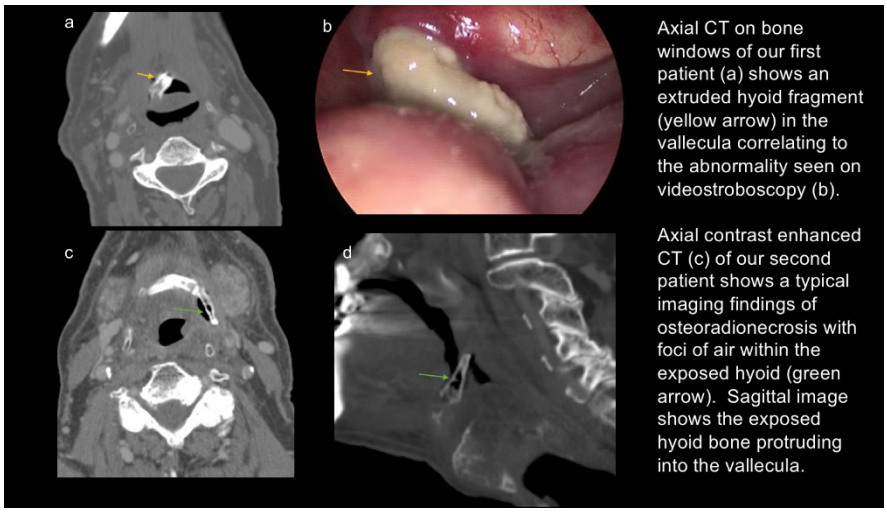

Carotidynia /TIPIC syndrome imaging: a 68-case series with follow-up evaluation

43 Carotidynia /TIPIC syndrome imaging: a 68-case series with follow-up evaluation

AA Dórea, RW Murakoshi, DV Sumi, RL Gomes, RM Loureiro, MM Daniel, CR Soares, H Tames

Hospital Israelita Albert Einstein
Brazil

Purpose: The purpose of this study is to identify imaging findings of carotidynia syndrome (recently also described by the proposed acronym: transient perivascular inflammation of the carotid artery - TIPIC syndrome) in Doppler ultrasound, computed tomography (CT) and magnetic resonance (MR) imaging, and correlate them with clinical aspects, including follow-up. Materials and Methods: Retrospective observational study included 68 patients with clinical history of cervical pain, admitted to our hospital emergency department from 2009 to 2017, and who underwent at least one of the following imaging exams: Doppler ultrasonography, CT and / or MR. Images were analyzed in order to identify structural alterations directly and indirectly related to this disease, and to demonstrate its characteristic findings. Patients were stratified in gender and questioned, by telephone, about symptoms, treatment performed and if there had been clinical improvement or recurrence of symptoms. Eight patients underwent follow-up imaging studies, which we examined to assess resolution of imaging findings and to exclude differential diagnoses of carotidynia/TIPIC syndrome. Results: Forty-nine (72%) patients were females and 19 (28%) males. Local edema associated with pain was reported in 45 (66%) patients, of which 35 were women (78%) and 10 men (22%). Focal thickening in the carotid artery wall, especially in the carotid bulb, was seen in 100% of the patients. Obliteration of adjacent fat planes was also observed, as well as lymph node enlargement and contrast enhancement on CT and MR. All patients had clinical follow-up and eight patients underwent follow-up imaging studies; 7 (88%) underwent ultrasound and 1 (12%) CT. All 8 cases presented improvement of imaging findings. Regarding treatment, 54 patients (79%) used anti-inflammatory / corticosteroid drugs for at least 3 days, with significant improvement of symptoms. The remainder of the patients did not use medication, but nonetheless reported improvement of symptoms in 5 to 15 days after diagnosis. Complete remission of symptoms and imaging findings was observed in up to 3 months after treatment, regardless of medication use. Conclusion: Imaging findings of carotidynia/TIPIC syndrome in Doppler ultrasound, CT and MR demonstrated similar findings as those reported in the literature. Follow-up evaluation showed complete regression of imaging findings in all 8 patients. All patients reported remission of clinical symptoms. Carotidynia/TIPIC syndrome should be remembered among diagnostic hypothesis in patients with unilateral neck pain, in the topography of the carotid arteries, with or without edema, especially in women.

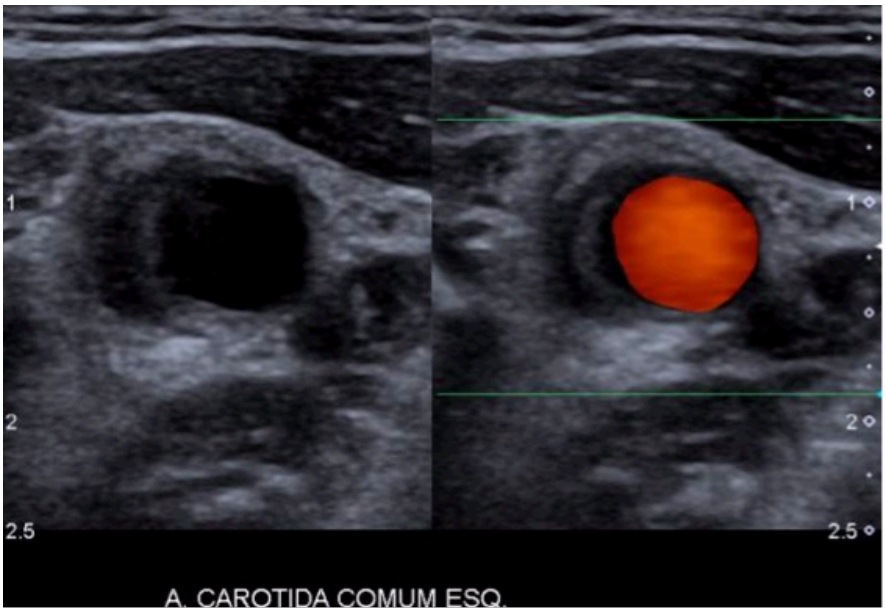
1
2
2.5
1
2
2.5
A. CAROTIDA COMUM ESQ.

Dermatofibrosarcoma protuberans of the face arising in pregnancy: A rare diagnosis

44 Dermatofibrosarcoma protuberans of the face arising in pregnancy: A rare diagnosis

M Patino, E Friedman, R Karni

University of Texas Health Science Center at Houston
United States

Purpose: To present cases of dermatofibrosarcoma protuberans arising in the face, two of which developed in pregnant women, and to contrast these lesions with the imaging appearance of other cutaneous facial masses. Discussion: Dermatofibrosarcoma protuberans (DFSP) is a rare, typically low-grade malignancy that arises from the dermis, with an estimated incidence of 0.8-4.5 cases per million persons per year in the United States. Up to 90% of cases occur in the trunk or extremities, with the remaining cases developing in the head and neck region, the overwhelming majority of which arise in the scalp. Clinically, the tumor begins as one or multiple painless small nodules that progress to an indurated plaque and multiple nodules with surrounding red to blue skin discoloration. Larger, advanced lesions may be painful and ulcerate. Peak incidence is in people in the 3rd - 5th decades of life. DFSP in its early stage is frequently treated by a dermatologist. DFSP is a locally aggressive tumor with a tendency for local recurrence if not completely resected, and head and neck lesions are more likely to recur than those occurring elsewhere in the body. Metastasis is uncommon. DFSP is most commonly a slowly progressive tumor, but may undergo periods of accelerated growth. Imaging is helpful to delineate the extent and depth of larger lesions. The most common imaging appearance on CT is a noncalcified mass in the skin and subcutaneous soft tissues which has similar attenuation to muscle, and on MRI is isointense to muscle on T1 and hyperintense on T2-weighted imaging. Typically, the mass shows diffuse enhancement, which may be heterogeneous in larger lesions. Larger lesions in the scalp may thin and remodel the underlying bone, but osseous destruction is uncommon, in distinction to invasive squamous cell carcinoma and malignant melanoma. We present five cases of DFSP that arose in the face, two of which developed during pregnancy. The facial soft tissues are an uncommon site of origin for DFSPs, as most of these lesions in the head and neck arise from the scalp. Some DFSPs express estrogen and/ or progesterone hormone receptors, and this may account for the interesting development or growth of these tumors during pregnancy in some instances. We will review the typical imaging features of DFSP in comparison to other cutaneous masses and neoplasms that could be confused with DFSP. Summary: DFSP is a rare cutaneous malignancy that uncommonly involves the face. Knowledge of the typical imaging and clinical characteristics of this lesion can help to distinguish from other cutaneous masses.

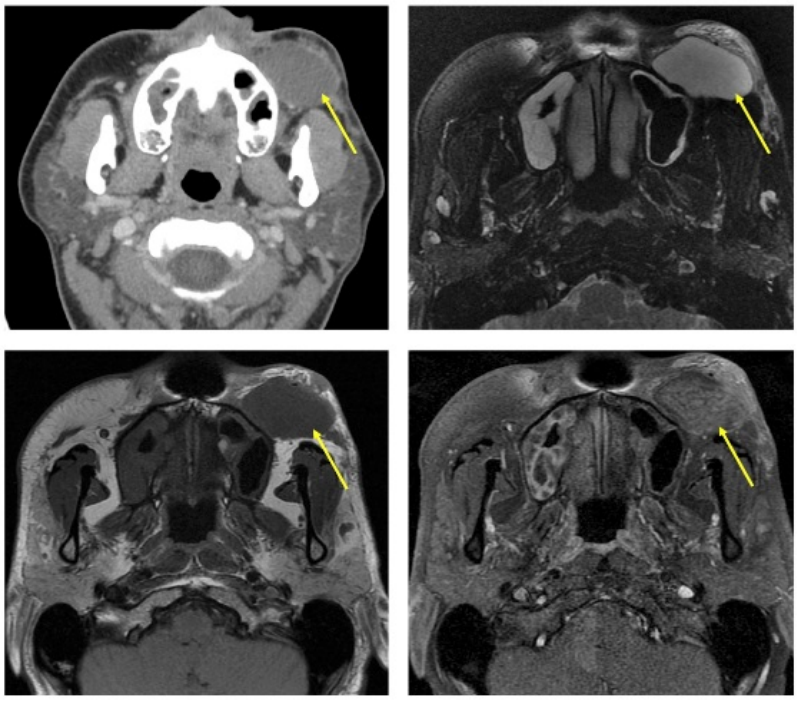

Don't Get Cheeky! An Imaging Review of Cheek Masses

45 Don't Get Cheeky! An Imaging Review of Cheek Masses

K Riley, N Supakul, K Mosier

Indiana University School of Medicine
United States

Purpose Cross-sectional imaging including CT, MRI, and ultrasound is frequently requested for evaluation of patients presenting with cheek masses. The differential diagnosis is broad and includes infectious/inflammatory, neoplastic, and congenital abnormalities. The purpose of this exhibit is to review the most common imaging manifestations of cheek masses likely to be encountered by the head and neck radiologist. Description Evaluation of patients presenting with a clinical history of "cheek mass" can be difficult. While physical examination and the history can sometimes be helpful, cross-sectional imaging is typically required to define the space of origin and extent of the lesion as well as narrow down the differential diagnosis. Lesions presenting as a cheek mass may potentially arise from several of the head and neck spaces including the parotid, masticator, or buccal spaces as well as within the superficial subcutaneous tissues. CT and MRI are most often performed although ultrasound may be obtained as well. A retrospective search was performed using a database of all radiologic exams performed at our institution. Representative cases of common and uncommon etiologies of cheek masses are presented with multimodality imaging correlates. These include infection/inflammation (abscess), neoplastic (benign mixed tumor, Warthin tumor, carcinomas), congenital (accessory parotid gland, 1st branchial cleft cyst, hemangioma, vascular malformation, benign hypertrophy of the masticator muscle). Rare entities include schwannoma and synovial chondromatosis. The key features of these different masses will be illustrated and their use in guiding the differential diagnosis will be highlighted. Summary Evaluation of patients presenting with cheek masses is difficult given a wide range of possible sites of anatomic origin as well as an extensive differential diagnosis. CT and MRI are typically the first-line imaging modalities for evaluation of these lesions and can define their anatomic origin and extent as well as narrow what would otherwise be a broad-differential diagnosis. Knowledge of the most common etiologies, anatomy and key imaging findings are critical to the head and neck radiologist to contribute to the care of these patients. References: Tart RP, Kotzur IM, Mancuso AA, et al. CT and MR imaging of the buccal space and buccal space masses. Radiographics. 1995 May;15(3):531-50. https://entokey.com/cheek-mass/

A Rare Case of Ectopic Pituitary Adenoma Presenting as a Nasopharyngeal Mass

46 A Rare Case of Ectopic Pituitary Adenoma Presenting as a Nasopharyngeal Mass

MH Hanna, R Marta, P Som

Mount Sinai
United States

INTRODUCTION Pituitary adenomas are benign neoplasms accounting for 10-15% of all primary intracranial tumors . The majority of pituitary adenomas occurs within the sella turcica, however, they can develop in other sites. Ectopic pituitary adenomas (EPA) are defined by the World Health Organization as benign pituitary gland neoplasms occurring separate from the sella, without connection to the normal anterior pituitary gland. They are rare and can occur in various areas including the sphenoid sinus, suprasellar cistern, cavernous sinus, clivus, nasal cavity, sphenoid wing, temporal bone, superior orbital fissure and the third ventricle. Although exceedingly rare, they can also appear as a nasopharyngeal mass. We report a case of a patient with a nasopharyngeal mass; after resection in which the histopathology revealed an EPA. PURPOSE We present a rare case of a middle aged male who complained of nasal congestion and epistaxis. A non-enhanced computed tomography (NECT) of the paranasal sinuses was performed, revealing a soft tissue mass extending from the nasopharynx into the left sphenoid sinus with erosion of the sphenoid sinus floor and the anterior clivus. A magnetic resonance (MR) was also performed. There was a lobulated mass centered to the nasopharynx, measuring about 2.8 cm x 2.6 cm x 4.5 cm in maximal diameters (AP x TR x CC). The patient underwent a total mass resection via endoscopic anterior cranial base approach, with extradural tumor resection, reconstruction of the skull base and a nasoseptal flap. Histopathology revealed pituitary adenoma tissue, favoring a null cell type. DISCUSSION The exact pathogenesis of EPA is not fully established. Some authors hypothesize that they originate from the embryological development of the anterior pituitary. The anterior pituitary primordium appears around the 4th week of embryogenesis. During the 8th week, the pituitary divides into sellar and pharyngeal components. At this point there is a superior attachment to the pituitary stalk and an inferior invagination known as Rathke’s pouch, consisting of an infolding of the buccopharyngeal membrane. This Rathke´s pouch will eventually push upward through the developing sphenoid bone into the sella, giving rise to the adenohypophysis and meeting the neurohypophysis. Remnants of this pouch can remain along the course of the craniopharyngeal canal, from the upper pharynx to the sella. Purely EPA are rare lesions and the most frequent site is the sphenoid sinus. However, they can also appear in different sites such as the nasopharynx. Our case illustrates a patient with a nasopharyngeal mass detected on a NECT of the paranasal sinus and further examined through MR imaging. The differential diagnosis included squamous cell carcinoma, chordoma, chondrosarcoma, lymphoma and granulomatous disease. Albeit uncommon, an EPA needs to be considered as a differential diagnosis of a nasopharyngeal, sphenoid sinus or clival mass, so that there can be appropriate medical and surgical management.

Ectopic Pituitary Adenoma presenting as a Nasopharyngeal

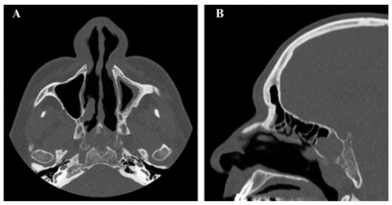

Figure 1. Axial (A) and sagittal (B) NECT images of the paranasal sinus, depicting a soft tissue mass involving the sphenoid sinus, the nasopharynx and the clivus. Notice the normal sella turcica.

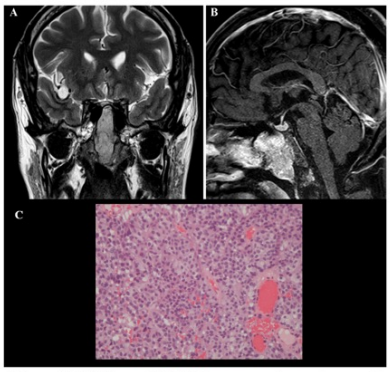

Figure 2. (A) Coronal T2WI demonstrating an intermediate hyperintense lobulated mass in the nasopharynx, extending into the sphenoid sinus. (B) Post-contrast sagittal T1WI shows avid enhancement of the mass; involvement of the clivus is also depicted. Note the intact sella and normal enhancing pituitary gland within it. (C) Pituitary adenoma: Monomorphic tumor cell population with pale, granular cytoplasm and bland nuclear features. H&E x200.

Temporal bone trauma; beyond fractures

47 Temporal bone trauma; beyond fractures

RL Gonzalez-Odriozola, EJ Labat-Alvarez

University of Puerto Rico Medical Sciences Campus, Department of Radiological Sciences
Diagnostic Radiology Division
Puerto Rico

The purpose of this exhibit is to review high resolution computed tomography of temporal bone trauma complications, specifically those cases involving critical structures that will determine patient management and establish a prognosis. These structures include the external ear canal, ossicles, cochlea, vestibule, semicircular canals, carotid canal, jugular fossa and facial nerve canal. Injury to these structures may have serious complications, such as conductive hearing loss, perilymphatic fistulas, sensorineural hearing loss, dizziness and balance dysfunction, vascular injury, facial nerve paralysis and cerebrospinal fluid leaks. Description: Complications of temporal bone trauma will be depicted in several temporal bone CTs. The first structure is the external Auditory Canal. Identifying fractures here are clinically relevant because if untreated, they could result in canal stenosis. This may be prevented by temporarily packing the canal. Next is the ossicles. The ossicular chain may be disrupted at multiple sites and usually results in conductive hearing loss. Ossicular dislocation is more common than ossicular fracture. There are five general types of dislocation: incudomalleolar joint separation, incudostapedial joint separation, dislocation of the incus, dislocation of the malleoincudal complex, and stapediovestibular dislocation (which may result in a perilymphatic fistula). We continue with evaluation of the carotid canal and jugular fossa. Patients with fractures that extend to the carotid canal or jugular fossa are at an increased risk for carotid artery injury and venous thrombosis, respectively. Vascular injuries include arterial dissection, pseudoaneurysm, complete transection, occlusion, and arteriovenous fistulas. CT angiography should be performed when fractures involving the carotid canal are identified. Next is the facial Nerve. Cranial nerve VI is divided into six segments: intracranial , intracanalicular , labyrinthine , tympanic , mastoid and extracranial segments. The facial nerve is injured in 7% of patients with a temporal bone fracture. Most injuries occur in the labyrinthine segment, particularly at the geniculate ganglion. Immediate post traumatic paralysis is concerning for transection of the nerve or compression by an osseous fragment. Delayed onset of paralysis may be explained by development of edema, swelling, or an expanding hematoma causing neural compression with an intact nerve. Injury to the cochlea, cochlear nerve, or cochlear nuclei is associated with sensorineural hearing loss. Sensorineural hearing loss also may occur when no definitive temporal bone fracture is present, an occurrence known as cochlear concussion. The vestibule is the central chamber of the osseous labyrinth. It is continuous with the cochlea anteriorly and the semicircular canals posteriorly. Injury to the vestibular apparatus may result in vertigo. We conclude this review with the semicircular canals. There are three semicircular canals: the lateral, posterior, and superior semicircular canals. As with vestibular injuries, trauma to the semicircular canals results in vertigo. Summary: Temporal bone trauma complications are numerous. Injuries in this region may have serious complications, such as conductive hearing loss, perilymphatic fistulas, sensorineural hearing loss, dizziness and balance dysfunction, vascular injury, facial nerve paralysis and cerebrospinal fluid leaks. Identification of injury to critical structures is vital to guide further management and predict prognosis in patients with temporal bone trauma.

Temporal bone CT

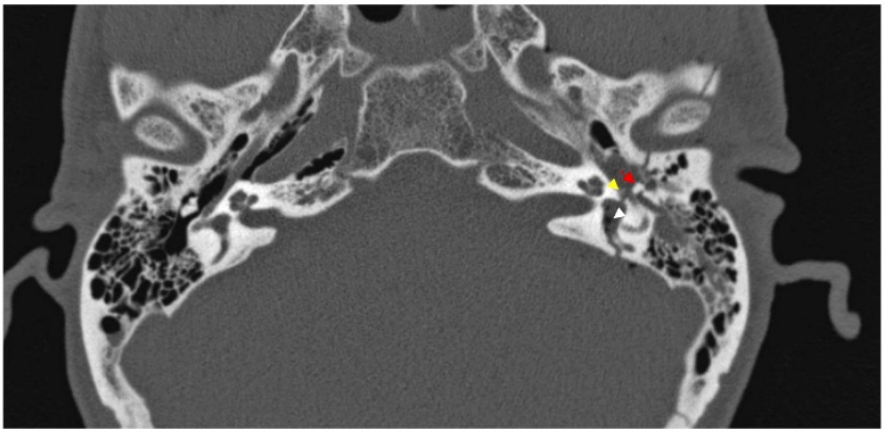

Transverse fracture with otic capsule involvement (posterior semicircular canal, vestibule) Air bubbles are seen within the vestibule (white arrowhead). Fracture lines extend through the tympanic segment of the facial nerve (yellow arrow). There is also an incudomalleolar dislocation (red arrow). Fracture line through the anterior and posterior condylar fossa walls. Blood products are seen at the left mastoid air cells and middle ear cavity.

Primary Optic Nerve Germinoma

48 Primary Optic Nerve Germinoma

DK Hill, L Eckel, K Schwartz, F Diehn

Mayo Clinic Rochester
United States

Purpose: This educational exhibit describes a rare case of a primary left optic nerve germinoma tumor in a 19-year old male presenting with diabetes insipidus, headaches, and progressive vision loss. Germ cell neoplasms are rare, accounting for 0.1% to 3.5% of all intracranial tumors, and are known to occur predominantly in the sella, pineal gland, and basal ganglia. Previously, there have only been 2 reported cases of intraorbital optic nerve germinomas, and 8 optic chiasmal germinomas. Of the reported optic chiasm germinoma cases, 100% suffered from visual deficits, 50% were diagnosed with diabetes insipidus, and 62.5% reported some form of endocrine abnormality. The previously reported cases of intraorbital optic nerve germinomas presented with vision loss only without endocrine abnormalities. Our case is unique in that this is the first reported germinoma affecting only the intraorbital optic nerve with associated endocrine abnormalities. Description: A 19-year old male presented with four years of progressively worsening headaches, left vision loss, and diabetes insipidus. His vision loss responded to steroid therapy for approximately one year, improving from 20/300 to 20/115, but has progressively worsened since then. He reports drinking several gallons of fluid daily resulting in difficulties in school from frequent urination and incontinence. Due to worsening symptoms, he underwent a head MRI which demonstrated left optic nerve enlargement and enhancement extending from the globe to the orbital apex. No abnormalities of signal or enhancement of the sella, infundibulum, chiasm, hypothalamus, or pineal region were present. Hematologic studies were significant for a mildly elevated prolactin of 17.4, and low urine osmolality of 117. He subsequently underwent an incisional biopsy of the left optic nerve with pathology consistent with germinoma. Summary: Germinomas involving the optic nerve and chiasm are rare. With involvement of the optic chiasm, there are associated endocrine abnormalities more than 50% of the time. This is the first reported case demonstrating endocrine abnormalities in a germinoma isolated to the orbital optic nerve. MRI findings alone yield a broad differential diagnosis including optic glioma, optic neuritis, meningioma, or pseudotumor. When seen in the setting of endocrine abnormalities, germinoma should also be considered in the differential.

Chaudhry NS, Ahmad FU, Whittington E, Schatz N, Morcos JJ. Primary intrinsic chiasmal germinoma. J Neuroophthalmol. 2015 Jun; 35(2):171-4.

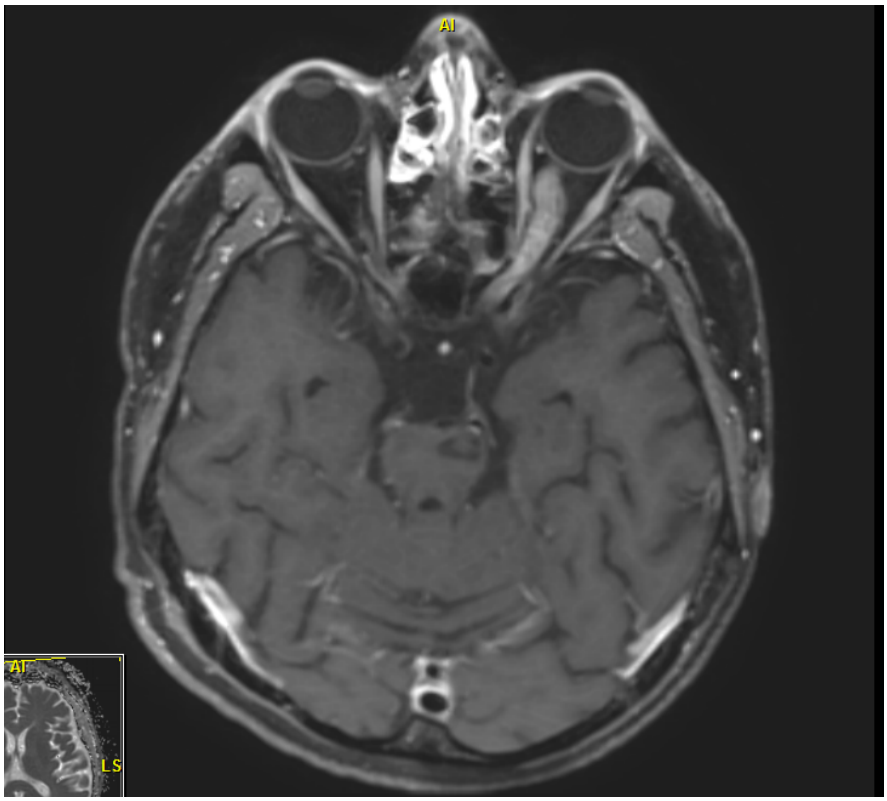
AI
AI
LS

Eye Popping Tumors: Review of Aggressive Orbital Tumors

49 Eye Popping Tumors: Review of Aggressive Orbital Tumors

T Li, D Pranav, V Starcevic, B Griffith, M Patel

Henry Ford Hospital
United States

Purpose: Our presentation aims to review uncommon aggressive orbital neoplasms and review the various predominantly CT and MRI imaging characteristics of patients from our institution. Description: We present 8 patients with aggressive Orbital neoplasms derived from our institution at Henry Ford Hospital in Detroit. We initially review normal anatomy orbital anatomy in a mostly pictorial review. We will then present mainly CT and MRI images of various aggressive orbital neoplasms and detail the findings and in some cases follow-up imaging to demonstrate disease course/progression . Uncommon neoplasms reviewed will include Malignant Fibrous Histiocytoma. Squamous Cell Carcinoma of the lacrimal gland, Hemangiopericytoma, Granulocytic Sarcoma, Undifferentiated carcinoma, Chondrosarcoma, Lymphoma and Ocular Melanoma. We will highlight imaging features that will aid in differentiating one neoplasm from another when possible, diagnostic pitfalls and discuss differential diagnosis. Summary: Imaging findings obtained from cross-sectional imaging such as CT and MRI provide valuable information and aid in the diagnosis of various orbital neoplasms. While many imaging findings can overlap between neoplasms and other inflammatory process certain key imaging figures can help in differentiation. Other neoplasms will require histologic confirmation, nevertheless imaging provides valuable information on extent of disease, staging, and aid in determining prognosis.

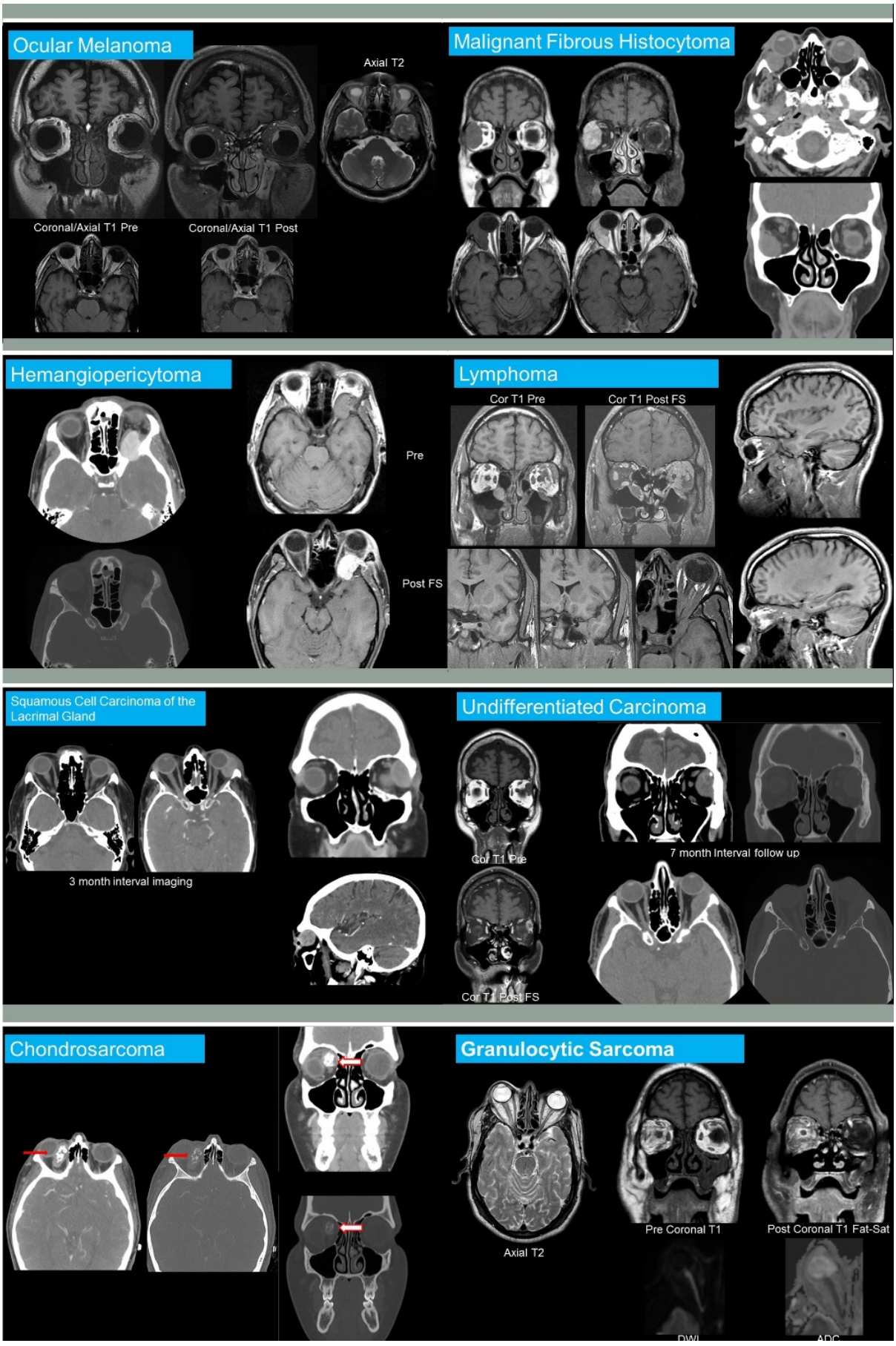
Ocular Melanoma
Axial T2
Coronal/Axial T1 Pre
Coronal/Axial T1 Post
Malignant Fibrous Histocytoma
Hemangiopericytoma
Pre
Post FS
Lymphoma
Cor T1 Pre
Cor T1 Post FS
Squamous Cell Carcinoma of the Lacrimal Gland
3 month interval imaging
Undifferentiated Carcinoma
Cor T1 Pre
7 month interval follow up
Cor T1 Post FS
Chondrosarcoma
Granulocytic Sarcoma
Axial T2
Pre Coronal T1
Post Coronal T1 Fat-Sat
DWI
ADC

Teeth that don't bite : A rare case of masticator space odontome

50 Teeth that don't bite : A rare case of masticator space odontome

J Kumar, A Mehndiratta, A Garg

MAULANA AZAD MEDICAL COLLEGE
India

LEARNING OBJECTIVE: To report a case of extragnathic odontome of masticator space and to highlight that imaging is the key to diagnosis. CASE SUMMARY: Odontomes are the most common benign tumors accounting for 22% of all odontogenic tumors of the jaws. Odontomes occurring in sites other than the jaws are extremely rare. Existing literature reveals few cases of extragnathic odontomes involving intracranial regions, middle ear, nasopharynx and mastoid. We present a rare case of extragnathic odontome involving the masticator space. Patient is an 8-year-old boy who presented with difficulty in speech. Oral examination revealed bilateral palatal palsy and a slight bulge on right side pushing the soft palate. The radiographs showed an irregular shaped radio-opacity abutting the right maxilla. NCCT face revealed radiopaque teeth-like structures with a thin capsule in the right masticator space. However, rest of the visualized teeth were grossly normal. The patient also had hypoplastic coronoid processes of mandible bilaterally with heterotopic bone in bilateral infratemporal fossa. To our knowledge, this is the first case report of odontome involving the masticator space. CONCLUSION: Extragnathic odontome is a clinicoradiological diagnosis which may present with unusual symptoms and may go undiagnosed for long periods unless imaging is carried out.

Tracing the dots and lines : Ossicular and facial nerve anomalies in congenital aural atresia

51 Tracing the dots and lines : Ossicular and facial nerve anomalies in congenital aural atresia

J Kumar, R Gautam, G Pradhan, J Passey, R Meher

MAULANA AZAD MEDICAL COLLEGE
India

LEARNING OBJECTIVES: The aim of this review is to delineate ossicular and facial nerve abnormalities found in patients with congenital aural atresia using High Resolution Computed Tomography. BACKGROUND: Congenital aural atresia is a common congenital anomaly in the clinics of otology. Patients present with varying degrees of microtia and hearing loss which may impede their speech, language and cognitive development. Various ossicular and facial nerve anomalies are associated with it. Thus, high resolution computed tomographic evaluation of the ossicular anatomy and facial nerve course is essential in guiding the selection of candidates, who will gain benefit from hearing aid implants or corrective surgeries. IMAGING FINDINGS: The patients presenting with microtia are imaged using high resolution computed tomography. Various anomalies of ear ossicles and facial nerve that may be associated with congenital aural atresia are: Stapes • Foot plate fixation • Absence of stapes superstructure • Absence of stapes Incus • Hypoplasia or Aplasia of long process of incus • Posterior fixation of long process of incus • Absence of icudo-stapedial articulation • Fibrous incudostapedial joint Malleus • Absence of malleo-incudal complex(deformity or dislocation) • fusion of malleus and incus • manubrium- short and curved or absent • fixation of the head of the malleus to the epitympanic wall • malleus neck fused to atretic plate • abnormal orientation of handle of malleus with increased distance from promontory Facial nerve anomalies • anterior displacement of posterior genu and mastoid segment • tympanic part running across oval window • exit of mastoid part of facial nerve at skull base displaced to enter into TMJ • bifurcation of one or more segments of facial nerve • facial canal dilatation CONCLUSION: Imaging plays a crucial role in delineating ossicular and facial nerve anomalies in patients with congenital aural atresia which further helps in planning appropriate management and improving hearing and speech outcome in such patients.

Internal carotid artery dissection presenting with hypoglossal nerve palsy

52 Internal carotid artery dissection presenting with hypoglossal nerve palsy

AC Tsai, S McNally, R Wiggins, E Quigley

University of Utah
United States

We present the case of a 59-year-old male who presented with approximately one weeks' history of left neck pain, dysphagia, speech slurring, and twelfth cranial nerve palsy on examination. The initial MRI, which was skull base protocol for the evaluation of cranial nerves, showed abnormal T1 and T2 signal surrounding the left carotid sheath and no evidence of hypoglossal nerve denervation effect. Subsequent CT angiography demonstrated a dissection with intramural hematoma involving a long segment of the left internal carotid artery (ICA), including extra- and intracranial segments. The patient was also noted to have dissections involving multiple other cervical arteries, raising the question of an underlying vasculopathy. Imaging findings at MRI and CTA in ICA dissections are discussed. The uncommon presentation as well as proposed pathophysiology of cranial palsy in ICA dissection are discussed.

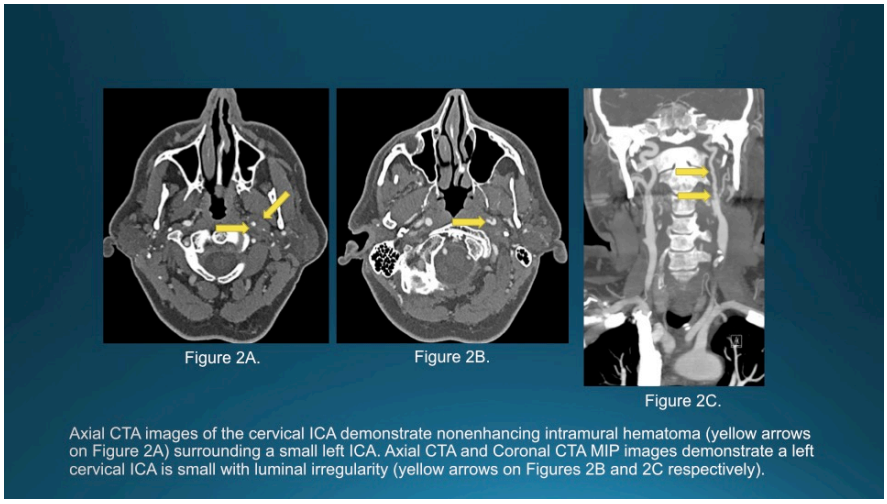

Uncommon intraorbital tumors: clinical, radiological and pathological correlation

53 Uncommon intraorbital tumors: clinical, radiological and pathological correlation

H Lee, M Siddiqi, EA Nimchinsky

Rutgers University, New Jersey Medical School
United States

Purpose: The orbit is a complex structure containing the optic nerve, muscles, fat, vessels, and connective tissues. The most common adult orbital masses are lymphoid tumors, metastatic disease, and cavernous malformations. Other masses commonly arise from surrounding structures and metastatic lesions. We present 7 uncommon intraorbital tumors representing a range of cell types, with often overlapping appearances. Methods We did a retrograde review of 7 cases of pathologically proven uncommon intraorbital masses. All patients underwent CT and/or MRI examination. Clinical, imaging and pathologic correlation is presented. Findings: All the described masses were well circumscribed, rounded or cone-shaped, with mass effect. Both Schwannomas and malignant peripheral nerve sheath tumors (MPNSTs; malignant neurolemmomas) appeared as T2 hyperintense, avidly enhancing masses, essentially indistinguishable on imaging. Neither was associated with bony destruction. Solitary fibrous tumor was associated with bony remodeling. Chondrosarcoma, in contrast, demonstrated significant osseous erosion as well as internal calcifications not seen in other masses. Adenoid cystic carcinoma of the lacrimal gland was notable for edema in the surrounding tissues, which was not seen with most other masses. Cystic epithelial choristoma was distingished by a fat-fluid level, easily seen on CT. Metastatic gastric carcinoma in a patient with no gastric symptoms demonstrated no characteristic features on imaging, and the primary tumor itself was only identified following orbital biopsy. Discussion: In adults, cavernous malformations are the most common benign primary orbital mass, appearing as well-circumscribed, enhancing masses in the intraconal or extraconal orbit. We present seven uncommon orbital masses, all of which also presented as well-circumscribed orbital masses. Some of these have imaging characteristics that may aid in their identification, but many are nearly indistinguishable on imaging. Schwannomas are rarely seen in the orbit, and account for 1-4% of intraorbital tumors. When present, they most commonly arise from branches of the fifth nerve. MPNSTs, which are extremely uncommon in the orbit, may be more aggressive, but may be indistinguishable from benign Schwannomas. Solitary fibrous tumor is a spindle cell neoplasm of mesothelial surfaces, with relatively few cases described in the orbit, although it may be more common than previously thought. Cartilagenous lesions are believed to account for less than 1% of orbital masses, and chondrosarcoma, a rare but aggressive tumor, may cause significant osseous destruction. Calcifications may help in its identification. Adenoid cystic carcinoma, constituting approximately 5-7% of orbital masses, is the most common malignancy of the lacrimal gland and may be indistinguishable from pleomorphic adenoma. Choristomas are congenital benign, proliferative masses, including dermoids and epidermoids. While common in children, they constitute less than 10% of orbital masses overall. Consisting of a cystic mass with an epithelial lining, they may present as cystic or partially cystic intraorbital lesions. Metastases from other malignancies represent 1-13% of orbital masses. The most common orbital metastasis are of breast origin, and gastrointestinal malignancies account for only 2% of orbital masses. Despite their vastly different origins, a wide range of orbital lesions may have a similar radiologic appearance, emphasizing the importance of tissue sampling for diagnosis.

Multimodality Appearance of Mastoiditis and Potential Associated Complications

54 Multimodality Appearance of Mastoiditis and Potential Associated Complications

M Cai, M Cedillo, N Voutsinas, P Som

Mount Sinai Department of Radiology
United States

Purpose: The purpose of this educational exhibit is to discuss a multimodality imaging approach to diagnose acute mastoiditis and the use of CT and MR venography for evaluating dural sinus thrombosis, a known complication. Description: The presentation will introduce mastoiditis by first discussing the pathogen etiologies including bacterial, fungal, and tuberculous. Radiographic features of mastoiditis will be highlighted using cases featuring both CT and MR imaging. Dural sinus thrombosis will also be characterized through both CT and MR venography. CT and MR imaging examples of other known complications will be included. Summary: Acute mastoiditis is most commonly a pediatric disease which occurs when acute otitis media spreads into the mastoid air cells. Diagnosis is critical as the complications can be life threatening, but early diagnosis prior to appearance of complications can lead to treatment with antibiotics alone. Mastoiditis typically is caused by bacterial etiologies, most commonly Streptococcus pneumoniae. More rare etiologies can be associated with other complications, for example H. influenzae meningitis and aspergillus associated facial nerve dysfunction. CT is the best initial study for evaluation of suspected mastoiditis and will demonstrate opacification of the mastoid air cells and possibly the middle ear cleft. More aggressive cases will also demonstrate erosion of the bony structures such as the bony septum. Contrast enhanced imaging is useful to evaluate for dural venous thrombosis, overlying subperiosteal abscesses, temporal bone osteomyelitis (rare), and intracranial extension which is manifest as meningitis, empyema, or cerebral abscess. MRI can help confirm the diagnosis as there should be evidence of soft tissue enhancement or diffusion restriction associated with mastoid air-cell fluid signal. CT and MR venography can be used in conjunction to evaluate for dural sinus thrombosis. Sinus thrombosis usually occurs secondary to intracranial extension of infection which is usually seen as post-contrast enhancement extending to the dural sinuses. MR venograms can be performed as non-contrast 2-D time of flight images, which can then be processed into thicker maximum intensity projections (MIPs).

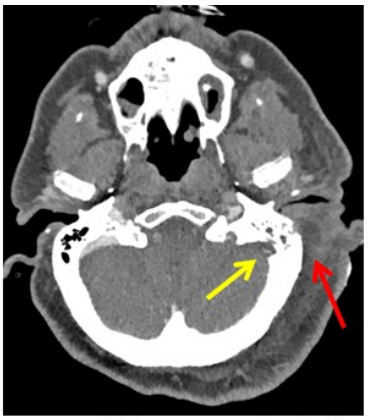

Narrowed left transverse sinus (yellow arrow) subjacent to the collection (red)

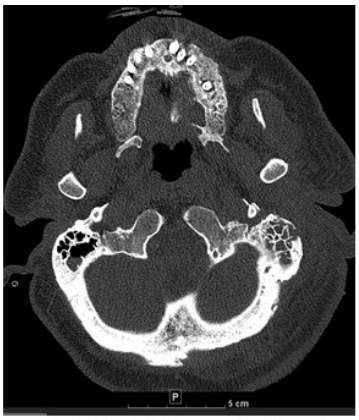

Fluid filled left mastoid air cells with adjacent bony destruction

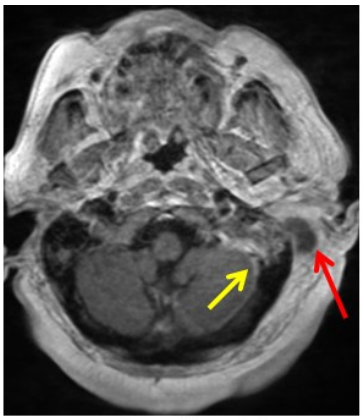

Contrast enhanced T1 axial MRI showing enhancement adjacent to the narrowed left traverse sinus (yellow arrow), which may be inflammatory changes secondary to the overlying collection (red arrow).

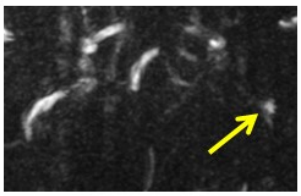

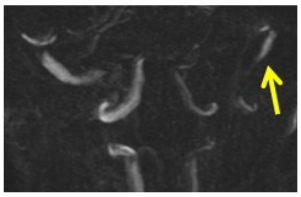

MR Venogram Imaging

Top: Axial 15mm slice multiplanar reconstruction
Bottom: Coronal 15 mm slice multiplanar reconstruction

MR venogram demonstrate a filling defect in the left sigmoid sinus. The left distal transverse sinus (yellow arrow) tapers down prior to the filling defect.

Training A Deep Learning System to Classify Pathology on CT Sinus Scans

55 Training A Deep Learning System to Classify Pathology on CT Sinus Scans

R Lufkin

UCLA
United States

PURPOSE: Deep learning artificial intelligence with convolutional neural networks has been shown to exceed human performance in certain complex visual recognition tasks. Training these networks for applications in radiology requires specialized software and large amounts of data. We describe the use of available tools to develop a deep learning system in classification of CT sinus pathology. MATERIALS AND METHODS: We used a commercially available medical AI development platform [dmed.ai, Santa Monica, CA]. A standard neural network architecture template was selected from several choices with the input matrix size matching CT sinus scans. The default hyperparameters were selected and then modified as training progressed. A standard CT sinus database with various pathologies labeled was selected from several radiology database options. The data was completely anonymized and no identifiable patient information was included. The model was trained using 50% of the data with the remaining amount set aside for validation testing. Two different network performance levels were selected for review. RESULTS: The networks were able to be trained to recognize and exclude a number of pathologies. Examples of various pathology and the classification rates are described. Performance tradeoffs versus parameters chosen were also evaluated. CONCLUSION: It is possible to train deep learning systems to classify pathology on CT sinus scans using commercially available tools. Further investigation is warranted.

Pediatric inner ear anomalies in genetic syndromes and multisystem associations

56 Pediatric inner ear anomalies in genetic syndromes and multisystem associations

KS Traylor, S Dodson, R Radhakrishnan, SF Kralik, CY Ho

Indiana University School of Medicine
United States

Purpose: To provide an overview of the many different inner ear anomalies seen in various pediatric syndromes, as well as, the inner ear anomalies that are isolated and related to certain known genetic mutations. Description: This educational exhibit will discuss inner ear anomalies known to be associated with pediatric syndromes including cochlear hypoplasia, semicircular canal hypoplasia/aplasia, and semicircular canal-vestibular globular anomalies. These inner ear anomalies have been associated with the following syndromes: Branchio-otorenal syndrome, CHARGE syndrome, Down's syndrome, Waardenburg syndrome, Alagille syndrome, Apart Syndrome, Trisomy 21, Pendred Syndrome, and 22q11.2 deletion syndrome. Furthermore, several genetic mutations that result in isolated inner ear anomalies will also be discussed, including: labyrinthine aplasia, common cavity malformation, cochlear incomplete partition type II, large vestibular aqueduct, and the stapes gusher. If one of these findings is identified on routine imaging, the neuroradiologist must search for additional findings that may provide the only clue to the patients underlying syndrome or genetic mutation. Summary: This educational exhibit provides an overview of inner ear anomalies that are

Retrospective Review of Otic Capsule Contour and Thickness in Otosclerosis and Normal-Hearing Patients on CT

57 Retrospective Review of Otic Capsule Contour and Thickness in Otosclerosis and Normal-Hearing Patients on CT

N Sanghan, T Chansakul, ED Kozin, HD Curtin, KL Reinshagen

Department of Radiology, Prince of Songkla University
Thailand

Purpose: Otosclerosis is commonly identified on CT as a focus of hypodensity in the otic capsule (OC) anterior to the oval window (OW). However, otosclerosis can have a sclerotic phase, approximating the density of normal bone making diagnosis challenging. This study assesses differences in OC contour and thickness anterolateral to the anterior margin of the oval window in otosclerosis compared to normal-hearing patients. Materials and Methods: Axial CT of 104 ears with clinically-diagnosed otosclerosis and 108 consecutive ears of audiometrically-normal individuals were retrospectively reviewed. Two radiologists independently evaluated the pattern of otosclerosis, OC contour and bone thickness on standardized axial images at the level of the OW and cochleariform process (CP). Measurements were made from the posterolateral margin of the cochlea to the most convex contour of the OC just anterolateral to the anterior margin of the oval window. In the absence of a convex contour, the sulcus between the OW and CP was identified, and measurement to the depth of the sulcus was used. ROC analysis determined the best cutoff value of OC thickness. Results: Mean OC thickness (2 standard deviations) was 3.08 (0.93) mm and 1.82 (0.31) mm in otosclerosis and normal-hearing patients, respectively (p-value < 0.001) with excellent interobserver agreement. OC thickness > 2.3 mm had 96.2% sensitivity, 100% specificity, 100% PPV, and 96.4% NPV for otosclerosis. Bulging/convex contour of the OC had 68.3% sensitivity, 98.1% specificity, 97.3% PPV, and 76.3% NPV. Conclusion: Using a standardized axial plane parallel to the lateral semicircular canal, bulging or convex contour of the otic capsule relative to a line drawn between the anterior margin of the oval window and the cochleariform process occurred with high specificity and positive predictive value in patients with otosclerosis. Thickness of the otic capsule along the anterior margin oval window at the level of the cochleariform process is significantly thicker in otosclerosis patients compared with normal-hearing individuals. Use of a quantitative assessment of the otic capsule may help the radiologist accurately diagnose otosclerosis.

Quiz Yourself on Pediatric ER Neck CT: Don't-Miss Diagnoses for Residents on Call

58 Quiz Yourself on Pediatric ER Neck CT: Don't-Miss Diagnoses for Residents on Call

A Farkas, M Jordan, E Parker, D Joyner

University of Mississippi Medical Center
United States

Purpose: Interpretation of soft tissue neck CT of the pediatric patient can be a challenging task for novice residents on call. As imaging is often used to evaluate pediatric patients in the emergency department and clinicians rely on imaging to direct management, it is crucial that residents are familiar with critical finding to correctly interpret and rapidly communicate findings to providers. This interactive exhibit will provide an overview of pertinent imaging findings and important clinical features of not-to-miss diagnoses on pediatric soft tissue neck CT ordered from the emergency department at a tertiary care center. Description: This exhibit is an interactive case-based review of common and uncommon pediatric soft tissue neck CT diagnoses encountered on call from the emergency department of a busy tertiary care center. The cases will include the spectrum of those encountered from the emergency department, from acute infectious/inflammatory processes and trauma to other processes that are not considered emergent, but which are evaluated in the emergency department. Cases will include orbital cellulitis, Pott's puffy tumor, Ludwig's angina, epiglottitis, peritonsillar abscess, Bezold abscess, and suppurative lymphadenitis. Cases will be presented as unknowns with subsequent explanation of key findings, follow-up questions, and key clinical points presented. Basic anatomy with emphasis on spaces will be reviewed for each case. The presentation will be optimized for viewing on mobile phones and tablets as well as computer viewing stations. Summary: After review of this interactive exhibit, residents will have an increased familiarity and comfort level with diagnoses encountered on pediatric soft tissue neck CTs performed on an emergent basis.

Mandibular condyle fractures : A pictorial review

59 Mandibular condyle fractures : A pictorial review

J Kumar, A Mehndiratta, A Manchanda, S Mohanty

MAULANA AZAD MEDICAL COLLEGE
India

LEARNING OBJECTIVES: Various classification systems describing mandibular condylar fractures have been developed and published. The universal application of a single classification system is highly controversial, if not impossible, because of variability in terminology, grammatical differences, native language challenges, and regional preferences for a specific system. Lindahl published the most comprehensive description of mandibular condylar head fractures to date within the literature. Hence, we have used this system to classify all cases presenting with condylar fractures. BACKGROUND: Although the condylar process of the mandible locates away from the direct traumatic insults, it is a structure with frequent facial traumatic injury. The forceful impact brings the fracture at this long thin anatomical structure by the transmission of the traumatic forces. It might be categorized as one of the controversial fractures in its diagnosis and management for facial bone fractures. Many radiological modalities have been used in the past for evaluation and classification of condylar fractures such as plain radiographs, OPG, etc but computed tomography is now considered the mainstay for complete evaluation and classification of injury. IMAGING FINDINGS The images were analysed on the following parameters according to the Lindahl's classification: • 1: Fracture level o 1a: condylar head o 1b: condylar neck o 1c: subcondylar/condylar base • 2: Deviation and displacement o 2a: bending/deviation with medial overlapping segments o 2b: bending/deviation with lateral overlapping segments o 2c: bending/displacement without overlapping o 2d: nondisplaced fracture without deviation • 3: Relation between condylar head and fossa o 3a: no dislocation o 3b: slight dislocation o 3c: moderate dislocation o 3d: severe and/or complete dislocation • 4: Condylar head fracture o 4a: horizontal o 4b: vertical o 4c: compression fracture CONCLUSION: Computed tomography is the gold standard for evaluation of such injuries. Radiologist plays a key role in deciding the operative/ non-operative management of these patients and a descriptive standardized classification system is the need of hour.

Looking Beyond the Ear: Demystifying Secondary Otalgia

60 Looking Beyond the Ear: Demystifying Secondary Otalgia

C Norris, AJ Stuckey, KS Traylor, S Burgin, K Mosier, NA Koontz

Indiana University School of Medicine
United States

Purpose: The first-line evaluation of otalgia is otoscopy. However, when otoscopy is normal, secondary causes for referred otalgia must be evaluated. Often, imaging of the inner ear/temporal bone, temporomandibular joint (TMJ), neck, and/or brain via CT or MR are useful to evaluate pathologies that may be responsible for causing referred ear pain (secondary otalgia). The purpose of this exhibit is to review common and uncommon secondary causes of otalgia, and the typical imaging characteristics thereof. Description: Secondary otalgia is a complex diagnostic dilemma because the sensory innervation of the ear involves several different nerves. The auricle is innervated by cranial nerves V, VII, and X; the external auditory meatus and canal by cranial nerves V, VII, and X; the tympanic membrane by cranial nerves VII, IX, and X; and the middle ear by cranial nerves V, VII, and IX. Scrutiny of each aforementioned cranial nerves must be conducted from the level of the primary nucleus to the end organ. Additionally, portions of the auricle are also innervated by cervical nerves C2 and C3, necessitating inspection of the cervical spine. If examination of the nerves yields no definitive abnormalities, then further interrogation of the anatomic structures sharing the same ganglia and second order neurons is warranted. In accordance with the policies of the institutional review board, a HIPAA-compliant retrospective search was performed using a database of all radiologic exams performed at our institution. We present an image-rich collection of cases that highlight important degenerative, neoplastic, infectious, and inflammatory etiologies of secondary otalgia, as well as a review of the current medical literature. Summary: When otoscopy is normal in patients with ear pain, causes of secondary otalgia must be sought out. Generally, the next diagnostic step is cross sectional imaging of the head and neck, including consideration of specialized protocols and targeted anatomic scans to better assess specific etiologies of referred otalgia. Knowledge of the common etiologies of secondary otalgia can help the radiologist add diagnostic support to the primary physician when otoscopy is normal.

References: 1. Earwood JS et al: Ear Pain: Diagnosing Common and Uncommon Causes. Am Fam Physician. 97(1):20-27, 2018 2. Lecler A et al: TIPIC Syndrome: Beyond the Myth of Carotidynia, a New Distinct Unclassified Entity. AJNR Am J Neuroradiol. 38(7):1391-1398, 2017 3. Harrison E et al: Otalgia. Aust Fam Physician. 45(7):493-7, 2016 4. Petscavage-Thomas JM et al: Unlocking the Jaw: Advanced Imaging of the Temporomandibular Joint. AJR Am J Roentgenol. 203(5):1047-1058, 2014 5. Kim DS et al: Dental otalgia. J Laryngol Otol. 121(12):1129-34, 2007 6. Kuttila S et al: Characteristics of subjects with secondary otalgia. J Orofac Pain. 18(3):226-34, 2004 7. Weissman JL: A pain in the ear: the radiology of otalgia. AJNR Am J Neuroradiol. 18(9):1641-51, 1997 8. Schellhas KP: Temporomandibular joint injuries. Radiology. 173(1):211-6, 1989

Rare cause for orbital mass in an African American female

61 Rare cause for orbital mass in an African American female

A Pathrose, S Gupta, J Keshavamurthy

Madras Medical College
India

Introduction: While sarcoidosis is a disease process that classically affects the lung parenchyma, the presentation of sarcoidosis can be extrapulmonary in up to 30% of the cases. Essentially any organ can be involved in sarcoidosis; however, particular patient populations and risk factors are associated with varying extrapulmonary sarcoidosis involvement. In particular, orbital sarcoidosis has been shown to be more common in women who are at least 50 years old although it still rarer than other common ophthalmic involvement such as uveitis (approximately 25-60% of patients with systemic sarcoidosis). Furthermore, orbital involvement as a presentation of sarcoidosis has had few reported cases with conflicting statistics on incidence. Case: A 59-year-old African American female with a past ophthalmologic history of cataract extraction was referred to oculoplastic surgery from her optometrist for post-traumatic pain and pressure surrounding her left eye lasting over a month with a gradual increase in symptoms. She also described increased proptosis, unilateral lacrimation, and a burning sensation upon downward gaze. Prescription ophthalmic NSAID drops provided minimal relief of symptoms. Upon review of systems, pertinent positives included dizziness and a sense of balance issues. Physical exam was notable for left-sided proptosis, hyperglobus, lagophthalmos, and a palpable mass inferotemporally and superonasally. Preliminary differential diagnosis included lymphoma versus metastatic lesions. CT scan of the orbits revealed diffuse inflammatory process surrounding the left orbit with pre-septal and post-septal involvement. An orbitotomy without bone flap procedure allowed for biopsy of the periorbital tissues with pathology results of a non-necrotizing granuloma with mild non-clonal lymphoplasmacytic infiltrate. Findings were highly suggestive of extra-pulmonary sarcoidosis. Subsequently, CT scan of the thorax was performed which revealed an 8 mm left, upper lobe pulmonary nodule and enlarged middle mediastinal lymph nodes. The patient has been referred to pulmonology for biopsy of the pulmonary nodule to assess for pulmonary sarcoidosis. Currently, the patient is being treated with oral prednisone. Discussion: This case provides evidence for maintaining a broad, yet critical differential diagnosis. Because sarcoidosis can present in a variety of locations, mimicking many other disease processes, it should be considered in the differential, particularly in relevant patient population, particularly in African American populations, and within endemic areas, such as the CSRA. Regarding management of orbital sarcoidosis, the treatment plan is dependent upon the presence or absence of systemic disease. In most cases, systemic steroid administration is the preferred method as it concurrently treats any other organ involvement of sarcoidosis. However, in the absence of systemic disease, intralesional injection of steroids has been shown to be effective as well. Surgical excision has not been proven to be an effective method due to the recurrence of disease and the risk of structural damage to the orbit.

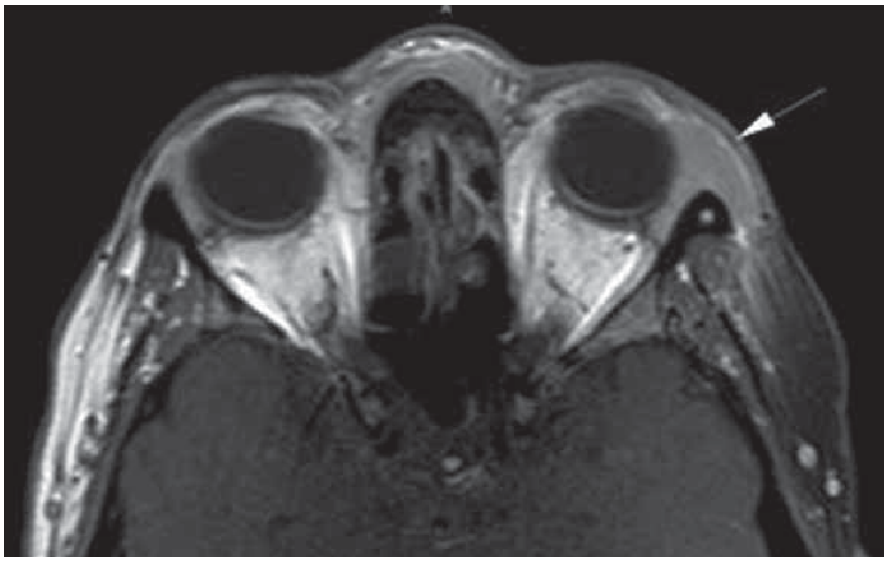

A New Approach to Facial Fullness: Extensive Five Year Institutional Review of Lesions of the Parotid Gland and Their Intimate Association with the Facial Nerve.

62 A New Approach to Facial Fullness: Extensive Five Year Institutional Review of Lesions of the Parotid Gland and Their Intimate Association with the Facial Nerve.

JD Gupta, ND Gupta

Southeastern Louisiana Veterans Healthcare System
United States

Purpose: The purpose of the project is to do an extensive review of all diverse pathology effecting the parotid glands as noted at our institution over a five year period with specific detail on underlying anatomy, morphology, physiology, treatment of the presenting parotid lesion and with additional specific emphasis on the relation of the primary parotid lesion to the underlying facial nerve. Our hope is to do a detailed imaging and anatomical review of the facial nerve as it affects all parotid lesions so as to augment and enhance a further value added report for referring head and neck surgeons and other treating referring physicians. Our ultimate goal is for decreased morbidity secondary to facial nerve injury post surgery by offering a more detailed pre operative imaging evaluation of the parotid lesion in association with the facial nerve. Approach/Methods: A series of diverse parotid gland pathology from over a five year period will be collected from our institution and all imaging will be reviewed and presented. We will do a detailed review of the anatomy, imaging course, and morphology of the facial nerve as it intimately affects the parotid gland and soft tissues. We will correlate facial nerve anatomy and facial nerve interaction with cases that we present from our institution with additional emphasis on pre surgical, surgical, and post surgical documentation so that we can further devise a system to enhance imaging reports to help decrease morbidity from facial nerve injury and help our surgeons with surgical planning. In summary, we will present a representative group of parotid gland lesions to review parotid gland pathology, then will focus on the facial nerve anatomy and its relation with the parotid gland, and finally we will marry both topics for a complete analysis. Findings/Discussion: A more detailed anatomical descriptive imaging report of diagnosed parotid gland pathology with specific detail on interaction with surrounding soft tissues to include deep and superficial parotid gland lobe, parapharyngeal fat space, lymph nodes, osseous structures, vascular structures, and specifically detailing the potential interaction of the facial nerve with the parotid gland lesion by reviewing and understanding the intimate detailed course of the facial nerve led to better value added radiology reports, improved pre surgical planning by the Head and Neck surgeon, decreased patient morbidity and mortality, and led to an overall improved patient experience. Summary: Upon reviewing our collection of parotid gland cases with review of the underlying facial nerve anatomy, it became imperative that understanding the intimate course of the facial nerve and its interaction with the parotid gland resulted in improved valued added radiology reports, improved surgical planning by our Head and Neck Surgeons, decreased patient morbidity and mortality specifically revolving around the facial nerve, and improved patient experience in patients. It is imperative that the interpretating Neuroradiologist have an exquisite understanding of the facial nerve as it interacts with the underlying parotid gland lesions before interpretation. We hope to give a concise but detailed review for our Neuroradiology colleagues.

Visualization of the lower cranial nerves within the carotid sheath: usefulness of three-dimensional double-echo steady-state with water excitation (3D-DESSWE) MR imaging

63 Visualization of the lower cranial nerves within the carotid sheath: usefulness of three-dimensional double-echo steady-state with water excitation (3D-DESSWE) MR imaging

Y Kim, H Kim, M Seong, Y Kim, S Kim

Department of Radiology, Samsung Medical Center, Sungkyunkwan University School of Medicine Republic of Korea

Purpose: To evaluate the normal appearances of the lower cranial nerves (LCNs) within the carotid sheath (CS) using three-dimensional double-echo steady-state with water excitation (3D-DESSWE) MR imaging. Materials and Methods: We evaluated 3D-DESSWE images in 50 subjects (M:F=23:27; mean age, 53 years; range, 21-74 years) without signs of LCN dysfunction using a 3T MR scanner (Skyra; Siemens). Axial images were obtained from the medulla to the hyoid bone by using a 32-channel head coil with the following parameters: TR/TE=13.62/5ms, FA=30°, FOV=200x200mm, matrix=384x250, effective section thickness=0.5mm, slab thickness=10.4cm, and scan time=5m 39s. We also generated axial, sagittal, and coronal thin slab MIP images (3-mm thick) from the axial source images. One hundred each of LCNs (CN IX-XII) for either side were assessed by the consensus of two neuroradiologists on 3D-DESSWE images with focus on the visibility and course of the nerves within the CS. The visibility of the nerves was graded with a 4-point scale: grade 4, the whole course of the nerve continuously traceable; grade 3, the course of the nerve minimally discontinuous but still well traceable; grade 2, the course of the nerve severely discontinuous and mostly untraceable; and grade 1, the whole course of the nerve hardly visible. We regarded the nerves with grade 3 or 4 as visible, while those with grade 1 or 2 as invisible. Results: Of 100 nerves each, the visibility of LCNs within the CS was 91% for CN IX (grade, 3.66±0.78 [mean±SD]), 96% for CN X (grade, 3.81±0.56), 96% for CN XI (grade, 3.83±0.51), and 99% for CN XII (grade, 3.88±0.36) on 3D-DESSWE images. Only 5 nerves were assessed as grade 1 including 2 CN IX, 2 CN X, and 1 CN XI. CN IX entered the CS first among 4 LCNs. Within the CS, it passed forward between the internal carotid artery (ICA) and internal jugular vein (IJV). CN IX also left the CS first, coursing between the lateral aspect of ICA and stylopharyngeus muscle. CN X was the only nerve that did not leave the CS, once it entered the sheath. It maintained the constant position within the CS behind and between the ICA and IJV. CN XI entered the CS lateral to CN X. Within the CS, it coursed either anteriorly or posteriorly in relation to the IJV. Of 96 nerves visible on MR images, 40 and 56 nerves passed anterior and posterior to the IJV, respectively. CN XI was the only nerve that coursed in the posterolateral direction after the exit from the CS. CN XII entered the CS last among 4 LCNs at the most medial aspect of the CS. Within the CS, it moved laterally behind CN X, hooked around CN X, and then coursed in anterolateral direction between the ICA and IJV. CN XII left the CS, coursing between the lateral aspect of the ICA and posterior belly of the digastric muscle. Conclusion: 3D-DESSWE MR imaging is useful for evaluating the anatomy of the LCNs within the CS.

Characteristic CT and MR findings of odontogenic keratocysts in the maxillomandibular region: 159 cases.

64 Characteristic CT and MR findings of odontogenic keratocysts in the maxillomandibular region: 159 cases.

Y Kawashima, O Sakai, S Masaaki, K Kuyama, T Kaneda

Department of Radiology, Nihon University School of Dentistry at Matsudo
Japan

Backgrounds: Odontogenic keratocyst (OKC) is an odontogenic cyst characterized by a thin, regular lining of parakeratonized stratified squamous epithelium with palisading hyperchromatic basal cells. OKCs account for 10-20% of odontogenic cysts and are the third most common cyst of the jaws. They occur over a wide age range, with a peak incidence in the second to third decades of life and a second smaller peak among patients aged 50-70 years. Most studies find a slight male prediction. OKCs are most frequently found in the mandible, with as many as half of the lesions located in the posterior mandibular body and ramus. Radiographs show well-demarcated radiolucent lesions, often with corticated margins. The lesions may be unilocular (with or without a scalloped margin) or may be multilocular. However, CT and MR findings of OKCs in the maxillofacial region have not been fully described in the literature. The purpose of this study was to evaluate CT and MR imaging characteristics of OKCs in the maxillofacial region. Methods: This study was approved by our institutional review board. A retrospective review of our imaging data base was performed to identify patients with pathologically proven OKCs who underwent CT or MR imaging between April 2006 and April 2017. The location, margin, bone expansion, tooth root resorption, signal intensity of the internal component, enhancement of the lesion wall were recorded. The margins of the lesions were classified as either well- or ill-defined. Results: One hundred fifty nine patients with pathologically proven OKCs (90 males and 69 females; mean age 43years; age range 6 to 90 years) were identified. Of the 159 patients, 100 patients had CT, 59 patients had MRI and 58patients had both CT and MR imaging, and. Contrast-enhanced MR imaging was performed in 9 patients. Forty patients had maxillary lesions and 119 patients had mandibular lesions. Of the 40 maxillary lesions, 15 lesions were seen in the posterior maxilla to maxillary sinus. Of the 119 mandibular lesions, 28 lesions were in the posterior mandibular body and ramus. One hundred fifty-eight lesions showed well-defined margins. Of the 40 maxillary lesions, 15 lesions showed buccal expansion. Of the 119 mandibular lesions, 45 lesions showed both buccal and lingual bone expansion. Of the 40 maxillary lesions, 2 lesions showed tooth root resorption. Of the 119 mandible lesions, 5 lesions showed tooth root resorption. The internal components showed low to intermediate signal intensity on T1-weighted images, low to high signal intensity on T2-weighted images in all cases. The cysts wall showed week enhancement in all of 9 lesions. Conclusion: OKCs were mostly seen in the mandible. By location, the posterior mandibular body and ramus was the frequent region. Margin was well defined most of the lesion. 34% of the cases showed both buccal and lingual bone expansion. 5% of the cases showed tooth root resorption. The signal intensity of the internal components can reflect the presence of material in the cystic lumen that consists of desquamated keratin.

Diagnostic Benefits of Routine Clinical Spectral CT in Head and Neck Imaging: An Imaging Review

65 Diagnostic Benefits of Routine Clinical Spectral CT in Head and Neck Imaging: An Imaging Review

TA Reher, K Mosier, NA Koontz

Indiana University School of Medicine Department of Radiology and Imaging Sciences
United States

Introduction: Spectral CT utilizes a dual-layer detector to identify photons of variable energy levels simultaneously and differs from traditional dual-energy CT in that spectral data is always being collected, thus allowing retrospective analysis and materials composition imaging without need for specifying photon energy levels prior to image acquisition. This also allows for synthesized monoenergetic image generation, by which the radiologist can retrospectively toggle between energy levels for the purposes of improved contrast enhancement or reduction streak artifact. Spectral CT presents new opportunities to investigate pathology of the head and neck, yet little has been reported on its utility. The purpose of this investigation is to report the utility of Spectral CT in head and neck imaging. We detail scenarios in our practice where routine use of Spectral CT imaging has altered image interpretation, thus affecting patient management. Methods: In this IRB-approved HIPAA-compliant study, we prospectively and retrospectively identified cases where Spectral CT made a meaningful difference in interpretation and subsequent patient management at our institution, a large academic radiology practice with associated Otolaryngology-Head & Neck Surgery referral center. We present an image-rich compilation of such cases, detailing the underlying physics and technique of spectral detector-based CT, clinically useful examples of synthesized monoenergetic images and spectral composition mapping (e.g., iodine no water, virtual noncontrast, and effective atomic number maps), and provide a comparison of Spectral CT imaging with routine multidector CT imaging for such cases. Discussion: Spectral CT (IQon Spectral CT, Koninklijke Philips, Amsterdam, Netherlands) was performed in 26,231 cases between December 2016 and May 2018 at our institution. Of these, 7,168 were dedicated head and neck studies. In our experience, spectral CT has shown utility in improved lesion detection/differentiation of lesion enhancement due to exploitation of the k-edge of iodide contrast over different keVs, improved detection of leptomeningeal and intracranial metastases on soft tissue neck CT imaging, improved discrimination of salivary gland calculi, increased sensitivity for detecting potential thyroid cartilage invasion by laryngeal squamous cell carcinoma, improved visualization of cutaneous malignancy, increased conspicuity of disease recurrence in the setting of post-operative flap margin recurrence, streak artifact reduction due to orthopedic hardware or dental amalgam, and salvage of contrast-enhanced examinations due to suboptimal iodinated contrast bolus or bolus timing. Furthermore, Spectral CT has been helpful in differentiation of calcium from contrast to assist in lesion characterization without further radiation exposure of an additional phase CT or patient inconvenience of a call-back for repeat imaging. Conclusions: Spectral CT shows significant promise in early implementation in head and neck imaging. Further studies can quantify the value of Spectral CT in the care of individual patients and across the health care system. References: 1. Perez-Lara A, et al. Spectral computed tomography: technique and applications for head and neck cancer. Magn Reson Imaging Clin N Am 2018;26(1):1-17 2. Al

Ajmi E, et al. Spectral multi-energy CT texture analysis with machine learning for tissue classification: an investigation using classification of benign parotid tumours as a testing paradigm. Eur Radiol 2018. Epub ahead of print.

Pediatric Head and Neck Infections: SpectrumFacial Weakness: A Comprehensive Review for Head and Neck Imagers

66 Facial Weakness: A Comprehensive Review for Head and Neck Imagers

AJ Stuckey, C Norris, MW Sim, K Mosier, NA Koontz

Indiana University School of Medicine
United States

Purpose: The purpose of this educational exhibit is to provide a comprehensive review of facial nerve anatomy, indications for imaging, and the multimodality imaging appearance of various pathologies that may result in facial nerve palsy. Particular focus will be given to acute versus insidious onset facial nerve weakness, as well as sections dedicated to important surgical and clinical considerations. Description: In compliance with policies of the institutional review boards at the authors' institution and HIPPA regulations, a literature review and retrospective review of the electronic medical record and PACS was performed. Illustrative cases of common imaging diagnoses of facial nerve weakness are presented. Particular focus is given to the complex anatomy of the facial nerve, extending from the facial nerve nuclei, the intracranial and intratemporal segments of the facial nerve, and the extracranial nerve branches to the end organs innervated. We highlight the various pathologic considerations for acute and insidious onset facial nerve weakness, including vascular, infectious, inflammatory, neoplastic, and traumatic etiologies, providing multimodality imaging examples and detailing the appropriate indications and approaches for imaging in patients with facial weakness. Additionally, we provide intraoperative image correlates, detail important pitfalls in the imaging of facial weakness, and report future directions for imaging of patients with cranial nerve 7 dysfunction. Summary: Facial nerve weakness is a common indication for radiologic imaging. Imaging of the facial nerve presents a significant diagnostic challenge due to the complex anatomy and potential for numerous pathologies along its course from brainstem to end organ. Head and Neck imagers must be familiar with the typical imaging findings of these pathologies, as well as surgical management considerations in order to better assist our referring clinicians and avoid misdiagnosis. References: 1. Gupta, Sachin et al. "Imaging the Facial Nerve: A Contemporary Review." Radiology Research and Practice 2013 (2013): 248039. 2. Kuya, Junko, et al. "Usefulness of High-Resolution 3D Multi-Sequences for Peripheral Facial Palsy: Differentiation Between Bell's Palsy and Ramsay Hunt Syndrome" Otology & Neurotology. 38(10):1523-1527, DEC 2017 3. Lim, H.K., et al. "MR Diagnosis of Facial Neuritis: Diagnostic Performance of Contrast-Enhanced 3D-FLAIR Technique Compared with Contrast-Enhanced 3D-T1-Fast-Field Echo with Fat Suppression" American Journal of Neuroradiology 2012 33(4) 779-783 4. Park, Sang Uk et al. "The Usefulness of MR Imaging of the Temporal Bone in the Evaluation of Patients with Facial and Audiovestibular Dysfunction." Korean Journal of Radiology 3.1 (2002): 16-23.

Jugular Foramen Lesions and Associated Lower Cranial Neuropathies: An Imaging Review

67 Jugular Foramen Lesions and Associated Lower Cranial Neuropathies: An Imaging Review

DM Krause, RE Seltman, AJ Stuckey, C Norris, TA Reher, K Mosier, NA Koontz

Indiana University School of Medicine
United States

Purpose: The purpose of this educational exhibit is to provide a comprehensive review of jugular foramen lesions that may manifest with complicated lower cranial neuropathies, including multimodality imaging findings of common and uncommon pathologies, differential diagnosis, and diagnostic pitfalls. Description: Located in the clef between the temporal and occipital bones, the jugular foramen is divided into two parts: the pars nervosa and the pars vascularis. The pars nervosa contains CN IX, the tympanic branch of the glossopharyngeal nerve (Jacobson's nerve), as well as the inferior petrosal sinus. The pars vascularis contains CN X and XI, the auricular branch of the vagus nerve (Arnold's nerve), the posterior meningeal artery, and the jugular bulb. Jugular foramen lesions correctly identified on head and neck imaging can lead to early detection of disease thereby limiting morbidity, guide appropriate management, and halt a workup in the setting of normal variants. CT and MR are often complementary tools for working up jugular foramen lesions, with the CT better delineating associated osseous changes (occasionally "pathognomonic") and MRI better at delineating the extent of the lesion and offering improved soft tissue resolution. In this IRB-approved, HIPAA-compliant study, we reviewed our institution's electronic medical record, imaging database, and pathology database for illustrative cases of jugular foramen lesions manifesting with lower cranial neuropathies. We present an image-rich collection of cases, including neoplastic (paraganglioma, meningioma, schwannoma, metastases, chondrosarcoma, and nasopharyngeal carcinoma) and infectious/inflammatory entities, highlighting multi-modality imaging findings, and important imaging pitfalls. We also present a review of the current medical literature. Summary: Appropriate knowledge of the jugular foramen contents facilitates recognition of important pathology and normal variants. Head and neck imagers should be familiar with the imaging characteristics, differential diagnosis, and potential pitfalls regarding jugular foramen lesions that may present with lower cranial neuropathies. References: 1. Thomas AJ, et al. Nonparaganglioma jugular foramen tumors. Otolaryngol Clin North Am 2015;48(2):343-59 2. Patel VA et al: End-organ radiographic manifestations of cranial neuropathies: A concise review. Clin Imaging 2017;44:5-11 3. Lopci E et al: Gallium-68 DOTANOC imaging in paraganglioma/pheochromocytoma: presentation of sample cases and review of the literature. Q J Nucl Med Mol Imaging 2013;57(2):134-45 4. Sharma P et al: 68Ga-DOTANOC PET/CT for baseline evaluation of patients with head and neck paraganglioma. J Nuc Med 2013;53(6):841-7

A pictorial review of endolymphatic hydrops utilizing delayed contrast enhanced FLAIR MRI

68 A pictorial review of endolymphatic hydrops utilizing delayed contrast enhanced FLAIR MRI

O Elbuluk, S Karnezis, A Vijayasarathi

David Geffen School of Medicine at UCLA
United States

Purpose: To review the key imaging findings observed in endolymphatic hydrops, a hallmark of Meniere's disease, utilizing delayed post-contrast fluid attenuated inversion recovery imaging. Description: Meniere's disease remains a challenging entity to diagnose both from a clinical and imaging standpoint. Clinically, Meniere's disease is characterized by vertigo, tinnitus, sensorineural hearing loss and aural fullness. From a postmortem histopathologic standpoint, endolymphatic hydrops is a defining feature of Meniere's disease. Recently, a noninvasive specialized MRI protocol using a delayed contrast enhanced FLAIR sequence has shown promise in diagnosing endolymphatic hydrops in vivo. This protocol has been in clinical use for over 5 years at our institution. The PACS and departmental teaching files will be queried for instructive examples of endolymphatic hydrops as well as normal controls. This educational exhibit will detail the imaging protocol, demonstrate normal inner ear anatomy, normal appearance of endolymphatic structures, and highlight a variety of cases of endolymphatic hydrops. Additionally, a systematic approach to the interpretation of these specialized studies will be offered. Summary: The accurate imaging diagnosis of endolymphatic hydrops allows for the possibility of confirmation of a challenging and incompletely understood diagnosis. Neuroradiologists may be able to aid in the diagnosis, understanding and future research endeavors related to Meniere's disease by becoming familiar with the imaging protocol and detection of endolymphatic hydrops on MRI.

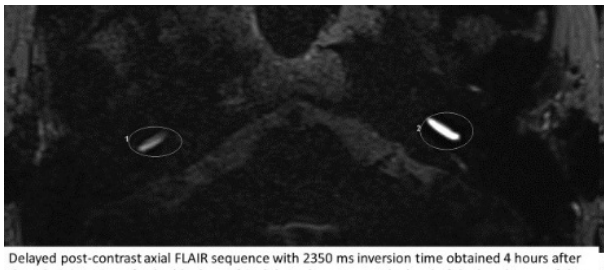

Delayed post-contrast axial FLAIR sequence with 2350 ms inversion time obtained 4 hours after the administration of a double dose of Gadobutrol contrast at the level of the basal turns of the cochlea. The left cochlea demonstrates asymmetrically high signal compared to normal contralateral side, consistent with abnormal blood-labyrinth barrier permeability, a finding that can be seen with Meniere's disease.

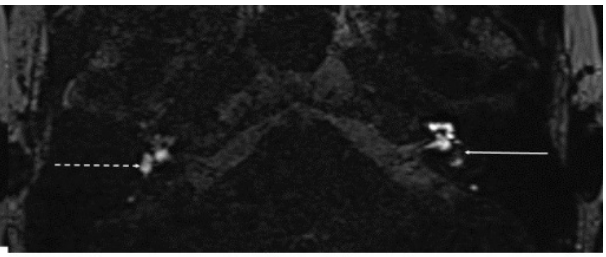

Delayed post-contrast axial FLAIR sequence at the level of the vestibules. The solid white arrow demonstrates the dark signal associated with dilated endolymphatic structure (saccule). The dashed white arrow demonstrates the normal appearance of the right vestibule without endolymphatic hydrops.

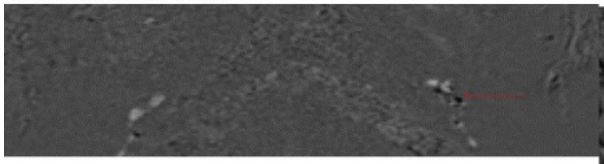

Subtraction image which demonstrates perilymph signal as white, endolymph signal as black, and surrounding tissues as grey. The left cochlear duct is dilated as evidenced by increased black endolymphatic signal compared to the normal contralateral side (red solid arrow). The subtraction images help distinguish membranous labyrinth from surrounding otic capsule.

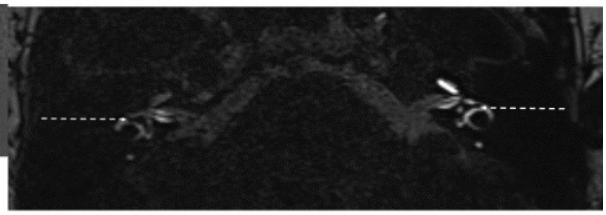

Delayed post-contrast axial FLAIR sequence at the level of the lateral semicircular canals. Dashed white arrows demonstrate symmetric appearance of the normal triangular utricles bilaterally.

Overall, this case is consistent with unilateral left sided endolymphatic hydrops involving the left cochlear duct and saccule. The utricle is uninvolved.

Radiologic Findings of Hemorrhagic Labyrinthitis

69 Radiologic Findings of Hemorrhagic Labyrinthitis

GS Suarez Duran, N Thangaraj, V Potigailo

Drexel/ Hahnemann University Hospital
United States

Purpose: To review key radiologic features seen in hemorrhagic labyrinthitis and help differentiate them from other similar pathologies (such as an intracochlear schwannoma) while aiding in determining prognosis. Description: In this case, we report a 56 year old male who presented to the emergency department with sudden onset of vertigo. The symptoms were associated with otalgia and tinnitus prior to onset. Other than hypertension controlled with metropolol, the patient had no significant prior medical history. Contrast enhanced MRI of the brain revealed increased T1 and FLAIR signal intensity in the right cochlea and horizontal semicircular canal with mild decrease in T2 signal intensity. Summary: Hemorrhagic labyrinthitis is a rare sequela of trauma or infection, particularly in patients with hematologic disease or on anticoagulation, that can result in permanent hearing loss. In this report we will review key MR findings seen in hemorrhagic labyrinthitis and help aid in determining prognosis using certain sequences. Accurate and prompt diagnosis is essential given that immediate treatment with steroids has been demonstrated to significantly improve outcomes.

A Rare Case of Adult Pleomorphic Rhabdomyosarcoma of the Neck

70 A Rare Case of Adult Pleomorphic Rhabdomyosarcoma of the Neck

SS Kahlon, N Pham, J Chang

University of California, Davis
United States

Purpose To describe the clinical presentation, imaging, and pathologic findings of a rare case of adult pleomorphic rhabdomyosarcoma (PRMS) of the neck. Description A 52-year-old woman presented with a rapidly enlarging posterior left neck mass, which had nearly doubled in size over the course of 9 months. The mass was initially painless; however, it became painful and began to limit the patient's range of motion as it increased in size. Physical examination was notable for a large 9 x 9 cm firm, but mobile mass centered within the posterior left neck. CT demonstrated a large, heterogeneously enhancing mass, interposed between the trapezius muscle and levator scapulae, and extending from the level of C2 to C7. Subsequent MRI demonstrated a T1 isointense and T2 hyperintense circumscribed mass with avid enhancement. PET/CT showed low FDG uptake of the primary mass and no evidence of regional or distant disease. The patient was referred to ENT and a core biopsy was performed. The core biopsy specimens were highly cellular and comprised of pleomorphic and spindle cells with histologic and immunohistochemical stains positive for vimentin, actin, desmin, and myogenin, most consistent with rhabdomyoblastic differentiation. A diagnosis of PRMS was established. Induction chemotherapy was then initiated with a plan for surgical resection and adjuvant radiation treatment. Summary Rhabdomyosarcoma is an exceedingly rare tumor in adults. Overall, soft tissue sarcomas constitute less than 1% of all adult malignancies of which undifferentiated pleomorphic sarcoma is the most common. Rhabdomyosarcoma only accounts for 1-3% of adult soft tissue sarcomas whereas it is the most common pediatric soft tissue sarcoma, accounting for more than 50%, with 80% occurring in children less than 12 years of age. Given the infrequency of adult rhabdomyosarcoma, treatment has largely been based on retrospective review of cases. The frequency of rhabdomyosarcoma histologic subtypes also varies with age. In adults, the following frequencies have been reported: 36% pleomorphic, 32% embryonal, 27% alveolar, and 6% variants of botryoid and spindle cell/sclerosing histologic subtype. The relative proportion of aggressive pleomorphic sarcomas increases with age, as in our case, however, truncal and extremity involvement is more common, with rare involvement of the head or neck. In summary, PRMS is an uncommon adult tumor but is an important differential consideration in a rapidly growing mass within the head and neck region.

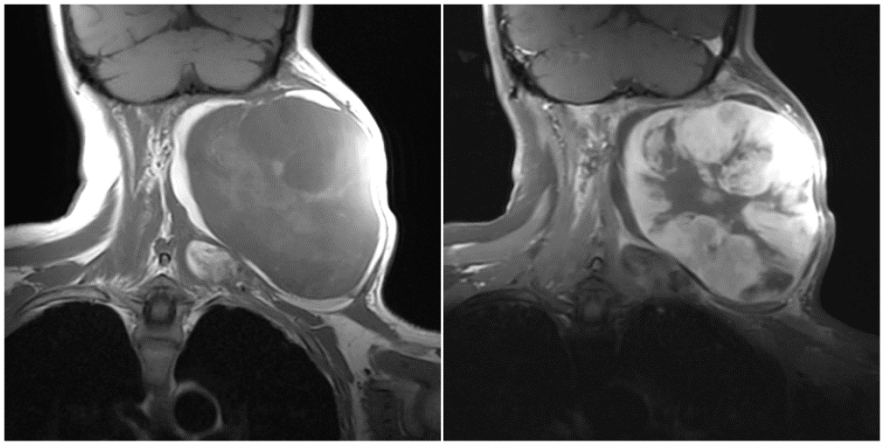

Abscess, Mass, or Mess? A Review of Thyroid Abscess Ultrasound Findings in Patients with 3rd/4th Branchial Anomalies

71 Abscess, Mass, or Mess? A Review of Thyroid Abscess Ultrasound Findings in Patients with 3rd/4th Branchial Anomalies

SL Rebolledo, R Ramakrishnaiah, J McCarty

UNIVERSITY OF ARKANSAS FOR MEDICAL SCIENCES
United States

Purpose: The goal of this case series is to summarize the sonographic imaging findings and pitfalls of branchial anomaly related thyroid abscess, utilizing sonographic and cross-sectional imaging. Description: Due to the inherent antimicrobial nature of the thyroid gland (high iodine content, encapsulation, separation by fascial planes, rich blood supply and lymphatic drainage), thyroid abscess is a rare entity associated with third and fourth branchial remnant anomalies. Third and fourth branchial arch remnants represent less than 10% of all branchial lesions. They are lateral structures and >90% localize to the left thyroid lobe. Differentiation between third or fourth branchial remnant is made at time of surgery, based on the location of the tract in the piriform sinus and relationship to the superior laryngeal nerve. Patients often present in the pediatric age group with fever, swelling, and a palpable neck mass. There is an association with recent upper respiratory illness and cervical lymphadenopathy. Ultrasound is primarily utilized as the initial imaging modality due to lack of ionizing radiation and excellent visualization of the superficially located gland. Common sonographic characteristics include unilobular enlargement with hypoechoic, mass-like areas and peripheral hypervascularity. Overlying skin thickening and subcutaneous edema may be present. A thyroid abscess can appear more echogenic and complex than an abscess in other anatomic locations. Due to its rare nature, a thyroid abscess can be mistaken as a mass with aggressive features if the interpreting radiologist is not provided with a clinical history suggestive of infection or if they are unfamiliar with this diagnosis. Cross-sectional imaging may be important to assess the location, size and extent of involvement. Common CT findings are similar to an abscess seen elsewhere in the body, with well-circumscribed, rim-enhancing, hypoattenuating collections. Fascial planes are not preserved in the setting of infection, especially if a biopsy has already been performed. Misdiagnosis can prompt unnecessary interventions as well as delays in proper clinical management and definitive surgical excision. Complications can be life threatening with local extension of disease to critical structures (mediastinitis, thrombosis of the internal jugular vein, and tracheal compression/obstruction). A case series of thyroid abscess in a pediatric population are presented with key sonographic and cross-sectional imaging findings. Original diagrams are presented to summarize imaging findings. Summary: This case series will highlight the pitfalls and key features of ultrasound imaging of thyroid abscess.

Masslike Left Thyroid Abscess

Introduction
Anatomy
Embryology
Presentation
Ultrasound
CT
Fluoro
Treatment
Conclusion

Complex, mass-like abscess in the left thyroid lobe with heterogeneous echogenicity and internal septation

Overlying skin is thickened and echogenic from edema

Masslike Left Thyroid Abscess

Introduction
Anatomy
Embryology
Presentation
Ultrasound
CT
Fluoro
Treatment
Conclusion

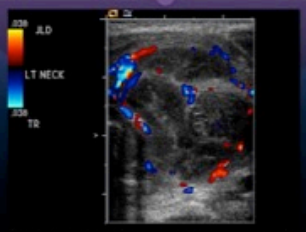

Peripheral and internal hypervascularity

Associated findings

Introduction
Anatomy
Embryology
Presentation
Ultrasound
CT
Fluoro
Treatment
Conclusion

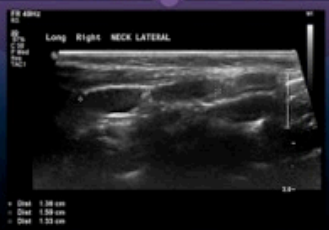

Reactive cervical lymphadenopathy

CT of the Same Patient

Introduction
Anatomy
Embryology
Presentation
Ultrasound
CT
Fluoro
Treatment
Conclusion

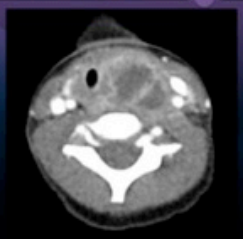

Mass-like areas of hypodensity with internal septation and peripheral enhancement

Mass-effect on trachea which is deviated right and mildly narrowed

Orbital Interstitial Fluid: A Pathway for Extracranial CSF Absorption?

72 Orbital Interstitial Fluid: A Pathway for Extracranial CSF Absorption?

J Sachs, M Zapadka

Wake Forest Baptist Health
United States

Purpose:The aim of the study was to describe the prevalence and characteristics of orbital interstitial fluid seen on magnetic resonance (MR) images of infants and young children. Materials & Methods:Fat-suppressed axial T2-weighted MR images of 100 consecutive infants and young children (<6 years) without orbital pathology were retrospectively reviewed by 2 neuroradiologists. The presence, location, and extent of high-signal orbital interstitial fluid were characterized and tabulated as a function of age. Results: Orbital interstitial fluid was detected in 90 (90%) of the 100 subjects overall, present in 100% (75/75) of infants and children younger than 3 years, 75% (12/16) of those aged 3 to 5 years, and 33% (3/9) of those aged 5 to 6 years. The fluid was bilateral and symmetric in all cases. Two morphologic patterns were distinguished, which often co-existed: (1) a focal discrete curvilinear band of fluid in the posterior-lateral orbit, more common in younger patients, and (2) an ill-defined, lace-like pattern primarily in the superior orbit seen in subjects of all ages. Conclusions:Orbital interstitial fluid as detected by fat-suppressed T2-weighted MR imaging is a nearly universal finding in infants and young children and should not be considered pathologic. It may have either a focal or lace-like pattern or both. Orbital interstitial fluid decreases in size and prevalence as a function of age but is still present in nearly half of children aged 4 to 6 years. Possible explanations concerning the nature and origin of this fluid are presented, including the fascinating possibility that the fluid represents an extracranial pathway for outflow of cerebrospinal fluid.

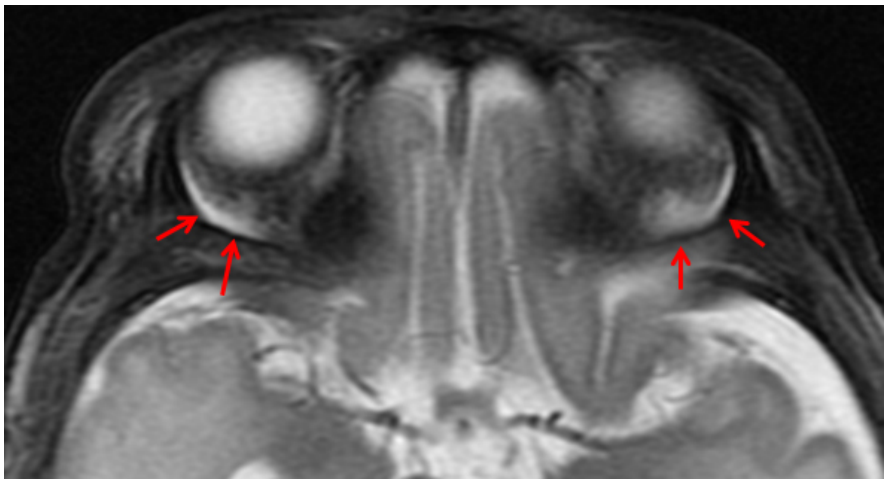

Diffusion weighted imaging for characterization of odontogenic cysts and tumors

73 Diffusion weighted imaging for characterization of odontogenic cysts and tumors

J Kumar, R V, A Manchanda, R Meher, S Mohanty

MAULANA AZAD MEDICAL COLLEGE
India

Objective: Odontogenic keratocysts (OKCs) are one of the most common jaw lesions encountered in clinical practice. However, they may be difficult to differentiate from other odontogenic cysts and tumors based on their morphological features alone. Diffusion weighted imaging can help characterize these lesions better and differentiate them from other odontogenic lesions. Methodology: A total of 26 patients with odontogenic cysts and tumors were included in the study. After MDCT and conventional MR evaluation including post contrast assessment, these patients were taken up for Diffusion weighted imaging using b values of 50, 400 and 800 s/mm2 The ADC value was calculated by placing a circular region of interest with minimum area of 1cm2 in the lesion separately for solid and cystic components of the lesion. Results: Out of 26 patients, 17 cases were diagnosed as OKC, 5 cases as ameloblastoma, 3 cases as dentigerous cyst and 1 case as odontogenic myxoma, based on histopathology. All 17 cases of OKCs were cystic with only peripheral enhancement. On diffusion weighted imaging, 12/17 OKCs showed restricted diffusion with a mean ADC value of 0.978 x 10-3 mm2/s. Only 5 /17 OKCs show facilitated diffusion. In 5 cases of ameloblastoma, all enhancing solid components showed restricted diffusion while all non-enhancing cystic components showed facilitated diffusion. All the 3 cases of dentigerous cyst showed facilitated diffusion with mean ADC value of 2.150 x 10-3 mm2/s. One case of odontogenic myxoma showed facilitated diffusion with mean ADC value of 2.552 x 10-3 mm2/s. There was a significant difference between the ADC cut-off value of cystic ameloblastoma and OKC (p value 0.03, Mann Whitney U test). The cut off with which OKC and cystic component of ameloblastoma were optimally differentiated was 2.138 x 10-3 mm2/s, which yielded 100% sensitivity and 83% specificity. Conclusion: We concluded that diffusion weighted imaging can play an important role in differentiating OKC from other cystic odonotogenic lesions.

Sinonasal Teratocarcinosarcoma With Intracranial Extension in a 40-year Old Male: A Discussion of Imaging Characteristics With Histopathological Correlate

74 Sinonasal Teratocarcinosarcoma With Intracranial Extension in a 40-year Old Male: A Discussion of Imaging Characteristics With Histopathological Correlate

A Rizvi, KT Golden, S Bobra, H Mehta, M Tenner, D Jourdy, C Bowers, G Kleinman, E Gulko

Westchester Medical Center
United States

PURPOSE We present a case of sinonasal teratocarcinosarcoma with intracranial extension in a 40-year old male. We review pre-operative and post-operative imaging characteristics with CT and MR, and provide histopathological correlation. We will discuss disease management, and review other pathology which may have similar appearance on imaging. BACKGROUND Sinonasal teratocarcinosarcoma is a rare malignant neoplasm of the head and neck with an adult male predominance (male:female ratio of 4:1). Histologically, the tumor has neuroectodermal elements with malignant epithelial and mesenchymal components. The tumors contain areas of squamous carcinoma and adenocarcinoma. They primarily originate from the ethmoid sinus and maxillary antrum, and present with nasal obstruction and epistaxis. These tumors are locally aggressive with the potential to metastasize to distant sites, such as the lungs. The average survival is less than 2 years with recurrence being common within 3 years. Early diagnosis and aggressive follow-up is critical, with total excision plus chemotherapy (with or without radiation therapy) the standard treatment. IMAGES Pre-operative MRI of the sinuses demonstrates a heterogeneously enhancing expansile mass with areas of T2 hyperintensity within the left nasal cavity extending into the left maxillary sinus and nasopharynx. There is effacement of the nasopharynx with evidence of intracranial extension. A T2 hyperintense air-fluid level is seen within the right maxillary sinus. Pre-operative non-contrast CT of the sinuses demonstrates the paranasal sinus mass with convex bulging and osseous thinning at the left lamina papyracea. There is slight mass effect upon the left medial rectus muscle. Additionally, there is a focal osseous defect within the left cribriform plate. CONCLUSION We will present a case of sinonasal teratocarcinosarcoma with intracranial extension in a 40-year old male. This is a rare malignant neoplasm of the head and neck with neuroectodermal, epithelial and mesenchymal components. These locally aggressive tumors have a high mortality and high rate of recurrence. We will discuss imaging characteristics on CT and MRI, and correlate with histopathological photomicrographs. We will review the prognosis and management, and conclude with a discussion of differential diagnoses and key points.

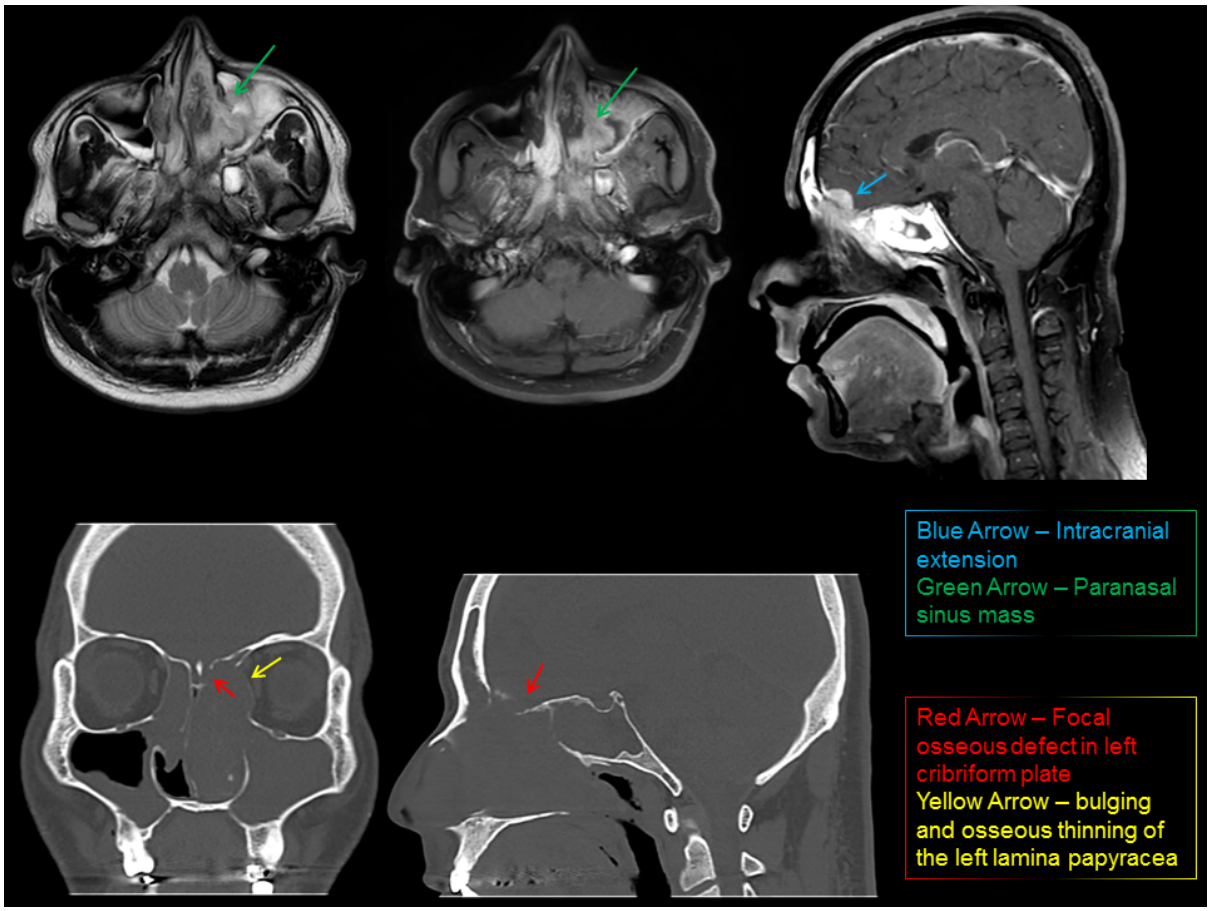
Blue Arrow – Intracranial extension
Green Arrow – Paranasal sinus mass
Red Arrow – Focal osseous defect in left cribriform plate
Yellow Arrow – bulging and osseous thinning of the left lamina papyracea

Organized Hematoma of the Maxillary Sinus: An Uncommon Tumor Mimic

75 Organized Hematoma of the Maxillary Sinus: An Uncommon Tumor Mimic

I Corcuera-Solano, N Swinburne, J Deutsch, S Govindaraj, M Fowkes, P Som

Icahn School of Medicine at Mount Sinai
United States

Case report A 24 year-old male with occasional cocaine use presented to his primary care physician with a toothache, right facial pain, and nasal congestion. He was afebrile and in no acute distress. His otolaryngologic examination was unremarkable except for nasal congestion. He was placed on a course of empirical antibiotics. When only little improvement occurred, a CT scan of his paranasal sinuses was obtained which showed complete opacification of the right maxillary sinus with bony remodeling and focal destruction and extension into the lower orbit (Fig. 1). The patient was referred to the ENT department of our institution. Nasal endoscopy demonstrated an edematous middle meatus, an enlarged inferior turbinate and a nasal mass. An MRI of the sinuses showed a well delineated, expansile, heterogeneous mass filling the right antrum and most of the right nasal cavity (Fig 2). The patient was taken to the operating room for sinus endoscopy and biopsy, which demonstrated polypoid fragments of edematous respiratory mucosa with chronic inflammation. However, given the high clinical suspicion for a potential neoplasm, the decision was made to proceed to a right maxillary antrostomy and middle turbinectomy. Histopathologic evaluation showed a benign respiratory mucosa-lined mass with stromal expansion by a prominent organizing hematoma and chronic rhinosinusitis. The patient has done well since surgery. Discussion An organized hematoma is a rare non-neoplastic entity occurring in patients in the age range of 20-40 years. (1) They have been primarily described involving the maxillary sinus (2), with few cases reported in the sphenoid and frontal sinuses (3-5). The most common presenting complaint is frequent epistaxis, followed by nasal congestion and facial pain. (6) Although most hematomas resolve without causing significant clinical problems, some may persist and present as slowly expanding lesions mimicking a neoplasm. The differential diagnosis of a unilateral paranasal sinus mass is extensive and includes neoplasms such as inverted papilloma, odontogenic tumor, squamous cell carcinoma, adenocarcinoma and melanoma, in addition to infectious and inflammatory processes. Sinonasal organized hematoma is believed to result from an accumulation of blood in the paranasal sinus that progresses to chronic hematoma formation followed by a process of organization through neovascularization and fibrosis. (7) Poor ventilation and drainage, accompanied by the formation of a fibrous capsule, prevent resorption of the hematoma. The organized hematoma progressively expands, resulting in bony remodeling and erosion. The characteristic CT appearance of an organized hematoma is an expansile mass of heterogeneous high density with thinning and erosion of the adjacent bony sinus walls. (8) MRI demonstrates markedly heterogeneous signal intensity, reflecting blood products of varying stages and areas of fibrosis. Heterogeneous contrast enhancement occurs. Although demographic, clinical and imaging findings are helpful in the approach to a patient with a paranasal sinus mass, the overlapping imaging and clinical features between an organized hematoma and a neoplasm makes this differentiation challenging and confirmatory histologic evaluation is generally necessary. (9) Surgical resection is mandatory to remove the organized hematoma in patients with persistent symptoms and lesion expansion.

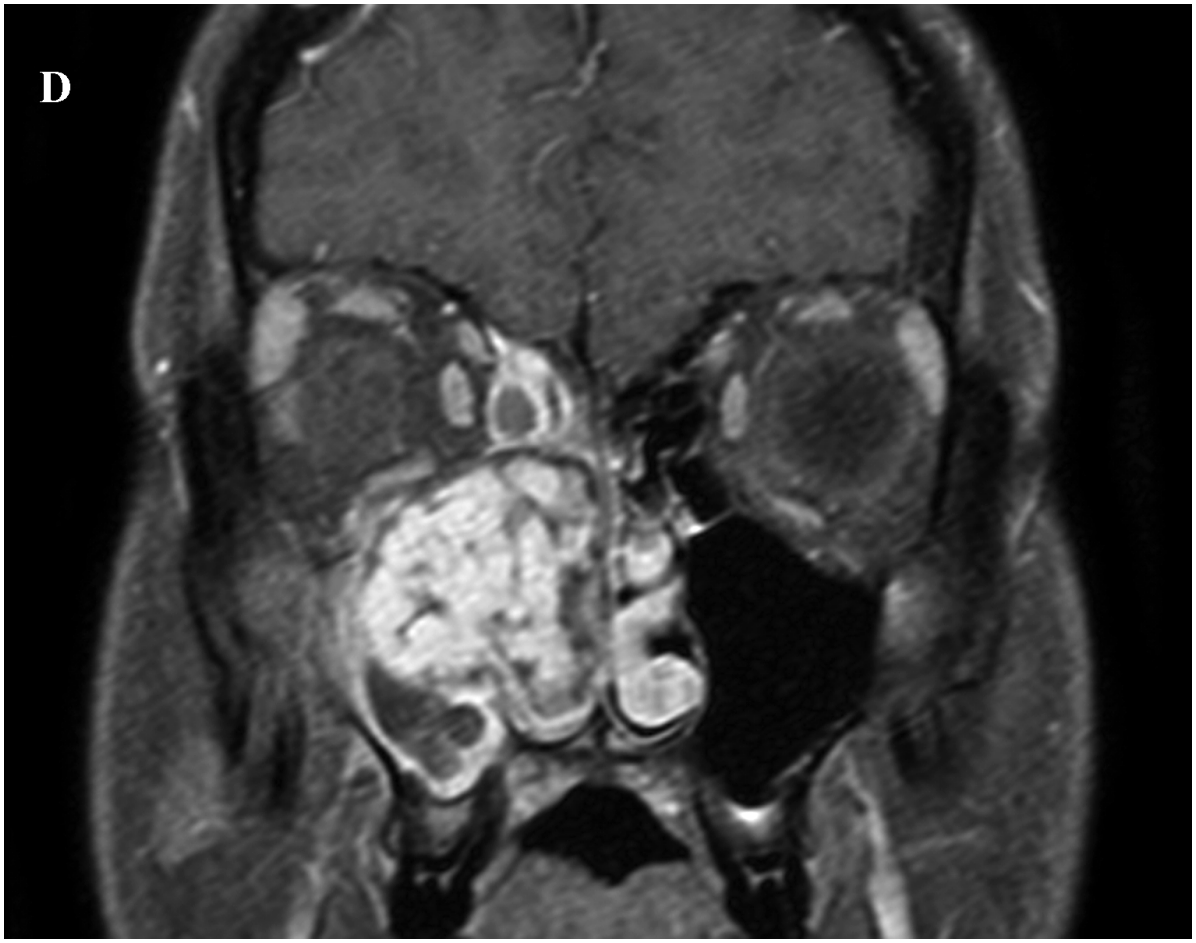
D

Apex Predators, Innocent Bystanders, and the Wrongfully Accused: An Imaging Review of Petrous Apex Lesions

76 Apex Predators, Innocent Bystanders, and the Wrongfully Accused: An Imaging Review of Petrous Apex Lesions

RE Seltman, K Mosier, NA Koontz

Indiana University School of Medicine
United States

Purpose: The purpose of this educational exhibit is to provide a comprehensive review of the salient anatomy, as well as the imaging findings and diagnostic pitfalls of common and uncommon lesions of the petrous apex. Description: The petrous apex is the pyramidal-shaped, medial segment of the petrous temporal bone located at the skull base and interposed between the intracranial compartment and suprahyoid neck. Understanding its contents and adjacent structures is critical in formulating an accurate and clinically-relevant differential diagnosis. Due to variable degree pneumatization, the petrous apex may give rise to several congenital, infectious, and inflammatory lesions of pneumatized air cells including cholesteatoma, cholesterol granuloma, mucocele, trapped fluid, and apical petrositis. Additionally, various vascular, infectious, inflammatory, and neoplastic processes which arise from the adjacent internal carotid artery, intracranial compartment, or suprahyoid neck may secondarily involve the petrous apex. Lastly, the petrous apex may give rise to primary and secondary lesions of bone including chondrosarcoma and bony metastases. In this HIPAA compliant, IRB approved study, we performed a literature review and retrospective review of the electronic medical records and PACS at the author's affiliated institution (academic medical center with tertiary neuroradiology and Otolaryngology-Head and Neck surgical referral). In an image-rich format, we present a selection of illustrative cases of primary and secondary lesions of the petrous apex, including multi-modality (CT, MRI, angiography, and nuclear medicine) imaging, as well as report important diagnostic dilemmas and pitfalls. Summary: The petrous apex is a critical structure at the skull base, interposed between the intracranial compartment and suprahyoid neck. Radiologists should be familiar with common and uncommon lesions of the petrous apex, potential mimics, distinguishing features of each utilizing multimodality imaging, and the limitations and diagnostic pitfalls of each modality. References: 1. Chapman PR, Shah R, Curé JK, Bag AK. Petrous apex lesions: pictorial review. AJR Am J Roentgenol 2011;196(3 suppl):WS26-WS37. 2. Moore KR, Harnsberger HR, Shelton C, Davidson HC. 'Leave me alone' lesions of the petrous apex. AJNR 1998; 19:733-738. 3. Razek AA, Huang BY. Lesions of the petrous apex: classification and findings at CT and MR imaging. RadioGraphics 2012;32(1):151-173.

The Ophthalmic Artery (OA): Mission Beyond Vision

77 The Ophthalmic Artery (OA): Mission Beyond Vision

E Supsupin, O Adesina, SV Mukhi

University of Texas Health Science Center McGovern Medical School Department of Diagnostic & Interventional Imaging
United States

Purpose: Apart from its fundamental role in vision, the ophthalmic artery (OA) is a complex arterial network that has important implications in the treatment of various pathologies. We study the ophthalmic artery, focusing on its clinically relevant anatomy. Objectives: 1. Review the angiographic anatomy of the OA 2. Identify important anatomic variants of the OA 3. Discuss important anastomoses of the OA and potentially dangerous and beneficial collaterals 4. Illustrate clinical scenarios where the OA may impact treatment approach to various pathological entities Discussion: The OA is the first intracranial branch of the internal carotid artery after emerging from the cavernous sinus. Its central retinal artery branch is fundamental in vision. Detailed understanding of the anatomy and anatomic variants of the OA, and recognizing dangerous collaterals, are crucial in safely carrying out endovascular treatment procedures. The clinical importance of the communication between the OA and internal maxillary artery (IMAX) branches such as the middle meningeal artery (MMA) and ethmoidal arteries lies in the potential complication of blindness during embolization of head and neck tumors and intractable epistaxis. The OA may provide an important collateral in carotid occlusive disease. The anatomy and course of the OA is important in the treatment approach to ophthalmic artery aneurysms. Understanding the anatomy is crucial in correct catheter placement during intra-arterial fibrinolysis in cases of central retinal artery occlusion, and in delivering intra-arterial chemotherapy for treatment of retinoblastoma. Summary: The OA not only plays a fundamental role in vision, but also impacts treatment approach in various clinical scenarios. Thorough knowledge of relevant angiographic anatomy and dangerous anastomoses is required in safely carrying out endovascular treatment procedures.

Fluorescein angiography depicting normal arteriovenous blood flow in mid transit phase

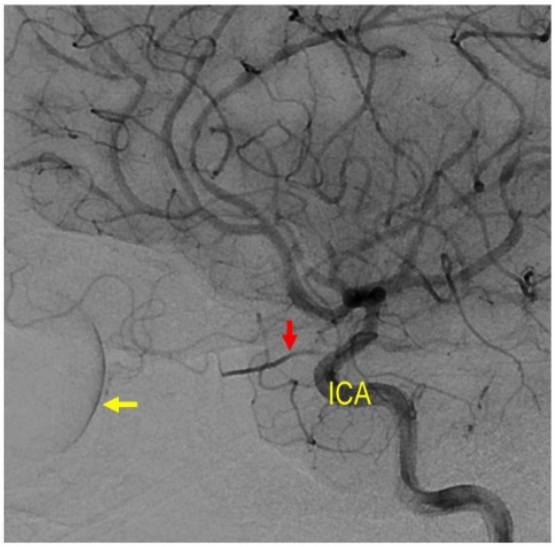

Lateral DSA (digital subtraction angiography) of the internal carotid artery (ICA) showing the ophthalmic artery (red arrow) & the normal choroid blush (yellow arrow)

Pediatric Cystic Neck Masses

78 Pediatric Cystic Neck Masses

A Farkas, M Jordan, E Parker, D Joyner

University of Mississippi Medical Center
United States

Purpose: Cystic neck masses are a common finding in the pediatric population. An understanding of the development and anatomy of this region is strongly associated with the consideration of a differential diagnosis. This exhibit will provide an overview of the cystic neck masses in the pediatric population with an emphasis on anatomy, multimodality imaging appearance, and clinical features of the findings. Description: This is an interactive case-based review of pediatric cystic neck masses. Cases will be presented as unknowns with follow-up questions and explanations of key imaging findings and clinical points. Cases will include CT and MR images of branchial cleft cysts, dermoids, lymphatic malformations, ranulas, and thyroglossal duct cysts as well as suppurative lymphadenitis. The presentation will be optimized for viewing on mobile phones and tablets as well as computer viewing stations. Summary: After review of this interactive exhibit, residents will have increased familiarity with the differential diagnosis of cystic neck masses in pediatric population, the anatomy and development of this region and how it relates to the differential diagnosis, and understanding of important clinical features and management of these masses.

The postcricoid venous plexus revisited- a retrospective review of an overlooked normal anatomic structure

79 The postcricoid venous plexus revisited- a retrospective review of an overlooked normal anatomic structure

M Gule-Monroe, T Vu, LE Ginsberg

MD Anderson Cancer Center
United States

Purpose Review the imaging appearance of the postcricoid venous plexus (PCVP) on multiphasic CT imaging of the neck. Materials and Methods A retrospective review was performed of 31 CT neck studies obtained using a multiphasic 4D-CT protocol for the evaluation of parathyroid adenoma. Each CT was obtained with non-contrast, arterial, venous and delayed venous acquisitions. Images were reviewed by a board certified neuroradiologist. The presence or absence of PCVP enhancement was identified. A PCVP was considered measureable if thickness was greater than or equal to 3mm. The density of a measurable PCVP, ipsilateral common carotid artery and an anterior jugular vein was quantified in Hounsfield units on non-contrast, arterial, venous and delayed venous phase acquisitions. Results Our sample population included predominantly women (87%) with a mean age of 60 years. This demographic skew is consistent with the demographics of parathyroid adenomas, the indication for the study. A PCVP was evident in 71% of patients (n=22), identified as separate from normal postcricoid hypopharyngeal mucosal enhancement. A PCVP was not visible in 26% (n=8) of patients. The post cricoid region was obscured by metal streak artifact from cervical hardware in one patient. The majority (88%) of the visible PCVPs were very thin and in the 1-2 mm range. A PCVP was measureable in 6 of the 22 patients (22%) with a visible PCVP at 3 mm or greater in thickness. The mean thickness of all measurable PCVP was 4.1 mm with the greatest at 6 mm. No mass effect on the adjacent airway or hypopharynx was identified. All the patients (n=6) with a measurable PCVP demonstrated enhancement characteristics that followed contrast enhancement of the ipsilateral anterior jugular vein. Conclusion The presence of a venous plexus in the postcricoid and posterior hypopharynx is well established in the anatomic literature and has been described as a “postcricoid impression” on fluoroscopic studies. There is a paucity of literature about the appearance of this normal anatomic structure on cross-sectional imaging. We have demonstrated that a PCVP is visible on CT in almost 2/3 of imaged patients and can differ in size and conspicuity. The lack of familiarity with PCVP and the variations in its imaging appearance may lead to misdiagnosis of a normal structure as pathology.

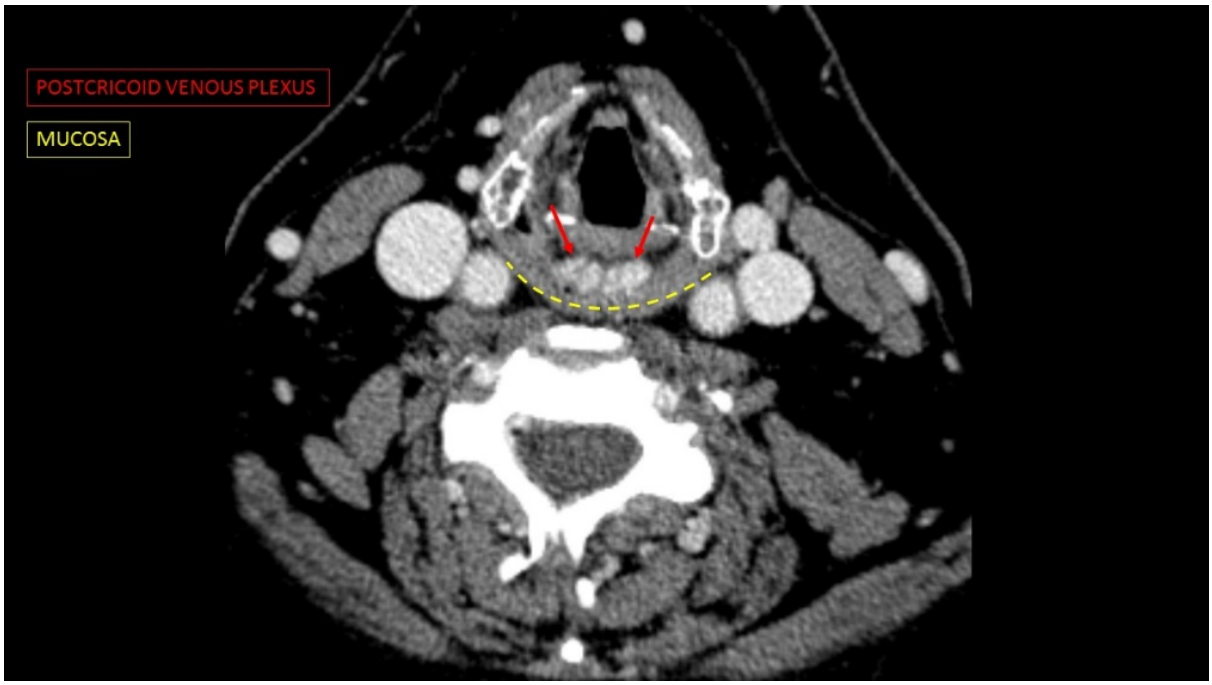
POSTCRICOID VENOUS PLEXUS
MUCOSA

Chew On This: A Radiographic Review of the Anatomy and Pathology of the Temporomandibular Joint

80 Chew On This: A Radiographic Review of the Anatomy and Pathology of the Temporomandibular Joint

A Arneja, MH Hanna, A Bansal, R Gupta, P Som

The Mount Sinai Hospital
United States

Purpose: To review the normal anatomy and function of the temporomandibular joint, dysfunctional temporomandibular joint and various pathologic abnormalities. Description Temporomandibular joint dysfunction is a common cause of pain and often results in obtaining radiologic imaging for diagnosis. A basic knowledge of the normal anatomy of the TMJ as well as common pathologies are key to the radiologist's interpretation of the images. We perform a multimodality review of the anatomy and basic pathologies of the temporomandibular joint. We review the relevant normal anatomy on both the open and close mouth sagittal MRI pulse sequences. We specifically focus on evaluation of the disc, presence of joint effusion, osteoarthritic changes, displacement and relocation. We discuss direct and indirect signs of displacement. We then review various pathologies of the TMJ including, dislocation with and without recapture, ankylosis, traumatic injuries, grafts and total joint replacement. Thus, we provide a comprehensive approach to the temporomandibular joint which allows for radiologists a more comprehensive understanding of the normal anatomy and relevant pathology. Summary We present a review of the temporomandibular joint with a systematic multimodality case-based approach. A thorough understanding of the normal anatomy and abnormal pathology that can be seen on MR and CT imaging may help the radiologist in providing vital information to define the cause of a patient's clinical symptoms. This allows for a greater diagnostic accuracy and improved patient care.

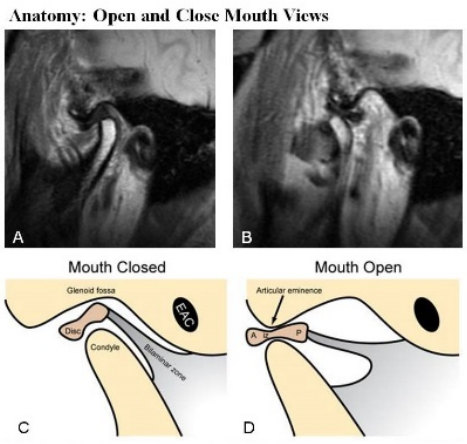

Figure 1: MRI of the left temporomandibular joint in (A) closed and (B) open mouth views demonstrating anterior displacement without recapture. Illustration of the normal anatomy of the TMJ (C and D, Courtesy of Dr Behrang Amini , Radiopaedia.org, rID: 36418.)

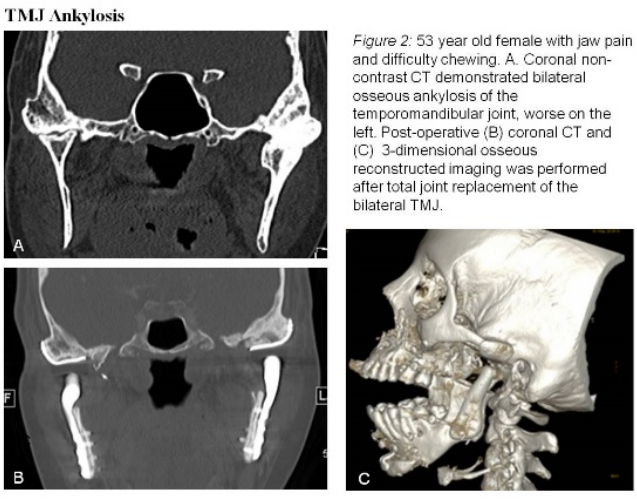

Figure 2: 53 year old female with jaw pain and difficulty chewing. A. Coronal non-contrast CT demonstrated bilateral osseous ankylosis of the temporomandibular joint, worse on the left. Post-operative (B) coronal CT and (C) 3-dimensional osseous reconstructed imaging was performed after total joint replacement of the bilateral TMJ.

Prominence of the retroarticular venous plexus in patients with prolonged open-mouth position: A potential diagnostic pitfall

81 Prominence of the retroarticular venous plexus in patients with prolonged open-mouth position: A potential diagnostic pitfall

AA Nagelschneider, K Krecke, J Lane, D DeLone

Mayo Clinic-Rochester
United States

Purpose: The retro-articular venous plexus (RAVP), also variably referred to in the literature as the retro-discal vascular plexus or genu vasculosum, is a venous network situated within the retro-discal tissues of the temporomandibular joint. It is well-documented in the anatomical literature but seldom mentioned in the radiology literature. This may be due to the fact that it is often not well seen on conventional outpatient MRIs. However, in patients who have a prolonged open-mouth position, such as those patients undergoing an MRI under general endotracheal anesthesia, this plexus can become quite prominent. Since the venous plexus can appear as prominent enhancement involving the temporomandibular joint or even as an enhancing “mass”, it may lead to diagnostic confusion with inflammatory, degenerative, or neoplastic entities. Our review sought to determine the frequency with which this venous plexus may be evident in patients with prolonged open-mouth vs. resting neutral position, as well as describe the variable appearance of this imaging artifact of normal anatomy. Description: Fourteen consecutive patients with MRIs performed under endotracheal anesthesia as well as 14 consecutive non-sedated outpatients were reviewed by two fellowship-trained neuroradiologists. Of the anesthesia patients, 79% demonstrated prominence of the RAVP and a total of 19/28 (68%) temporomandibular joints were involved. Of the non-sedated outpatients, 27% demonstrated prominence of the RAVP and a total of 5/28 (18%) temporomandibular joints were involved. Summary: The retro-articular venous plexus (RAVP) is a normal vascular structure that is often not well seen on conventional outpatient MRI, but can become quite prominent in patients who have a prolonged open-mouth position such as those undergoing an MRI under general endotracheal anesthesia. This finding may be related to passive filling of the plexus with anterior translation of the mandibular condyle and disc. In these cases, the vascular plexus can have the appearance of an enhancing multicystic lesion, and may be misinterpreted as inflammatory, degenerative, or neoplastic pathology. Understanding of the normal variation of the appearance of the retro-articular venous plexus, particularly with open-mouth position, is important in avoiding this diagnostic pitfall which may result in unnecessary additional imaging or intervention.

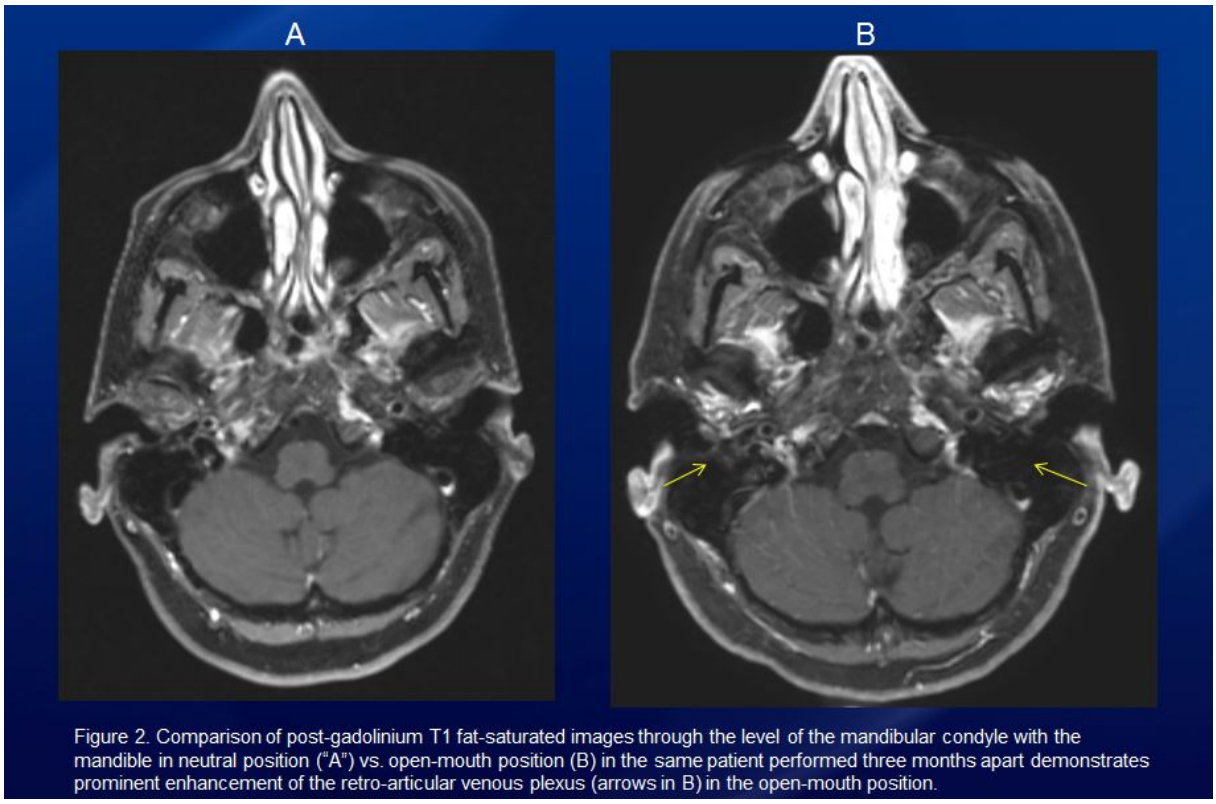

Figure 2. Comparison of post-gadolinium T1 fat-saturated images through the level of the mandibular condyle with the mandible in neutral position ("A") vs. open-mouth position (B) in the same patient performed three months apart demonstrates prominent enhancement of the retro-articular venous plexus (arrows in B) in the open-mouth position.

8th Edition American Joint Committee on Cancer (AJCC) Head and Neck Cancer Staging: What has changed and how does it affect me?

82 8th Edition American Joint Committee on Cancer (AJCC) Head and Neck Cancer Staging: What has changed and how does it affect me?

M Agarwal, MA Michel

Medical College of Wisconsin
United States

Purpose: In this exhibit we will 1) Outline the changes to head and neck cancer staging according to the recently released 8th edition American Joint Committee on Cancer (AJCC) cancer staging manual; 2) Describe the relevance of these changes to the interpreting head and neck radiologist; and 3) Demonstrate the differences between the current and prior staging systems using relevant imaging cases. Description: The AJCC Staging Manual was established to predict tumor prognosis and determine systematic therapeutic regimens on the basis of clinical, imaging and pathological tumor features. With advancing knowledge of tumor pathophysiology and behavior, and with emerging innovations in treatment, the manual is frequently updated to reflect changing trends. The most recent revision of this manual was published in December 2016. Significant changes were made to head and neck cancer staging including the addition of new chapters on 1) HPV+ oropharyngeal cancer, 2) soft tissue sarcomas of the head and neck, 3) cutaneous carcinomas of the head and neck, and 4) non-viral-related head and neck cancer of unknown primary. There has been modification of the T and N staging for nasopharyngeal cancer as well as modification of T staging for oral cavity cancer. During this period of transition, head and neck imagers and oncologists are making changes to their reporting and treatment protocols and it is important for all to fully understand these changes and their implications. Summary: Head and neck imagers and oncologists are transitioning to the staging system established by the new 8th edition AJCC manual. An overview of the new system, its implications to the head and neck imager, and the differences from the previous staging system are demonstrated in this exhibit.

Imaging of Acquired Sensorineural Hearing Loss

83 Imaging of Acquired Sensorineural Hearing Loss

G Avey, J Roche, J Brucker, T Kennedy

University of Wisconsin School of Medicine and Public Health
United States

Purpose: Sensorineural hearing loss is a common clinical entity and is frequently imaged to assess for potential underlying treatable conditions. Our understanding of this entity is evolving, with a greater appreciation of the role of synaptopathic noise-induced hearing loss. Other previously underappreciated imaging based prognostic features, such as increased T1 and FLAIR signal intensity within the cochlea, are actively being reported and evaluated in the radiology literature. This evolving literature presents an opportune moment to review both the newly appreciated and familiar causes of acquired sensorineural hearing loss. Description: Sensorineural hearing loss can be divided into both sensory (cochlear) and neural (retrocochlear) etiologies. This case based electronic exhibit reviews the causes of sensorineural hearing loss starting with abnormalities of the bony labyrinth, the membranous labyrinth, the cochlear synapses, the vestibulocochlear nerve, and finally central causes of sensorineural hearing loss. This format both explores the relevant pathology of sensorineural hearing loss and reinforces a relevant search pattern for related imaging studies. Summary: Imaging can play a central role in determining the etiology of sensorineural hearing loss and in helping to assess prognosis and potential treatment options. In order to fully evaluate a patient with sensorineural hearing loss the radiologist must be familiar with the anatomy, physiology, and pathology of the bony labyrinth, the membranous labyrinth, and vestibulocochlear nerve.

A rare pediatric case of aggressive mandibular central giant cell granuloma

84 A rare pediatric case of aggressive mandibular central giant cell granuloma

BD Owen, O Raslan, J Chang, N Pham, M Bobinski, A Ozturk

University of California Davis
United States

Purpose We present imaging findings of a pediatric case of mandibular central giant cell granuloma (GCG) with aggressive features. Description A 14 year old male developed soreness of the right mandibular tooth and numbness in the right lower jaw and lip, which was evaluated by an outside oral surgeon who performed a biopsy. The outside pathologic evaluation demonstrated a central interosseous giant cell granuloma with secondary aneurysmal bone cyst-like areas. He was initially treated with steroid injections, however after the third treatment, his family noticed a significant change in the size of the lesion, causing visible distortion of the mandible. He was then referred to our department of otolaryngology for surgical evaluation. On physical examination, he had an expansile large lesion asymmetrically involving the mandible more on the right side with involvement of multiple teeth, and intact overlying mucosa. There was anesthesia along the distribution of right trigeminal nerve mandibular division. Computed Tomography (CT) demonstrated a large expansile lesion with central cystic and peripheral solid enhancing components involving the symphysis and right mandibular body with separation and lateral displacement of the adjacent teeth. The peripheral margins of the lesion demonstrate significant cortical thinning/remodeling and expansion. There was associated mass effect along the floor of mouth but no adjacent soft tissue infiltration. The patient underwent partial resection of the mandible with osteo-cutaneous fibular free-flap reconstruction of mandible and floor of mouth. Histopathological result from the surgical specimen also confirmed the diagnosis of a central giant cell granuloma. Summary GCG is a non-odontogenic tumor occurs only in the head and neck region, typically affecting the maxilla and mandible. The majority of these lesions are found in the anterior mandible as in our case. Although it is a benign entity, it can sometimes be locally aggressive. GCG is believed to be a single pathology in a spectrum of altered vascular and reactive responses within the bone. The lesion most frequently occurs in females in the second or third decades of life, and is rare in children. It can mimic an odontogenic cyst as a unilocular osteolytic lesion with evolution into a multilocular morphology with thin osseous septations, and may cross the midline of the mandible. There may be associated osseous erosion, expansion, remodeling of cortex, or root resorption. Locally aggressive GCGs can affect children at an earlier age, can be larger at the time of diagnosis, and recur more frequently than a non-aggressive type. GCGs should be considered in the differential diagnosis of cystic osteolytic lesions of the mandible, particularly in the pediatric age group, which can require extensive surgery for definitive management.

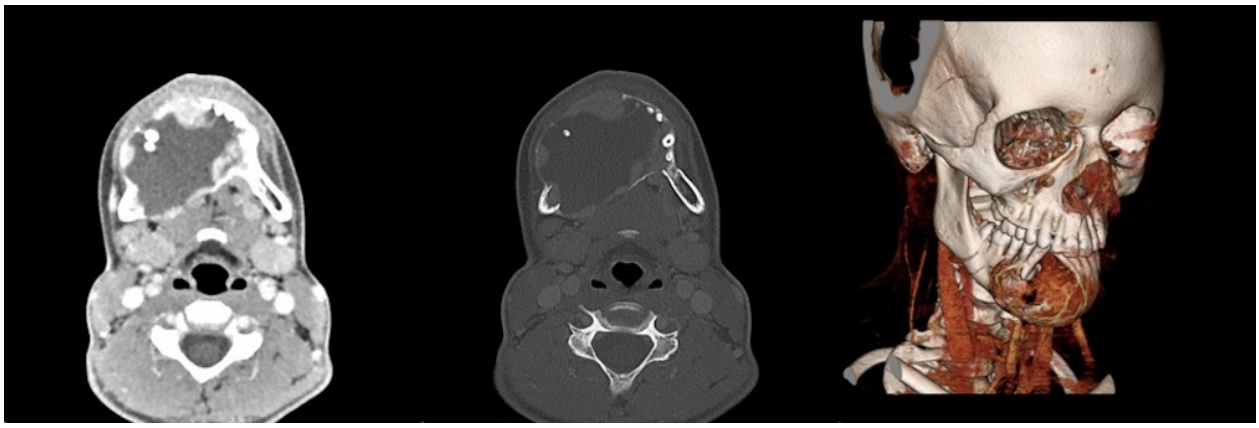

It is not just a snot: Imaging review of sinonasal , inflammatory and neoplasic disease

85 It is not just a snot: Imaging review of sinonasal , inflammatory and neoplasic disease

K Jonguitud, M Campos-Coy, J Menchaca

Hospital Universitario Jose Eleuterio Gonzalez
Mexico

Purpose: To review the most common manifestations and the main indications of imaging modalities of sinonasal pathology such as infectious, inflammatory and neoplasic diseases. Description This educational exhibit will explain the utility and role of imaging modalities (computed tomography and magnetic resonance) for the characterization of infectious, inflammatory and neoplasic disease, explaining the most characteristics radiologic features of each process. Summary Most individual have experience symptoms related to sinonasal disease, requiring imaging studies when patients are unresponsive to medical therapy or when symptoms are chronic. Given this clinical scenario, radiologists should know the differential diagnosis of sinonasal disease, in order to differentiate infection from inflamatory and neoplasic disease. Among those differential diagnoses are acute and chronic rhinosinusitis, fungal infections (mycetoma, invasive fungal sinusitis and allergic fungal sinusitis) and inflammatory processes (sinonasal polyposis, sinonasal solitary polyps, silent sinus syndrome, sinonasal mucocele and granulomatosis with polyangiitis); each with different clinical and radiological features. It is also important to distinguish benign neoplasms (juvenile angiofibroma, inverted papiloma, hemangioma, osteoma, ossifying fibroma and fibrous dysplasia) from malignant tumors (squamous cell carcinoma, adenoid cyst carcinoma, esthesioneuroblastoma, adenocarcinoma, melanoma and non-Hodgkin Lymphoma). An understanding of the different radiological patterns of sinonasal dissease will allow the radiologist to play a crucial role in alerting the clinician to use appropriate diagnostic techniques for diagnosis.

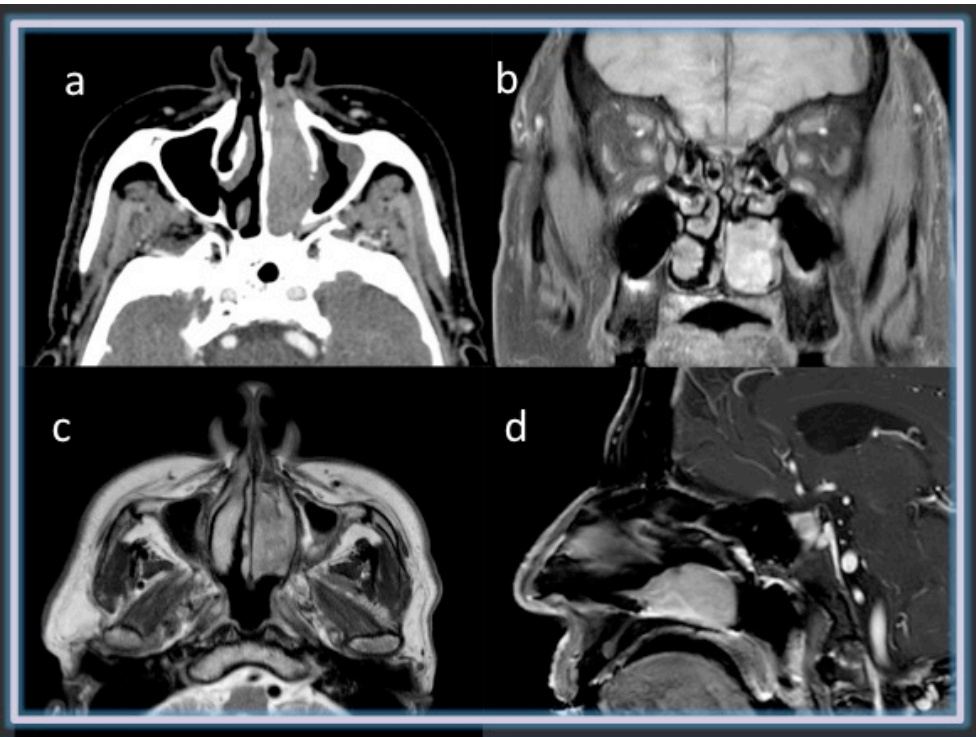

Fig. 2. Sinunasal melanoma (a) Axial CT image shows a soft tissue mass involving the left inferior turbinate. (b) Coronal T1W fat sat images demostrate high signal intensity . (c) On the axial T2W the mass reveal low signal intensity. (d) Contrast-enhacement fat sat suppressed T1W MRI, the lesion display enhacement.

Head & Neck Vascular Anomalies: Diagnostic and Interventional Manual for the Neuroradiologist

86 Head & Neck Vascular Anomalies: Diagnostic and Interventional Manual for the Neuroradiologist

LB Eisenmenger, D Cooke, C Glastonbury, C Hess, CF Dowd

University of California, San Francisco
United States

Purpose: To provide a practical framework for clinical classification of vascular anomalies of the head and neck. To provide a review of the clinical presentation, important imaging findings, and available treatment options emphasizing the information that is most important for the neuroradiologist to know and convey to clinicians. Description: Vascular anomalies affect approximately 1 in 22 children with sixty percent found in the head and neck. Through case-based examples with clinical presentation as well as clinical, radiologic, intra-procedural, and post-treatment images, we will highlight the importance of a multi-disciplinary approach. In this educational exhibit, we not only review these anomalies and syndromes but more importantly provide a practical framework for clinical classification and treatment of vascular anomalies of the head and neck. These lesions can present throughout antenatal and perinatal period as well as during childhood development and into adulthood. They broadly fall into two categories: vascular tumors and vascular malformations. Their impact is determined by both pathological type and location. While many of these lesions follow an uncomplicated course, more complex and/or progressive anomalies can cause significant morbidity and mortality from mass effect, hemorrhage, or large volume arteriovenous shunting. Vascular tumors include infantile hemangioma, congenital hemangioma [both rapidly involuting congenital hemangioma (RICH) and noninvoluting congenital hemangioma (NICH)], and the more aggressive kaposiform hemangioendothelioma (KHE) and tufted angioma (TA). Management options for vascular tumors include conservative measures, oral medications, and surgical intervention with a treatment determined by tumor type, location, and associated complications. Vascular malformations are not tumors and represent malformed blood vessel elements, including arteriovenous, capillary, lymphatic, and venous malformations, or a combination thereof. Arteriovenous malformations are a heterogeneous group of dynamically changing, high flow arteriovenous shunting lesions primarily treated with an endovascular or surgical approach. Lymphatic and venous malformations (together often referred to as "low-flow" vascular malformations) are frequently treated by sclerotherapy, surgery, or medical management. Vascular anomalies may also be indicative of more extensive underlying syndromes and their associated pathology, including but not limited to hereditary hemorrhagic telangiectasia, Sturge-Weber syndrome, and 'PHACES' syndrome. Figure 1 shows an example case with pre-procedural clinical (A) and MR (B) images of an infant with a large lymphatic malformation as well as decreased size of the malformation after sclerotherapy (C and D). Ultrasound images during treatment show a small portion of the treated malformation with a pre-procedural image (E), an image after aspiration (F), and an image after sclerotherapy injection with echogenic injectate (G). A single sagittal fluoroscopic image (H) shows the areas of the lymphatic malformation treated in this stage of therapy. Summary: Vascular anomalies are an important cause of morbidity in children extending into adulthood. Accurate and efficient identification, diagnosis, and management of these lesions is essential. Through a case-based approach, this educational exhibit will provide a practical framework for classification of vascular anomalies of the head and neck as well as highlight the important information the neuroradiologist must know to effectively contribute to the multi-disciplinary treatment effort.

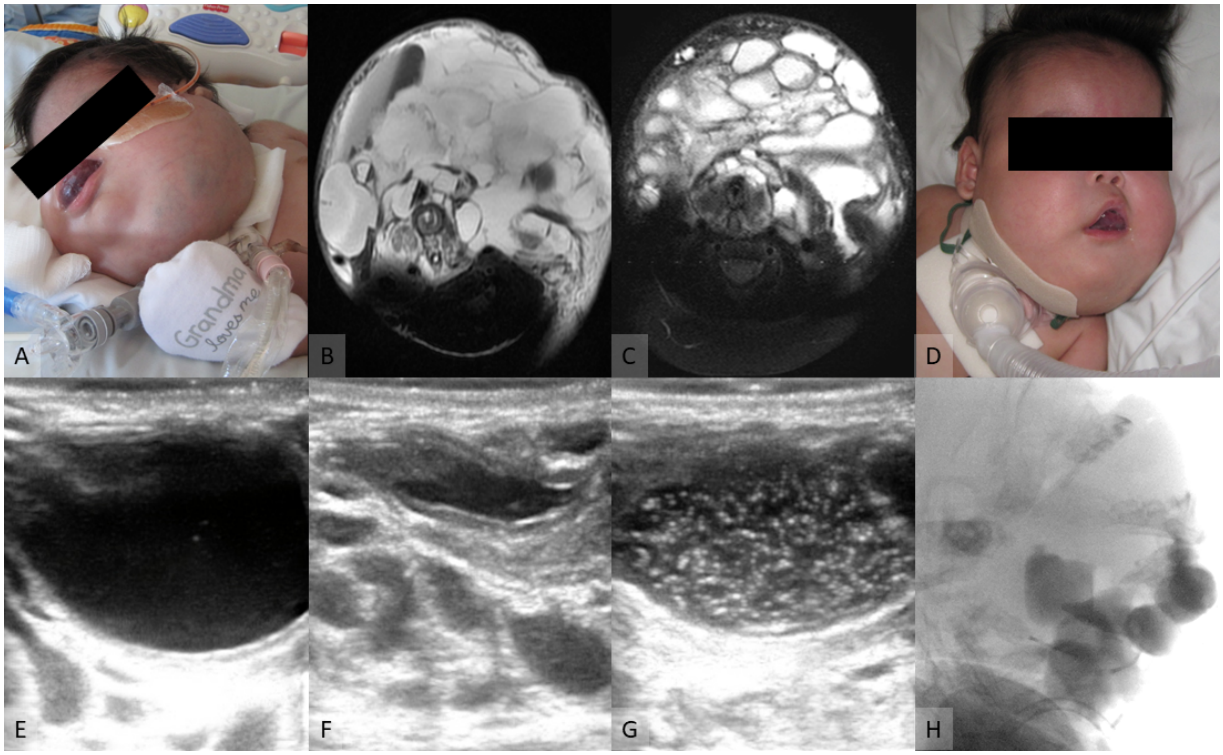
A
B
C
D
E
F
G
H

“Oh Myeloma!” A Pictorial Spectrum of Plasma Cell Neoplasms Involving the Head and Neck

87 “Oh Myeloma!” A Pictorial Spectrum of Plasma Cell Neoplasms Involving the Head and Neck

R Gupta, MH Hanna, A Arneja, A Bansal, P Som

Mount Sinai Hospital - Icahn School of Medicine
United States

Purpose: To illustrate the various manifestations of plasma cell neoplasms in the head and neck as part of a disease continuum. Description: Plasma cell neoplasms include multiple myeloma, solitary plasmacytoma of bone, and extramedullary multiple myeloma, which are histologically similar, but may have differing clinical presentations and treatment approaches. They are relatively rare in the head and neck and can mimic other entities causing a diagnostic dilemma. We present here a case series of plasma cell neoplasms involving the head and neck including the skull base, cranial nerves, retina and orbit, paranasal sinuses, and mandible with radiological pearls. Summary: Plasma cell neoplasms are rare in the head and neck, however, differentiating them from other entities carries clinical relevance with treatment implications, and thus imperative for radiologists to understand.

Plasma Cell Neoplasms in the Head and Neck
Selected Examples

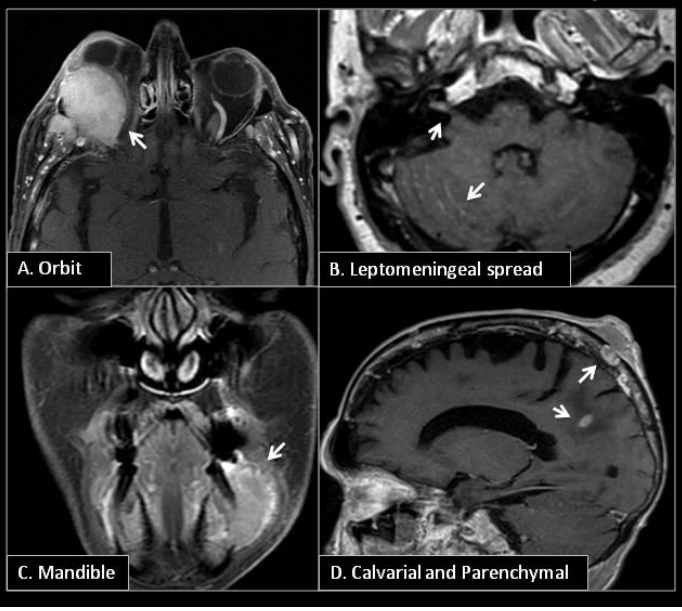

Fig A. Axial Post C+ MRI of the Orbits: Large enhancing mass in the Right orbit.

Fig B. Axial Post C+ MRI through skull base shows leptomeningeal spread involving the Left CN VII-VIII complex and cerebellar folia.

Fig C. Coronal Post C+ MRI: Enhancing osseous and extra-osseous mass involving the Left mandible.

Fig D. Sagittal Post C+ MRI: Calvarial and extra-calvarial lesions as well as a parenchymal lesion with surrounding edema in the parietal lobe.

What's the matter with matted nodes? Significance of matted lymph nodes in HPV-related oropharyngeal squamous cell carcinoma

88 What's the matter with matted nodes? Significance of matted lymph nodes in HPV-related oropharyngeal squamous cell carcinoma

K Huang, R Banerjee, B Debenham, A Patel, F Sabiq, H Lau, D Skarsgard, J Lysack, G Chen, H Quon

Vancouver General Hospital
Canada

PURPOSE: HPV-related oropharyngeal squamous cell carcinoma (OP SCC) is associated with favorable survival outcomes compared to non-HPV related OP SCC. Given its poor prognostic significance, the presence of matted lymph nodes was added to other exclusion criteria to some treatment de-escalation trials. However, its prognostic significance should be independently validated and the radiologic criteria for matted nodes needs to be further defined. MATERIALS & METHODS: Patients diagnosed with p16+ OP SCC, treated with curative intent, diagnosed between January 2007 to April 2013, with available diagnostic CT images were retrospectively reviewed. Pre-treatment images were independently scored by a neuroradiology fellow according to 4 radiologic nodal groups: discrete non-abutting lymph nodes (LNs) without extranodal extension (ENE) (group D); abutting LNs without ENE (group A); abutting LNs with ENE in their intervening fat plane only (group I); single LN with ENE or abutting LNs with ENE in their intervening fat plane and around their non-abutting borders (group E). Overall survival (OS) and local, regional and distant recurrence free survival (RFS) was calculated based on Kaplan-Meier (KM) method and compared by log-rank test. Multivariate analysis, accounting for age, sex, comorbidity, smoking status, primary treatment modality, subsite and stage, was also performed. RESULTS: 260 patients with locally advanced p16+ OP SCC were diagnosed and treated with curative intent. Median follow-up was 4.96 years (range 0.21-5.00 years) and mean age was 57 years (± SD 8). Distribution of radiologic nodal groups is as follows: D (n= 81), A (n=54), I (n=79) and E (n=46). OS at 5 years was 79.6% (A) vs 78.6% (D), p=0.87; 81.0% (I) vs 77.9% (no I), p=0.57; and 65.2% (E) vs 81.8% (no E), p=0.01. RFS at 5 years was 81.5 (A) vs 84% (D), p=0.66; 86.1% (I) vs 82.3% (no I), p=0.45; and 72% (E) vs 86% (no E), p=0.02. By univariate analysis, the presence of E nodes was significantly associated with reduction in OS, RFS, and distant RFS (all p=0.01); and the presence of I nodes was significantly associated with reduction in local RFS (p=0.02). By multivariate cox regression analysis, at 5 years, the presence of E nodes was statistically significantly associated with reduction in distant RFS with a hazard ratio (HR) of 5.2 (95% confidence interval 1.2-22.1, p=0.02. CONCLUSION: In this multi-institutional study, the prognostic significance of 4 different radiologic nodal groups in p16+ OP SCC is evaluated. The presence of group E nodes was significantly associated with reduction in 5-year OS, RFS, and distant RFS by univariate analysis and reduction in distant RFS by multivariate analysis. This suggests that ENE is a strong prognostic indicator and should be considered in clinical decision-making, and for inclusion in future AJCC staging systems for p16+ OP SCC.

A case of styloid process radiation necrosis and concurrent tumor recurrence evaluated using dual energy CT

89 A case of styloid process radiation necrosis and concurrent tumor recurrence evaluated using dual energy CT

G Romero Sanchez, LE Ginsberg, A Elakkad, R Forghani

Jewish General Hospital, McGill University
Canada

Purpose: Radiation necrosis of the styloid process as a complication of head and neck cancer treatment is a rare event, with no published description in the peer reviewed literature so far. In this report, we describe an interesting case of biopsy proven styloid process radiation necrosis with concurrent cancer recurrence. Materials and Methods: We present a case of a 63-year-old-male who was treated with chemoradiation for a p16+ right tonsil SCC who diagnosed in February 2016. After completion of the treatment, patient developed a new dysphagia and globus sensation when eating. A CT scan was requested to rule out necrosis vs tumor progression and biopsy was performed. The CT scan was performed in dual-energy CT (DECT) mode. In addition to 65 keV virtual monochromatic images (VMIs) typically considered similar to a standard single energy CT acquisition when using DECT, low energy VMIs (40 keV) and iodine-water material decomposition maps were also generated and quantitative region of interest analysis was performed with generation of spectral Hounsfield unit attenuation curves. Results: The DECT showed abnormal solid enhancement extending adjacent to the right styloid process. However, there was also a small rim enhancing collection and gas along part of the styloid process that was fragmented, without evidence of solid invading mass accounting for the fragmentation. On DECT iodine maps, there was a combination of poorly enhancing tissue suggestive of post-treatment changes and radionecrosis as well as tissue with a high content concerning for tumor. Because of this unusual presentation, the possibility of styloid process radionecrosis, with secondary inflammatory changes and possibly concurrent tumor recurrence, was raised. Biopsy confirmed co-existent recurrent invasive poorly differentiated SCC. Conclusions: Styloid process radiation necrosis can occur as a rare complication after treatment of oropharyngeal SCC and it is important to be aware of this complication. However, the presence of radiation necrosis does not exclude concurrent tumor recurrence and careful evaluation for any solid tissue component is mandatory for identifying concurrent tumor recurrence and DECT could be helpful in this regard by improving visualization and extent of solid enhancing tissues.

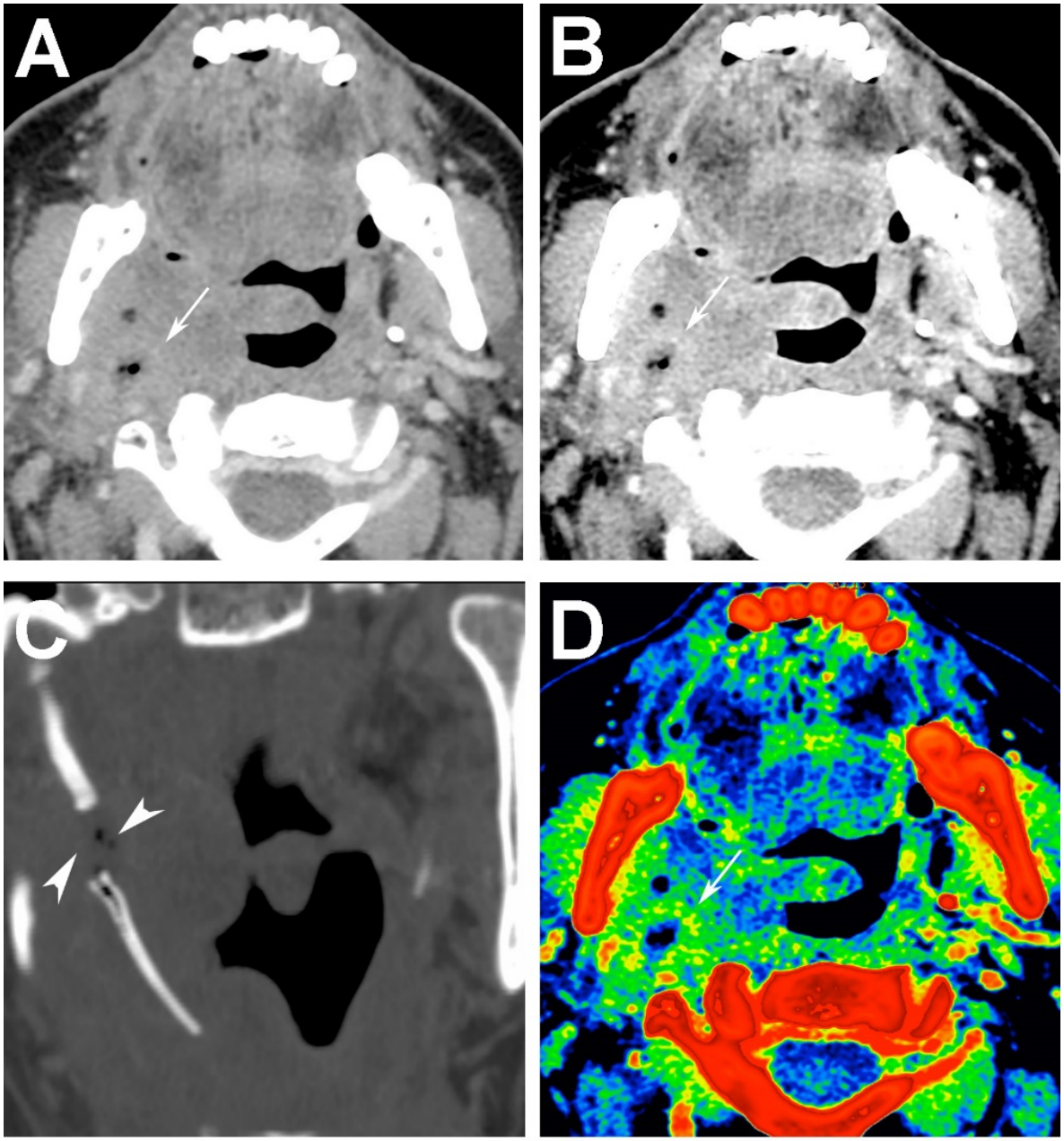

Figure 1. (A) 65 keV VMI, (B) 40 keV VMI, (C) coronal reformatted 65 keV VMI displayed bone windows, and (D) iodine map are shown. There is a pocket of fluid and gas along the broken off part of styloid process (arrowheads). There is mixed attenuation tissue in this area, including solid iodine containing component that is well seen on the iodine map (white arrows).

Papillary Cystadenoma: A Rare Benign Minor Salivary Gland Neoplasm

90 Papillary Cystadenoma: A Rare Benign Minor Salivary Gland Neoplasm

K Riley, N Supakul, K Mosier

Indiana University School of Medicine
United States

Purpose Papillary cystadenoma is a rare benign salivary gland neoplasm which may present clinically as a cheek mass. The purpose of this exhibit is to review the CT and ultrasound features of this entity most likely to be encountered by the head and neck radiologist. Description Papillary cystadenoma (PC) is a rare, benign and indolent neoplasm predominantly involving the minor salivary glands which typically presents as an asymptomatic cheek mass. Current literature describing the imaging features of PC is sparse, and to date only the histologic and pathologic features have been characterized in detail. PC histologically resembles the much more common Warthin's tumor (also known as papillary cystadenoma lymphomatosum) however it lacks a lymphoid component. Differentiating these two entities is location, as Warthin's tumor occurs within the parotid gland the vast majority of the time. Furthermore, while there is a known strong association between smoking and Warthin's tumors, no such association with PC is known as the risk factors are not well-understood. Given the high utilization of cross-sectional imaging for evaluation of facial masses it is important to be aware of PC and its appearance on imaging which may help differentiate it from other more aggressive neoplasms also occurring within the minor salivary glands including cystadenocarcinoma, mucoepidermoid carcinoma, and adenoid cystic carcinoma. A retrospective search was performed using a database of all radiologic and pathology exams performed at our institution. Pathologically-proven cases of salivary gland papillary cystadenoma were identified and all available imaging studies were reviewed. We highlight the common features of these cases on CT and ultrasound imaging that are of importance to head and neck radiologists. Summary Papillary cystadenoma is an uncommon benign salivary gland neoplasm that may present as a cheek mass or other facial mass. While the histologic features of this mass have been well-characterized, description of its features on cross-sectional imaging within the literature is lacking. Knowledge of its appearance on CT and ultrasound will help the head and neck radiologist formulate a more complete differential diagnosis and add value to patient care. References Tjioe KC, de Lima HG, Thompson LD, et al. Papillary Cystadenoma of Minor Salivary Glands: Report of 11 Cases and Review of the English Literature. Head Neck Pathol. 2015 Sep;9(3):354-9. Barnes L., Everson J.W., Reichart P., Sidransky D. (Eds): World Health Organization Classification of Tumours. Pathology and Genetics of Head and Neck Tumours. IARC Press; Lyon 2005.

Skull Base Osteomyelitis: Rare, but worth revisiting. We present an unusual case of clival osteomyelitis in a patient with remote nasopharyngeal carcinoma.

91 Skull Base Osteomyelitis: Rare, but worth revisiting. We present an unusual case of clival osteomyelitis in a patient with remote nasopharyngeal carcinoma.

TW Plauche, N Emerson

Ochsner Health System
United States

Skull base osteomyelitis (SBO) is a rare, but potentially life threatening entity typically occuring secondary to otitis externa in immunocompromised patients. SBO of the clivus is referred to as central skull base osteomyelitis to differentiate this entity from “typical” SBO commonly involving the temporal bones. SBO is treatable with antibiotics, however expeditious diagnosis is of utmost importance. Diagnosis is often delayed due to vague clinical presentation allowing for a wide spectrum of differentials. Additionally, radiographic features of SBO on common imaging modalities are indistinguishable from neoplastic disease and tissue sampling is often required. We present an interesting case of clival SBO precluded by a remote history of nasopharyngeal carcinoma along with a review of radiographic and clinical features to aid in the expedient diagnosis and treatment of SBO. Discussion: A 72 year-old male presented to our institution with a 2 month history of progressive occipital headaches, upper cervical neck pain, fatigue, and 20lbs weight loss. Symptoms progressed to include fever and AMS (confusion/disorientation and slurred speech) 48 hours prior to admission. Patient was oriented to self only and medical history was obtained from family. Pertinent past medical history included remote nasopharyngeal carcinoma in remission treated with chemo-radiation therapy 18 years prior to admission. Initial CT imaging revealed a destructive lytic lesion centered at the clivus with mucoperiosteal thickening of the sphenoid sinuses. Differential diagnosis included primarily recurrent neoplasm vs delayed radiation necrosis. Further imaging with MRI revealed more extensive skull base erosion along with a rim-enhancing epidural collection which raised concern for SBO to the top of our differential. ENT and NSGY consultation was obtained with subsequent endoscopic sphenoidotomy and biopsy was performed. Endoscopy revealed “boggy, edematous mucosa” in the sphenoid sinus “resembling a polypoid mass” as well as “frank yellow-white purulence.” Antibiotic therapy was initiated and cultures grew Mycobacterium avium intracellulare complex. The patients clinical symptoms subsequently resolved and serial imaging revealed stability of radiographic features. Conclusion: SBO is a potentially life threatening, yet treatable entity with imaging features mutual to both infectious and neoplastic processes. Established clinical and radiographic findings include cranial nerve deficits, headaches, and osseous erosion of the skull base. Special attention should be paid to markers of inflammation such as elevated WCC and CRP, presence or absence of fluid collections, and presence of immunocompromised state. These features should prompt early initiation of empiric antibiotic therapy once identified. Direct tissue sampling confirms diagnosis and should not be delayed once suspicious imaging findings are discovered.

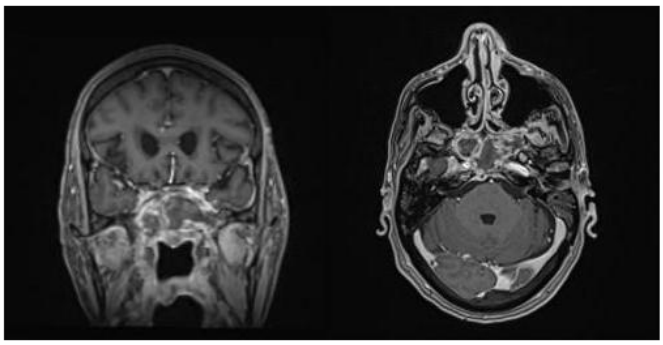

Coronal and Axial FSPGR - post contrast

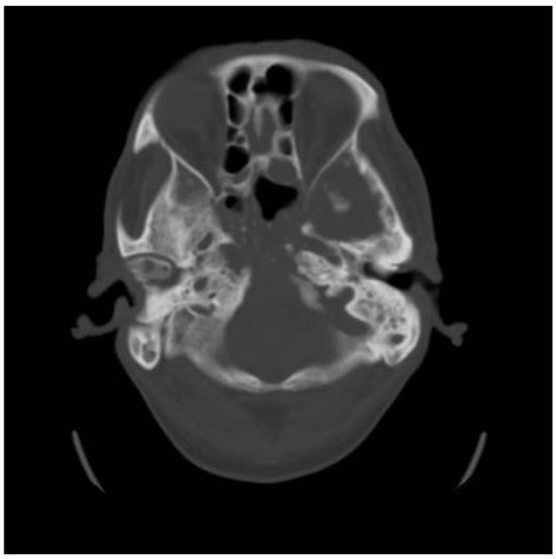

Axial CT head

Radiation Dose and Image Quality in Pediatric Neck CT

92 Radiation Dose and Image Quality in Pediatric Neck CT

M Spampinato, D Patel, S Stalcup, M Matheus, S Tipnis

MUSC
United States

Purpose: To evaluate the image quality of pediatric neck CT studies before and after the implementation of low dose protocols. Materials and Methods: We retrospectively reviewed 179 pediatric neck CT studies, 75 before and 104 after the implementation of low dose protocols, performed in children aged 0-16 years. The two cohorts were divided into 3 age groups, 0 to 4 years, 5 to 9 years, and 10 to 16 years. All studies were performed with tube current modulation on multidetector CT scanners. Target CTDIvol values for pediatric neck CT were set at 6 mGy, 8 mGy, and 15 mGy for the 0 - 4, 5 - 9, and 10 - 16 years groups respectively. We obtained CT scanning parameters, CT dose index (CTDIvol), and dose-length product (DLP) from the Picture Archiving and Communication System. A quantitative assessment of image quality was performed by measuring the background noise (BN) and calculating signal-to-noise ratio (SNR) on the axial CT image through the true vocal folds. Three neuroradiologists assessed the image quality of the same CT image using a 5-point scoring system, where 1 = non-diagnostic and 5 = excellent diagnostic quality, and scores equal to or greater than 3 indicated satisfactory diagnostic quality. We compared CTDIvol, DLP, average image quality ratings, and SNR of studies conducted at baseline and with low dose protocols using the Mann-Whitney test. Results were considered statistically significant when $p < 0.05$. Results: CTDIvol and DLP were significantly lower in studies performed using the low dose protocols than at baseline in children aged 0-4 and 10-16 ($p < 0.001$ for both variables), but there was no significant change in CTDIvol and DLP in the 5-9 year old group. Image quality ratings and SNR were lower in the low dose than in the baseline cohort in children aged 10-16, but not in children aged 0-4 and 5-9 years. Despite the decrease in image quality scores in children aged 10-16 years, 97% of the studies (73/75) in the baseline patient cohort and all studies (104/104) in the follow-up patient cohort were considered of sufficient image quality. Conclusion: Following the implementation of low dose pediatric neck CT protocols, we observed no degradation of diagnostic image quality. Our initial results suggest that there may be an opportunity for further radiation dose reduction without compromising diagnostic image quality using iterative reconstruction algorithms.

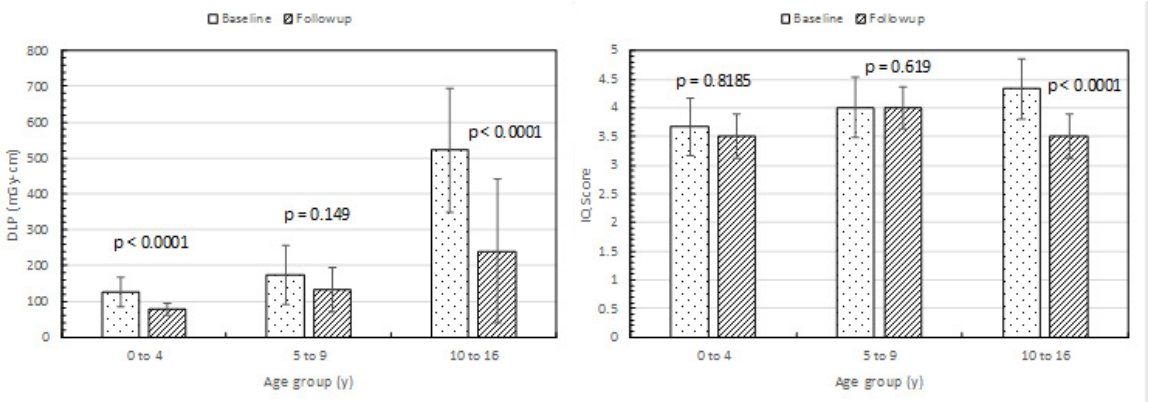

Imaging Findings in Temporal Bone of Patients with Fanconi Anemia and Conductive Hearing Loss

93 Imaging Findings in Temporal Bone of Patients with Fanconi Anemia and Conductive Hearing Loss

L Coelho, K Mahfouz, D Bertholdo, G Santos, A Carvalho Neto

DAPI
Brazil

Purpose: To demonstrate temporal bone anatomical abnormalities in patients with Fanconi anemia (FA) and conductive hearing loss using computed tomography (CT). Background: FA is a rare autosomal recessive disorder (1 to 5 in 1,000,000), characterized by pancytopenia, multiple congenital anomalies and increased susceptibility to malignancy. Skin pigmentation, radial ray deformities, renal and urinary tract anomalies are the most frequent congenital anomalies. Otologic and audiologic manifestations in FA patients have also been described, particularly in patients with abnormal radii. The prevalence of hearing loss and ear anomalies in patients with FA varies from 10 to 20%. Findings: Seven patients (2 male, 5 female; mean age 13 years, from 5 to 44 years) with FA and conductive hearing loss were evaluated with temporal bone CT, performed using a 64-channel multidetector. Six patients depicted ear malformations. One patient had chronic inflammatory changes on both mastoid and erosion of the inferior margin of the manubrium of malleus bilaterally, probably post infection. The most common malformation found was hypoplasia, aplasia or thinning of the manubrium of malleus, seen bilaterally in all 6 patients. Other abnormalities found were: reduced diameter of the tympanic membrane (5 patients), narrowed external auditory canal (3 patients), thin facial canal nerve, lateral semicircular canal dysplasia and oval window atresia (all 1 patient). Conclusion: Although the exact frequency and types of ear malformations in FA are unknown, our patients presented mainly with malleus and external ear abnormalities, which could play a role in conductive hearing loss in FA patients.

What’s wrong with that tongue?: Imaging approach to hypoglossal nerve pathology

94 What’s wrong with that tongue?: Imaging approach to hypoglossal nerve pathology

AP Guarnizo, R Glikstein, C Torres

University of Ottawa, The Ottawa Hospital
Canada

Purpose: 1. To review the anatomy and course of the 12th cranial nerve 2. To discuss the common and rare pathologies that affect the hypoglossal nerve along its five segments 3. To review the imaging features of hypoglossal nerve denervation Approach/Methods: A retrospective review of the imaging findings in patients with isolated hypoglossal nerve palsy was performed. Different disorders affecting the hypoglossal nerve were identified along its course. Detailed CT and MR imaging features of the lesions causing CN 12 palsy and the associated findings that result from hypoglossal denervation were described. Findings: Multiple lesions can affect the hypoglossal nerve along its five segments. Within its medullary segment, we found lesions such as neoplasms, vascular malformations and demyelinating disease. Primary neoplasms, metastatic disease, traumatic injury and vascular pathologies involved the cisternal, skull base and the carotid segments. Squamous cell carcinoma was the most common pathology involving the sublingual segment of the nerve. Chronic hypoglossal denervation was seen as atrophy and fatty replacement of the muscles in the affected hemitongue . In addition, a "pseudomass appearance" secondary to posterior bulging could be seen and signal changes vary on MRI depending on the acuity or chronicity of the nerve injury. Summary: The hypoglossal nerve gives motor innervation to the intrinsic and extrinsic muscles of the tongue. Injury to this nerve manifests with particular features that involve the imaging appearance and movement of the tongue. It is important to be familiar with the anatomy and the imaging findings of hypoglossal denervation in order to identify or suspect an underlying pathology.

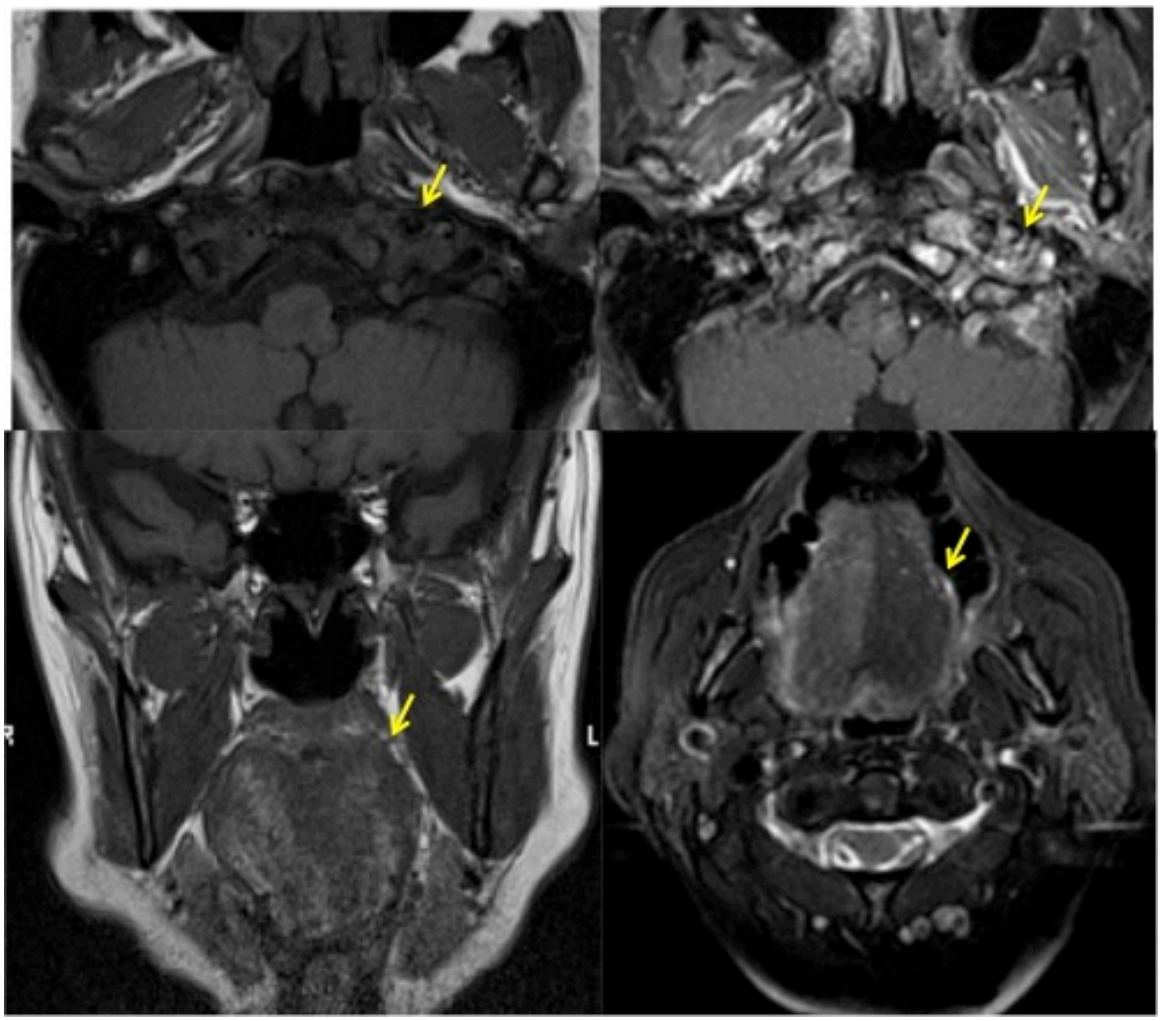
R
L

Imaging Features of Benign Salivary Gland Tumors

95 Imaging Features of Benign Salivary Gland Tumors

D Ginat

University of Chicago
United States

Purpose: This exhibit reviews the multimodality diagnostic imaging features of benign neoplastic and nonneoplastic tumors associated with the major salivary glands. Description: Examples of neoplastic conditions that are depicted and discussed include pleomorphic adenoma, Warthin tumor, oncocytoma, peripheral nerve sheath tumors, lipoma, and hemangiomas or hemangioendotheliomas. Examples of nonneoplastic conditions that are depicted and discussed include ranulas, benign lymphoepithelial lesions, Kimura disease, and vascular malformations. Summary: Specific imaging and clinical features of these conditions are emphasized in this article.

Assessment of Proton Resonance Frequency Shift MR Thermography for Head and Neck Tumors

96 Assessment of Proton Resonance Frequency Shift MR Thermography for Head and Neck Tumors

D Ginat, G Christoforidis, S Sammet

University of Chicago
United States

PURPOSE Adequate image quality is necessary for implementing MR thermography during MRI-guided laser ablation of head and neck tumors. The goal of this study is to objectively characterize the image quality of phase contrast MR thermography sequences in patients with head and neck tumors. METHOD AND MATERIALS Phase contrast MR thermography (TR: 30 ms, TE: 10 ms, flip angle: 19.5 degrees, slice thickness: 3.0 mm, number of excitations: 1, matrix size: 252x126, field of view: 240 mm) was performed on 3T scanners (Ingenia dStream; Philips Healthcare, Best, The Netherlands) in a series of patients with head and neck tumors. The signal-to-noise and contrast-to-noise ratios of the lesions on the images were computed in order to gauge image quality. RESULTS A total of 9 lesions in 8 patients were assessed, including one parotid tumor, one oral tongue squamous cell carcinoma, one tongue base squamous cell carcinoma, one paravertebral squamous cell carcinoma metastasis, four level 4 lymph nodes with metastatic squamous cell carcinoma, and one level 4 lymph node with metastatic squamous cell carcinoma. The average signal-to-noise for the lesions was 515.8 (range: 9.3 to 1973.4; standard deviation: 643.0), while the average contrast-to-noise ratio for the lesions was 98.0 (range: 0.03 to 320.6; standard deviation: 113.0). CONCLUSION The signal-to-noise and contrast-to-noise ratios of lesions in the head and neck depicted on phase contrast MR thermography is highly variable. Factors that may contribute to the variability include coil selection, coil positioning, the nature of the lesion and surrounding tissues in terms of susceptibility effects, patient motions, and blood flow effects. CONCLUSIONS Since the image quality of MR thermography of head and neck lesions can vary considerably, it is important to obtain this sequence as part of thermal ablation planning to ensure that it would be adequate for use during the procedure. For example lesions with a signal-to-noise ratio less than 100 have a temperature uncertainty of greater than 3 degrees Celsius, which was the case for one-third of the lesions in this series.

Lesions involving the tongue in children (part one) - pertinent anatomy and embryology

97 Lesions involving the tongue in children (part one) - pertinent anatomy and embryology

HD Segall, J Qi, T Deshmukh

Medical College/ Children's Hospital of Wisconsin
United States

This presentation will emphasize the anatomy of the tongue and adjacent structures. The practical anatomy that is most important in diagnosing, localizing and treating lesions involving the tongue will be emphasized. The intrinsic and extrinsic musculature of the tongue as well as the muscles at the floor of the oral cavity will be reviewed using anatomic illustrations and cross-sectional imaging. The anatomical relationships of the lingual artery and nerve, sublingual space and pertinent salivary gland tissue and ducts will also be demonstrated on anatomic illustrations and cross-sectional imaging. The anlage of the thyroid starts off in the region of the foramen cecum of the tongue; dynamic illustrations will be used to show the descent of the thyroglossal duct. This embryology is important to know when evaluating cystic lesions of the tongue, thyroglossal duct cysts and ectopic thyroid. It also helps to explain the various reasons for performing the Sistrunk procedure.

Lesions involving the tongue in children (part two) - cystic lesions

98 Lesions involving the tongue in children (part two) - cystic lesions

HD Segall, M Jang, JF Southern

Medical College/ Children's Hospital of Wisconsin
United States

The first part of this presentation has dealt with important anatomy and embryology that is worth understanding when evaluating cystic lesions involving the tongue. In this second part congenital and acquired cystic lesions are considered. Examples of ranulas and other mucocoels, dermoid and epidermoid cysts, thyroglossal duct cysts, foregut duplication cysts, etc. will be shown.

Lesions involving the tongue in children (part three) - other lesions

99 Lesions involving the tongue in children (part three) - other lesions

HD Segall, T Kelly, M Maheshwari

Medical College/ Children's Hospital of Wisconsin
United States

The first and second parts of this presentation have dealt with the anatomy and embryology and a review of cystic lesions involving the tongue. In this third part infections, congenital and vascular vascular lesions and neoplasms are considered. Examples of abscesses, actinomycosis, ectopic thyroid, venous and lymphatic malformations and numerous neoplasms (including a variety of sarcomas, lipoblastoma, teratoma and other tumors) will be shown.

Imaging Review of the 2017 4th Edition World Health Organization (WHO) Classification of Head and Neck Tumors

100 Imaging Review of the 2017 4th Edition World Health Organization (WHO) Classification of Head and Neck Tumors

D Ginat, N Oren

University of Chicago
United States

Purpose: The goal of this exhibit is to review the imaging features of lesions with updated 2017 WHO nomenclature. Description: The major WHO changes include refinement of existing entities, description of new tumor types, elimination of defunct categories, and an update on the biology of various tumor types. In particular, the changes and updates of the following conditions will be reviewed: • tumors of the nasal cavity, paranasal sinuses, nasopharynx, and skull base, including new entities such as NUT carcinomas, and HPV-related carcinoma with adenoid cystic-like features. • tumors of the hypopharynx, larynx, trachea, and parapharyngeal space, including nomenclature revisions for laryngeal neuroendocrine tumors. • tumors of the oral cavity and oropharynx, including squamous cell carcinoma and ectomesenchymal chondromyxoid tumor. • tumors and tumor-like lesions of the neck and lymph node, with a discussion spanning developmental cysts, metastases and heterotopia associated neoplasia. • tumors of salivary gland, including issues related to high grade transformation and nomenclature for polymorphous adenocarcinomas. • odontogenic and maxillofacial bone tumors, including the reversal of terminology for certain cystic lesions. Summary: There are many recent updates to the WHO classification of head and neck tumors, with some changes that are relevant to head and neck imaging.

Many faces of granulomatous lesions of head and neck

101 Many faces of granulomatous lesions of head and neck

CF Lôbo, VT Gonçalves, FA Dalprá, RW Murakoshi, MR Garcia, RL Gomes, EM Gebrim

Radiology Institute of the University of Sao Paulo
Brazil

Educational Exhibit Purpose: - Illustrate and discuss the most frequent imaging findings of granulomatous diseases (GDs) affecting the head and neck, through an anatomical approach; - Highlight the importance of the identification of the possibility of a GD by the radiologist avoiding inappropriate treatment. Description: The spectrum of clinical manifestations of the GDs is variable, as they can affect different organs and systems. Detailed clinical history, laboratory results and epidemiological data are crucial information that radiologists must look for when analysing these cases. Radiological findings associated with these diseases are often nonspecific and overlap. The authors describe etiologies of GDs that affect head and neck through an anatomical approach and illustrate the general findings associated with these diseases, emphasizing the most specific ones. Findings are illustrated with computed tomography and magnetic resonance imaging. Diseases illustrated are: - Sinonasal cavity: granulomatosis with polyangiitis, paracoccidioidomycosis, murcomycosis, leishmaniasis, myiasis and Churg-Strauss syndrome. Special consideration is given on nasal septal perforation. General findings of GDs involving the sinonasal cavities are mucosal thickening and polyps, osseous and cartilage destruction, intraorbital and cranial extension and nasal septal perforation. - Orbits: sarcoidosis, syphilis and granulomatosis with polyangiitis General findings of GDs involving the orbits are enhancing soft tissue masses involving extraocular muscles, lacrimal gland enlargement, masses, extension to apex of the orbit and intracranially and intra and extraconal soft tissue with coarse calcification. - Temporal bone: tuberculosis, myiasis, syphilis, candidiasis, granulomatosis with polyangiitis and cholesterol granuloma General findings of GDs involving the temporal bone are soft tissue occupying the external auditory canal, middle ear and mastoid air cells, sclerosis of the mastoid and erosion and destruction of the mastoid air cells and ossicles. - Aerodigestive tract: granulomatosis with polyangiitis, relapsing polychondritis, tuberculosis, leishmaniasis, paracoccidioidomycosis and actinomycosis (jaw) General findings of GDs involving the aerodigestive tract are infiltrative diffuse mucosal involvement, often ulcerative that may progress to fibrosis, scarring and calcification; glottic and paraglottic thickening and subglottic stenosis. - Lymph nodes: tuberculosis, paracoccidioidomycosis, cat scratch disease and sarcoidosis GDs affecting the lymph nodes often manifest necrotic, suppurative or homogenous lymphadenopathy. Calcifications are observed in tuberculosis and sarcoidosis. Some miscellaneous disorders that involve granuloma formation are also described, such as: giant cell reparative granuloma, Langerhans cell histiocytosis and Rosai-Dorfman granuloma. Summary: - Diagnosis of GDs involves the conjunction different aspects, the clinical history, laboratory exams and imaging findings. - Radiologists should known the differents presentations of granulomatous diseases in head and neck. - Imaging findings may overlap, but some findings are more specific and may help the diagnosis.

Many faces of granulomatous lesions of head and neck

- Granulomas are histological findings consisting of a compact and organized collection of activated macrophages (epithelioid macrophages) surrounded by mononuclear cells. Epithelioid cells may fuse, forming the multinucleated giant cells.
- The spectrum of clinical manifestations of the granulomatous diseases is variable, as they can affect different organs and systems. **Detailed clinical history, laboratory results and epidemiological data are crucial information that radiologists must look for when analysing these cases.**
- Radiological findings associated with these diseases are often nonspecific and overlap. Nonetheless, some diseases exhibit relative specific findings that may aid in the diagnosis. The major differential diagnosis is neoplasm and radiologists should identify the possibility of a granulomatous disease, consequently avoiding inappropriate treatment.

Sinonasal cavity

- Mucosal thickening and polyps;
- Osseous and cartilage destruction;
- Intraorbital and cranial extension;
- Nasal septal perforation;

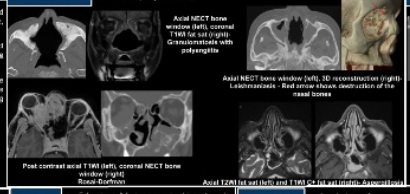

Temporal bone

- Soft tissue occupying the external auditory canal, middle ear and mastoid air cells;
- Sclerosis of the mastoid;
- Erosion and destruction of the mastoid air cells and ossicles;

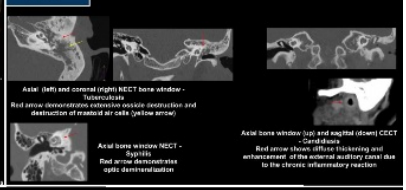

Pharynx and Larynx

- Infiltrative diffuse mucosal involvement, often ulcerative;
- May progress to fistula, scarring and calcification;
- Glottic and paraglottic thickening;
- Subglottic stenosis;

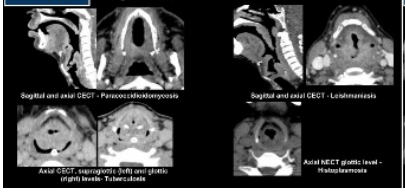

Orbit

- Enhancing soft tissue masses involving extraocular muscles;
- Lacrimal gland enlargement, masses;
- May extend to apex of the orbit and intracranially;
- Intra and extraconal soft tissue with coarse calcifications

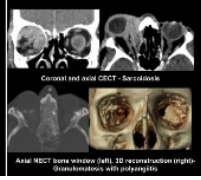

Lymph nodes

- Lymphadenopathy
- Necrosis, suppurative, homogeneous
- Calcifications - tuberculosis and sarcoidosis

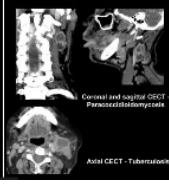

Salivary Gland Small Cell Neuroendocrine Tumors: The Importance of CK20

102 Salivary Gland Small Cell Neuroendocrine Tumors: The Importance of CK20

RL Delfanti, B Julie

UCSD
United States

Purpose: Small cell neuroendocrine carcinomas arising in the salivary glands tumors are rare. Immunohistochemistry, with evaluation of CK-20 expression, can further classify them into Merkel cell or pulmonary varieties, holding promise for prognostic significance. Description: Major and minor salivary gland anatomy is presented on both CT and MRI. Subsequently, the unique characteristics of these small cell neuroendocrine tumors are discussed with consideration given to histology, staging, and outcome. Cross-sectional imaging from a single institution experience is showcased to demonstrate primary salivary small cell neuroendocrine tumors and contrast these to metastases arising from non-salivary neuroendocrine primaries. These examples followed by a self-assessment quiz will stress the importance of a thorough imaging work-up when a neuroendocrine tumor is identified in the neck. Summary: At the end of this exhibit the learner will: 1) be able to identify the major and minor salivary glands; 2) understand the classification of salivary neuroendocrine tumors; 3) direct an appropriate systemic imaging evaluation based on pathologic diagnosis of a neuroendocrine tumor in the neck.

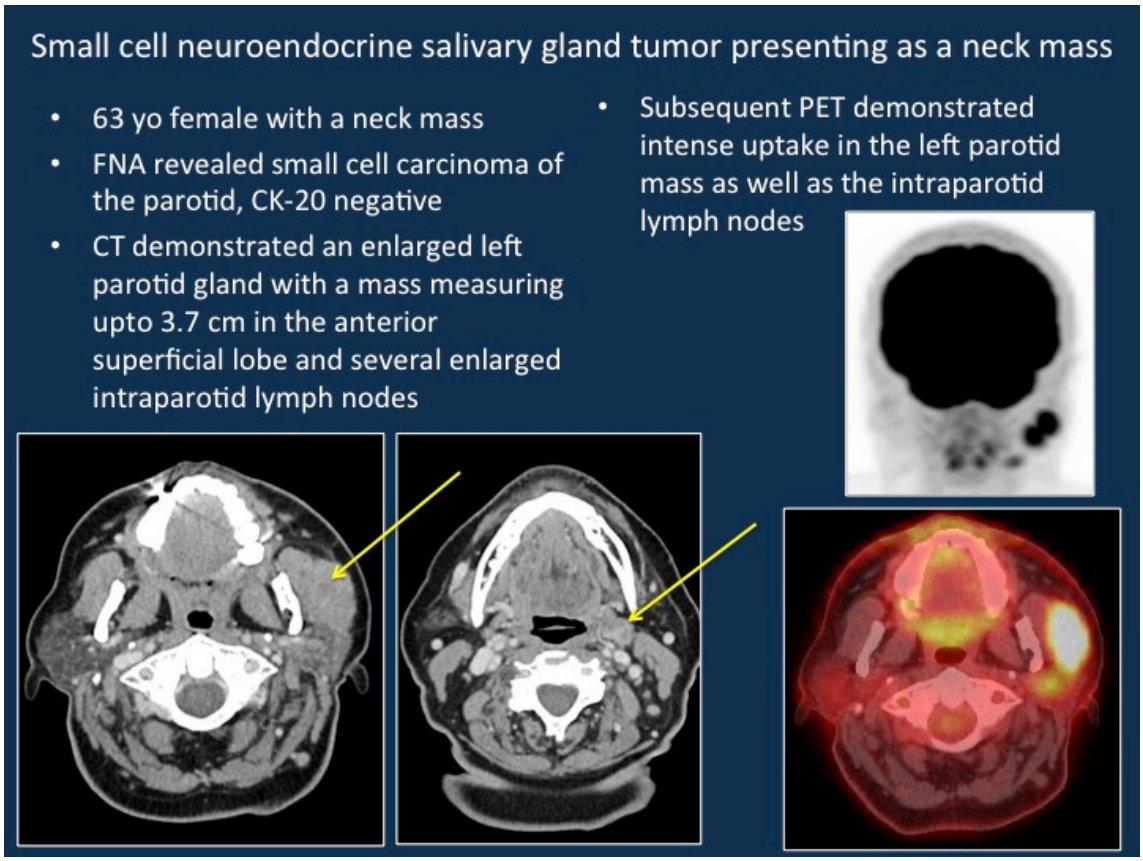

MR imaging findings of basal cell adenoma of the parotid gland: comparison with other parotid gland tumors

103 MR imaging findings of basal cell adenoma of the parotid gland: comparison with other parotid gland tumors

K Takumi, H Hakamada, N Hiroaki, Y Fukukura, E Sung, O Sakai, T Yoshiura

Boston University School of Medicine, Kagoshima University Graduate School of Medical and Dental Sciences
Japan

Purpose: To characterize the MR imaging features of basal cell adenoma (BCA) of the parotid gland and to compare with those of other parotid gland tumors. Material and Methods: The population of this retrospective study consisted of 101 patients with 110 parotid gland lesions (9 BCAs, 33 pleomorphic adenomas (PAs), 44 Warthin tumors (WTs), and 24 malignant tumors (MTs)). The MRI features (tumor size, marginal morphology, presence of capsule, cystic or necrotic change, hemorrhagic change, intensity of T1W and T2W images, enhancement pattern, and apparent diffusion coefficient (ADC) value) were compared between BCAs and other parotid gland tumors. Results: The mean tumor size of BCAs was 19.3±7.0 mm. BCAs showed regular margin (100%, 9/9), presence of complete capsule (100%, 9/9), and rapid and prolonged dynamic contrast

enhancement pattern (78%, 7/9). The mean ADC of BCAs was 1.10±0.29 ×10-3mm2/sec. BCAs showed significant differences in contrast enhancement pattern and ADC values in comparison with PAs (p=0.013 and 0.006, respectively) and WTs (p<0.001), while no significant differences were seen between BCAs and MTs. Smaller size, regular margin, and presence of complete capsule were significantly more common in BCAs than in MTs (p=0.002, 0.005, and <0.001, respectively). Conclusion: BCAs typically demonstrated small size, regular margin, presence of a capsule, rapid and prolonged dynamic contrast enhancement pattern, and mean ADC value of 1.10±0.29 ×10-3mm2/sec. Contrast enhancement pattern and ADC values were useful for differentiating BCAs from PAs and WTs, while the morphological features can help differentiate between BCAs and MTs.

Destructive spondyloarthropathy an increasingly recognized entity in hemodialysis patients. Spectrum of imaging findings.

104 Destructive spondyloarthropathy an increasingly recognized entity in hemodialysis patients. Spectrum of imaging findings.

A Ghasemiesfe, M Rahimian, M Afzaal, P Sharma, G Marrinan

Yale New Haven Health, Bridgeport Hospital
United States

Purpose: To review the pathophysiology, clinical manifestations and imaging findings of destructive spondyloarthropathy in hemodialysis patients. Description: Destructive spondyloarthropathy is an increasingly recognized entity mostly described in patients undergoing maintenance hemodialysis. The pathogenesis of destructive spondyloarthropathy remains unclear. It is thought to be related to a hemodialysis-associated amyloidosis. This spondyloarthropathy correlates with the duration of dialysis but not with severity of laboratory abnormalities associated with hyperparathyroidism. Imaging features: The condition most frequently involves the lower segment of the cervical spine, although the craniocervical junction may also be affected. It can involve a single level or multiple spinal disc levels. Imaging features range from superficial erosions to large bony defects. Discovertebral erosions or destruction, disc space narrowing and ligamentous laxity or instability are the most common findings usually in the absence of common degenerative elements. Computed tomography is the most sensitive method to evaluate the bone destruction, revealing osteolytic areas, with bone sclerosis of adjacent vertebral endplates, and minimal osteophytosis. The intervertebral spaces are usually significantly involved with narrowing or obliteration. The disorder may mimic the imaging characteristics of spondylodiskitis. However, absence of high signal intensity on T2-weighted images can favor a non-infection etiology. Summary: Radiographic features can be similar to an infectious process and it may progress and further destruct vertebral bodies with collapse and development of spinal instability. It is crucial for radiologist to fully understand the imaging findings of this entity especially in hemodialysis patients with a practical approach to describe the location, morphology, extent of the abnormality and associated complications. Severe complications may compromise the spinal cord warning surgical decompression, with or without spinal stabilization.

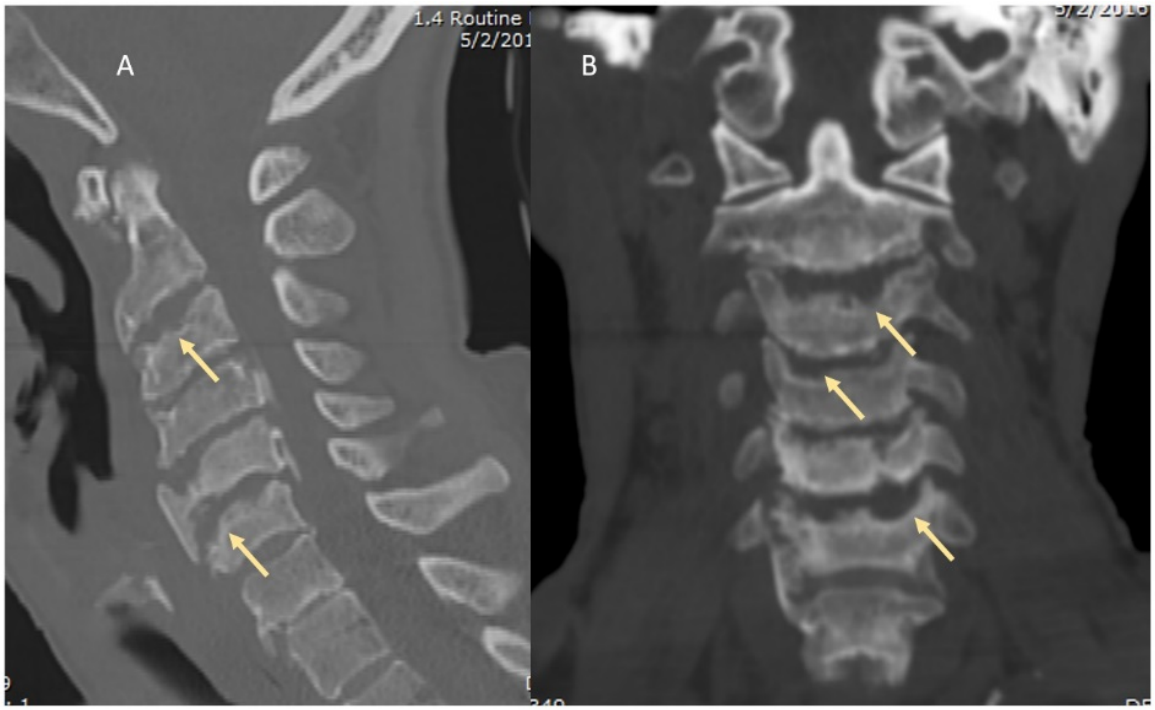

A and B; Sagittal and coronal CT images reveal multilevel large erosions along the endplates with disc space narrowing and vertebral body height reduction in a patients with long-term dialysis developing severe cervical pain.

Feasibility of 3D pseudo-continuous arterial spin labeling: differentiation of benign and metastatic cervical lymph nodes in patients with head and neck squamous cell carcinoma

105 Feasibility of 3D pseudo-continuous arterial spin labeling: differentiation of benign and metastatic cervical lymph nodes in patients with head and neck squamous cell carcinoma

K Takumi, H Hakamada, N Hiroaki, Y Fukukura, E Sung, O Sakai, T Yoshiura

Boston University School of Medicine, Kagoshima University Graduate School of Medical and Dental Sciences
Japan

Purpose: To evaluate the feasibility of 3D pseudo-continuous arterial spin labeling (pCASL) for the differentiation of benign and metastatic lymph nodes in head and neck squamous cell carcinoma in comparison with the apparent diffusion coefficient (ADC) value. Materials and Methods: The study population consisted of 10 patients with 34 cervical lymph nodes (16 metastatic and 18 benign). All patients were evaluated using 3D pCASL on 3T MRI before treatment. 3D pCASL was used to calculate quantitative blood flow (BF). BF values of the lymph nodes were compared using the Mann-Whitney U test. Receiver operating characteristic (ROC) curve analyses were generated to evaluate the accuracy in diagnosing metastatic lymph nodes, and the optimal cutoff values were chosen by using a threshold criterion determined by the largest Youden index. Results: The mean BF value in metastatic lymph nodes was significantly higher than in benign lymph nodes (63.2±11.7 vs. 45.8±15.8 mL/100 g/min, $p<0.001$). The optimal threshold BF value for differentiating metastatic from benign lymph nodes was 55.7 mL/100 g/min with a sensitivity of 81.2%, specificity of 88.9%, PPV of 86.7%, NPV of 84.2, and accuracy of 85.3%. Conclusion: Measurement of BF using 3D pCASL may play a role in pretreatment diagnosis of cervical lymph node metastases.

Going Through the Pyramid. Anatomy and Pathology of the Pterygopalatine Fossa. A simplified approach.

106 Going Through the Pyramid. Anatomy and Pathology of the Pterygopalatine Fossa. A simplified approach.

FM Ferraro, LA Miquelini, J Rogondino, C Rugilo, A García, S Mukherji

Department of Radiology, British Hospital of Buenos Aires, Argentina
Argentina

Purpose -Review the detailed anatomy of the Pterygopalatine Fossa and various pathways and communications. -Describe various pathologies that involve the Pterygopalatine Fossa and the mechanisms of spread to adjacent regions. Presentation Summary The Pterygopalatine Fossa is a complex region located between the maxillary sinus and central skull base that is not familiar to most radiologists. The intent of this exhibit will be to discuss the bony anatomy of the Pterygopalatine Fossa and its contents. This educational exhibit will also discuss the communication pathways and explain how disease that involves the Pterygopalatine Fossa can spread to adjacent areas. This information is important for initial diagnosis, understanding disease spread and treatment planning for various malignancies that involve this region.

Fallopian Canal Meningocele

107 Fallopian Canal Meningocele

A Silberzweig, A Khorsandi, G Moonis, M Cosetti, C Hadjipanayis

University of Pennsylvania
United States

The purpose of this presentation is to report the clinical and imaging presentation of 4 cases of congenital fallopian canal meningoceles. Otorrhea is a common presentation in patients with ear disease. Identification and differentiation of CSF otorrhea from otitis medial needs to be made initially. Identification of CSF otorrhea in patients without history of infection, trauma, surgery or neoplasm can be difficult. Here we present four cases of CSF otorrhea in patients with meningoceles extending through the fallopian canals and the middle ear. All patients had positive b transferrin from the otorrhea collection. On CT of Temporal bone and MRI examination, enlargement of the canal for labyrinth portion of the facial nerve was noted with opacification of the mastoid and middle ear. On Fiesta and T2 weighted MRI imaging, a sac like CSF signal out pouching was seen contiguous with the enlarged CSF containing Fallopian canal. The CT of the temporal bone did not reveal any other areas of defect of the Temporal-Cranial Junction. The MRI examination did not reveal other areas of meningoceles at the Temporal-Cranial junction. The MRI examination did not reveal other signs of increased intracranial pressure. On imaging there was no enlargement of the Meckels Cave, empty sella turcica , Chiari malformation or papilledema. Operative confirmation of one of the four cases has been made so far. There are eleven reported cases of Fallopian Canal Meningoceles. Fallopian canal meningoceles are rare entities. Understanding the varied clinical presentation and radiologic appearances may aid in diagnosis and treatment of this entity.

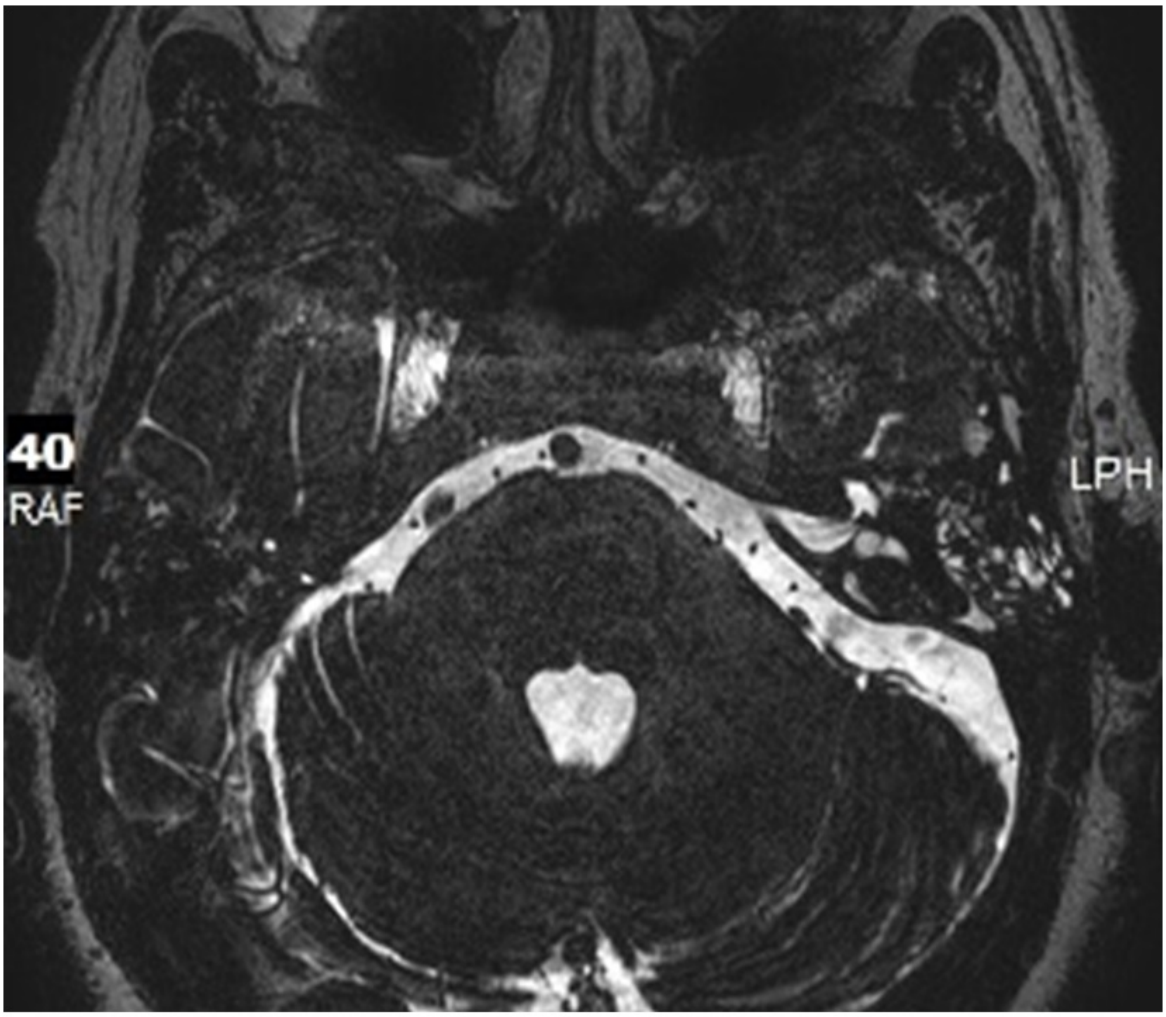
40
RAF
LPH

2018 Cancer Staging Update: Tips and Tricks for Tumor Boards

108 2018 Cancer Staging Update: Tips and Tricks for Tumor Boards

R Lobo

University of Michigan
United States

Purpose: This electronic exhibit will summarize the important changes in the newest AJCC 2018 cancer staging manual, with images and explanations for radiology representatives to tumor boards. Description: The AJCC 2018 cancer staging manual made several important changes in its newest iteration. Being familiar with the terminology is important for presenting radiologists at head and neck tumor boards, it gives us a shared language with our otolaryngology, radiation oncology and medical oncology colleagues. This electronic exhibit will explain the rationale behind the newest changes with special attention to useful tips and tricks for the consulting radiologist. Representative head and neck cancers from multiple locations are used to show features that help categorize the T station. Nodal staging is summarized for NPC, HPV OPSCC, and non-NPC/non-HPV cancers with imaging examples. Special attention is given to NPC and OPSCC as these are new and distinct categories. The complimentary modalities of CT (+/-PET) and MR are used to show strengths and limitations of each. Summary: Radiologists are crucial members of the head and neck cancer treatment team. Having familiarity and fluency with the AJCC 2018 manual gives us a shared language with our surgical and medical colleagues. By speaking in relevant terminology, we help enable efficient discussion and appropriate triage of care.

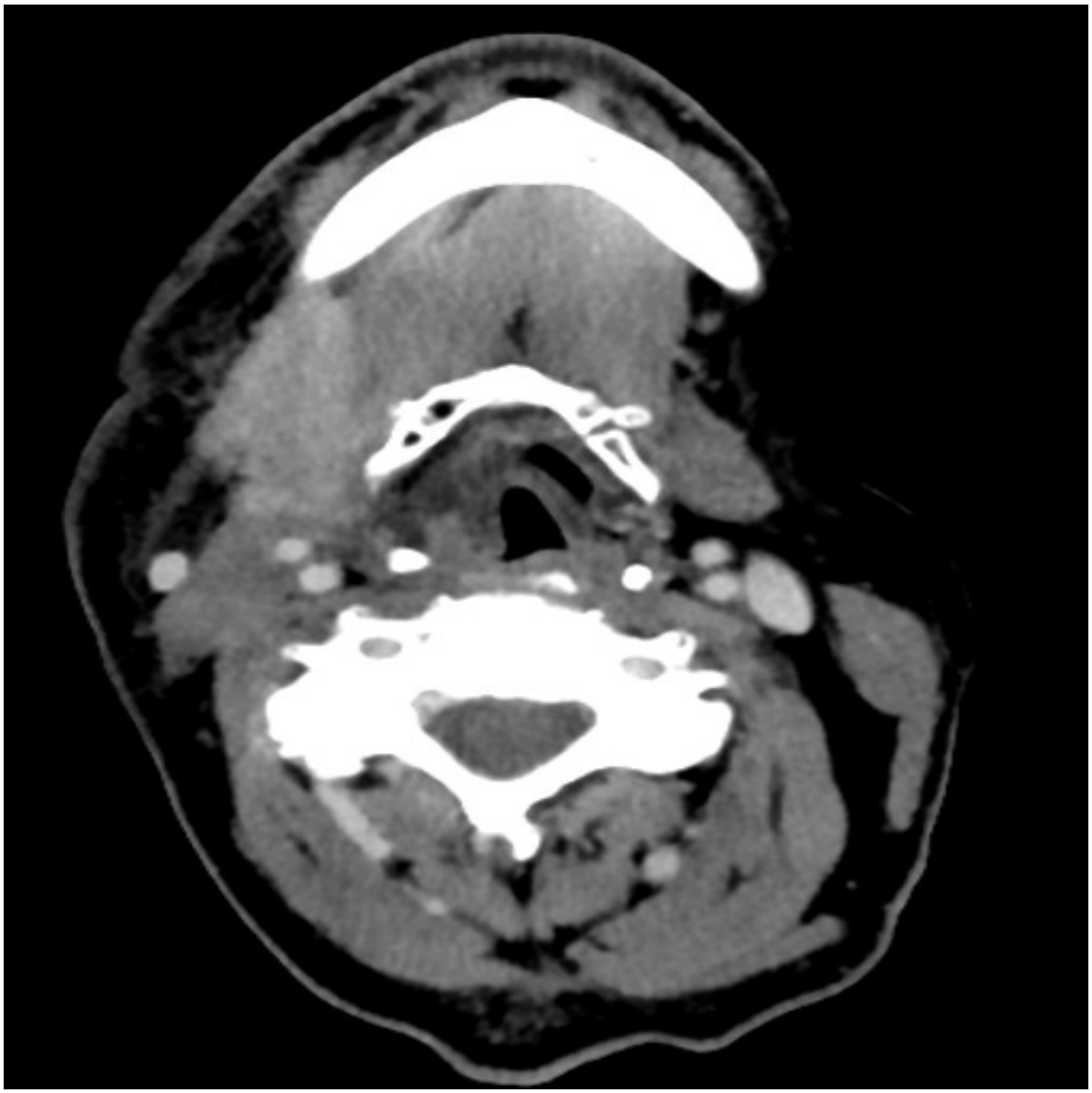

Don't forget to look at the teeth!

109 Don't forget to look at the teeth!

R Lobo

University of Michigan
United States

Purpose: This exhibit shows multiple examples of cystic and solid lesions along the teeth and adjacent maxilla/mandible. Description: The teeth are a common source for pathology when imaging the head and neck. This exhibit begins by describing basic anatomy of the teeth and the adjacent maxilla/mandible. Multiple examples of various pathology arising from the teeth are shown, with special attention to defining features that help narrow the differential diagnosis. Additional examples of cystic and solid lesions of the maxilla/mandible are also included. Common routes of spread for infection and inflammation are addressed. Anatomic considerations are described in specific disease processes. Post-surgical cases are also illustrated, along with tips and tricks to evaluate for disease recurrence. Examples are shown where both CT and MR are used in conjunction, illustrating benefits and limitations of each. Summary: The teeth and adjacent structures are a common source of pathology in the head and neck. By paying special attention to these spaces and using a series of characteristic imaging features, we can generate narrow differentials and evaluate common routes of spread.

“Jaw dropping:” A Radiographic Review of Benign and Malignant Lesions of the Mandible

110 “Jaw dropping:” A Radiographic Review of Benign and Malignant Lesions of the Mandible

MH Hanna, A Arneja, A Bansal, R Gupta, P Som

Mount Sinai
United States

Purpose: The purpose of this project is to review both benign and malignant imaging findings of lesions involving the mandible using various modalities including CT and MRI. We will also aim to identify specific imaging characteristics that can refine the differential diagnosis and identify features that would prompt tissue biopsy for a definitive diagnosis. Description There are numerous lesions that may involve the mandible ranging from both benign and malignant entities. They range from benign cystic lesions such as odontogenic cysts or nonossifying fibromas to malignant solid tumors such as squamous cell carcinoma. The aim of this project is to review both benign and malignant lesions of the mandible and review their radiographic features. It is essential for radiologists to able to identify characteristic features of particular entities in order to better refine their differential diagnosis. Additionally, understanding the anatomy and location of a particular lesion may help differentiate among pathologic conditions. Summary Mandibular lesions have a wide array of radiologic imaging findings and range from cystic to solid lesions, benign and malignant. There are a wide array of pathologic features which may have similar imaging findings, however, having a basic understanding and identifying key features along with certain locations may help narrow the differential diagnosis. Thus, the radiologist can guide patient treatment as they can improve in their contribution to identifying the abnormality and refining their differential.

FIGURE 1: Ameloblastoma

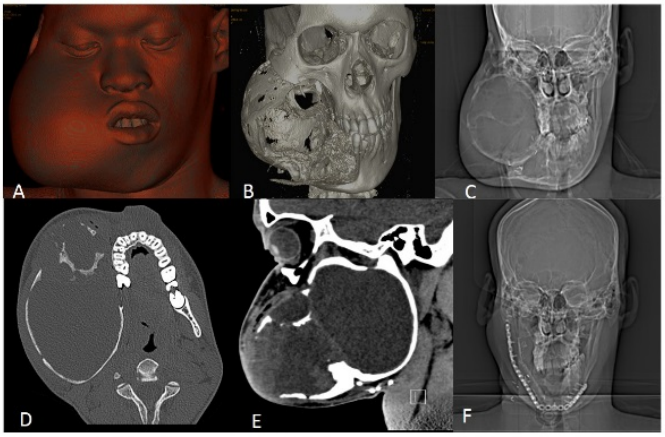

19-year-old male presenting with a large mass. A and B. Volume rendering soft tissue and bone images demonstrates a large mass along the right cheek. C. Scout image demonstrates the relative lucency through the mass. D and E. Axial CT bone algorithm and Sagittal soft tissue window demonstrates a large multiloculated expansile lesion of the right mandible which is predominately fluid filled and with peripheral nodular and soft tissue components. There is adjacent bony remodeling. F. Scout image from a postoperative CT scan of the facial bones demonstrates surgical hardware along the right mandible. The diagnosis was ameloblastoma.

FIGURE 2: Giant Cell Tumor

a. 3D volume rendering, b. Axial noncontrast CT, c. Sagittal noncontrast CT, d. Coronal noncontrast CT-partially sclerotic and cystic expansile mass involving the mandible from the first molar on one side to the other first molar on the opposite side. This has a complex cystic appearance and is consistent with a giant cell tumor.

Think beyond the brain! : Search pattern to avoid missing clinically significant extra-cerebral findings.

111 Think beyond the brain! : Search pattern to avoid missing clinically significant extra-cerebral findings.

RG Hegde, P Kochar, H Sawhney, M Rosovsky

Bridgeport Hospital Yale New Haven Health
United States

INTRODUCTION: Extracerebral findings on MRI Brain studies can be seen in the calvarium, upper cervical spine, orbits, paranasal sinuses/mastoids, nasopharynx and in the upper neck. Although not ordered for detection of these findings, it is the responsibility of the reading radiologist to be aware and comment about them especially when they are of clinical significance. Their detection is akin to detecting the 'corner of the film' finding on radiographs. The vast majority of times, they may not be of clinical significance; however, if looking for these structures is not part of the reader's search pattern, there is a good chance of missing out on a finding that is of clinical significance. EXHIBIT CONTENT: The exhibit will review a series of cases to highlight significant extracerebral findings seen on MRI Brain studies. For example, the cases would include the following: 1. Calvarium- metastatic disease, 2. Upper cervical spine- trauma, cord demyelination/ tumor, Orbits- inflammatory disease, intracranial hypertension, paranasal sinuses/mastoids- inflammatory/neoplastic disease, nasopharynx - infection/ inflammation/ neoplasm and in the upper neck- skull base tumors, parapharyngeal masses, parotid lesions. The exhibit will also review the pertinent literature regarding the frequency of these findings and their detection rate. CONCLUSION: What the mind does not know the eyes do not see! Awareness of commonly seen and significant extracerebral findings on MRI Brain studies is an essential skill. Developing and applying a methodical search pattern, although cumbersome and time-consuming at times in a busy practice is important in order to prevent missing a clinically important finding.

¡Eye Caramba! Globe pathologies that every radiologist needs to know.

112 ¡Eye Caramba! Globe pathologies that every radiologist needs to know.

A Bansal, A Arneja, MH Hanna, R Gupta, M Mafee, P Som

University of Virginia
United States

Purpose: The purpose of this educational exhibit is to: (1) review normal ocular anatomy and (2) review the radiographic appearances of a wide variety of globe pathology, including benign, malignant, congenital, acquired and traumatic entities. Description: Although most lesions of the eye and orbit are detected and diagnosed by physical and ophthalmologic examination, radiologic imaging can play a significant role in further characterization of these abnormalities. The orbits are often, albeit incompletely, included in routine non contrast imaging of the head and therefore many times, findings are made incidentally. Thus, it is imperative that the interpreting radiologist be familiar with a wide gamut of pathologic orbital entities. While CT can provide quick information in situations involving trauma, for dedicated orbital evaluation, we often recommend MRI imaging as it provides superior contrast and high sensitivity for detecting pathology. As there are too many orbital entities to present in a single exhibit, this review will specifically focus on the globes, showcasing a variety of benign, malignant, congenital, acquired and traumatic entities that we have encountered in our practice and feel should be on every radiologist's radar. Summary: This educational exhibit aims to review normal ocular anatomy and the radiographic appearances of a wide variety of pathologies affecting the globe, including benign, malignant, congenital, acquired and traumatic entities. In doing so, the interpreting radiologist will be able to improve their ability to provide a specific diagnosis or refine the differential diagnosis.

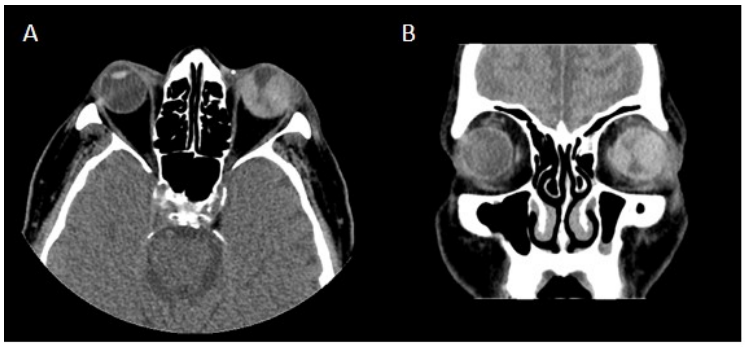

Figure 1. 71-year old male with eye pain. Noncontrast axial (A) and coronal (B) images of the orbits demonstrate increased density reflecting hemorrhage throughout much of the left globe, with some sparing centrally, suggestive of choroidal detachment. Increased density within the posterior aspect of the vitreous body may reflect the dislocated lens and/or additional hemorrhage.

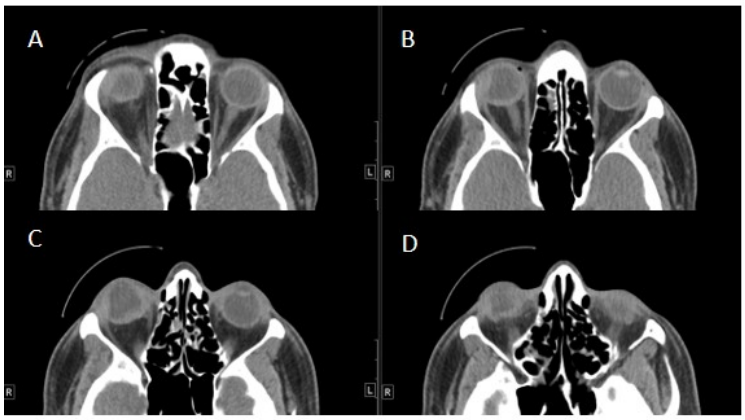

Figure 2: 46-year old male presents with screwdriver injury to the right eye. A-D Sequential axial noncontrast CT images through the orbits demonstrate a shallow anterior chamber of the right globe. The right lens is displaced laterally against the wall of the eye. Compared to the left globe, the right globe is flat along its posterior pole. Findings are consistent with globe rupture.

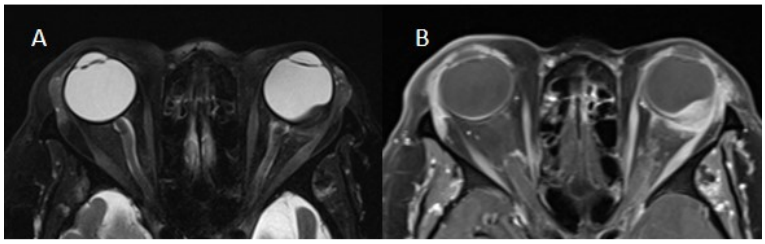

Figure 3: 86-year old female with uveal melanoma. Axial T2W (A) and contrast enhanced T1W (B) MR images through the orbits demonstrate a 13 mm x 4 mm segment of thickened uvea along the posterolateral margin of the left globe, consistent with uveal melanoma. The tumor also extends outside of the globe and into the intraconal portion of the orbit.

Cochlear-Facial Dehiscence:

113 Cochlear-Facial Dehiscence:

N Salastekar, A Salinas, A Duleep, S Destian, K Petropoulou

SUNY Upstate Medical University
United States

Purpose While dehiscence of the superior semicircular canal is a well recognized entity, the cochlear-facial dehiscence is an unusual third window. A case of cochlear-facial dehiscence will be presented along with review of the literature on otic capsule third window however outside the dehiscence of superior semicircular canal. Description A 42 year old female with a two year history of vestibular migraine presented with a new symptom of autophony which prompted the CT of the temporal bone. The semicircular canal was intact bilaterally. Analysis of the axial, coronal, Stenvers and Poschl views revealed a 1.3 mm dehiscence at the superior aspect of the basal turn of the cochlea at the crossing point of the labyrinthine segment of the facial nerve bilaterally. The CT diagnosis of this rare third window was followed by audiogram and vestibular evoked myogenic potential (VEMP) testing. Summary A third window may exist outside the superior semicircular canal. In a symptomatic patient with intact superior semicircular canal on temporal bone CT, the otic capsule should be further scrutinized for rare sites such as carotid artery-cochlear, internal auditory canal-cochlear as well as cochlear-facial dehiscence.

Incidental Paranasal Sinusitis on Brain MRI - Can regional findings stratify causal mechanisms?

114 Incidental Paranasal Sinusitis on Brain MRI - Can regional findings stratify causal mechanisms?

PA Rosenthal, DP Massoglia, K Lundy, E Payne, M Gebregziabher

Ralph H Johnson VAMC
United States

Object or Purpose of Study Incidental Paranasal Sinusitis (IPS) is often seen but its origins are unclear. Like Chronic Rhinosinusitis (CRS), its causes are likely polygenic. Regional findings and IPS patterns may provide clues, e.g. diffuse inflammation may be due to airborne exposures (allergens or viral infections); localized processes may be odontogenic, or from ostiomeatal obstruction, seen directly or inferred, e.g. fluid levels or fully "opaque" Maxillary Antra (MA). We test if analysis of IPS patterns may stratify the prevailing mechanisms. Materials, Methods, and Procedures A random cohort - first 15 Brain MRs per month in 2009, no duplicates. Mostly on sagittal T2 sequences, a previously validated IPS scoring system and MA IPS pattern scheme were recorded, with - nasal passage patency, posterior maxillary tooth count, fully-filled MAs, fluid levels, cysts and polyps. Based on average sinus volumes, IPS scores were: 0 - 6 for each MA; 0 - 3 for each non-MA sinus; maximum possible summed IPS score was 30. Isolated tiny mural foci were scored as 0.5. Previously validated threshold of Significant IPS (Sig IPS) was 6/30. Analyses included 1) prevalence of each feature or pattern; 2) number of subjects by IPS score; 3) mapping of IPS by sinus type, by grade of IPS Results Of 180 subjects, 7 excluded, leaving 173; males 156, 90.2%; females 17, 9.8%; mean 62.4 years, (M 64.1 yrs: F 46.3 yrs) range 23.3 - 97.7 years; Whites 104, 60.1%; Blacks 66, 38.2%; other minorities 3. IPS reactions were almost all T2 fluid-bright. Essentially clear sinuses were recorded in 92 (53.2%) subjects, but almost half, 25.4%, had mostly 1, or a few, tiny T2 bright mural foci (IPS 0.5). The remaining 81 (46.8%) had IPS scores from 1 - 22/30. Mean subject IPS score was 2.20/30; SD 3.24. Sig IPS seen in 20/173, 11.6%. Plotting the number of subjects by IPS score resembled a standard decay curve - higher numbers of low IPS scores and numbers declining with each step-up of IPS severity. Mapping by sinus type showed - 1) MA IPS exceeded all other sinuses combined; 2) declining gradients of IPS volume with increasing distances of each sinus from the MA floors. Potential and actual obstructive features: "opaque" MA in 3 (1.7%), including 1 with mucocele; MA fluid levels, 2.3%; partial nasal passage obstruction, 2.3%. Even combined, visible and inferred obstructive features were non-dominant in all IPS and Sig IPS. Isolated size-able MA cysts were 2.9%; and no polyps were seen. Posterior maxillary tooth count analysis revealed no IPS correlations, but bilateral absence of teeth (64/173; 37.0%) was associated with age >/= 65 - OR 6.1, p< 0.001. Significance of Conclusions MA dominance and declining gradients of IPS ascending the sinuses favor causes near the MA bases, i.e. odontogenic defects, including periodontitis. We previously reported a strong association of Sig IPS with history of cerebrovascular disease in the same cohort, best explained as co-related effects of periodontitis. The current study is an alternative analysis of the same cohort, and yields congruent results.

Schematic representation of sinus volume scores by sinus type:
Gradients declining consistently with distance from Maxillary Sinus floors (↑)
(All subjects' total severity scores shown from A – G: whole cohort scores H.)

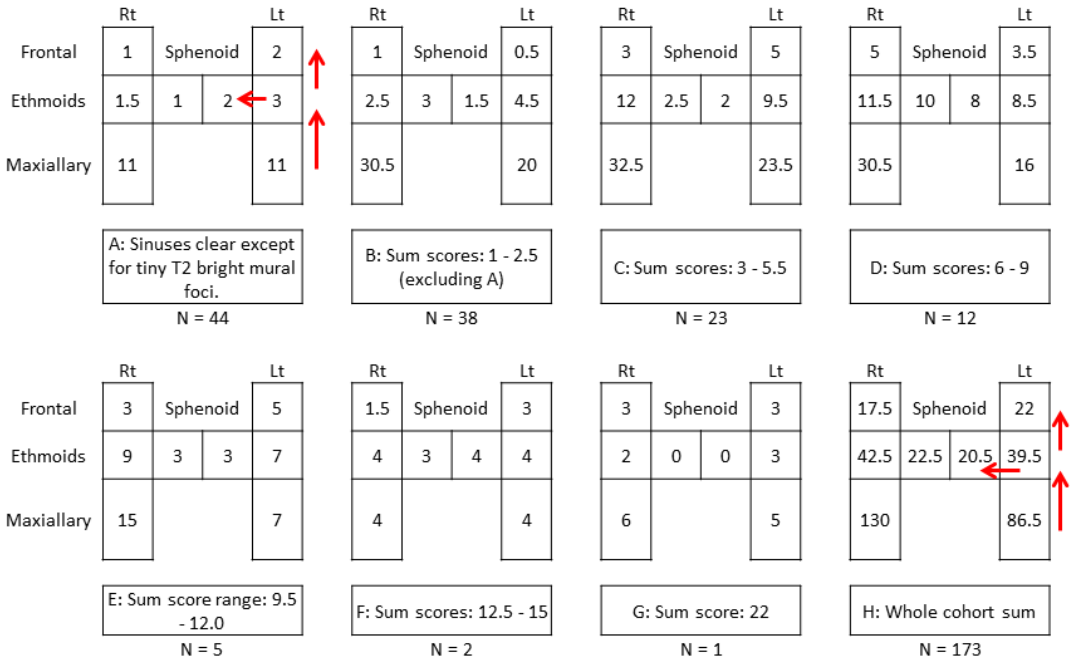

Ecchordosis Physaliphora: Typical Imaging Findings and Differential Diagnoses

115 Ecchordosis Physaliphora: Typical Imaging Findings and Differential Diagnoses

M Albertson, J Cramer, M Keiper, J Helvey

University of Nebraska Medical Center
United States

Purpose: Become familiar with the typical CT and MRI imaging features of Ecchordosis Physaliphora (EP) and learn how to differentiate it from other benign and malignant lesions that commonly affect the clivus through several example cases. Description: What is EP and where is it found? EP is a benign lesion of hamartomatous ectopic notochordal tissue which is usually found in the clivus or prepontine cistern, but can occur anywhere along the midline from the sella to the coccyx (just like chordoma). What is the typical imaging appearance of EP? On CT: EP is a well-defined lytic lesion in the clivus containing low attenuation material surrounded by a thin sclerotic rim. Occasionally there may be an ossified stalk arising from the clivus connecting to the lesion. If the lesion is predominately in the prepontine cistern, it may not be seen on CT since it has similar attenuation to CSF. The hallmark of EP is the ossified stalk, which is not present in other clival lesions. On MRI: EP has Low T1 signal, high T2 signal, NO enhancement (unlike chordoma), and can have restricted diffusion. When EP is small in size, the lesion may blend in with surrounding CSF, limiting detection. EP has similar characteristics to an epidermoid cyst on MRI, but EP is only midline and may not restrict diffusion. The ossified stalk may not be visible in all MRI cases, but is best demonstrated on T2WI if present. What is the prognosis of EP? EP is histologically similar to chordoma, but is considered benign and often incidental with very little growth over time. Since EP is benign and indolent, it may actually be more common than it's malignant counterpart, the chordoma, with EP reportedly present in 2% of autopsies. Because of it's benign nature, surgical intervention is usually only considered in cases of brainstem compression. It can also be difficult for pathologists to confidently make a diagnosis between chordoma and EP, so the radiologist's interpretation is important. What is included in the differential for EP? Other lesions that occur near the clivus include: chordoma, chondrosarcoma, metastases/myeloma, nasopharyngeal carcinoma, lipoma, epidermoid cyst, and meningioma. However, EP can usually be differentiated from these other lesions based on imaging characteristics and specific location. Summary: What should the radiologist remember about EP? 1) Consider EP in your differential diagnosis when there is a benign-appearing lesion in the clivus or prepontine cistern with homogeneous high T2 signal and NO enhancement. 2) If there is an ossified stalk arising from the posterior midline clivus, strongly consider EP. 3) EP has similar MRI characteristics of an epidermoid cyst and could look like a chordoma, EXCEPT midline retroclival epidermoids are rare and a chordoma will generally enhance.

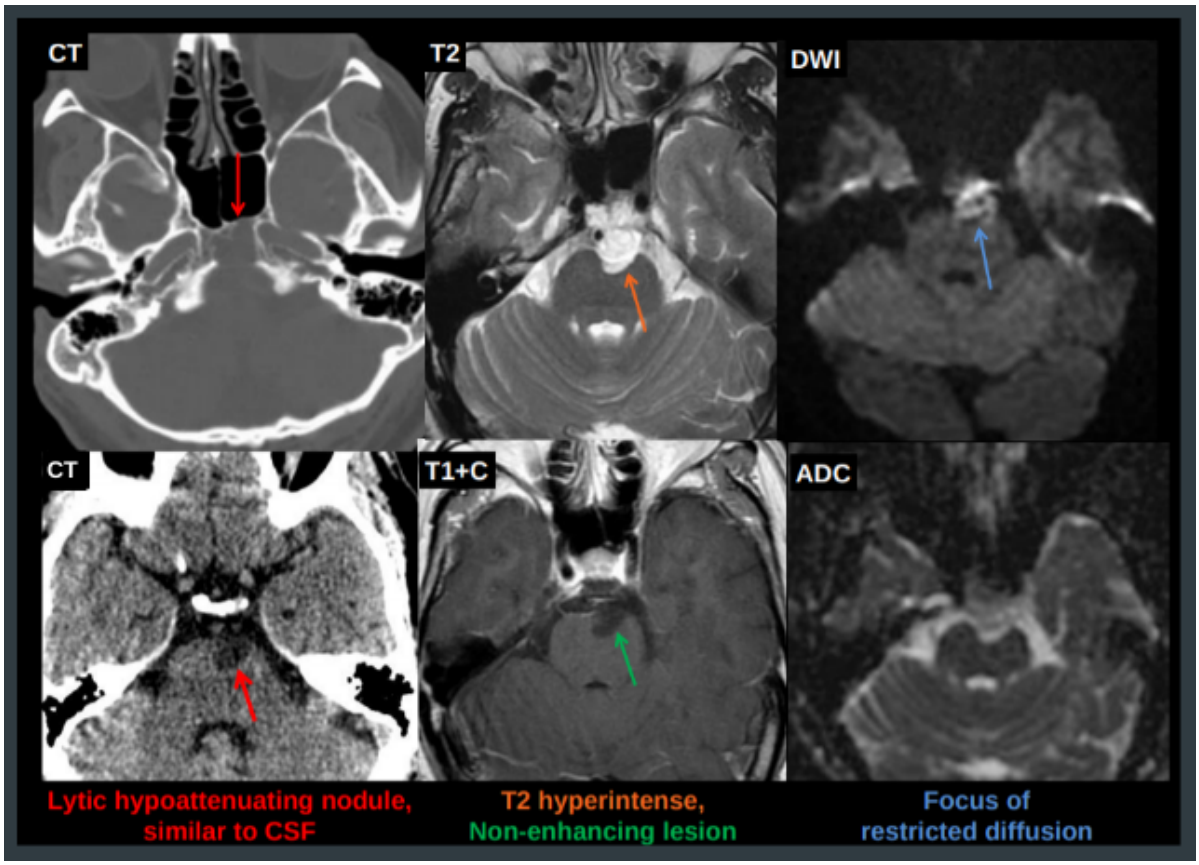
CT
T2
DWI
CT
T1+C
ADC
Lytic hypoattenuating nodule,
similar to CSF
T2 hyperintense,
Non-enhancing lesion
Focus of
restricted diffusion

“Can’t Miss” Head and Neck Emergencies: A Symptom-Based Imaging Review

116 “Can’t Miss” Head and Neck Emergencies: A Symptom-Based Imaging Review

M Roseland, T Alves, A Srinivasan, S Chong

University of Michigan
United States

Purpose: -To present a systematic approach for imaging of various head/neck clinical complaints based on focused differential diagnoses. -To describe imaging features of critical and potentially subtle diagnoses associated with each presenting symptom, as well as clinically significant complications. -To provide imaging pearls and pitfalls to aid radiologists in confidently identifying these conditions. Background: Non-traumatic head and neck complaints are encountered frequently in the emergency setting, and patients often require imaging for definitive diagnosis. Since many infectious, inflammatory, and vascular pathologies have potentially grave complications if management is delayed, accurate and prompt radiologic diagnosis is crucial. Description: Common symptoms of the head and neck for which imaging is often requested will be introduced, including airway compromise, throat pain, vision loss, facial/tooth pain, ear pain/hearing loss, epistaxis, and acute neurologic symptoms/bleeding suggestive of a vascular injury. Based on the differential diagnosis of each presenting complaint, several emergent radiologic diagnoses and their complications will be described. Examples of these conditions include epiglottitis, angioedema, orbital cellulitis, optic neuritis, deep neck abscesses, Ludwig’s angina, calcific tendinosis of the longus colli, arterial dissection, carotid blowout, and mastoiditis. For each complaint and specific diagnosis, evidence-based imaging recommendations will be provided. Summary: A thorough understanding of emergent head and neck diagnoses associated with common clinical scenarios is essential for radiologists, both to identify these diseases and their complications accurately and rapidly, as well as to suggest the proper imaging modality/technique for a given complaint.

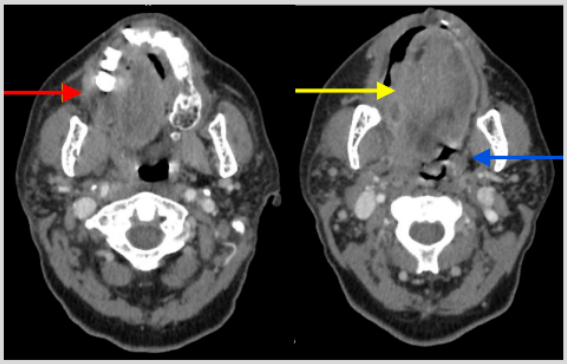

Ludwig's angina: Multiloculated, enhancing fluid collection arising from the right floor of the mouth (red arrow), extending into the sublingual and submandibular spaces, with edema and medial displacement of the tongue (yellow arrow), effacement of the right glossotonsillar sulcus and severe narrowing of the oropharyngeal airway (blue arrow).

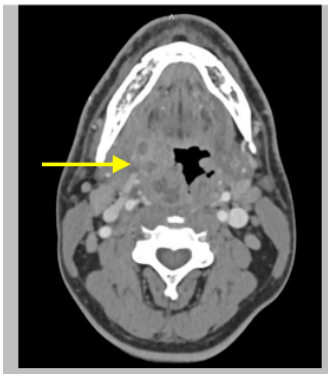

Peritonsillar abscess: Large, multiloculated, thick-walled fluid collection centered at the right palatine tonsil, with moderate narrowing of the oropharyngeal airway (yellow arrow).

Retropharyngeal abscess with mediastinal extension: Enhancing fluid collection in the retropharyngeal space (red arrow), extending into the danger space and descending into the superior mediastinum (yellow arrow).

Atypical Allergic fungal sinusitis causing osseous destruction with intracranial and intraorbital extension. We present a comprehensive review with two case illustations.

117 Atypical Allergic fungal sinusitis causing osseous destruction with intracranial and intraorbital extension. We present a comprehensive review with two case illustations.

S Gaddamanugu

Academic/Federal
United States

Purpose:The purpose of this exhibit is to highlight and review the clinical and imaging manifestation of atypical allergic fungal sinusitis which present on imaging with bone destruction and extension outside the Sino nasal cavity. Description: Allergic fungal sinusitis is the most common type of fungal sinusitis. Allergic fungal sinusitis typically presents as hyper dense polypoidal Sino nasal masses with no osseous destruction. This disease typically occurs in an immuno-competent individuals. The fungal mycelia incite a severe allergic reaction which induces proliferation of mucin. In occasional cases, the proliferation of fungus and mucin is strikingly remarkable and causes severe expansion of the sinuses and nasal cavity leading to ischemic necrosis of the bone. The bone destruction facilitates extension of the soft tissue outside the sino-nasal cavity into the orbit and extra-axial spaces of the brain. However in such patients with invasive-appearing allergic fungal sinusitis, the fungus remains on the surface of the mucosa and is not invasive to the bone, brain and meninges as in patients with true invasive fungal sinusitis. The most common fungi which cause this condition are Aspergillus and members of the Dematiaceae family of fungi. This condition will mimic other sino-nasal pathologies such as tumors and invasive fungal sinusitis. Treatment of this condition includes surgical debridement of the fungus with postoperative corticosteroid treatment. Our presentation will review the clinical presentation of these patients with invasive-appearing allergic fungal sinusitis and its clinical diagnostic criteria and imaging findings.Our exhibit will be facilitated by the clinical presentation and imaging illustrations of two patient's with this condition. Summary: Allergic fungal sinusitis can occasionally appear "invasive" with osseous destruction and extension outside the sino-nasal cavities. It is important to consider this entity and suggest appropriate management.


A

Imaging Weirdomas in the Head and Neck with Pathology Correlation

118 Imaging Weirdomas in the Head and Neck with Pathology Correlation

D Ginat

University of Chicago
United States

Purpose: Weird cases in the head and neck selected from our institution's educational radiology-pathology conferences will be reviewed. Description: The imaging features and corresponding histopathologic characteristics and relevant differential diagnosis for the following conditions are reviewed: disseminated malignant extrarenal rhabdoid tumor of the head and neck, lingual desmoid, secretory carcinoma of the cheek, sclerosing epitheloid fibrosarcoma of the mandible, solitary fibrous tumor of the orbit, salivary ductal carcinoma ex pleomorphic adenoma, Kikuchi disease, histiocytic necrotizing lymphadenitis, sinonasal meningioma, maxillary aneurysmal bone cyst, oral cavity foregut duplication cyst, and parotid angiosaroma. Summary: Radiology-pathology correlation of strange and unusual lesions in different anatomic regions of the head and neck are reviewed, providing a comprehensive review of rate and common conditions through the associated differential diagnoses.

A pictorial review of inner ear abnormalities on CT and MRI

119 A pictorial review of inner ear abnormalities on CT and MRI

K Onoue, B Setty, K Takumi, V Carlota Andreu, O Sakai

Boston Medical Center
United States

Purpose: The focus of this educational exhibit is to present pictorial reviews of various inner ear abnormalities and describe their important CT and MR imaging features. Description: The inner ear is comprised of the membranous labyrinth containing endolymph and the encasing bony labyrinth separated by a small quantity of perilymph. It is subdivided into three major parts: cochlea, vestibule and semicircular canals. Inner ear anomalies are an important cause of sensorineural hearing loss. These are most often detected in young age, however some patients become symptomatic later in life. These abnormalities could arise due to underlying genetic causes or due to in utero and other environmental factors, often infection or trauma, most leading to premature arrest of the normal inner ear development. Syndromic causes such as Alport, Waardenberg and CHARGE comprise approximately 30% of genetic causes1. Recent advancement in imaging techniques allows for careful evaluation of the inner ear anatomy, with high resolution CT affording superior depiction of the osseous structures and MR imaging providing complimentary information of the membranous labyrinth and the vestibulocochlear nerve. Accurate and timely diagnosis of inner ear abnormalities is critical as many of the affected patients require assistive intervention and it is important for evaluating the utility of performing cochlear transplants2. Cases of inner ear anomalies detected on dedicated temporal bone CT and MR imaging will be presented. Our institution's temporal bone CT protocol includes axial images through the temporal bones at 0.625mm slice thickness with 0.3 mm interval reconstructions with coronal reformats in bone and soft tissue kernels by 64-MDCTs. Temporal bone MR imaging protocol includes high resolution axial 3D T2-weighted imaging with 0.8mm slice thickness, axial and coronal pre and post-contrast T1-weighted imaging at 2mm slice thickness on 1.5 or 3T magnets. Summary: Various cases of inner ear anomalies as detected on dedicated temporal bone CT and/or MRI are presented with focus on their important imaging features. The imaging manifestation is broad, ranging from complete aplasia of the inner ear structures to hypoplasia to more subtle findings that differ only minimally from the normal anatomy. High resolution CT and MR imaging afford differing but complimentary information and together provide valuable tools for the radiologist to make the correct diagnosis. Firm knowledge of these anomalies will help make accurate and timely diagnosis which in turn help guide clinical management for the patients. References: 1. RSZ Yiin et al. "Review of congenital inner abnormalities on CT temporal bone." The British Journal of Radiology 2011 84:1005, 859-863. 2. Varsha M. Joshi et al. "CT and MRI imaging of the inner ear and brain in children with congenital sensorineural hearing loss." RadioGraphics 2012 32:3, 683-698.

Support Images: Examples of inner ear abnormalities as seen on CT and MRI

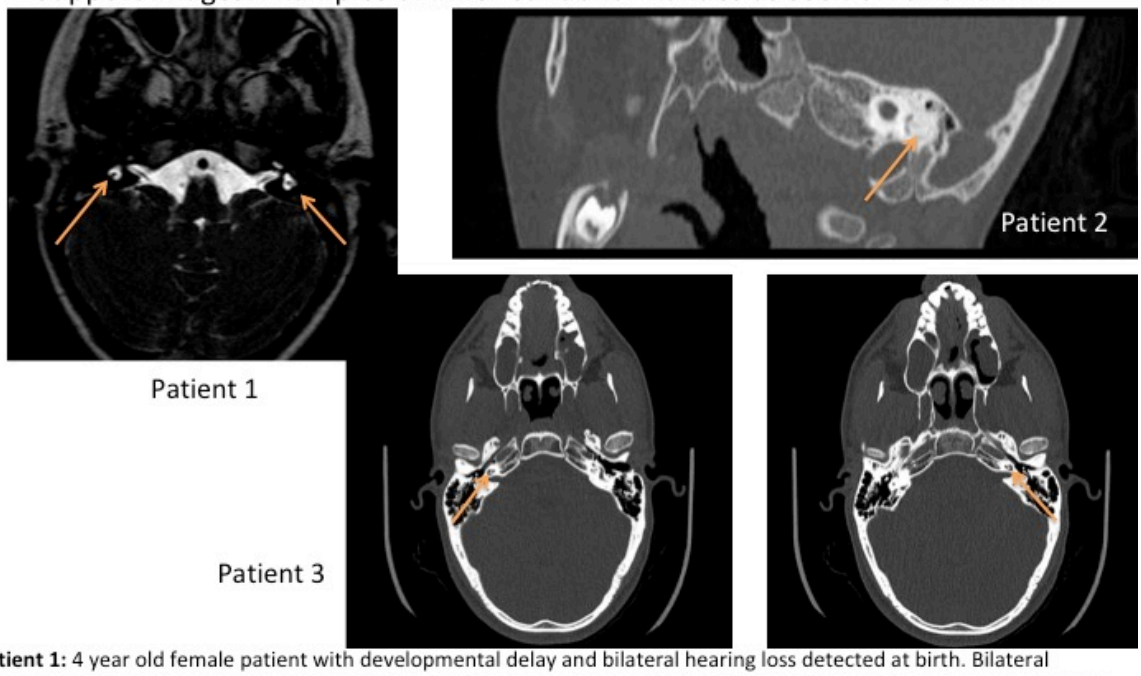

Patient 1: 4 year old female patient with developmental delay and bilateral hearing loss detected at birth. Bilateral hypoplasia of the semicircular canals with incomplete posterior canals (arrows) and aplasia of lateral and superior canals. Cochlea were noted to be abnormal with hypoplasia of apical and possibly middle cochlear turns. **Patient 2:** 8 year old female patient with asymmetric hearing loss in left ear. There is narrowing of the left posterior semicircular canal with increased sclerosis/ossification (arrow), suggestive of labyrinthitis ossificans. **Patient 3:** 23 year old male patient with congenital hearing loss. Mild flattening of the apical turn of the cochlea bilaterally (arrows) with small cochlear nerve hole, suggestive of bilateral cochlear dysplasia.

A Bridge from the Neck to the Skull Base. Anatomy and Pathology of the Masticator Space.

120 A Bridge from the Neck to the Skull Base. Anatomy and Pathology of the Masticator Space.

FM Ferraro, J Rogondino, LA Miquelini, C Rugilo, A García, S Mukherji

Department of Radiology, British Hospital of Buenos Aires, Argentina
Argentina

Purpose • Review the anatomy and components of the masticator space. • Review the foramina related to the masticator space and establish landmarks in order to find them. • Define various pathologies that involve the masticator space and the transition between the neck itself and the skull base. Presentation Summary The masticator space represents a transition space between the suprahyoid neck and the skull base. It is important to understand its anatomy in order to recognize the origin of different pathology, especially those which has the ability of perineural spread such as melanoma. The intent of this exhibit is to describe the anatomy of the Masticator Space, including related skull base foramina and,therefore, understand the origin and extension of various pathologies.

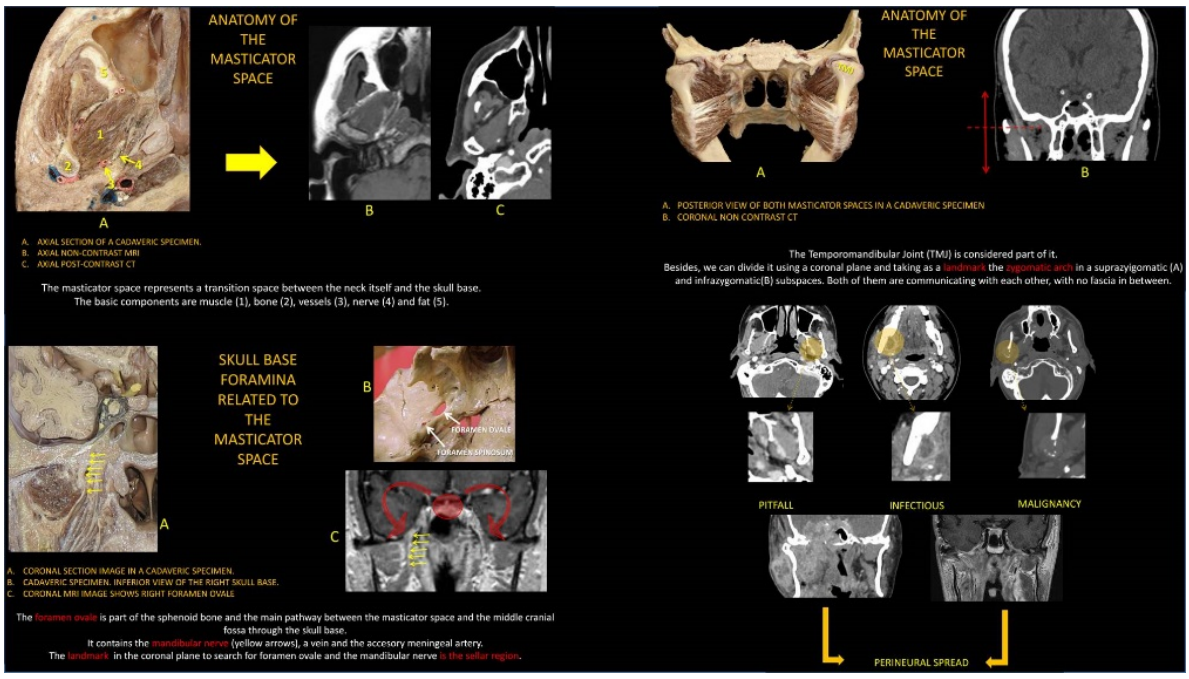

Normal Anatomic Structures and Variants that can Mimic Lesions on Head and Neck Imaging

121 Normal Anatomic Structures and Variants that can Mimic Lesions on Head and Neck Imaging

D Ginat, G Moonis

University of Chicago
United States

Purpose: The appearance of various normal structures in the head and neck potentially can be misinterpreted as pathology on diagnostic imaging. The goal of this exhibit is to illustrate these anatomic variants and how they differ from actual lesions. Description: The imaging features of normal variants review in this exhibit include orbital calcifications, temporal bone fissures, sutures, and clefts, asymmetric fatty marrow within the petrous apex, fibrous dysplasia-like appearance of the frontal process of the maxilla, arrested pneumatization of the sinuses, Stafne cyst, herniated sublingual gland through the mylohyoid gap, accessory parotid gland, Zuckerkandl tubercle and pyramidal eminence of the thyroid gland, laryngeal cartilage mineralization, levator claviculae muscle, and various vascular structures, such as the jugular bulb pseudomass, carotid body, and jugular phlebectasia. Examples of lesions that can be mimicked by these normal variants on imaging are also depicted for comparison and distinguishing features are highlighted. Summary: Familiarity with the variety of normal variants on imaging can help avoid misconstruing these as actual lesions.

Laryngeal HPV-associated squamous cell carcinoma in young patients, presumed perinatal transmission

122 Laryngeal HPV-associated squamous cell carcinoma in young patients, presumed perinatal transmission

B Wang, LE Ginsberg

MD Anderson Cancer Center
United States

Purpose: Perinatal route of transmission of human papillomavirus (HPV) has been demonstrated in many studies [1]. HPV is a major risk factor for specific cancers of the head and neck, particularly malignancies of the tonsil and base of the tongue. The role of HPV in the development of laryngeal cancer is less well established [2]. However, recent research has shown HPV infection, especially infection due to the high-risk type HPV-16, to be significantly associated with the risk of laryngeal squamous cell carcinoma (SCC) [2, 3]. We present imaging findings of laryngeal SCC associated with HPV in young patients who presumably acquired the infection perinatally, likely through birth canal, which to our knowledge have not received much attention in radiology literature. Materials & Methods We retrospectively searched the radiology and pathology reports in the last 10 years at our tertiary cancer intuition for laryngeal cancer in patients younger than 30. We found 3 cases of HPV+ or P16+ primary laryngeal cancer. HPV status is yet to be confirmed in the 3 other cases because the tissues were obtained many years ago. CT, MRI, and PET/CT imaging findings were reviewed. The location and staging of the primary cancer were studied. Results The patients in our study range from 14 to 24 years old, with 4 female and 2 male. Only 1 out the 6 patients smoked cigarettes. Initial stage of the cancer ranges from carcinoma in situ of vocal cords to T4bN2bM0. 3 out of the 6 patients had recurrence after initial treatment. 3 other patients were lost to follow up after no recurrence for 2-10 years; all these 3 patients had radiation therapy. Our youngest patient was born transvaginally. Shortly after her birth her birth mother was diagnosed with cervical cancer and subsequently died. She is adopted. The patient presented with progressive hoarseness and throat pain over 2 years which intensified to the point of prompting a tonsillectomy/adenoidectomy but continued to have worsening voice quality and throat pain. CT, PET/CT, and MRI showed a T4bN2bM0 laryngeal cancer (Figure 1). Anteriorly there is involvement of the strap muscles and posteriorly tumor extends into the retropharynx and possibly prelaryngeal space. She has been on chemotherapy with some initial response; however, follow up imaging only 3 weeks later showed massive disease progression. Conclusion We presented the clinical and imaging findings of laryngeal SCC associated with HPV in young patients who presumably acquired the infection perinatally, which to our knowledge have not received much attention in head and neck radiology literature. References [1] Trottier H, Mayrand, M, Coutlée F, et al. HPV perinatal transmission and risk of HPV persistence among children: Design, methods and preliminary results of the HERITAGE study. Papillomavirus Research, 2016:2, 145-152. [2] Hernandez B, Goodman M, Lynch C, et al. HPV Prevalence in Invasive Laryngeal Cancer in the United States. PLoS One 2014:9(12). [3] Li X, Gao L, Li H, et al. HPV Infection and Laryngeal Cancer Risk: A Systematic Review and Meta-Analysis, The Journal of Infectious Diseases, 2013:207 (3), 479-488.

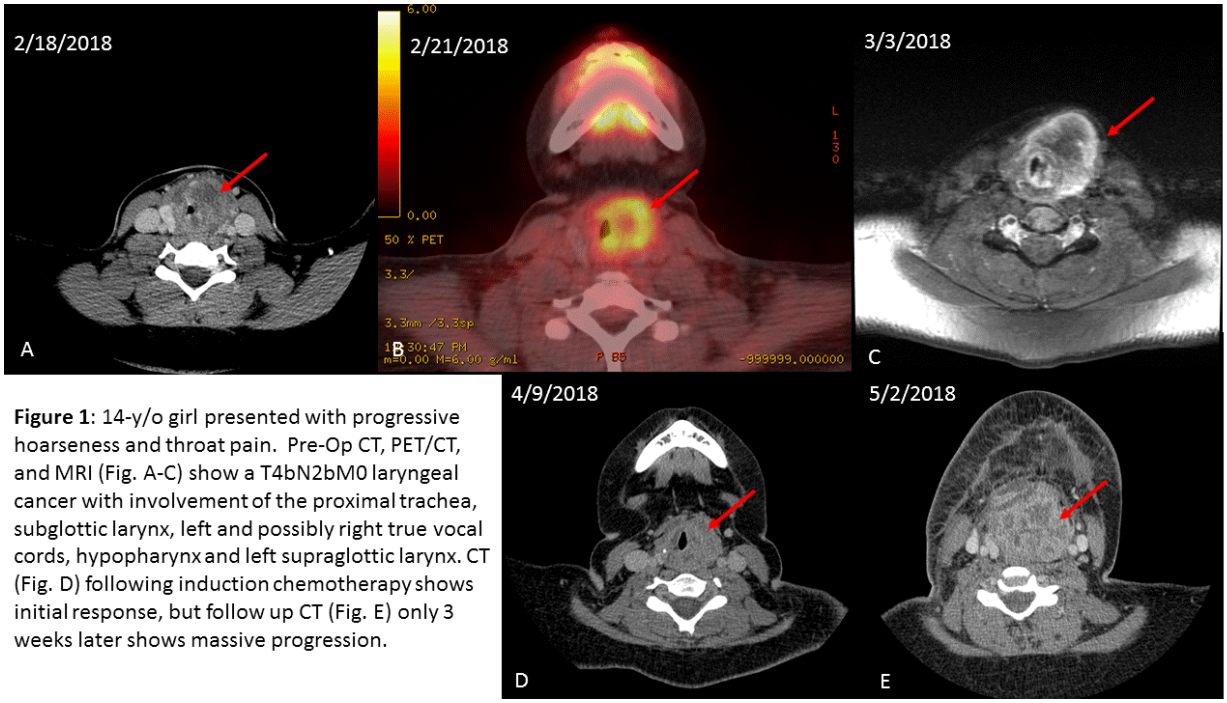

Figure 1: 14-y/o girl presented with progressive hoarseness and throat pain. Pre-Op CT, PET/CT, and MRI (Fig. A-C) show a T4bN2bM0 laryngeal cancer with involvement of the proximal trachea, subglottic larynx, left and possibly right true vocal cords, hypopharynx and left supraglottic larynx. CT (Fig. D) following induction chemotherapy shows initial response, but follow up CT (Fig. E) only 3 weeks later shows massive progression.

Destructive transcranial carcinoma ex-pleomorphic adenoma in an infant

123 Destructive transcranial carcinoma ex-pleomorphic adenoma in an infant

M Bashir

Loyola University Medical Center
United States

The purpose of this electronic exhibit is to report the first case of a transcranial carcinoma ex-pleomorphic adenoma of the parotid gland in an infant. This has not been previously reported to our knowledge. A 5 month old female patient with history of failed right sided newborn hearing tests thought to be due to external auditory canal (EAC) stenosis presented with 1 month of right ear drainage and bleeding. After a failed course of antibiotics, she developed a right temporal and right cheek mass. MRI was performed for further evaluation, revealing a large, heterogeneous mass replacing the right parotid gland, invading the right masticator space, EAC and middle ear cavities, and extending superiorly into the middle cranial fossa with dural invasion and mass effect upon the inferior surface of the right temporal lobe. There was no definite intraparenchymal involvement. Pathology of tissue sampled through the EAC was resulted as a pleomorphic adenoma. Subsequently, collaborative surgery was performed with neuro-otology from otolaryngology as well as skull base neurosurgery, which included resection of the preauricular infratemporal fossa, total right parotidectomy, right neck dissection, right lateral temporal bone resection, and attempt at dural resection. The procedure was aborted given the mass was invading dura. Surgical pathology revealed myoepithelial carcinoma ex pleomorhphic adenoma. The patient was referred to pediatric oncology and radiation oncology for further management. In summary, this is the first known case of transcranial carcinoma ex-pleomorphic adenoma in an infant. While salivary gland neoplasms are rare overall in children, the most common solid parotid neoplasm is a pleomorphic adenoma. Though the risk of malignant degeneration of pleomorphic adenoma to carcinoma ex pleomorphic adenoma is well known, the risk is thought to be time-dependent, and therefore our patient's young age of 5 months at presentation makes this case very unusual. It is unclear if the mass was present in utero. The extensive intracranial involvement can be explained by open sutures; the tumor likely extended from the right masticator space to the middle cranial fossa through the open sphenosquamousal suture. This case illustrates the importance of considering carcinoma ex pleomorphic adenoma in the pediatric population, particularly in invasive and transcranial parotid tumors.

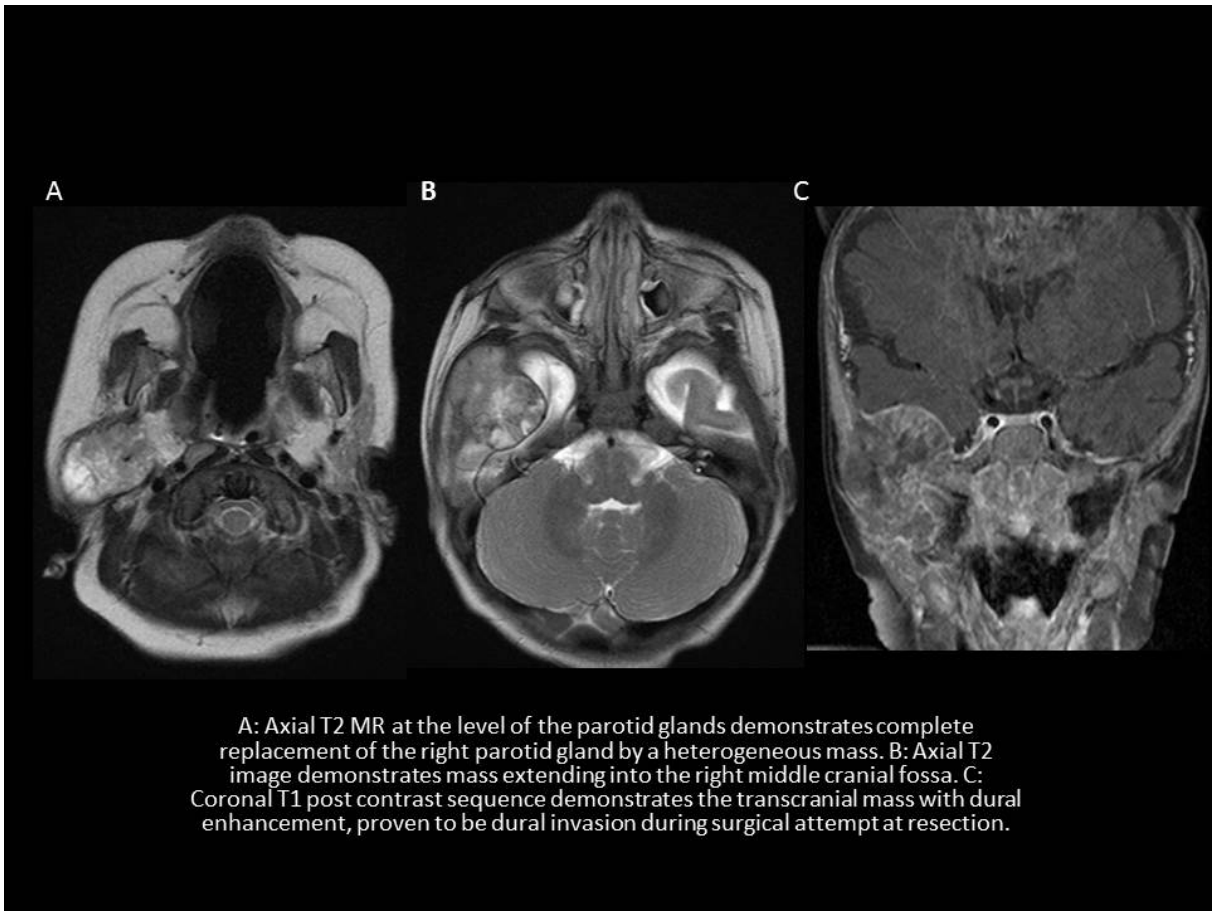

A: Axial T2 MR at the level of the parotid glands demonstrates complete replacement of the right parotid gland by a heterogeneous mass. B: Axial T2 image demonstrates mass extending into the right middle cranial fossa. C: Coronal T1 post contrast sequence demonstrates the transcranial mass with dural enhancement, proven to be dural invasion during surgical attempt at resection.

Ring - Ring… Imaging Evaluation Of Tinnitus

124 Ring - Ring… Imaging Evaluation Of Tinnitus

J Ortiz Jimenez, C Torres Pardo

McGill University
Canada

Purpose: Tinnitus is a condition affecting 15 to 20% of the world's population. Approximately 25% of patients with tinnitus, consider it a condition that interferes with their daily life. We want to create an interactive presentation that will serve as a learning tool in the diagnosis of different causes of tinnitus. We will use images extracted from the database of the Montreal University Health Centre in Montreal, QC. These include the use of 4D CTA in the diagnosis of dural fistulas as a cause of tinnitus. Approach/Methods: An interactive electronic presentation will be created in order to explain the relevant anatomy of the temporal bone and the differential diagnoses of pulsatile and non-pulsatile tinnitus. Findings/ Discussion: Tinnitus is a challenging diagnosis. CT and MRI can rule out some of the treatable causes. A precise knowledge of anatomy, anatomical variants, and associated pathological entities are fundamental prior to offering an adequate treatment. Summary/Conclusion: Our interactive presentation will allow the viewer to learn about the relevant anatomy, imaging protocols, radiological findings and differential diagnosis of tinnitus. References: 1. Santon, CL, Fatterpekar GM. Imaging Interpretation of Temporal Bone Studies in a Patient with Tinnitus. A Systematic Approach. Neuroimag Clin N Am 2016; 26: 207-225. 2. Baomin LI, Xiangyu CAO, Xinfeng LIU et al. Interventional diagnosis and treatment of vasculogeneic pulsatile tinnitus. J Otol 2014; 9(1): 7-15. 3. Swain SK, Nayak S, Ravan JR et al. Tinnitus and its current treatment - Still an enigma in medicine. J Formos Med Assoc. 2016; 115: 139-144. 4. McCormack A, Edmonson-Jones M, Somerset S. A systematic review of the reporting of tinnitus prevalence and severity. Hear Res 337; (2016) 70-79

46 y/o woman, pulsatile tinnitus
Retrotympanic mass

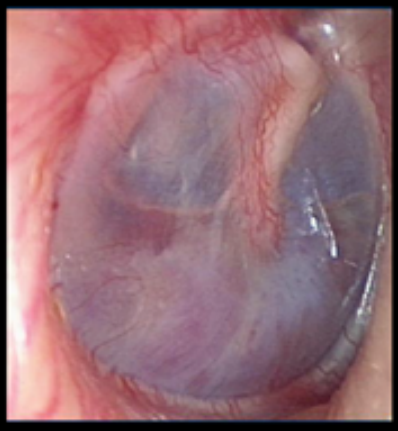

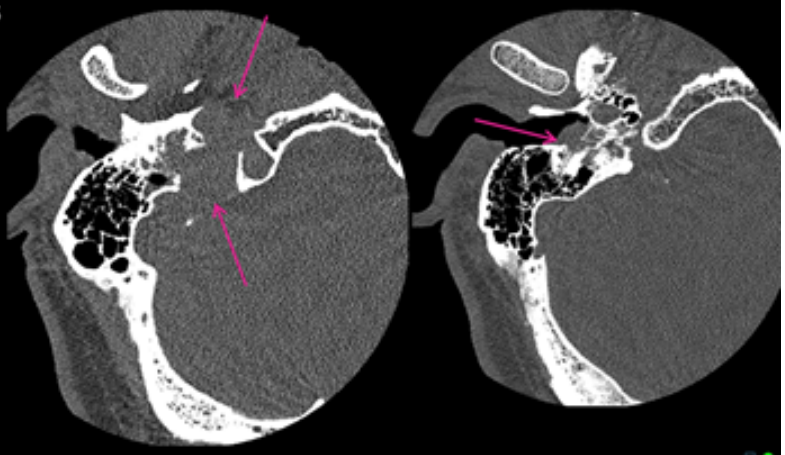

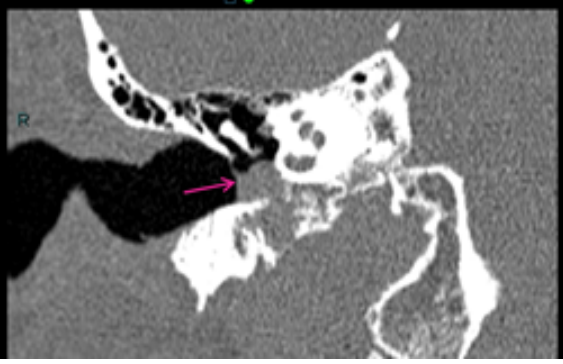

-Jugular foramen mass
-Permeative pattern of bone
-Middle ear extension

Optimal Adaptive Statistical Iterative Reconstruction Settings for the Evaluation of the Neck using Low Energy Dual Energy CT Virtual Monochromatic Images

125 Optimal Adaptive Statistical Iterative Reconstruction Settings for the Evaluation of the Neck using Low Energy Dual Energy CT Virtual Monochromatic Images

G Romero Sanchez, Z Lahijanian, R Forghani

Jewish General Hospital, McGill University
Canada

Purpose: Dual-energy CT (DECT) low energy virtual monochromatic images (VMIs) have been shown to improve visibility of head and neck cancers and the tumor-soft tissue boundary. However, the higher image noise on these reconstructions may represent a relative barrier to more widespread adoption and subjective acceptance. In this study, we evaluated the optimal iterative reconstruction settings for reducing image noise and improving quality of low energy VMIs. Material & methods: DECT scans from 30 consecutive patients were evaluated. All subjects were scanned with a 64-section scanner with fast kVp switching and low energy VMIs at 40 keV were reconstructed using different Adaptive Statistical Iterative Reconstruction (ASIR) settings (no ASIR, 20%, 40%, 60%, 80%, 100%). Image quality and noise was evaluated quantitatively and subjectively by evaluating normal tissues at different levels in the neck. This consisted of muscles at 6 different levels as well as different glands (parotid, sublingual, submandibular, and thyroid). Quantitative analysis was performed using three circular ROIs per structure. Standard deviation (SD) was used as a measure of image noise (IN). In addition, the signal to noise ratio (SNR) was calculated by dividing the CT attenuation (in Hounsfield units) by the SD. Results: A total of 6750 ROIs were evaluated, with an average ROI area of 9.46 mm2. The IN derived from muscles and glands progressively decreased, with a negative correlation of -0.6 for the glands and -0.9 for the muscles ($p < 0.05$). At all the ASIR settings, the muscle IN demonstrated a statistically significant difference in comparison with the control (no ASIR) (1-way ANOVA with Dunnett multiple-comparisons test $p < 0.005$). The lowest ASIR setting in the gland IN that showed a statistically significant difference was an ASIR of 40%. Muscle and gland SNR progressively increased at higher ASIR settings, with a positive correlation of 0.6 for the glands and 0.8 for the muscles ($p < 0.05$). The best quantitative results were obtained with an ASIR setting of 100. Although quantitatively the SNR progressively increased with increasing ASIR, subjectively, the best image quality was achieved at ASIR settings between 20 and 40%. Conclusion: 40 keV VMIs reconstructed using ASIR settings between 20 and 40% decrease image noise, increase SNR, and improve subjective image quality in the neck.

'Jaw Dropping' Lesions

126 'Jaw Dropping' Lesions

N Shekhrajka, M Forman, G Moonis

New York Presbyterian Hospital/Columbia University Medical Center
United States

Purpose: 1. To discuss the indications and appropriate imaging modalities for suspected mandibular/jaw lesions. 2. To discuss the various types of benign/malignant, cystic/solid and odontogenic/non-odontogenic mandibular lesions with multi-modality pictorial examples and differential diagnoses. 3. To discuss the treatment options including surgery and post operative imaging findings. Description: We plan to present the following pathologies with multi-modality imaging. CYSTIC LESIONS: Periapical/Radicular cyst Dentigerous cyst Odontogenic Keratocyst Primordial Cyst Solitary Bone cyst Aneurysmal bone cyst Stafne cyst BENIGN ODONTOGENIC SOLID LESIONS: Odontoma Ameloblastoma Odontogenic Myxoma Cementoblastoma Ameloblastic Fibroma MALIGNANT ODONTOGENIC SOLID LESIONS: Odontogenic carcinoma Odontogenic sarcoma and carcinosarcoma BENIGN NON-ODONTOGENIC SOLID LESIONS: Cemento-ossifying fibroma Juvenile ossifying fibroma Torus mandibularis Osteoma Fibrous dysplasia Paget disease Central giant cell granuloma Eosinophilic granuloma Neurofibroma Schwannoma MALIGNANT NON-ODONTOGENIC SOLID LESIONS: Squamous cell carcinoma Osteosarcoma Ewing sarcoma Chondrosarcoma Metastasis Multiple myeloma/plasmacytoma Lymphoma/leukemia

“Jaw Dropping” Jaw Lesions

Odontogenic Keratocyst

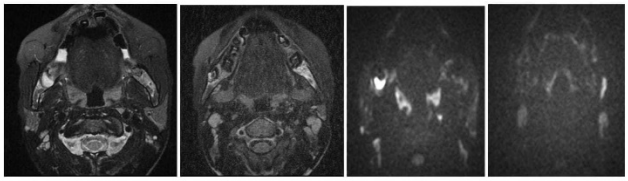

Axial T2 (left two images) and Axial DWI (right two images) through the mandible shows diffusion restricting T2 hyperintense lesions in the bilateral mandibles and maxilla in a patient with Gorlin-Goltz syndrome. These lesions were proved to be Odontogenic Keratocysts on pathology.

Stafne Cyst

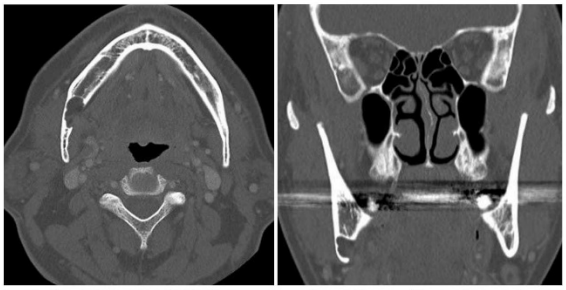

Axial (left) and Coronal (right) CT in the bone window through the mandible showing a shallow defect through the medial cortex of the right mandible with a corticated rim without soft tissue abnormalities, consistent with a Stafne Cyst.

“Jaw Dropping” Jaw Lesions

Cemento-ossifying Fibroma

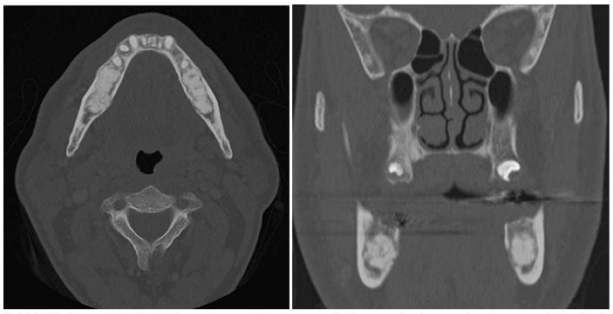

Axial (left), Coronal (right) CT through mandible shows well-circumscribed mineralised masses in the bilateral mandibles with bony expansion consistent with Cemento-Ossifying Fibroma.

Mandibular metastasis

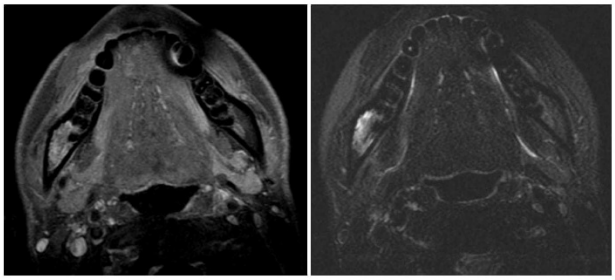

Axial T1 Fatsat post contrast (left) and Axial T2 Fatsat MRI sequences in a patient with Germ cell tumor of the testis showing a T2 hyperintense marrow signal in the right mandible adjacent to a soft tissue mass with enhancement. Biopsy of the lesion showed metastasis from patient’s known malignancy.

'Bullough Bump' : Protuberant fibro-osseous lesion of the temporal bone

127 'Bullough Bump' : Protuberant fibro-osseous lesion of the temporal bone

N Shekhrajka, G Moonis

New York Presbyterian Hospital/Columbia University Medical Center
United States

Protuberant fibro-osseous lesion (FOL) of the temporal bone or "Bullough Bump/Lesion" is a benign lesion of unknown etiology. To our knowledge only 6-8 cases of protuberant FOL of the temporal bones have been reported in the literature. With this case report we aim to discuss the clinical, radiological, pathological features and differential diagnosis for this lesion.

'Bullough Bump' : Protuberant fibro-osseous lesion of the temporal bone

Bullough Bump : Plain Radiograph

Plain skull radiograph showing bony thickening of the right temporal bone with mineralized densities within the overlying soft tissues.

'Bullough Bump' : Protuberant fibro-osseous lesion of the temporal bone

Bullough Bump : CT Scan

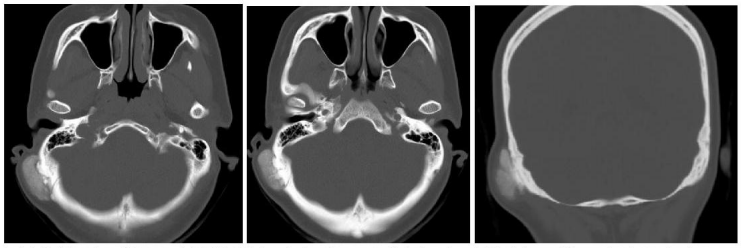

Axial (left two) and Coronal (right) CT head showing a well-defined, calcified, broad-based retroauricular mass emanating from the outer table of the right temporal bone without intraosseous or intracranial extension.

Bullough Bump : MRI

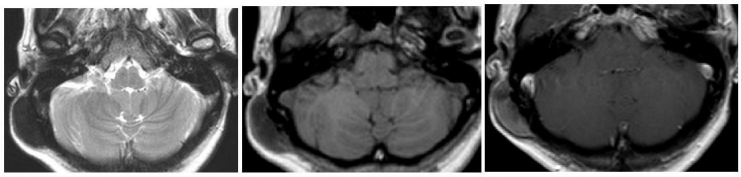

Axial T2 (left), Axial T1 pre contrast (middle) and Axial T1 post contrast (right) through right temporal bone showing a T1 and T2 hypointense, mildly enhancing post auricular lesion emanating from the outer table of the right temporal bone.

'Bullough Bump' : Protuberant fibro-osseous lesion of the temporal bone

Bullough Bump : Postoperative CT Scan

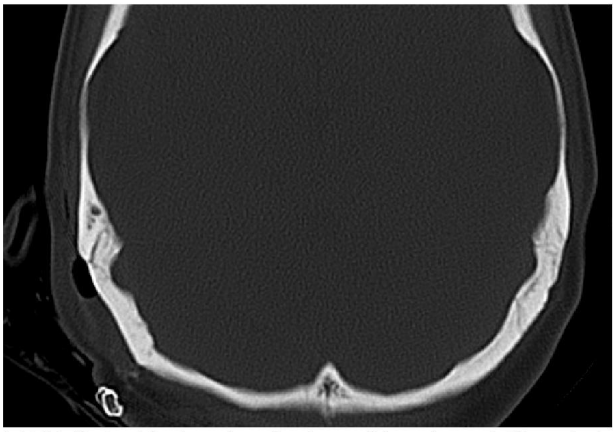

Axial CT of the head showing postoperative changes status post removal of the previously seen post auricular right temporal bone lesion.

Coexistent cholesteatoma: diagnosing the patient with the 'pearl earring'

128 Coexistent cholesteatoma: diagnosing the patient with the 'pearl earring'

J Choi, E Friedman, M Patino

UT McGovern Medical School University of Texas at Houston
United States

Coexistent cholesteatoma: diagnosing the patient with a “pearl earring” PURPOSE: Cholesteatoma diagnosis can be challenging even with high resolution CT and MRI techniques tailored to detect characteristic imaging findings. When cholesteatoma is coexistent with additional pathologies, compounded diagnoses may be missed in the setting of “satisfaction of search” pattern in describing and diagnosing the cholesteatoma. This presentation will demonstrate cases where cholesteatoma diagnosis was accompanied by coexisting or complicating pathologies. DESCRIPTION: Even with imaging techniques such as non EPI DWI that have near 100% specificity and up to 92% sensitivity in detecting cholesteatoma as small as 2 mm, there can be difficulties in making the diagnosis. When there are coexisting pathologies such as superimposed acute infection with abscess and chronic inflammatory sequelae such as cholesterol granuloma, underlying cholesteatoma can be overlooked. We will present cases underscoring the need to adhere to a consistent search pattern in evaluating coexisting cholesteatoma pathologies and complications. SUMMARY: Diagnosing cholesteatoma, primary or residual/recurrent, is challenging even in the face of additional techniques such as non EPI DWI that have been introduced. In the face of coexisting diagnoses or complications related to chronic inflammatory conditions, it is important not to give in to the “satisfaction of search” impulse. References: Dremmen MHG, Hofman PAM, Hof JR, Stokroos RJ, Postma AA. The diagnostic accuracy on non-echo planar diffusion weighted imaging in the detection of residual and/or recurrent cholesteatoma of the temporal bone. AJNR. March 2012;33: 439-444. Lingam RK, Nash R, Majithia A, Kalan A, Singh A. Non-echoplanar diffusion weighted imaging in the detection of post-operative middle ear cholesteatoma: navigating beyond the pitfalls to find the pearl. Insights Imaging. Oct 2016; 7(5): 669-678.

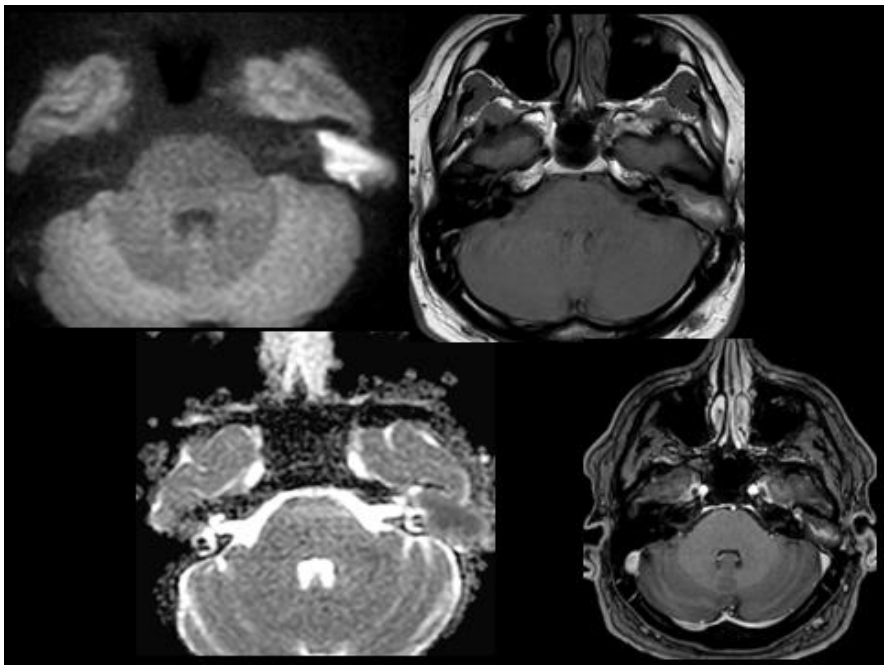

Strategies to Optimize Image guided biopsies and Cryoablation for Head and Neck Pathology .

129 Strategies to Optimize Image guided biopsies and Cryoablation for Head and Neck Pathology .

J Job

osu wexner medical center
United States

Purpose: The head and neck radiologist now plays an increasing role in patient management, with growing demand for percutaneous ablations and highly precise biopsies targeting regions of greatest concern on prior imaging using multiple modalities. Therapeutic advances, such as lower profile cryoablation probes with tightly controlled zones of ablation, have increased the potential role for ablative therapy in appropriate cases. Tailoring patient positioning, planning imaging protocols to specific head and neck pathology and patient anatomy (both in the pre and post operative setting) are crucial for accurate characterization of disease to optimize yield during image guided biopsies as well as treatment planning. Description: We first briefly review commonly encountered pitfalls and strategies to optimize and standardize imaging parameters for head and neck pathology with specific case examples, including: Methods to trouble shoot and consistently acquire optimal bolus timing to ensure adequate mucosal phase of enhancement for characterization of head and neck pathology. Routine acquisition of multiplanar reconstructions with bone and soft tissue algorithms as well as additional reconstructions specific to anatomy involved, pathology of interest and tailored to assist in treatment planning. Examples of Dual Energy CT to improve delineation of primary and regional disease. Methods to improve detection of pathology in the post treatment neck. For example: ventilation via stoma in the post operative neck with TEP device in place during imaging/biopsy/ treatment planning. This better delineates the walls of neopharynx and is similar in principle to puffed cheek acquisition for lesions involving buccal space. Methods to minimize commonly encountered artifacts. For instance, angled images to minimize artifact both for diagnostic imaging and for biopsy/treatment planning. If this is not possible by tilting gantry, we show examples of controlled patient head tilt after review of scout to ensure artifact will be out of plane of interest. Other commonly encountered challenges during CT guided biopsies of small deep space lesions and strategies to work around them. For example- in plane beam hardening artifact from biopsy device, which can obscure lesion of interest. We then review the role for ultrasound in head and neck intervention, with case examples demonstrating when it is optimal for both characterization of disease, tissue sampling and therapeutic intervention. Finally, we review cryoablation cases for treatment in head and neck cancers. We examine our patient selection process at OSU, pertinent regional anatomy with techniques to avoid critical structures - such as hydrodissection pre- cryoablation, and the importance of performing each case with appropriate ENT follow up, including swallow studies, assessment of vocal cord function etc. Summary: There are growing demands for targeted biopsy and therapy by the head and neck radiologist, which mandate the neuroradiologist remains up to date with optimizing and tailoring imaging protocols and aware of how to maximize yield and optimize outcomes from image guided intervention.

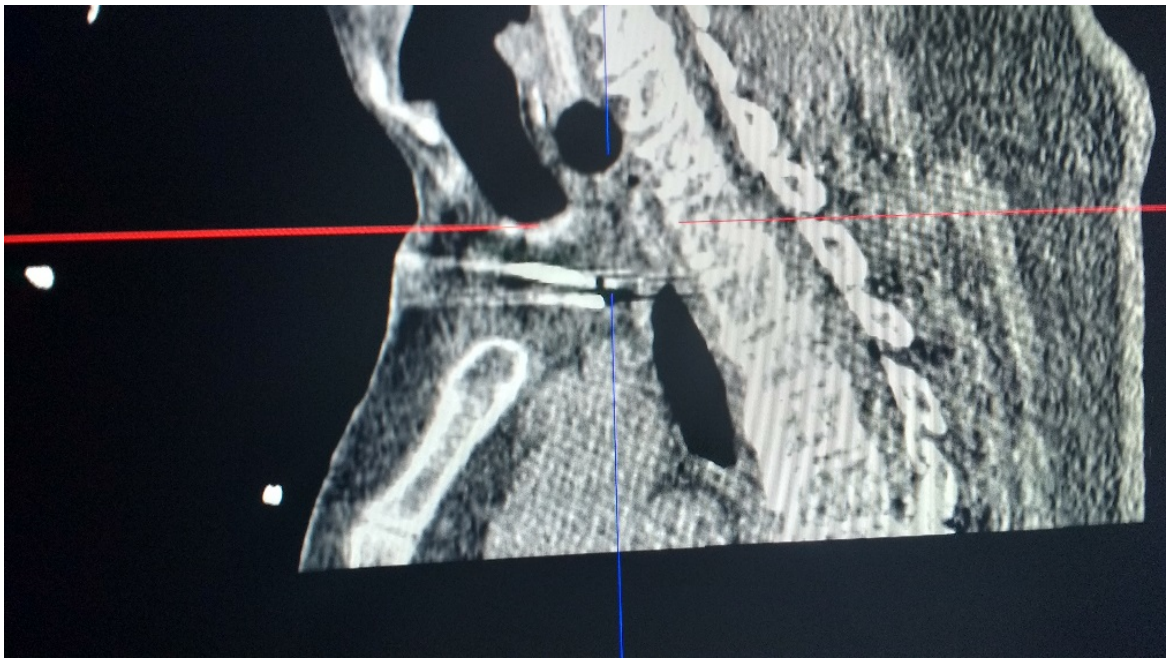

The hide and seek game of head and neck radiologists: An update on multimaging diagnostic approach of unusual ectopic abnormal parathyroid glands.

130 The hide and seek game of head and neck radiologists: An update on multimaging diagnostic approach of unusual ectopic abnormal parathyroid glands.

RA Moreno, RL Gomes, FL Montenegro, EM Gebrim

Hospital das Clinicas FMUSP
Brazil

The purpose of this exhibit is to: 1. Illustrate very unusual ectopic abnormal parathyroid glands locations, such as at the soft palate, pre-laryngeal, retropharyngeal and submandibular spaces. 2. Highlight relevant information provided by 4D-CT and MR imaging in cases with such particular locations and small dimensions. 3. Establish new imaging techniques advantages over the most commonly used first-line modalities, as nuclear medicine scintigraphy and ultrasound imaging. 4. Delineate a take-home message board, by the analysis of representative cases with imaging findings in agreement with those recently described in the literature. Primary hiperparathyroidism (PHPT) diagnosis is based on the biochemical evaluation, however, imaging plays an essential role, since a solitary parathyroid adenoma is the most common cause (89%). A precise localization of such lesions or any functioning parathyroid tissue, unresponsive to medical therapy, contributes to a more targeted surgical treatment, with high cure rates. It's also essential for those with persistent or recurrent PHPT since it contributes to reduce reoperation taxes and increases recognition of related conditions, such as multigland disease, ectopic and supernumerary glands. The choice of imaging algorithm evaluation is site specific and should be based on local resources, interdepartmental discussions and the experience of radiologists. Nuclear medicine scintigraphy and ultrasound are well-established modalities. Recently, multiphase or 4-dimensional computed tomography (4D-CT) is gaining acceptance as a first line study with several advantages. MR imaging is used less commonly. In summary, no imaging modality has demonstrated clear superiority, but we believe that 4D-CT is an easy method to localize these unusual ectopic parathyroid glands, particularly the suprahyoid ones.

SOFT PALATE ADENOMA

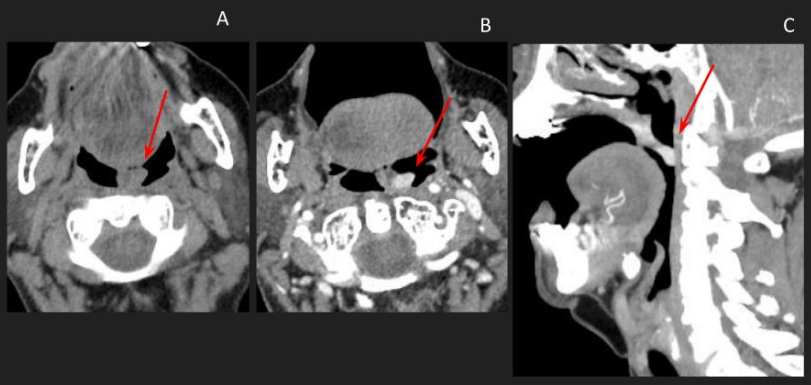

Patient presenting with throat discomfort on left side. CECT of the neck shows left uvulopalatal small nodule, proved to be a parathyroid adenoma by histopathological analysis. (A) Non-contrast phase axial image of the neck demonstrates a bump at uvula left lateral contour, with high contrast enhancement on CECT (B) (arrows). Reformatted left sagittal (C) images demonstrate that the lesion (arrows) obliterated partially the pharyngeal airway column, and probably was the responsible for the clinical complaint.

Whooshers: Pulsatile Tinnitus Etiologies and Advanced MR Techniques from Diagnosis to Intervention

131 Whooshers: Pulsatile Tinnitus Etiologies and Advanced MR Techniques from Diagnosis to Intervention

LB Eisenmenger, M Brozynski, C Glastonbury, V Shah, W Dillon, D Saloner, M Amans

University of California, San Francisco
United States

Purpose: To present the wide spectrum of pulsatile tinnitus etiologies emphasizing the most common causes and those with high risk for poor neurological outcome. To present a succinct imaging protocol and a systematic method of evaluating for critical imaging findings. To present cutting edge imaging techniques that offer promise for identifying the source of pulsatile tinnitus. Description: Pulsatile tinnitus is a rhythmic sound patients experience without extracorporeal source that is often associated with the cardiac cycle. Although pulsatile tinnitus in itself can be a debilitating condition due to the chronic and incessant nature of the symptoms, there are also many potentially dangerous causes of this condition that can lead to significant neurologic morbidity and mortality. Through case-based examples with clinical presentation as well as clinical, radiologic, intra-procedural, and post-treatment images, we will not only review the etiologies of pulsatile tinnitus, but more importantly provide a practical framework for evaluating this condition. Vascular causes of pulsatile tinnitus are among the most common underlying etiologies including arterial dissection, aneurysm, focal narrowing/atherosclerosis, and fibromuscular dysplasia as well as shunting lesions such as arteriovenous malformations and dural arteriovenous fistulas, venous abnormalities such as dural venous sinus narrowing and diverticulum, and more rare but well-described causes such as an aberrant internal carotid artery and persistent stapedial artery. Underlying osseous abnormalities including encephaloceles extending into the middle ear, active otosclerosis, and the vascular stage of Paget's disease as well as vascular masses including glomus tumors, hypervascular metastases, and some meningiomas will also be discussed. Through case presentations of both common and rare causes of pulsatile tinnitus, we will emphasize the important features the neuroradiologist should recognize. Advanced MRI techniques are the most potent of the noninvasive imaging tools to screen for most of the high-risk lesions. Arterial spin labeling may be used to increase the sensitivity for dural AVF and AVM detection. 4D flow MRI is a cutting-edge sequence that can be used to evaluate flow patterns in both normal and abnormal vasculature, sometimes helping to identify increased vorticity and flow patterns that can lead to pulsatile tinnitus and potentially identify higher risk lesions. We will present case examples of both common imaging modalities used in clinical practice as well as cutting edge techniques currently limited to the research setting. For example, in Figure 1, there are four example cases of 4D flow MRI in the internal jugular vein showing two patients with pulsatile tinnitus (the two on the right) and two patients without (the two on the left). The patients with tinnitus have higher helical pitch values compared to the asymptomatic individuals demonstrating one possible application of 4D flow MRI in this patient population. Summary: Through our exhibit, we will present pulsatile tinnitus cases and their defining features as well as emphasize high-risk, "don't miss" lesions. We will also present the innovative research imaging techniques that may become integrated into practice. This exhibit will provide an in-depth review of what the neuroradiologist needs to know regarding cases of pulsatile tinnitus.

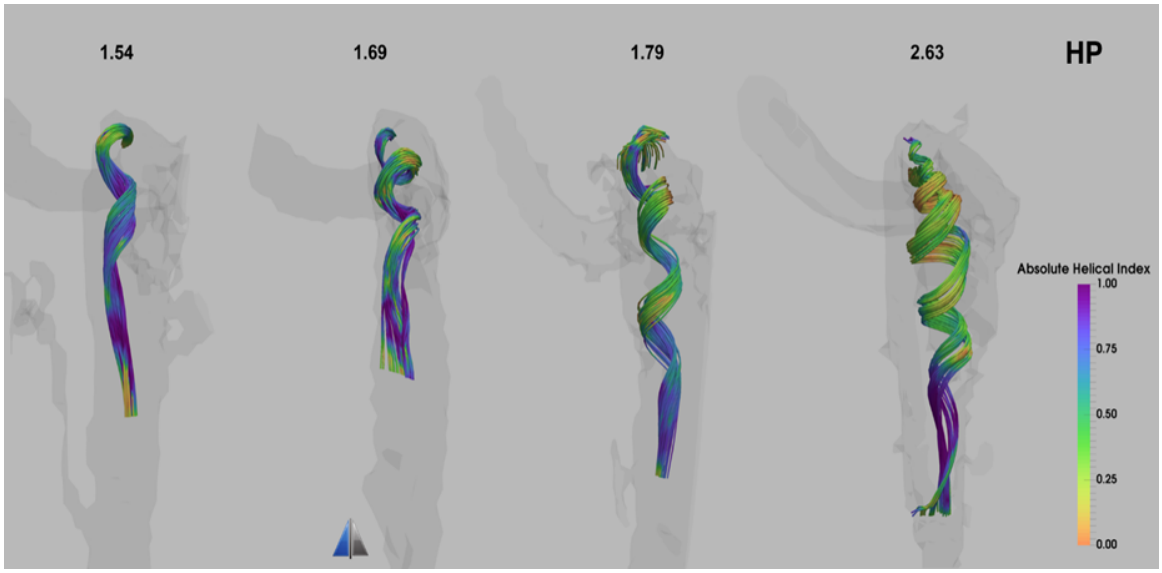
1.54
1.69
1.79
2.63
HP
Absolute Helical Index
1.00
0.75
0.50
0.25
0.00

Don't Biopsy Me: Commonly Encountered "Don't Touch" Lesions of the Head and Neck

132 Don't Biopsy Me: Commonly Encountered "Don't Touch" Lesions of the Head and Neck

G Mongelluzzo, T Ly, N Purdy, W Quinones

Geisinger Medical Center
United States

PURPOSE The purpose of this exhibit is to familiarize the radiologist, otolaryngologist, and interventionalist with imaging appearances and appropriate workup of various lesions and pseudolesions of the head and neck that may present on imaging, but should not be biopsied. DESCRIPTION There are a wide array of lesions found throughout the head and neck that should not be biopsied for one reason or another. These lesions may present as a palpable or symptomatic mass or may be found incidentally on imaging obtained for another reason. In some cases, a thorough knowledge of the relevant anatomy is all that is necessary to prevent any further unnecessary evaluation or worry. Awareness of specific lesions that arise in characteristic locations, such as the mylohyoid boutonniere defect, asymmetry of the pterygoid venous plexus, or unusual patterns of skull base pneumatization allow the interpreter to confidently dismiss normal variants. Other lesions may have a complex or nonspecific appearance on at least one imaging modality, such as CT, while diagnosis can easily be made by another modality if the appropriate recommendation is given. Such lesions include venolymphatic malformations that may be nondescript by CT. The most accurately targeted needle biopsy will certainly provide a nondiagnostic sample to the pathologist, while an MRI will often reveal fluid-fluid levels and thin enhancing septations, allowing a confident diagnosis to be made. As always, before inserting a needle into a lesion, consideration should be given to whether or not a lesion may be vascular. Enhancement within a venous malformation or pseudoaneurysm of the external carotid artery can appear surprisingly unimpressive on a routine delayed venous phase CT scan of the neck. Even in cases when a biopsy is not inherently risky, it may be lead to repeated unnecessary nondiagnostic procedures. The diagnosis of a schwannoma by fine needle aspiration, for instance, often proves difficult. Commonly, an inadequately cellular specimen is obtained; and even when the sample is adequately cellular, the diagnosis can be challenging for the pathologist. Contributing further to the dilemma, schwannomas are commonly FDG avid on PET/CT. The aforementioned examples provide just a glimpse of the scenarios encountered in a busy head and neck practice and highlight the role of the radiologist in contributing to appropriate guidance and management. SUMMARY This presentation aims to provide examples of routinely encountered “don’t touch” lesions in the head and neck, summarize imaging features that allow the radiologist to provide a definitive diagnosis based on imaging alone, and to describe locations or imaging findings that should prompt the radiologist to recommend an alternative imaging study before an unsafe or unneccessary biopsy is attempted or performed.

ORBITAL TUMORS: Insights from imaging

133 ORBITAL TUMORS: Insights from imaging

C Utrilla, PS García-Raya, A Arbizu, C Oterino, A Royo, G Garzon

Hospital Universitario La Paz, Madrid, Spain
Spain

Purpose - To provide a classification of orbital tumors based on compartmental location and age of presentation. - To describe the main radiologic features of orbital tumors, including the contribution of advanced imaging techniques. Description All orbital tumors registered in our center in the last ten years were reviewed, focusing on imaging finding. In order to simplify the approach of this wide range of pathologies, we divided the orbit into three compartments: preseptal, postseptal intraconal and postseptal extraconal. Tumors in the preseptal space include those related to skin (and appendages) and conjunctiva. Postseptal tumors can be classified using as reference the tissue of which they arise from. In the intraconal space: the globe, the optic nerve and sheath (meningioma and glioma) and involving tissues such us fat, extraocular muscles and blood vessels (slow flow venous malformation). The extraconal, which limits peripherally the orbit, will include the lacrimal system, walls of the orbit (fibrous dysplasia) and tumors from neighborhood (brain, nasal cavity and paranasal sinuses). Some tumors can affect more than one compartment or arise at any compartment: lymphoma, neurogenic tumors, veno-lymphatic malformation, rhabdomyosarcoma and metastasis. We will focus on the main radiologic features of these tumors, and on advanced MRI techniques, especially diffusion-weighted imagining (DWI). Summary Orbital tumors comprise a diverse group of lesions, complex to characterize and sometimes challenging to remember for radiologists. A useful strategy is to make a diagnosis based on compartmental location, combined with advanced MRI techniques, which can help to narrow our differential diagnosis.

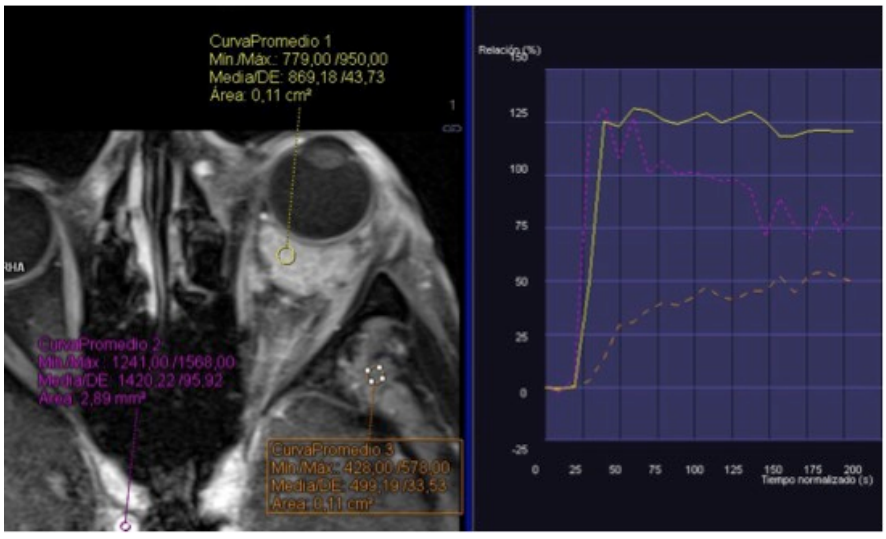

Diagnostic approach to parotid gland lesions: multiparametric magnetic resonance evaluation

134 Diagnostic approach to parotid gland lesions: multiparametric magnetic resonance evaluation

AP Freitas, C Amancio, L Silva, L Godoy, U Passos, C Costa Leite, EM Gebrim

Radiology Institute of the University of Sao Paulo
Brazil

Imaging of the salivary glands is a diagnostic challenge because of the great variety of disease processes that may show similar imaging findings. Many diseases including inflammatory, infectious, obstructive, systemic, and benign and malign neoplastic processes can inflict the salivary glands. Magnetic Resonance Imaging (MRI) techniques have been applied to differentiate between benign and malignant salivary gland lesions and have improved the parotid lesions evaluation. The purpose of this exhibit is to describe the detailed anatomy of the parotid gland, including its ducts, vascularization and innervation. To demonstrate how multiparametric evaluation such as diffusion and permeability of parotid lesions can help to narrow the broad differential diagnosis. Benign mixed tumor shows an ascending plateau in the perfusion curve, whereas Warthin tumor presents a rapid and intense uptake and a wash-out, exceeding 30%. Malignant tumors show an intense uptake and persistent or descending plateau. Cases of tumoral and non-tumoral lesions of parotid gland will be presented, including benign mixed tumor, Warthin tumor, mucoepidermoid carcinoma, adenoid cystic carcinoma, lymphoma, parotid abscess, Sjogren syndrome, venous malformations, lipoma and metastasis.

ANATOMY OF NORMAL PAROTID GLAND

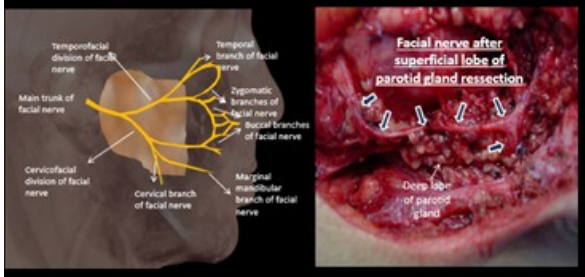

ADVANCED METHODS: NORMAL DCE OF PAROTID GLAND

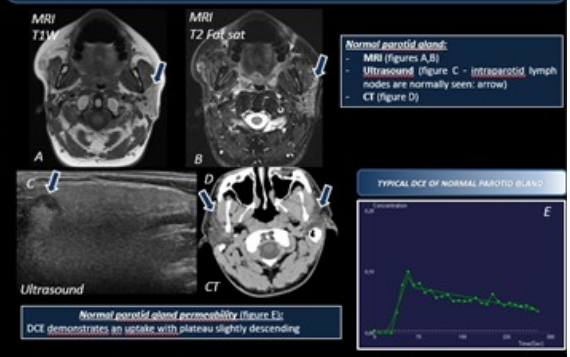

Normal parotid gland:
- MRI (figures A,B)
- Ultrasound (figure C - intraparotid lymph nodes are normally seen: arrow)
- CT (figure D)

Normal parotid gland permeability (figure E):
DCE demonstrates an uptake with plateau slightly descending

ADVANCED METHODS: LESIONS CARACTHERISTICS ON DCE

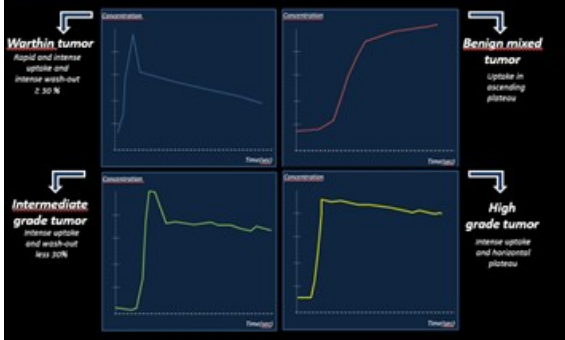

BENIGN MIXED TUMOR

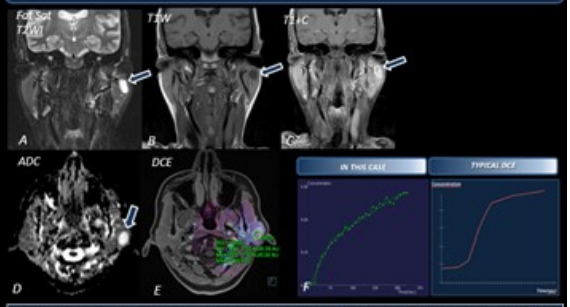

Solid nodule in the superficial portion of the left parotid gland with regular contours and hypersignal in T2 (figure A), hyposignal in T1 (figure B) and intense enhancement (figure C). Note the high value of ADC (figure D) and DCE curve shows a typical slow ascending plateau (figure F), suggestive of BMT.

WARTHIN TUMOUR

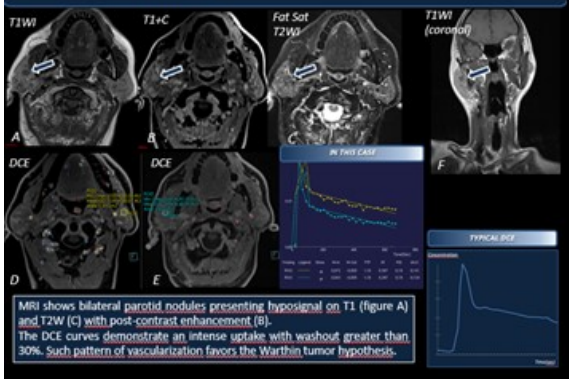

MRI shows bilateral parotid nodules presenting hyposignal on T1 (figure A) and T2W (C) with post-contrast enhancement (B).
The DCE curves demonstrate an intense uptake with washout greater than 30%. Such pattern of vascularization favors the Warthin tumor hypothesis.

ADENOID CYSTIC CARCINOMA

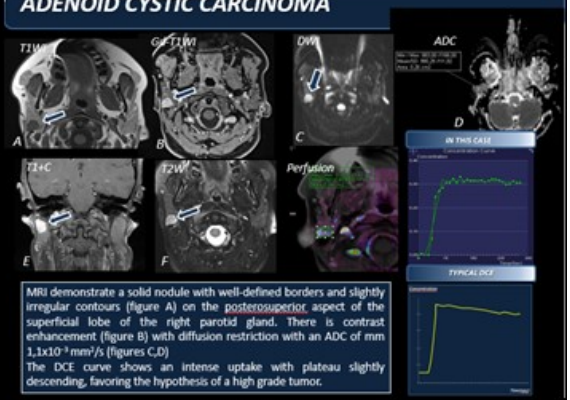

MRI demonstrate a solid nodule with well-defined borders and slightly irregular contours (figure A) on the posterosuperior aspect of the superficial lobe of the right parotid gland. There is contrast enhancement (figure B) with diffusion restriction with an ADC of mm $1{,}1 \times 10^{-3}$ mm²/s (figures C,D)
The DCE curve shows an intense uptake with plateau slightly descending, favoring the hypothesis of a high grade tumor.

A Match-Made in (Hospital) Heaven: The Growing Relationship between Neuroradiology and Oral and Maxillofacial Surgery

135 A Match-Made in (Hospital) Heaven: The Growing Relationship between Neuroradiology and Oral and Maxillofacial Surgery

M Forman, C Cooper, S Eisig, G Moonis

New York Presbyterian Hosptial, Columbia University Medical Center
United States

Purpose: The purpose of this exhibit is to portray the clinically meaningful, and productive relationship that the field of oral and maxillofacial surgery (OMFS) has developed with neuroradiology and the 3D lab. Approach: OMFS continues to expand and utilize its use of the capabilities of neuroradiology. Many facial reconstruction procedures such as corrective jaw surgery, pathology, or trauma cases can all have improved outcomes and shorter operating room times when employing virtual planning. Typically, a patient presents with an existing surgical problem (e.g., orbital floor fracture, mandibular tumor, skeletal discrepancy). The patient proceeds to get a maxillofacial computed tomography scan. With the help of the on-site 3D lab, a virtual surgical plan can be created together (e.g., segmentalization of a jaw lesion, making surgical margins). Once the patient model is printed, reconstructive materials such as a rigid fixation plate, mesh, or other implant can be prepared and customized to that case. This process would usually otherwise take place in the operating room increasing surgical, anesthesia and operating room time. Discussion: This relationship has improved the precision, accuracy, and operating room times for our patients. Through this exhibit we hope to describe the use of radiography, virtual planning, and 3D printing for maxillofacial cases including post-traumatic reconstruction, pathologic resection and corrective maxillomandibular surgery. Third party companies and engineers have become a mainstay of the field; however, by working with local, on-site radiologists and 3D labs, the independence of surgeons and institutions continues to grow. This expanding relationship promises to be an exciting part of the future for both fields. Conclusion: The use of neuroradiology, virtual surgical planning, and 3D printing have substantially changed the way that OMFS plans and completes surgery for its patients. In this exhibit we will highlight through individual cases, this collaborative experience at our institution.

Value of Doppler ultrasound in uveal melanomas treated with brachytherapy, an indicator of regression.

136 Value of Doppler ultrasound in uveal melanomas treated with brachytherapy, an indicator of regression.

C Utrilla, M Asencio, A Fernández-Zubillaga, G Garzon, A Royo, PS García-Raya

Hospital Universitario La Paz, Madrid, Spain
Spain

Purpose To evaluate tumor blood flow in uveal melanomas, before and after ruthenium-106/Iodine-125 episcleral plaque application, using pulse Doppler ultrasound. Materials & Methods A cohort of 40 patients with uveal melanoma treated with brachytherapy has been reviewed. Color Doppler ultrasound was used to evaluate the presence of vessels within the lesion and to measure blood flow velocity and vascular resistance index of these pathological vessels. The ultrasound was performed at diagnosis and every 6 months. The follow-up period is 22.5 months on average (range 6-56 months). Results 40 patients, 22 men and 18 women with uveal melanoma treated with brachytherapy. The average age was 59.27 years. 22 lesions affect the left eyed and 18 the right eye. Location: 32.5% posterior part of the globe, 22.5% equatorial, 17.5% peripheral, 15% cilliary body and 12.5% post-equatorial. 80% were melanotic, 12.5% amelanotic and 7.5% were mixed. 11 lesions showed vascularization within the tumor. The dose to the apex in all was 85 cGy and the average rate of dose was of 81,5 cGy/h. In all patients with vascularization within the tumor at diagnosis, it disappeared at month 18, except one, which showed recurrence. 6 that were non-vascularized at diagnosis, experienced new vascularization during the follow-up, 2 were related to neovascular glaucoma, 1 with recurrence, 1 with worsening of diabetic retinopathy and 2 with ecographic and ophthalmoscopic regression. There was only a case of metastasis during the follow-up and was in a regressed melanoma without vascularization. Conclusions The results of this study suggest that color Doppler ultrasound allow a noninvasive in vivo evaluation of tumor vascularity in uveal melanoma. It is an useful tool for monitoring uveal melanoma after brachytherapy, since the disappearance of the vessels together with the tumor decrease in size, measured by ultrasound are signs of regression. Cases with persistent vascularization are associated with tumor recurrence or vascular congestion due to neovascular glaucoma. Cases of appearance of new vascularization can be explained by persistence of vasculature that previously was not found.

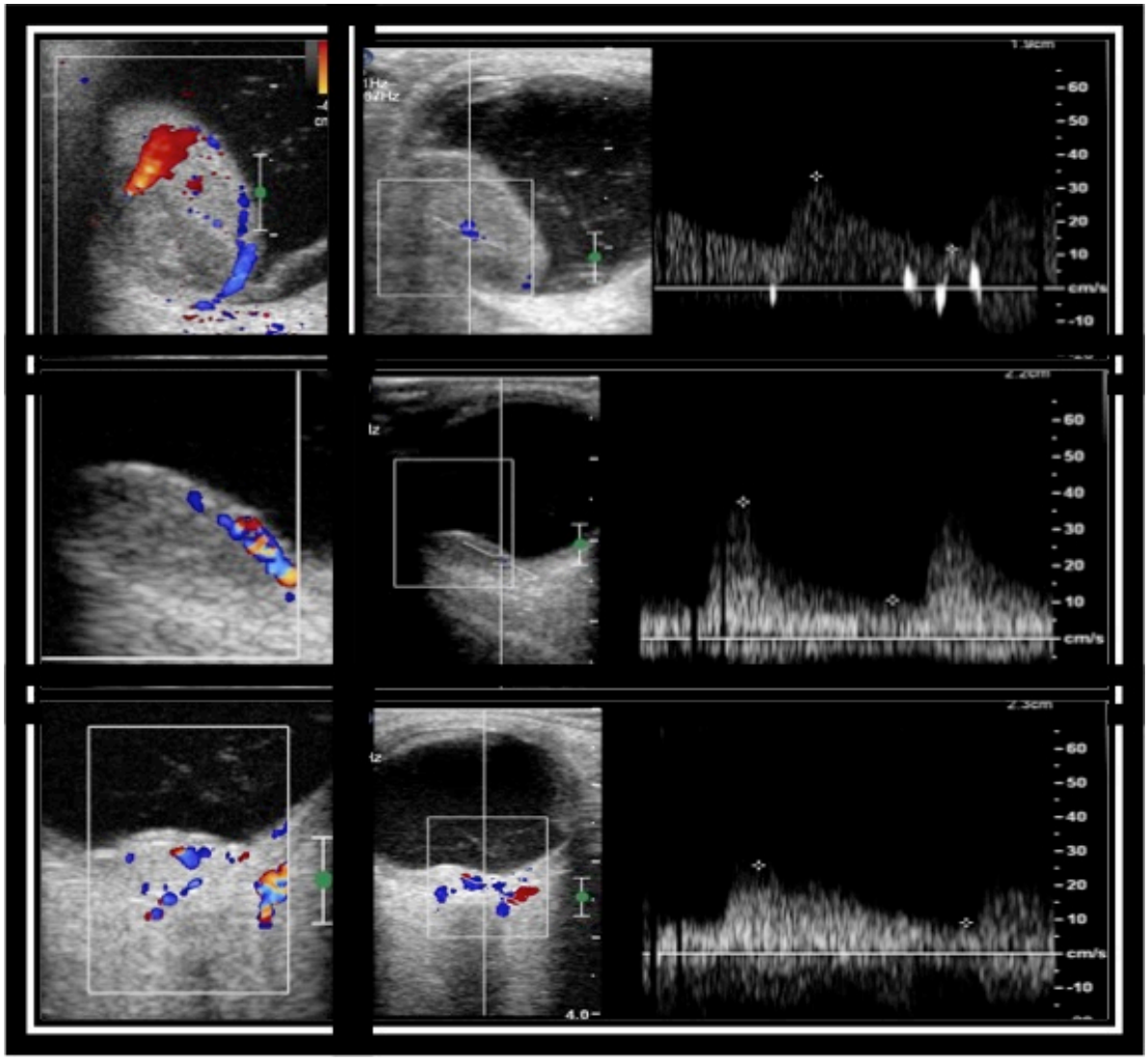
60
50
40
30
20
10
cm/s
-10
60
50
40
30
20
10
cm/s
60
50
40
30
20
10
cm/s
-10
4.0

The Oculomotor Nerve: Beyond Diplopia

137 The Oculomotor Nerve: Beyond Diplopia

LF Ramin, RA Moreno, H Tames, B Olivetti, CJ da Silva, RL Gomes, EM Gebrim

Radiology Institute of the University of Sao Paulo
Brazil

The purpose of this exhibit is to: Discuss functions of oculomotor nerve and symptomatology Show the normal anatomy of the oculomotor nerve through CT, MRI and schematic drawings Discuss the role of MRI for evaluation of oculomotor nerve pathway diseases and imaging recommendations for analysis of each segment Show selected pathologic conditions Delineate a take home message board by the analysis of didactic and representative cases of oculomotor nerve diseases Description: Oculomotor nerve is a mixed cranial nerve (motor and parasympathetic) which innervate extraocular muscles (levator palpebrae superioris, superior, inferior and medial rectus muscle and inferior oblique muscle), ciliary muscle and pupillary sphincter. It is divided into four anatomic segments (intra-axial, cisternal, cavernous, extracranial) and its parasympathetic fibers are peripherally distributed. Imaging plays a key role in the differential diagnosis of oculomotor nerve related symptoms. Summary: Introduction Oculomotor nerve function Anatomic considerations Selected Pathologic Conditions Tumoral: isolated schwannoma, NF related schwannoma Infectious: Lyme disease, cisternal tuberculosis Inflammatory: ophthalmoplegic migraine, neuritis, Tolosa Hunt syndrome Vascular: neurovascular conflict, aneurysmal compression, carotid cavernous fistula, cavernous sinus thrombosis Traumatic: nerve rupture, uncal herniation Others: orbital apex IgG4 related disease, cavernous sinus lymphoma, pituitary apoplexy, and more Take-home messages

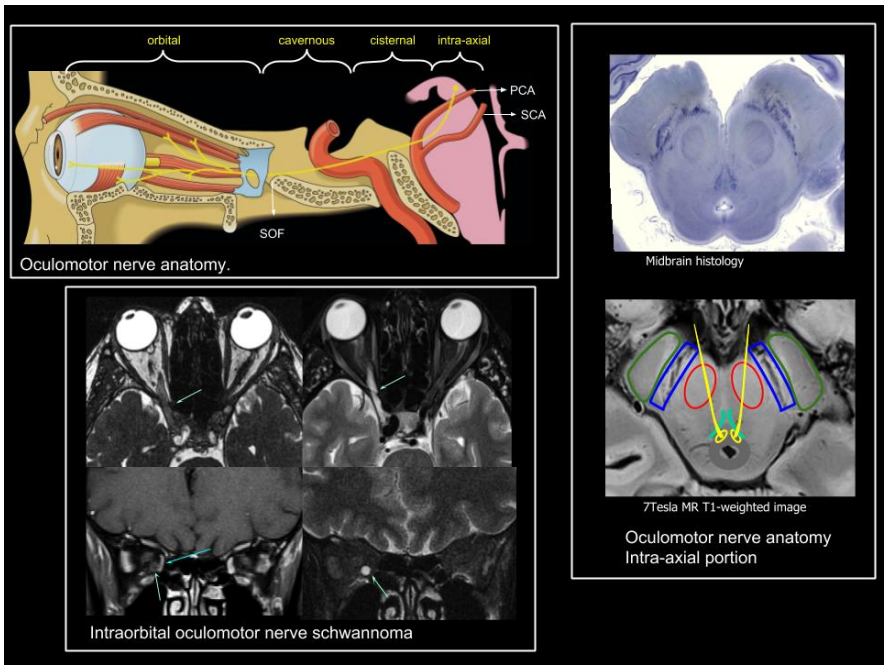
orbital
cavernous
cisternal
intra-axial
PCA
SCA
SOF
Oculomotor nerve anatomy.
Midbrain histology
7Tesla MR T1-weighted image
Oculomotor nerve anatomy
Intra-axial portion
Intraorbital oculomotor nerve schwannoma

Massive extracranial Arteriovenous Malformation: Case Report

138 Massive extracranial Arteriovenous Malformation: Case Report

M Lochocki, LA Miquelini, MP Larregina, FM Ferraro, A García, S Mukherji

British Hospital of Buenos Aires, Argentina
Argentina

Massive extracranial Arteriovenous Malformation: Case Report Purpose: • Describe the main radiological characteristics of the arteriovenous malformations. Presentation summary: Arteriovenous malformations (AVM) correspond to the group of high flow vascular anomalies which are characterized by direct communication between arteries and veins, lack of capillary network in between and for being locally aggressive. This is a case of massive AVM involving the neck, face and ear in a 34 years old female, which started to grow since the age of 15. It had many complications including almost fatal hemorrhages. CT angiography of the extracranial Head and Neck showed a giant mass comprised of multiple tortuous vascular structures, with the right vertebral artery as the main afferent vessel, and the external jugular vein, as the main efferent vessel. The aim of this report is to review the principal features of this abnormality, which often represents a real challenge for the radiologist due to its vascular architectural complexity.

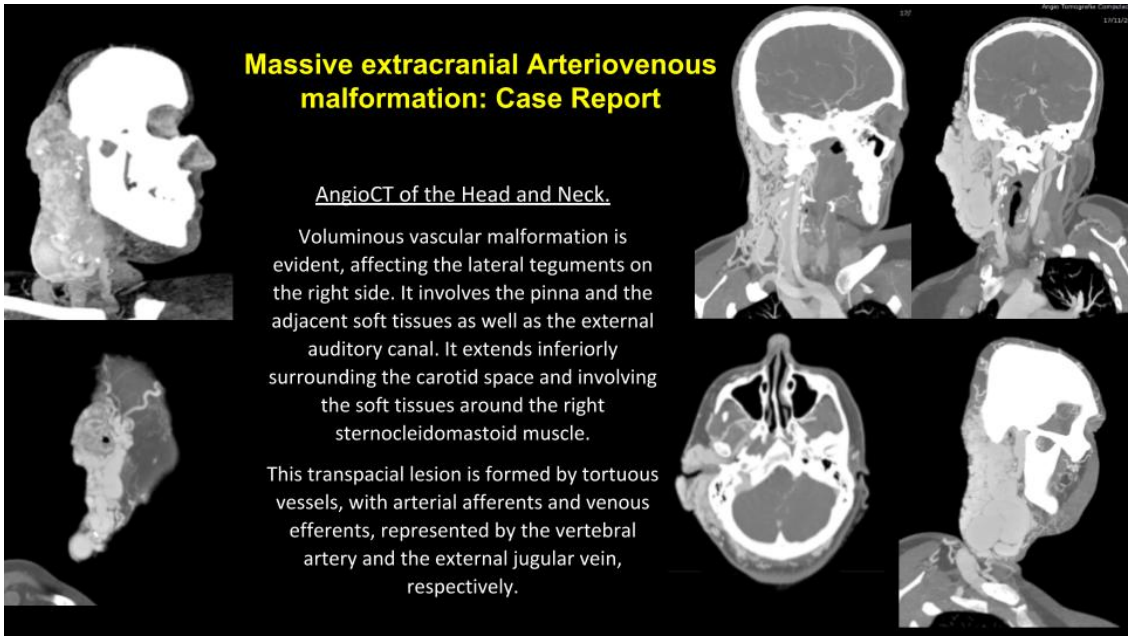

Case Presentation: Erdheim-Chester Disease

139 Case Presentation: Erdheim-Chester Disease

SP Onderi, U Sarmast, I Ikuta

Yale University School of Medicine
United States

Purpose: To present a pictorial evolution of Erdheim-Chester disease with orbital, pituitary, calvarial, and spine lesions. We report the radiologic appearance of this rare disease to promote prompt recognition, diagnosis, and treatment. Description: This 58-year-old woman with a medical history of hyperlipidemia and hypertension presented at an outside facility with significant polydipsia and polyuria. A diagnosis of central diabetes insipidus was presumptively made. Lab testing later showed decreased gonadotropin levels, and CSF testing was notable for rare small lymphocytes and monocytes, but otherwise unremarkable. Initial brain MRI study showed pituitary gland and stalk enlargement and enhancement. A presumptive diagnosis of lymphocytic hypophysitis was made at that time. PET-CT was performed which showed skeletal expansion and marrow activity involving the distal femora and proximal tibias. The patient was treated with dDAVP with improvement of polydipsia and polyuria. Serial follow up brain MRI studies demonstrated eventual resolution of the pituitary findings over a time period of 3 years. MRI of the brain performed 3 years later showed enhancing bilateral orbital masses. Orbital biopsy was notable for xanthogranulomatous inflammation with fibrosis, and foamy histiocytes. Molecular diagnostic testing showed BRAF gene V600E mutation. A presumptive diagnosis of Erdheim-Chester disease was then made. The patient was placed on Dabrafenib with continued follow up. Repeat PET-CT showed sclerosis with uptake in multiple skeletal structures including the bilateral tibias and distal femora. There was bilateral renal enlargement and increased FDG uptake, with perirenal soft tissue infiltration and increased FDG uptake. Follow up MRI demonstrated persistent intraorbital enhancing masses, with low signal intensity lesions in the right parietal calvarium and C3 vertebral body, suspected to represent additional foci of Erdheim-Chester disease manifestations. Summary: Erdheim-Chester disease is a rare non-Langerhans cell histiocytosis associated with multiorgan deposition of foamy, cholesterol-laden histiocytes associated with fibrosis. To date, only about 600 cases are described in the medical literature. Presenting symptoms are nonspecific, ranging from mild indolent presentation to life-threatening multi-organ disease. Diagnosis involves a combination of clinical investigation with radiology-pathology correlation in involved organs. Early recognition and diagnosis is crucial for initiation of early treatment to decrease morbidity and mortality associated with this disease.


Page: 10 of 17
IM: 10 SE: 14
cm

Ewings Sarcoma of the Temporal Bone: a Pictorial Essay

140 Ewings Sarcoma of the Temporal Bone: a Pictorial Essay

A Botsford, J Heidenreich

Dalhousie University Division of Neuroradiology
Canada

Purpose: Ewing's sarcoma is a small, round, blue cell tumour and the second most common tumour in children. Primary Ewing's sarcoma in the cranial bones, however, is exceptionally rare. Of the reported cases in the literature, to our knowledge the oldest patient with this diagnosis presented at 52 years of age with an occipital bone mass. The vast majority of patients however are under 10 years old. We report the case of a 54 year old female, who presented with scant brown drainage from the ear, cranial nerve V-VIII palsies and a progressively enlarging visible mass. The purpose of this report is to present and review the imaging, immunohistochemical and molecular findings in this rare condition. Description: Following initial clinical presentation, the patient underwent a CT which revealed a large 5.7 x 5.7x 5.2cm soft tissue mass, centered in the right temporal bone causing erosion into the vestibule, superior semicircular canal and internal auditory canal (Figures A and B). There were only scattered bony remnants of the temporal bone, with extension of the mass into the middle and posterior cranial fossae. The patient proceeded to MRI, where the mass was revealed to have mixed high/low T2 signal (Figure F) and avid enhancement with gadolinium (Figures C,D,E). Mass effect on the right side of the brainstem and right cerebellar hemisphere was noted. Vascular involvement was assessed using MR Venogram, which demonstrated occlusion of the jugular vein at the bulb as well as stenosis of the right sigmoid sinus. Subsequent direct biopsy was performed through the auditory canal. A fleshy, hemorrhagic tissue sample was obtained, and sent for pathology. Histological analysis demonstrated a tumor composed of densely packed blue cells (Figure G) and irregular nests of small epitheloid cells, with no identifiable rosette formation and a background of myxoid stroma with a fine vasculature. Immunohistochemistry revealed diffusely positive AE1/AE3, CK8/18, vimentin and CD99 (figure H). Tissue was subsequently sent for molecular diagnosis, which confirmed the presence of EWSR1 by FISH. A diagnosis of Ewings Sarcoma was made. Summary: Our case highlights many of the clinical, imaging and pathologic features of Ewings' sarcoma of the Temporal bone. The initial clinical features experienced by this patient were somewhat atypical: headache and vomiting are the usual reported features at presentation of skull base Ewing's sarcoma rather than the palpable mass, drainage and cranial nerve palsies in our case. Our clinical features may be atypical due to the abnormally large size of the tumour as well as the deep-seated location within the temporal bone. Our case illustrates many of the typical imaging features of primary cranial Ewings sarcoma such as avid enhancement, and presents some atypical features such as the mixed high/low T2 signal which is normally not seen and the absence of adjacent bony thickening on CT, which has been demonstrated in other case reports. We have highlighted many of the immunohistochemical features typical of these lesions such as expression of vimentin and CD99, as well as providing molecular diagnostics.

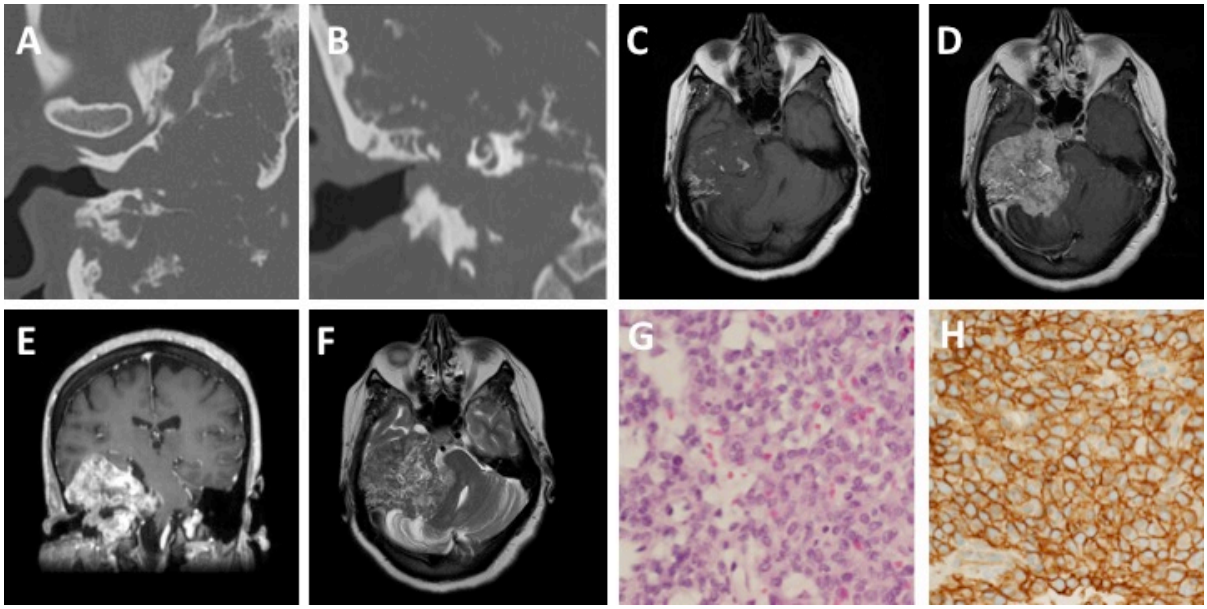
A
B
C
D
E
F
G
H

Radiologic spectrum of metastatic lymph nodes in HPV-related oropharyngeal squamous cell carcinoma

141 Radiologic spectrum of metastatic lymph nodes in HPV-related oropharyngeal squamous cell carcinoma

F Sabiq, A Patel, K Huang, H Quon, R Banerjee, B Debenham, H Lau, D Skarsgard, G Chen, J Lysack

Vancouver General Hospital
Canada

PURPOSE: The presence of matted lymph nodes in HPV-related oropharyngeal squamous cell carcinoma (OP SCC) is a poor prognosis marker and acts independently as a predictor of distant metastasis and overall survival. However, imaging-based definitions of matted nodes in the literature are variable and ambiguous. The purpose of our study is to examine and further define the radiologic patterns of metastatic lymph nodes (LNs) in HPV-related OP SCC and to analyse our grading system for reproducibility. MATERIAL & METHODS: The pre-treatment staging CT examinations performed at two centres were retrospectively reviewed for 148 patients diagnosed with p16+ OP SCCC between January 2007 to December 2011. The nodal metastases were scored independently by two neuroradiology fellows according to 4 radiologic nodal groups: discrete non-abutting lymph nodes (LNs) without extranodal extension (ENE) (group D), abutting LNs without ENE (group A), abutting LNs with ENE in their intervening fat plane only (group I), single LN with ENE or abutting LNs with ENE in their intervening fat plane and around their non-abutting borders (group E). The groups were further divided into subgroups A2 and A3; I2 and I3; and E1, E2 and E3, depending on the number of LNs in a cluster. Interrater reliability analysis was performed to determine consistency among raters using Kappa statistic. RESULTS: Agreement on the radiologic nodal groups amongst raters was achieved on 110 out of 148 CT examinations (74% agreement). By Kappa statistics, overall agreement was substantial (κ=0.73 including groups, 95% confidence interval [CI] 0.63-0.82 vs κ= 0.67 including subgroups, CI 0.60-0.74; all $p<0.0001$). Agreement was almost perfect for group D (κ=0.85, CI 0.69-1.00) and substantial for group A, I and E (κ=0.62, CI 0.46-0.78; κ=0.63, CI 0.47-0.79; κ=0.77, CI 0.60-0.93, respectively). The presence of ENE (groups I and E) was detected with substantial agreement (κ=0.74, CI 0.58-0.90). Amongst the subgroups, agreement was moderate for subgroup I3 (3 or more abutting LNs with ENE in their intervening fat plane only) (κ=0.58, CI 0.42-0.74) and substantial for subgroup E3 (3 or more abutting LNs with ENE in their intervening fat plane and around their non-abutting borders) (κ=0.71, CI 0.55-0.87). When assessing for the presence of matted nodes, which by definitions in the literature would include subgroups I3 and E3, agreement was substantial (κ=0.76, CI 0.60-0.92). CONCLUSION: In our study, we describe several radiologic patterns of metastatic LNs in HPV-related OP SCC. In a cluster of 3 or more abutting LNs on CT, ENE may be detected in their intervening fat plane only (subgroup I3) or in their intervening fat plane and around their non-abutting borders (subgroup E3). These two nodal subgroups are distinguishable with moderate to substantial agreement amongst raters. Definitions of matted nodes in the literature include both these subgroups. Their individual prognostic value should be further assessed.

Valentines and other Variations in the Incisive Foramen: A Peekhole into Developmental Neurobiology

142 Valentines and other Variations in the Incisive Foramen: A Peekhole into Developmental Neurobiology

JH Rees, RO DeJesus MD

University of Florida College of Medicine
United States

Purpose: To examine variations in the incisive foramen in humans, and to correlate these observations with the developmental biology of the vomeronasal gland and pathway Materials and Methods: Random selection of variations in shape of the incisive foramen encountered incidentally in a routine University Neuroradiology practice was performed. Results: The incisive foramina selected show variation in morphology ranging from rounded to bi-oval to valentine or heart shaped, and vary in size from 2-3 mm up to 6 mm in diameter. Review of developmental biology literature reveals that the incisive foramen is the vestigial aperture for receptor neurons of the vomeronasal organ or Jacobson's Organ, which in humans involutes during fetal life. The vomneronasal organ is an accessory olfactory gland which differs from our primary olfactory system in several ways. It is the mechanism whereby many vertebrates and other animals detect the presence of pheromones. Pheromones are molecules in the environment which convey important biological signals of a number of different types. They may convey information about readiness or suitability for sexual partnering. They may contain information about food sources. They may contain informational location, or directional maps to food and other locations particularly in insects. Whereas typical olfaction occurs via aerosolized molecules floating freely in air, which enter the nasal cavity and bind to receptors on the olfactory nerves after they penetrate the cribriform plate, pheromone detection often requires direct physical contact. Animals such as elephants use the prehensile tips of their trunks to grab and thrust material into the roof of their oral cavity in order to accomplish this, and other animals exhibit a wide variety of similar and different mechanisms for presenting material directly to their vomneronasal organs. Pheromones exhibit a wide variety of meaning and potency throughout the animal kingdom but in general they tend to produce an obligate neural response. When humans smell something, the sensation is initiated, processed and then routed to the cortex where it is stored and also compared to other stored scent memories allowing decision and judgement regarding the importance of the smell and whatever action its detection may incite. In animals without an olfactory cortex, the neural response through pheromones is more hardwired. Conclusion and Discussion: In evolutionary biology, it has been found that as neural structures become more complex, and specifically as animals develop olfactory cortex, the dominance of the vomneronasal organ and obligate pheromone signaling decreases. Hence in humans, the vomneronasal organ is generally considered absent or vestigial and the incisive foramen is an empty pathway. But yet olfaction in humans does in some ways resemble pheromones, as exhibited in the instinctive reactions to smells such as dead or rotting meat, and other pleasant and unpleasant odors. Variations in the morphology of the incisive foramen likely reflect the varied genetic histories of different humans which have evolved through our varied family trees which may have made variable use of pheromones versus typical olfaction in their struggle to survive and reproduce.

Smash Mouth! Principles of Orthognathic and Craniofacial Surgery and imaging correlates

143 Smash Mouth! Principles of Orthognathic and Craniofacial Surgery and imaging correlates

N Shekhrajka, M Forman, S Eisig, G Moonis

New York Presbyterian Hospital/Columbia University Medical Center
United States

Corrective jaw, or orthognathic surgery is performed by an oral and maxillofacial surgeon (OMFS) to correct a wide range of minor and major skeletal and dental irregularities, including the misalignment of jaws and teeth. Typically this involves an osteotomy wherein bone is cut, moved, modified, and realigned to correct a dentofacial deformity. These procedures include but are not limited to genioplasty, Sagittal split osteotomy, anterior segmental maxillary osteotomy and Le Fort I and III osteotomy. In this presentation we shall introduce and elucidate with clinical and imaging examples the basic principles underlying orthognathic surgery .

Smash Mouth! Principles of Orthognathic and Craniofacial Surgery and imaging correlates

21 y old female with microcephaly, hypotonia and significant developmental delay.
3 D reconstructions from a facial CT demonstrate a LeFort I osteotomy of the maxilla and bilateral sagittal split osteotomies of the mandible .

Texture Analysis of Diffusion-weighted Imaging in Head and Neck Squamous Cell Carcinoma: Diagnostic Value for Nodal Metastasis

144 Texture Analysis of Diffusion-weighted Imaging in Head and Neck Squamous Cell Carcinoma: Diagnostic Value for Nodal Metastasis

J Park, Y Bae, L Sunwoo, B Choi, C Jung, J Kim

Seoul National University Bundang Hospital
Republic of Korea

Purpose To evaluate the diagnostic performance of texture features of diffusion-weighted imaging (DWI) in differentiating nodal metastasis from benign lymph nodes in head and neck squamous cell cancer (SCC) patients. Materials and Methods Between June, 2016 and February, 2018, thirty-six patients with pathologically proven head and neck SCC were included in this study. All patients underwent preoperative magnetic resonance imaging (MRI) including DWI and conventional imaging at 3T. Total 204 MRI-detected lymph nodes including 176 subcentimeter-sized nodes were assigned to the benign or metastatic nodes according to pathology or positron emission tomography-computed tomography reports. Texture features including histogram and gray-level matrices was derived by drawing region-of-interest on lymph nodes while excluding necrosis on apparent diffusion coefficient (ADC) maps. Texture features between benign and metastatic nodes were compared using independent t-test, and hierarchical cluster analysis was performed to identify correlations between features. Multivariate logistic regression and receiver operating characteristic analysis were performed to assess diagnostic performance for metastatic nodes. Results Total 83 out of 204 lymph nodes in all size were confirmed as metastasis; 58 out of 176 subcentimeter-sized nodes were metastatic. Three discriminative texture features for differentiating metastatic from benign nodes were complexity (all-size, P<.001, odds ratio [OR] 1.0000022, 95% confidence interval [CI] 1.000001-1.000004; subcentimeter-size, P=.001, OR, 1.000002, 95% CI, 1.0000008-1.000004), normalized energy (P=.014, OR 1.000002, 95% CI 1.0000004-1.000004; P=.001, OR 1.000002, 95% CI 1.0000009-1.000004) and roundness (P=.008, OR 103.56, 95% CI 3.35-3675.25; P=.008, OR 116.88, 95% CI 3.39-4675.74). Area under the curves (AUCs) for all-sized and subcentimeter-sized nodes were 0.829 and 0.767 regarding complexity, 0.699 and 0.685 regarding normalized energy, and 0.671 and 0.638 regarding roundness. The combination of three features resulted in a higher AUC value of 0.836 and 0.781, respectively. Conclusions Texture analysis of DWI can be useful in diagnosing nodal metastasis in in head and neck SCC, especially in normal subcentimeter-sized lymph nodes.

Understanding CT and MRI artifacts in head and neck imaging: developing identification techniques through artifact visualization

145 Understanding CT and MRI artifacts in head and neck imaging: developing identification techniques through artifact visualization

EL Marshall, D Ginat, S Sammet

University of Chicago
United States

Purpose: Establish common CT and MRI imaging artifacts found in head and neck imaging. Develop an understanding of the physics principles behind these artifacts to work towards either the elimination of the artifact or the creation of an awareness regarding how the artifact may impact the image reading. Description: Patient images provide visual examples of all major CT and MRI artifacts alongside their clinical indications for exam. Each artifact example is accompanied by a direct explanation of the physics behind the artifact and works up to providing troubleshooting techniques to work towards eliminating the artifact. CT artifacts included in this exhibit are beam hardening, motion, partial volume, photon starvation, stair step, under-sampling, metal materials, and ring artifacts. MRI artifacts included in this exhibit are chemical shift, signal loss, motion, under-sampling, flow, susceptibility, slice cross-talk, under-sampling, Gibbs ringing, partial volume, and wrap-around. Explaining of the physics principles leading to the artifact creation empowers the radiologist to understand what underlying issues are causing these imperfections in the imaging chain. MRI motion artifacts, for example, are generally a result of the extended readout period observed in the phase-encoding direction. This length of time, on the order of tens of seconds, enables patients to move, resulting in blurry images. If the blurred line appears across an anatomical area of interest, the MRI signal can be collected in successive sequences with the phase and frequency encoding directions switched. This imaging solution becomes understandable when the physics principles behind the artifacts conception are understood. Summary: Exposure to clinical case studies containing artifacts provides practicing and training clinicians the opportunity to develop a familiarity with artifact presentation. Clinicians exposure to such cases and comprehensive understanding of the physics behind the artifact will help develop a subsequent comfort level leading towards swift detection.

Cystic Parotid Lesions: Pictorial review with an approach to diagnosis.

146 Cystic Parotid Lesions: Pictorial review with an approach to diagnosis.

RG Hegde, M Rosovsky, P Kochar

Bridgeport Hospital Yale New Haven Health
United States

PURPOSE: 1. Depict varied etiologies of cystic lesions in the parotid glands on imaging. 2. Devise a diagnostic approach to dealing with cases of parotid cystic lesions. DESCRIPTION: Parotid cystic lesions and solid-cystic lesions have a wide differential including developmental, idiopathic, inflammatory, infectious, benign neoplastic and malignant neoplastic etiologies. We present a spectrum of cases with parotid cystic lesions from varied etiologies like branchial cleft cyst, venolymphatic malformations, abscess, sjogren sydrome, HIV associated lympho-epithelial cysts, sialocele and Warthin'g tumor (Cystadenoma lymphomatosum). We review the clinical presentation and imaging features of these conditions on multiple modalities (US, CT, MR) to identify typical features. In summary, we present a diagnostic approach with conditions that are solitary or multiple and unilateral or bilateral. CONCLUSION: Review of multimodality imaging findings of cystic and solid cystic parotid lesions and developing a diagnostic approach for these lesions based on clinical information and imaging findings.

Ollier Disease-- When and How to Image

147 Ollier Disease-- When and How to Image

C Fleming

Omaha Children's Hospital
United States

Ollier disease is an entity generally classified as benign and without systemic implications. We will discuss the case of a 16 year old girl, who carried the diagnosis of Ollier disease. She presented with several nonspecific hypopharyngeal lesions, and was referred for an MRI of the neck/ hypopharynx. The lesions had imaging characteristics of hemangiomas, and this diagnosis was later confirmed surgically. A diagnosis of Maffucci syndrome was thus made. Further MR imaging revealed additional unsuspected internal hemangiomas. Our exhibit will review these entities with a review of the literature including the clinical significance of distinguishing the two. We will explore the question of when and how patients with Ollier disease should be screened for additional pathology. We will also discuss the head and neck manifestations of Ollier disease and Maffucci syndrome.

Case Report: Acute Bacterial Meningitis Secondary to an Indolent Encephalocele

148 Case Report: Acute Bacterial Meningitis Secondary to an Indolent Encephalocele

M Wu, D Luu, R Gilad, S Motivala, L Voutsinas, J Hwang, S Serras, M Raden, D Klein

Staten Island University Hospital
United States

Purpose: Acute bacterial meningitis is a relatively rare but serious infection of the meninges and subarachnoid space that often presents with fevers, headaches, and nuchal rigidity. Rarely, bacterial meningitis may occur secondary to a sinus encephalocele. This case report details an atypical presentation of acute bacterial meningitis as a result of an encephalocele within the left frontal sinus. Case Report: A 62 year old female with no significant past medical history presented to our emergency department complaining of 10-day history of generalized fatigue, lower extremity weakness, and the occasional low-grade fever. She did not report any headache, dizziness, or blurry vision. She did not report any recent trauma or illness. Two lumbar punctures performed 18 days apart were remarkable only for mild pleocytosis and an elevated opening pressure on the repeat lumbar puncture. Cerebrospinal fluid gram stain and culture were negative. A noncontrast CT of the head was obtained initially followed by an MRI without contrast and subsequently an MRI with contrast. Despite the imaging findings, the patient was treated conservatively given relative lack of acute symptomatology. A week later the patient deteriorated clinically and became lethargic and developed right upper and lower extremity weakness. A dural biopsy was performed, during which loculated purulent material was aspirated from the subarachnoid space overlying the vertex. Fluid culture grew Streptococcus pneumoniae, an organism known to colonize the nasal cavity, respiratory tract, and sinuses of frequently asymptomatic patients. After a course of antibiotics the patient recovered without residual defects. The encephalocele was repaired successfully a few weeks after the infection subsided. Image Findings: Noncontrast CT of the head demonstrates hypodense material filling the superior bilateral cortical sulci. There is a bony defect along the posterior wall of the left frontal sinus with a small left frontal sinus encephalocele extending through the defect. MRI of the brain without contrast demonstrates distention of the subarachnoid space near the vertex with restricted diffusion. Area of edema with expansile T2 hyperintensity were noted within the left frontal lobe subcortical region. Contrast enhanced images demonstrate corresponding dural and leptomeningeal enhancement surrounding the areas of restricted diffusion. A small left frontal encephalocele is demonstrated containing gliotic brain parenchyma and some susceptibility effect. Summary: Encephaloceles are herniations of meninges and brain parenchyma through cranial defects that may be congenital, post-traumatic, or erosive in origin. Infectious seeding of the meninges via the encephalocele, leading to purulent bacterial meningitis is rare. When an encephalocele is a cause of meningitis, the cranial defect needs to be repaired to prevent recurrence; thus, detection of the encephalocele by the radiologist is crucial. When meningitis is caused by an encephalocele, the symptoms may not be classic as in our case given the possibility for chronic exposure and the infection to be isolated. Imaging findings played a key role in diagnosing and treating this patient.

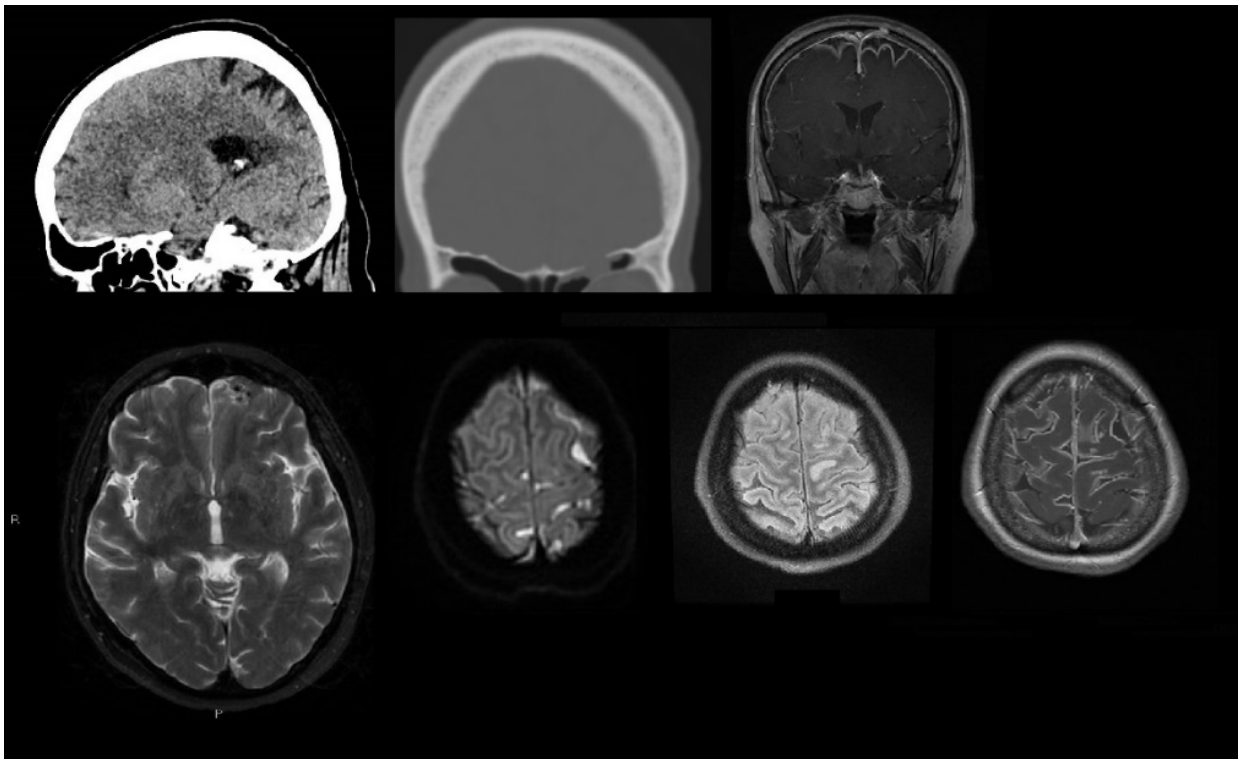
R
P

Radiomic MRI phenotyping of oropharyngeal tumor: differentiating squamous cell carcinoma and malignant lymphoma of the oropharynx

149 Radiomic MRI phenotyping of oropharyngeal tumor: differentiating squamous cell carcinoma and malignant lymphoma of the oropharynx

S Bae, Y Choi, B Sohn, H Park, C Park, J Kim

Department of Radiology, Severance Hospital, Yonsei University College of Medicine, Seoul, Korea
Republic of Korea

Purpose: To investigate whether radiomic feature-based machine-learning models differentiate squamous cell carcinoma (SCC) and malignant lymphoma of the oropharynx. Materials and methods: Pretreatment MR imaging from 89 consecutive patients with pathologically confirmed oropharyngeal SCC (n=70) and malignant lymphoma (n=19) were retrospectively reviewed. Enhancing tumors were manually segmented on each slice of the postcontrast T1-weighted images and registered to T2-weighted images. Radiomic features (n=741) were extracted from postcontrast T1-weighted and T2-weighted images, including 645 features from wavelet transformation. Variable combinations of feature selection (t-test, principal component analysis, recursive feature elimination) and machine learning algorithms (random forest, gradient boost machine, and linear discriminant analysis) were used for assessment of the strength of association between radiomic features and pathology of the oropharyngeal tumor. Results: Applying machine learning to radiomic features yielded moderate performance (area under the receiver operating characteristics curve: 0.651-0.800) to differentiate SCC and malignant lymphoma of the oropharynx. In terms of accuracy, only a few combinations showed higher accuracy than prediction by change. Conclusions: Our preliminary results suggest that radiomic phenotyping might differentiate SCC and malignant lymphoma of the oropharynx, and thus has potential as a practical imaging biomarker.

Greater Occipital Nerve: Radiological anatomy demonstrated by two cases of Tumour Perineural Spread

150 Greater Occipital Nerve: Radiological anatomy demonstrated by two cases of Tumour Perineural Spread

M Debowski, J Sommerville, M Gandhi

Royal Brisbane and Women's Hospital, University of Queensland
Australia

Background: The greater occipital nerve (GON) is a tortuous superficial cutaneous nerve supplying sensory innervation to the posterior scalp. Perineural spread (PNS) is an established form of local invasion but is rarely seen along the GON. Methods: We present two cases of PNS along the GON which underwent MRI and extensive resection. Results: A selection of annotated MR images and a diagram is used to illustrate anatomy of the GON which is relevant to the surgeon and radiologist. Conclusion: This is the first radiological portrayal of the course of perineural tumour spread of the GON as demonstrated on MRI.

Where did my voice go?: Unilateral Vocal Cord Paralysis Cases Presented with an Anatomic and Radiologic Review

151 Where did my voice go?: Unilateral Vocal Cord Paralysis Cases Presented with an Anatomic and Radiologic Review

JD Gupta, ND Gupta

Southeastern Louisiana Veterans Healthcare System
United States

Purpose: We will describe the anatomy and innervation of the vocal cords. We hope to describe imaging techniques useful for evaluation of potential causes of Vocal Cord Paralysis/Paresis (VCP). We plan to review common and uncommon causes of VCP with teaching cases from our institution and the literature. Description: Most common symptoms of vocal cord paralysis include hoarseness, dyspnea, vocal fatigue, loss of vocal pitch, aspiration, and dysphonia Vocal cord paralysis often develops in the post-procedural or post-infectious period. A neoplastic etiology should be considered in the setting of chronic tobacco use or known malignancy. Common Etiologies of vocal cord paralysis includes mass impingement or invasion of the vagus/recurrent laryngeal nerve secondary to malignancy or lymphadenopathy, traumatic nerve injury inclusive of surgical complications, infection, inflammation, and idiopathic etiologies. Damage or compression of the proximal Vagus Nerve(s) or the RLN's results in VCP. It is possible for a vagal brainstem nuclei lesion to cause VCP. A given lesion results in VCP of the ipsilateral side. The entire course of the vagal nerves from the skull base through the RLN's should be visualized. Summary: Vocal cord paralysis (VCP) can be a devastating condition that can impair one's ability to communicate with others and can make breathing difficult and laborious. VCP is a well-known complication of surgeries involving the neck. Common VCP symptoms include dyspnea, hoarseness, and dysphonia. Other etiologies of VCP include trauma, infection, inflammation, and mass infiltration or compression. Up to 20% of cases of unilateral VCP are idiopathic. The Anatomic Review, VCP Overview, and Case Presentations within this educational exhibit provide a thorough review of VCP and possible patient presentations for the practicing radiologist or imaging trainee.